DUAL REGULATION OF VOLTAGE- AND LIGAND-GATED CALCIUM CHANNELS BY COLLAPSIN RESPONSE MEDIATOR PROTEIN 2

Joel Matthew Brittain

Submitted to the faculty of the University Graduate School
in partial fulfillment of the requirements
for the degree
Doctor of Philosophy
in the Program of Medical Neuroscience,
Indiana University

December 2012

Accepted by the Faculty of Indiana University, in partial
fulfillment of the requirements for the degree of Doctor of Philosophy.

Rajesh Khanna, Ph.D., Chair

Theodore R. Cummins, Ph.D.

Doctoral Committee

Gerry S. Oxford, Ph.D.

Lawrence A. Quilliam, Ph.D.

November 12, 2012

Debbie C. Thurmond, Ph.D.

DEDICATION

This thesis is dedicated to my parents for all of the love and support they have given me. Knowing that they are there for me and that I can always count on them has given me a calm and strength to work hard to achieve my goals.

.

ACKNOWLEDGEMENTS

This thesis and the work therein would not be possible without the contributions and support of many people

I first thank my mentor Dr. Rajesh Khanna for guiding and challenging me in the laboratory. Dr. Khanna has been a mentor who truly cares about my future and strives to make me a better scientist. The experience of working in his laboratory and under his guidance has led me to mature as both a person and scientist. All of my past and future success is due to your diligence and hard work. I thank Dr. Cummins for convincing me to attend Indiana University and exposing me to the field of ion channel biology. Without your effort and invitation to visit the IUPUI campus I would not have the opportunity to come to IUPUI and become the person I am today. I thank Dr. Oxford, Dr. Thurmond, and Dr. Quilliam for their support and pushing me in the right direction. I thank Dr. Nick Brustovetsky for assistance with technical aspects of several experiments and for many enlightening conversations. I thank Dr. Fletcher White for his insightful conversations and unique perspectives that greatly aided in my research. I thank Dr. Cynthia Hingtgen, Dr. Michael Vasko, and Dr. Grant Nicol along with the rest of the sensory neuron lab meeting participants for challenging me to improve as a scientist and for the tough questions they routinely asked me. I thank Dr. Andy Hudmon for many discussion regarding experimental approach and assistance with aspects of my experiments.

I thank Nastassia Belton and Brittany Veal of Stark Neuroscience Research Institute for everything they have done to make my life as a graduate student easier. I thank Tracy Donhardt for helping me to improve my writing skills. I thank Dr. Djane Duarte, Dr. Weiguo Zhu, Dr. Haitao You, Dr. Andrew Piekarz, Matthew Ripsch, Dr. Naikui Liu, and Tatiana Brustovesty for the experiments they performed that have been included in thesis. I thank Dr. May Khanna for her technical assistance with protein purification and surface plasmon resonance. I thank Kashif Kirmani and Eric Thompson for work and assistance with virus production. I thank Dr. Andrei

Molosh, Dr. Michael Due, Dr. Brian Jarecki, and Dr. Patrick Sheets for their assistance with experiments and many enlightening conversations.

I thank the graduate students both on the 4th floor of R2 as well as throughout campus that have made graduate school fun even when the science did not work as planned. I thank Dr. Nicole Asphole, Dr. Michael Kalwat, Melissa Walker, Ben Thirlby, Natalie Case, Justin Babcock, Hoa Nyugen, and Sherry Pittman for their friendship and stimulating scientific conversations. I thank members of the Khanna lab for making the laboratory a fun and prosperous environment. I thank Sarah Wilson, Alicia Garcia, Omotore Eruvwetere, Kisan Shah, Stephanie Martinez, Weina Ju, Erik Dustrude, and Xiao-Fang Yang for all of their assistance and for laughing even when my jokes were not funny. I thank all of my friends and family for hanging with me through the ups and downs that graduate school can bring.

I lastly thank Alyssha Duncan who has been supportive of me throughout the all-encompassing process that is writing a thesis.

ABSTRACT

Joel Matthew Brittain

DUAL REGULATION OF VOLTAGE- AND LIGAND-GATED CALCIUM CHANNELS BY COLLAPSIN RESPONSE MEDIATOR PROTEIN 2

Synaptic transmission is coordinated by a litany of protein-protein interactions that rely on the proper localization and function of pre- and post-synaptic Ca^{2+} channels. The axonal guidance/specification collapsin response mediator protein-2 (CRMP-2) was identified as a potential partner of the pre-synaptic N-type voltage-gated Ca^{2+} channel (CaV2.2). CRMP-2 bound directly to CaV2.2 in two regions; the channel domain I-II intracellular loop and the distal C-terminus. Both proteins co-localized within presynaptic sites in hippocampal neurons. Overexpression in hippocampal neurons of a CRMP-2 protein fused to EGFP caused a significant increase in Ca^{2+} channel current density whereas lentivirus-mediated CRMP-2 knockdown abolished this effect. Cell surface biotinylation studies showed an increased number of CaV2.2 at the cell surface in CRMP-2–overexpressing neurons. Both activity- and CRMP-2-phosphoryation altered the interaction between CaV2.2 and CRMP-2. I identified a CRMP-2-derived peptide (called CBD3) that bound CaV2.2 and effectively disrupted the interaction between CaV2.2 and CRMP-2. CBD3 peptide fused to the HIV TAT protein (TAT-CBD3) decreased neuropeptide release from sensory neurons and excitatory synaptic transmission in dorsal horn neurons, and reversed neuropathic hypersensitivity produced by an antiretroviral drug.

Unchecked Ca^{2+} influx via *N*-methyl-D-aspartate receptors (NMDARs) has been linked to activation of neurotoxic cascades culminating in cell death (i.e. excitotoxicity). CRMP-2 was suggested to affect NMDAR trafficking and possibly involved in neuronal survival following excitotoxicity. Based upon these studies, I hypothesized that a peptide from CRMP2 could

preserve neurons in the face of excitotoxic challenges. Lentiviral–mediated CRMP2 knockdown or treatment with TAT-CBD3 blocked neuronal death following glutamate exposure likely via blunting toxicity from NMDAR-mediated delayed calcium deregulation. TAT-CBD3 induced internalization of the NMDAR subunit NR2B in dendritic spines without altering somal surface expression. TAT-CBD3 reduced NMDA-mediated Ca^{2+}-influx and currents in cultured neurons. The presented work validates CRMP-2 as a novel modulator of pre- and post-synaptic Ca^{2+} channels and provides evidence that the TAT-CBD3 peptide could be useful as a potential therapeutic for both chronic neuropathic pain and excitotoxicity following stroke or other neuronal insults.

Rajesh Khanna, Ph.D., Chair

TABLE OF CONTENTS

LIST OF TABLES

LIST OF FIGURES

FIGURE CONTRIBUTIONS

LIST OF ABBREVIATIONS

AMPAR	2-amino-3-(3-hydroxy-5-methylisox-azol-4-yl) propionate receptor
AP-5	D-(-)-2-Amino-5-phosphonopentanoic acid
BSA	Bovine serum albumin
CAD	Catecholamine A Differentiated
CaM	Calmodulin
CaMKII	Ca^{2+}-dependent CaM Kinase II
CAPS	N-cyclohexyl-3-aminopropanesulfonic acid
CASK	Ca^{2+} /CaM activated serine kinase
CaV1.2	L-type Ca^{2+} channel (α1C)
CaV2.1	P/Q-type Ca^{2+} channe (α1A)
CaV2.2	N-Type Ca^{2+} channel (α1B)
CBD	Ca^{2+} channel binding domain
Cdk5	Cyclin-dependent kinase 5
CRMP	Collapsin response mediator protein
DEAE	Diethylaminoethyl cellulose
DIV	Days *in vitro*
DsRed	*Discosoma* sp. red fluorescent protein
EGFP	Enhanced green fluorescent protein
EPSC	Excitatory post-synaptic current
FITC	Fluorescein isothiocyanate
GSK3β	Glycogen synthase kinase 3β
GST	Glutathione S Transferase
HEPES	4-(2-hydroxyethyl)-1-piperazineethanesulfonic acid
IP	Immunoprecipitation
MBS	MES buffered saline
MES	2-(*N*-morpholino)ethanesulfonic acid
mIgG	Mouse Immunoglobulin G
MK-801	(+)-5-methyl-10,11-dihydro-5H-dibenzo[a,d] cyclohepten-5,10-imine maleate
Munc18	Mammalian uncordinated 18
NMDAR	N-methyl-D-aspartate receptor
NR2A	NMDA receptor subunit 2A
NR2B	NMDA receptor subunit 2B
O/N	Overnight
PBS	Phosphate buffered saline
PDZ	PSD-95, *Drosophila* disc large tumor suppressor (Dlg1), zonula occludens-1 protein (zo-1)
PKA	Protein kinase A
PKC	Protein kinase C
PN	Post natal
PSD-95	Post-synaptic density 95
ROCK	Rho associated kinase
rIgG	Rabbit Immunoglobulin G
RT	Room termperature

SDS-PAGE	Sodium dodecyl sulfate polyacrylamide gel electrophoresis
SH3	Src homology 3
shRNA	Short hairpin RNA
siRNA	Small interfering RNA
TAT	Transactivator of transcription
TBST	Tris buffered saline with Tween-20
TrkB	Tyrosine-related kinase B
ω-CTX	ω-conotoxin GVIA

FOREWORD

I begin my thesis with an Introduction to the three main areas covered in my thesis research: CaV2.2, CRMP-2, and NMDARs. I then describe the Materials and Methods (Chapter 2) used to perform the experiments that comprise my thesis research. Next, I describe the results of my studies on the regulation of CaV2.2 by CRMP-2. This spans the initial biochemical and functional characterization between CaV2.2 and CRMP-2, the potential role CRMP-2 phosphorylation by Cdk5 plays in regulation of CaV2.2, and finally the development and characterization of the CRMP-2-CaV2.2 disrupting CRMP-2 peptide CBD3 and the use of a cell penetrant version of the CBD3 peptide in cell biology and animal studies (Chapter 3). The second part of my results present evidence for CRMP-2 regulation of NMDARs and putative roles in neuroprotection (Chapter 4). This is followed by an overall Discussion (Chapter 5), which synergizes the results, discusses the relevance to the literature, and presents future directions for the CRMP-2 and calcium channel fields.

CHAPTER 1. INTRODUCTION

1.1. CaV2.2

1.1.1. Identification of an "N-type" calcium current

The field of Ca^{2+} channels likely began with the seminal observation of a Ca^{2+} current during an examination of the electrical properties of crustacean muscle fibers (Fatt and Katz, 1953). During the course of recording Na^{+} current dependent action potentials, Paul Fatt and Bernard Katz noted that despite complete removal of Na^{+}, action potentials persisted. It was not until five years later that Fatt and Bernard Ginsborg concluded that Ca^{2+} was sufficient to support action potentials (Fatt and Ginsborg, 1958). Building on these early studies on Ca^{2+}-dependent excitability, using squid giant axons, Hodgkin and Keynes first measured activity-dependent $^{45}Ca^{2+}$ flux leading to their postulate that Ca^{2+} influx triggers neurosecretion (Hodgkin and Keynes, 1957). These early findings were prescient of a route for rapid entry of Ca^{2+} into the cell thereby paving the road for all subsequent studies on synaptic transmission and all other forms of fast Ca^{2+} signaling. The pathway for Ca^{2+} entry was eventually found to be pore-forming proteins called Ca^{2+} channels (Llinas et al., 1976). Importantly, these Ca^{2+} channels are responsible for converting the electrical signal contained in an action potential to the chemical signal of a neurotransmitter, were found to be regulated by the voltage across the cell membrane. Hence, these channels are now known as voltage-gated Ca^{2+} channels. A hint of diversity of Ca^{2+} channel first emerged when it was shown that two Ca^{2+} channels with unique properties existed in star fish eggs (Hagiwara et al., 1975). Some years later, two subtypes of Ca^{2+} channels that could be separated by the voltages at which they open were discovered in chick sensory neurons (Carbone and Lux, 1984). These subclasses of Ca^{2+} channels would be coined low voltage-activated (LVA) and high voltage-activated (HVA) channels. Using specific agonists and antagonists in cardiac cells, long lasting HVA currents that were termed "L-type" currents were identified (Hess et al., 1984). In neurons, despite complete block of L-type currents, an additional current was also present. This current was designated "N-type" (non-L-type and neuronal) and while requiring high voltage to activate like the L-type, it was biophysically different particularly

in its inactivation and activation properties (Nowycky et al., 1985). This neuronal N-type Ca^{2+} channel is the focus of my dissertation work but is it is important to acknowledge that there also exist other Ca^{2+} channels in neurons. A compendium of voltage-gated Ca^{2+} channels expressed in neurons is shown in Figure 1.1. These channel subtypes are distinguishable by their biophysical properties and/or drug sensitivities. Importantly, the identification of N-type Ca^{2+} currents explained previous reports of neurotransmitter release insensitive to L-type currents blockade. The isolation and detailed analyses of N-type Ca^{2+} currents was greatly advanced by the discovery of the cone snail toxin ω-conotoxin GVIA (ω-CTX) (Kerr and Yoshikami, 1984; Olivera et al., 1984) which was capable of blocking neurotransmission via directly antagonizing N-type Ca^{2+} currents (Dooley et al., 1987; Kasai et al., 1987). The N-type Ca^{2+} channel was subsequently purified and genetically isolated (Williams et al., 1992). Like the majority of Ca^{2+} channels, the N-type channel is composed of multiple subunits including the α1, β, α2δ, and γ subunits. The α1 subunit (classified as α1B) is the primary subunit and determines toxin selectivity and synaptic targeting (discussed in §1.1.8). Ca^{2+} channel α1 subunits contain four domains each consisting of six transmembrane regions. Richard Tsien, William Catterall and others proposed a nomenclature for Ca^{2+} channels that was approved by the International Union of Pharmacology and has been widely accepted (Catterall et al., 2005; Ertel et al., 2000). This nomenclature groups and labels the 10 known Ca^{2+} channels (as defined by their α1 subunit) using a CaVX.Y where X = number of Ca^{2+} channel subfamily and Y = number of the Ca^{2+} channel within this subfamily. According to this nomenclature, the N-type channel is known as CaV2.2 and the P/Q-type channel, which is part of the same subfamily, is designated as CaV2.1. A compendium of Ca^{2+} channels is outlined in Figure 1.1B. Ca^{2+} channel subtypes will be referred to using this nomenclature for the remainder of this thesis. A more indepth descriptive history of Ca^{2+} channels can be found elsewhere (Dolphin, 2006).

A

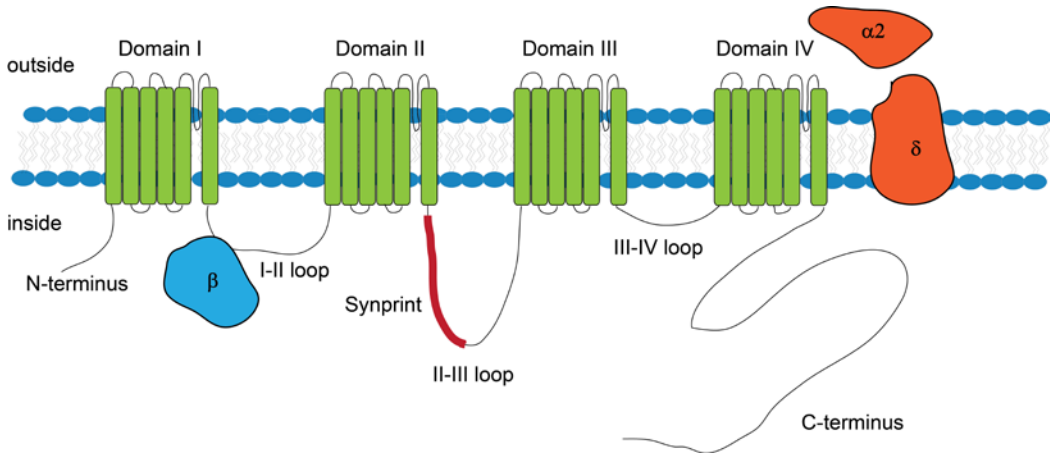

B

Channel	Current	alpha 1 subunit	HVA or LVA	Function
CaV1.1	L	S	LVA	Excitation-contraction coupling
CaV1.2	L	C	LVA	Excitation-contraction coupling, gene transcription, peptide release
CaV1.3	L	D	LVA	Gene transcription, peptide release, cardiac pacemaking
CaV1.4	L	F	LVA	Neurotransmitter release from photoreceptors
CaV2.1	P/Q	A	LVA	Release of neurotransmitters and peptides
CaV2.2	N	B	LVA	Release of neurotransmitters and peptides
CaV2.3	R	E	LVA	Regulation of firing patterns
CaV3.1	T	G	HVA	Regulation of firing patterns
CaV3.2	T	H	HVA	Regulation of firing patterns
CaV3.3	T	I	HVA	Regulation of firing patterns

Figure 1.1. Ca^{2+} channel structure and family

(**A**) This figure depicts the predicted structure of CaV2.2 based upon sequence analysis and homology to Na^{+} channels. Included in this depiction is the auxiliary subunits β and α2δ, in addition the synprint region of CaV2.2 (aa 718-963) is highlighted. (**B**) Table of Ca^{2+} channel family subtypes, the nomenclature used and proposed functions.

1.1.2. Relationship of Ca^{2+} influx via CaV2.2 to synaptic release

Even prior to the actual identification of Ca^{2+} currents and channels, it was well known that Ca^{2+} was *required* for synaptic transmission through classical experiments of Locke, Overton, and Mines (Mines, 1911; Rubin, 1970). As mentioned above it was further postulated, following discovery of Ca^{2+} currents, that Ca^{2+} influx was required for neurotransmitter release (Hodgkin and Keynes, 1957). Furthermore, it was observed that increasing Ca^{2+} leads to an increase in release despite a decrease in pre-synaptic response (Katz and Miledi, 1965a). These findings linked Ca^{2+} influx to neurotransmitter release and led to more intense studies into the relationship between Ca^{2+} and neurotransmitter release. In a seminal study exploring this relationship, Frederick Dodge Jr. and Rami Rahamimoff observed that the relationship between Ca^{2+} and post-synaptic response was exponential (Dodge and Rahamimoff, 1967). The exponent in their particular set of experiments in the frog muscular junction was found to be four. This number, designated cooperativity, states that for a quantum of neurotransmitter to be released four Ca^{2+} molecules are required. It was later found that the single quantum of release consisted of a single neurotransmitter containing vesicle (Heuser et al., 1979). Cooperativity has been proposed as a means to assess the efficiency of coupling of Ca^{2+} channels to synaptic vesicle release. Using the calyx of Held – a large mammalian auditory synapse which can be isolated intact – the cooperativity was found to be ~6 (Fedchyshyn and Wang, 2005). Synaptic connections within the cerebellum were found to have a cooperativity value of between 2.5 and 4, likely due to the differential contributions of CaV2.1 and CaV2.2 or CaV2.2 channels alone, respectively (Mintz et al., 1995). Consistent with the finding in the cerebellum and frog neuromuscular junction, experiments in hippocampal autapses predicted a cooperativity value of 4 (Reid et al., 1998). The observed variance in cooperativity values across synapses can be attributed to stronger coupling to specific channel subtypes (as shown by Mintz and colleagues for CaV2.1) which may ultimately be due to changes in the developmental program of the

channels themselves (see §1.1.4) as well as protein-protein interactions involved in transmitter release.

The coupling of pre-synaptic Ca^{2+} channels to vesicle machinery facilitates the release of neurotransmitters by allowing Ca^{2+} influx to trigger vesicle fusion. The resting cytosolic concentration of Ca^{2+} within the nerve terminal is quite low (~50-100 nM), which upon opening of Ca^{2+} channels rises locally near the mouth of the Ca^{2+} channels (~5-30 μM) (Evans and Zamponi, 2006; Tay et al., 2012). The increase in Ca^{2+} is detected by Ca^{2+} sensing proteins (i.e. synaptotagmins) present on neurotransmitter containing vesicles leading to vesicle fusion with the synaptic membrane (Chapman, 2008). The delay between Ca^{2+} influx and release of neurotransmitter is very short (~ 1ms) suggesting that Ca^{2+} channels must be in tight spatial proximity to the release machinery (Katz and Miledi, 1965b; Llinas et al., 1981). It is therefore not surprising that CaV2.2 directly couples to vesicle exocytotic proteins enabling the rapid release of neurotransmitter (Khanna et al., 2007a; Zamponi, 2003). The regions of pre-synaptic terminals that are responsible for release are commonly referred to as "active zones" and are defined as regions opposite of post-synaptic terminals that contain all of the machinery needed for synaptic release. The tight coupling of CaV2.2 and the synaptic release complex is further supported by the finding that current passing via a single channel is sufficient for release of neurotransmitter in some neurons (Stanley, 1993). CaV2.2 is the primary source of Ca^{2+}-influx required for transmitter release at many synapses throughout the central nervous system (Hirning et al., 1988; Maggi et al., 1990b; Weber et al., 2010; Wheeler et al., 1994). At most synapses where CaV2.2 is not dominant, CaV2.1 is responsible for regulating release (Meir et al., 1999). At most synapses, however, release is regulated by more than one channel subtype (Reid et al., 2003; Wheeler et al., 1994; Wu et al., 1999).

1.1.3. CaV2.2 expression and localization

The presence of CaV2.2 currents is defined by their pharmacological sensitivity to ω-CTX. Through the use of ω-CTX, CaV2.2 current has been found in many different neurons both in the peripheral and central nervous system. CaV2.2 currents were first observed in dorsal root ganglion sensory neurons (Nowycky et al., 1985). Since their initial discovery, CaV2.2 have been found in soma and axodendritic compartments of various types of neurons including sympathetic (Hirning et al., 1988), cortical (Lorenzon and Foehring, 1995), hippocampal (Wheeler et al., 1994), cerebellar (Haws et al., 1993), and thalamic (Kammermeier and Jones, 1997). While some of the CaV1 family of Ca^{2+} channels are expressed in many different tissues (Catterall et al., 2005), expression of CaV2.2 is primarily limited to neuro- and neuroendocrine tissues (Artalejo et al., 1992; Williams et al., 1992), although it has also been observed in glia and sperm (D'Ascenzo et al., 2004; Wennemuth et al., 2000).

One of the proposed theories for regulation of Ca^{2+} channels in the presynaptic terminals states that there are modular units of release machinery within the active zone that couple to a set number of channels defining a "slot". This concept arose from work performed in the 19070's hinting that Ca^{2+} channels associate with synaptic vesicles in an ordered manner along the active zone (Heuser et al., 1979). Because different synapses express a different complement of Ca^{2+} channels contributing to release, this theory posits that synapses have different "allotments" of subtype-specific slots. Using cultured cortical neurons from mice deficient in CaV2.1, Tsien and co-workers showed that (i) over-expression of CaV2.1 leads to competition for native CaV2.1 channels more so than with other channel subtypes and (ii) that the amplitude of excitatory post-synaptic current (EPSCs) in neurons lacking CaV2.1 or expressing low conductance CaV2.1 was not altered (Cao et al., 2004). These data suggested that while CaV2.1 selectively occupies a subset of slots, CaV2.2 is able to compensate for the reduction in active zone CaV2.1. The basis for the compensation by CaV2.2 was explored in a subsequently study which reported that there exists two slots of differential Ca^{2+} channel preference (Cao and Tsien, 2010). In this model, two

kinds of slots exist: those with CaV2.2, which only accommodate CaV2.2, and those with a CaV2.1 preference, which *prefer* CaV2.1 but *may* accommodate CaV2.2 if CaV2.1 are limiting. This may be explained by differential binding of synaptic proteins to specific Ca^{2+} channels, a mechanism which would also allow neurons to fine-tune slot preference by regulating expression of these synaptic proteins.

1.1.4. Developmental regulation of CaV2.2

Although CaV2.2 is the prominent source of Ca^{2+} influx at many synapses in the adult animal, CaV2.1 dominates other synapses within the adult. During ontogeny, there is a switch in expression of CaV2.2 to CaV2.1 at several synapses (Iwasaki et al., 2000; Iwasaki and Takahashi, 1998; Scholz and Miller, 1995). In order to monitor the effects of these Ca^{2+} channels in synaptic release, post-synaptic responses were monitored by recording EPSCs. The Ca^{2+} channel switch was first observed in hippocampal neuronal in cultures, where it was found that EPSCs were initially more sensitive to block by ω-CTX in immature cultures (grown for 10-15 days in vitro (DIV)) but were more sensitive to block by the CaV2.1 selective toxin ω-agatoxin IVA in cells grown in culture for longer times (20-25 DIV) (Mintz et al., 1992). A similar change was observed in brainstem slices maintaining the calyx of Held synapse where ω-CTX sensitivity decreased in animals at post-natal day (PN) 7-10. Expression of CaV2.2 within the hippocampus seems to follow a similar trend with expression peaking PN10-20 and reducing by about half by PN40 (Jones et al., 1997b). Another study examining multiple types of synapses through development found that this switch was specific to certain synapses: dorsal horn and cerebral cortical synapses showed no change in ω-CTX sensitivity while thalamic, cerebellar, and brainstem auditory synapses completely lost ω-CTX sensitivity in PN20 animals (Iwasaki et al., 2000). The mechanism for why some synapses remain sensitive to ω-CTX and why some lose their sensitivity is at present unknown. Still other studies using the calyx of Held found that the slow Ca^{2+} buffering reagent EGTA displayed stronger inhibition of synaptic release in immature

synapses (PN8-12) than in mature synapses (PN16-P18) (Fedchyshyn and Wang, 2005). As EGTA has a slow onset for the binding of Ca^{2+} it prevents release that occurs spatially distant from the Ca^{2+} channel. In constract, the fast Ca^{2+} buffering reagent BAPTA inhibited release regardless of the *age* of the synapse. The fast Ca^{2+} binding kinetics of BAPTA are able to prevent Ca^{2+} mediated signaling, including neurotransmission, independent of whether the release site is near the channel. These findings lead to the deduction that mature synapses likely have their release machinery that is spatially closer or tightly associated with the Ca^{2+} channel while a portion of immature release occurs via spatially distant release machinery. In addition the efficiency of transmission correlates with increased Ca^{2+} exposure within the pre-synaptic calyx (Yang and Wang, 2006). However, despite mature synapses exhibiting a net decrease in Ca^{2+} influx into the presynaptic terminal, the Ca^{2+} that enters the terminal initiates release more effectively. Collectively, these findings suggest that changes in the coupling of $Ca2^{+}$ channels to the release machinery reflect the maturation of a synapse designed to ensure synaptic fidelity. A recent study also found that among the voltage-gated Ca^{2+} channels it appears that CaV2.2 has the largest single channel conductance (Weber et al., 2010), suggesting that CaV2.2 may be more efficient than CaV2.1 in initiating release when a larger amount of Ca^{2+} is required. The developmental regulation of CaV2.2 likely coincides with that of a protein partner – perhaps collapsin response mediator protein 2 (CRMP-2) (see §1.2) – which is also present during neurogenesis and changes with development.

1.1.5. Structure and function of CaV2.2

Voltage-gated Ca^{2+} channels are multimeric proteins (Figure 1.1) consisting of the pore forming α1 subunit as well as ancillary subunits β, α2δ, and γ (Ahlijanian et al., 1990; Catterall, 1991a; Catterall, 1991b; Catterall et al., 1989; De Jongh et al., 1989). While the α1 subunit is sufficient to form the pore of the channel and conduct current, the other subunits largely facilitate proper trafficking and localization of the α1 subunit. When the first Ca^{2+} channel α1 subunit was

fully sequenced it was found to have high homology to previously identified Na^+ channels and was hence proposed to have a similar structure (Noda et al., 1986; Noda et al., 1984; Tanabe et al., 1987). As depicted in Figure 1.1, the α1 subunit of CaV2.2 (like all voltage-gated Ca^{2+} channels) contains four domains that each have six transmembrane regions. These domains are connected via large cytosolic linker sequences. It is within these intracellular regions where the majority of protein interactions with the channel occur (Chan et al., 2007; Li et al., 2006b; Maximov et al., 1999; Sheng et al., 1994; Sheng et al., 1997; Vance et al., 1999; Yokoyama et al., 1997b). CaV2.2, the focus of this dissertation, is encoded by the α1B subunit which is made up of 2339 amino acids (although with splice variants this can vary) and contains the sequences responsible for the Ca^{2+} permeation, ω-CTX sensitive interaction site, and voltage-dependent gating (Williams et al., 1992). While the expression of α1B alone in heterologous cells is sufficient to produce Ca^{2+} current, the presence of the auxiliary subunits greatly enhances the current amplitude (Kang et al., 2001; Yasuda et al., 2004) as described in the sections below.

The Ca^{2+} channel β-subunit is a family of cytosolic proteins translated from four genes (β_{1-4}) with ~24 splice variants yielding very diverse protein products (Buraei and Yang, 2010; Dolphin, 2003a). While CaV2.2 is known to associate with several different β-subunits in native tissues (e.g. β_3 in hippocampal neurons), the complete compliment of β-subunits that are important for CaV2.2 function is not clear (Jones et al., 1997b; Ludwig et al., 1997; Scott et al., 1996). All four β-subunits do, however, interact with the α1 subunit through a conserved region (379-396) within the I-II linker (commonly referred to as the I-II loop or L1) via binding to the alpha interaction domain (AID) of the β-subunit (Pragnell et al., 1994). The N- and C-termini of α1 subunits have also been suggested to interact with β-subunits (Qin et al., 1997; Stephens et al., 2000; Walker et al., 1998; Walker et al., 1999) although this data is considered controversial. The primary function of the β-subunit appears to assist with proper folding and trafficking of the α1 subunit to the membrane (Birnbaumer et al., 1998; Brice et al., 1997; Chien et al., 1995; Dolphin, 2003a); a detailed description of the contribution of the β-subunit on trafficking will be

discussed in §1.1.8. In heterologous expression studies, the β-subunits lead to changes in biophysical properties when co-expressed with α1 subunits. Expression of all four β-subunits appears to kinetically enhance activation and cause a hyperpolarizing shift in activation (Buraei and Yang, 2010). The effects of β-subunit expression on other properties, such as inactivation, seem to vary depending on the β-subunit (Buraei and Yang, 2010).

There are four isoforms of the α2δ subunit, a subunit that is made by disulfide bonds bridging of an α2 subunit and a δ subunit, (Davies et al., 2007). Co-expression of α2δ with α1B leads to a 2-4 fold increase in current and maximum conductance (Gao et al., 2000; Kang et al., 2001; Yasuda et al., 2004). The open probability and surface expression of CaV2.2 was found to be increased (4- and 3-fold respectively) by co-expression of α2δ with α1 in *Xenopus* oocytes (Shistik et al., 1995). Subsequent studies, however, using mammalian cells observed no change in open probability (Barclay et al., 2001; Brodbeck et al., 2002). The increase in conductance without an increase in the open probability suggested a role for a2δ in trafficking of the α1 subunit; the role of α2δ in trafficking of CaV2.2 will be discussed further in section 1.1.8. In addition to trafficking, the α2δ subunit also acts to regulate channel activation and inactivation (Kang et al., 2001; Yasuda et al., 2004). Altered biophysical properties of CaV2.2 by the α2δ subunit have been reported, however; these two studies reported effects in opposite directions for both the half voltage ($V_{1/2}$) of activation and steady state inactivation. These effects on biophysical properties appear to be synergistic with expression of the β-subunit. The synergism between α2δ and β-subunits also contributes to the enhancement of current amplitude.

The γ subunit is peculiar in its function as, in contrast to the other subunits, it appears to *antagonize* the function of the α1 subunit (Kang and Campbell, 2003; Kang et al., 2001). Out of all the subunits γ has been studied the least and may have gone even less studied if not for several studies linking mutations in the γ subunit to epilepsy (Leitch et al., 2009; Letts et al., 1998; Letts et al., 2003). The observed antagonism of CaV2.2 by γ only occurs in the presence of α2δ and

reduces expression in what appears to be via an unfolded protein response (Sandoval et al., 2007a; Sandoval et al., 2007b).

1.1.6. Activation and inactivation of CaV2.2

The voltage-gated ion channel family is defined by its responses to voltage across the cell membrane leading to changes in the gating of the channel. Gating refers to mechanisms by which an ion channel regulates its conductance (ability for ions to pass through the channels' pore) and transitions from one state of conductance to another. Using a relatively simple model, Ca^{2+} channels can exist in three states: closed, open, and inactivated. The properties of each state can vary greatly amongst the Ca^{2+} channel subtypes (Carbone and Lux, 1984; Nowycky et al., 1985). The closed state is the resting state in which the voltage-gate of the pore is in a non-conducting configuration. The transition between the closed state and the conducting open state is termed activation. LVA channels are closed at polarized potentials (~ –100 mV) and activate when the membrane is depolarized to intermediate voltages (~ –50 mV). Conversely HVA channels (including CaV2.2) activate at significantly lower potentials (~ –10 mV). Activation of Ca^{2+} channels, similar to voltage-gated Na^{+} channels, relies on charged residues in the S4 transmembrane region. The S4's charged residues are conserved between Na^{+} channels and CaV2.2 suggesting that the mechanism of activation is also conserved (Catterall, 1988; Williams et al., 1992). These charged residues move in response to changes in voltage causing a conformational change of the channel, which makes the channel conduct Ca^{2+}. Collectively, these residues are responsible for Ca^{2+} channel activation and are commonly referred to as the voltage sensor. Furthermore, activation can be indirectly observed through measuring gating current, which is due to charges within the sensor moving in relation to the membrane (Adams and Gage, 1976; Jones et al., 1999; Jones et al., 1997a).

During activation, Ca^{2+} channels transition to a state that is distinct from the closed state termed the inactivated state. The inactivated channel, like the closed state, is a conformation of

the channel that is unable to conduct current. This state, however, differs from the closed state as it is unable to directly transition to an open state, but rather must first transition to a closed state and is therefore refractory. CaV2.2 preferentially undergoes closed-state inactivation, which contrasts with classical open-state inactivation (Patil et al., 1998). CaV2.2 has a U-shaped curve for inactivation as a function of prepulse voltage, which is indicative of closed-state inactivation (Cox and Dunlap, 1994; Goo et al., 2006; Jones and Marks, 1989). Principally, this mechanism of inactivation leads to more channels becoming inactivated during a train of action potentials, a stimulation that engages in repetitive opening and closing, rather than a long depolarization. In addition to voltage-dependent inactivation CaV2.2 also displays Ca^{2+} dependent inactivation (CDI). CDI involves Ca^{2+} entering through the channel and binding an intracellular partner to induce channel inactivation. This phenomenon was first observed in *Paramecium* where the replacement of Ca^{2+} with Sr^{2+} or Ba^{2+} prevented inactivation of Ca^{2+} channel current without a reduction in current amplitude (Brehm and Eckert, 1978). In studies on L-type Ca^{2+} channels, it was ter determined that CDI occurs due to binding of the Ca^{2+} binding protein calmodulin (CaM) (Peterson et al., 1999; Zuhlke et al., 1999). CaV2.2 also displays CDI via this mechanism through a conserved CaM-binding sequences in the cytosolic C-terminus (Cox and Dunlap, 1994; Liang et al., 2003). Thus CDI is an important mechanism that allows CaV2.2 to regulate its own activity and control Ca^{2+} influx (Goo et al., 2006).

1.1.7. Pharmacology of CaV2.2

The most well studied and characterized antagonist that targets CaV2.2 is ω-CTX. Its discovery occurred through purification and isolation of toxins from the mollusk *Conus geographus* (Olivera et al., 1984). Commonly known as the cone snail, this organism rapidly immobilizes its prey by injecting it with venom containing ω-CTX . The finding that ω-CTX blocked presynaptic release at the frog neuromuscular junction supported the notion that this toxin is responsible for paralyzing prey (Kerr and Yoshikami, 1984). Composed of 27 amino

acids, ω-CTX is a peptide that contains three disulfide bridges giving the peptide its functional structure (Olivera et al., 1984; Olivera et al., 1994). Binding of ω-CTX occurs within the extracellular loops of CaV2.2 DIII (1334-5) leading to pore occlusion (Ellinor et al., 1994). In addition to ω-CTX there are several other toxins that also inhibit CaV2.2 (Catterall et al., 2005). Notably, ω-conotoxin MVIIA shows selective and reversible inhibition of CaV2.2, unlike the irreversible inhibition observed by ω-CTX (Yoshikami et al., 1989). A synthetic form of MVIIA, termed Ziconotide, was developed and is currently approved as a pain therapeutic (Schmidtko et al., 2010).

The role of CaV2.2 in pain (discussed in § 1.1.9) has led to extensive drug development efforts seeking specific antagonists of CaV2.2. Through utilization of fluorescence based high through-put screening, a recent study identified an *N*-triazole oxindole, named TROX-1, which targets CaV2.2 and appears to display increased potency under depolarized conditions (Abbadie et al., 2010). This drug displayed a more preferable therapeutic window compared to Ziconotide although a subsequent study found it to not be specific for CaV2.2 as it inhibited other CaV2 channels with similar potencies (Swensen et al., 2012). Several other chemical structures (e.g. piperidines, aliphatic monoamines) have been identified that inhibit CaV2.2, but there are currently no non-peptide specific inhibitors of CaV2.2 (Catterall et al., 2005; Hu et al., 1999a; Hu et al., 1999b; Hu et al., 2000; Lukyanetz et al., 2002).

1.1.8. Trafficking of CaV2.2

While the ability of CaV2.2 to function as a Ca^{2+}-conducting protein is vital to its function, the ability of Ca^{2+} influx via CaV2.2 in inducing synaptic release is reliant on proper channel localization and targeting (Simms and Zamponi, 2012). CaV2.2 must be translated from α1B mRNA, be post-translationally modified, co-assemble with α2δ, and β-subunits to form a functional channel complex that must then be trafficked to pre-synaptic active zones to facilitate coupling of CaV2.2 to neurotransmitter release. As such, trafficking of CaV2.2 may directly

impart its function as a regulator of synaptic release. As previously discussed, the accesory subunits, such as β and α2δ, aid in trafficking of CaV2.2, but there are also additional protein interactions required for localizing the channel to the active zone that are unique to CaV2 channels that will be discussed below.

The relative amount of surface expressed CaV2.2 is determined by the sum of forward trafficking and stability of channels once in the membrane. Forward trafficking of CaV2.2 requires export from the ER and transportation through the Golgi network to the surface (Simms and Zamponi, 2012; Waithe et al., 2011). Studies with CaV2.1 constructs reported that the interaction between the β-subunit and I-II loop of the Ca^{2+} channel masks an ER retention signal (aa415-90) leading to channels being exported from the ER ((Bichet et al., 2000). It was subsequently observed that the I-II loop of CaV2.2 had a similar level of retention (Cornet et al., 2002). More recent studies have not supported this conclusion, however, and rather suggest that the proximal portion of the C-terminus of CaV2.2 (1749-96) has a retention sequence (Altier et al., 2011; Waithe et al., 2011).

Recent elegant studies from the Dolphin and Zamponi groups have further delineated the mechanism whereby the β-subunit enhances total channel expression, namely by reducing proteasomal degradation of Ca^{2+} channels. While investigating the discrepancies between ER retention of CaV1.2 and CaV2.1 Ca^{2+} channels, it was observed that co-expression of the β_{1b} subunit greatly enhanced total channel expression (Altier et al., 2011). Investigations into how this may happen led to the intriguing discovery that the β_{1b} subunit reduces ubiquitination and subsequent degradation of L-type channels. Another study verified these findings for CaV2.2, leading to the conclusion that β-subunits prevent proteasomal degradation of other Ca^{2+} channels as well (Waithe et al., 2011).

In addition to the β-subunit, the α2δ subunit has also been implicated in CaV2.2 trafficking. Trafficking of the α1 subunits by α2δ has been observed in mammalian cells where mutations in α2δ greatly reduce surface expression of α1 subunits (Barclay et al., 2001; Canti et

al., 2005). However, in contrast to the forward trafficking bestowed by β-subunits upon Ca^{2+} channels, it appears that the α2δ subunit increases the amount of undegraded channels recycled back to the membrane during endosomal sorting (Tran-Van-Minh and Dolphin, 2010). Perhaps the most interesting aspect regarding the role of α2δ in CaV2.2 trafficking is the evidence supporting it as the target for the drugs Gabapentin (Neurontin) and Pregabalin (Lyrica) (Bauer et al., 2009; Belliotti et al., 2005; Field et al., 2006; Hendrich et al., 2008; Joshi and Taylor, 2006). Gabapentin and pregabalin are medications commonly prescribed for the treatment of epilepsy and neuropathic pain. The proposed mechanism for these drugs is to target α2δ and disrupt its ability to enhance surface expression of CaV2.2. This mechanism is further supported by the finding that only chronic (several days), but not acute, application of pregabalin or gabapentin reduces Ca^{2+} channel current density (Heblich et al., 2008; Hendrich et al., 2008; Vega-Hernandez and Felix, 2002). The α2δ subunit has been shown to be upregulated in models of neuropathic pain (Bauer et al., 2009; Field et al., 2000; Li et al., 2006a; Nguyen et al., 2009). The upregulation of α2δ leads to enhanced Ca^{2+} channel regulated synaptic transmission due to an enhancement in surface expression of Ca^{2+} channels. Presumably, this increase in transmission is what is targeted by gabapentin and pregabalin leading to a reduction in pain.

Consistent with its role in synaptic transmission, CaV2.2 is targeted to synaptic terminals in neurons (Westenbroek et al., 1992; Westenbroek et al., 1998). Maximov and Bexprozvanny specifically investigated synaptic targeting of the CaV2 family of channels, as these channels are known to mediate synaptic transmission (Maximov et al., 1999; Wheeler et al., 1994; Wu et al., 1998). They discovered that the synaptic-specific trafficking of CaV2.2 appears to be regulated by several binding sites within its C-terminus (Maximov and Bezprozvanny, 2002; Maximov et al., 1999). Specifically, there are PDZ (post synaptic density protein (PSD-95), *Drosophila* disc large tumor suppressor (Dlg1), zonula occludens-1 protein (zo-1)) and Src homology 3 (SH3) binding domains in the C-terminus which are responsible for binding to scaffolding proteins that aid in synaptic localization. PDZ domains are present in signaling molecules that commonly link

the PDZ containing protein to a transmembrane protein (Romero et al., 2011). The SH3 domain is found in many signaling molecules that interact with SH3 binding proteins to activate various cascades (Kaneko et al., 2008). The adaptor protein munc18 interacting protein 1 (Mint-1) contains a PDZ domain which binds to the last four amino acids in CaV2.2 (i.e. DHWC), while the SH3 domain in the adaptor protein Ca^{2+} activated serine kinase (CASK) binds to CaV2.2 through a SH3 binding domain in the medial C-terminus. Deletions of either the DHWC or the SH3 binding domain of CaV2.2 dramatically reduced localization of CaV2.2 with the synaptic marker synapsin, suggesting interactions with CASK and Mint-1 are vital for synaptic targeting of CaV2.2 (Maximov and Bezprozvanny, 2002). Trafficking of CaV2.2 through CASK also appears to be dynamically regulated through phosphorylation of CASK by cyclin dependent kinase 5 (Cdk5) (Samuels et al., 2007b). Namely phosphorylation of CASK by Cdk5 allows CASK to bind to CaV2.2 and facilitate an increase in channel surface expression. In a recent study, it was also shown that Cdk5 can directly phosphorylate CaV2.2 and lead to enhanced surface expression (Su et al., 2012). Mutation of potential Cdk5 sites in CaV2.2 was able to prevent this increase in surface expression. The regulation of CaV2.2 by Cdk5 has important implications for my thesis studies described in Chapter 3, which investigates the potential role of Cdk5-mediated phosphorylation of CRMP-2 as it relates to CaV2.2 interaction and function.

In addition to the C-terminus, the synaptic protein interaction (*synprint*) region (718-963) within the II-III loop also assists in synaptic targeting (Szabo et al., 2006). The *synprint* region is so named as it is responsible for binding to several synaptic proteins, the most well characterized being syntaxin (Leveque et al., 1994; Sheng et al., 1996; Sheng et al., 1994). The *synprint* region is specific to CaV2.2 and CaV2.1 channels. Splice variants of CaV2.2 lacking portions of the *synprint* region (Δ756-1139 and Δ737-1001) reduce synaptic localization, further supporting that these interactions are critical for synaptic localization of CaV2.2 (Szabo et al., 2006). In addition to being necessary, the *synprint* sequence appears to be sufficent for synaptic targeting as transplanting the CaV2.1 *synprint* region into L-type channels localizes them ectopically to

synapses (Mochida et al., 2003). Summarizing then, it it appears that synaptic targeting of CaV2.2 is achieved by interactions with proteins with the II-III loop and the C-terminus regions of the channel itself.

Once CaV2.2 reaches the membrane, it can be internalized and degraded or internalized and recycled back to the membrane. Recent work has shown that the closely related CaV2.1 is recycled via a ras associated in brain 11(Rab11)-dependent endocytic sorting mechanism (Tran-Van-Minh and Dolphin, 2010). This finding is likely true for CaV2.2 as well as this recycling pathway relies on interaction with the conserved Ca^{2+} channel subunit α2δ. Labeling of a heterlogous cell line expressing α1B/α2δ/β1b with radioactive ω-CTX found that ~55% of the channels were internalized in 24 hours (Bernstein and Jones, 2007). A similar time scale for internalization was previously observed using the same approach in hippocampal rat membranes (Jones et al., 1997b). These studies suggest that the lifetime of a channel on the membrane is likely on the order of a few days. This is consistent with results from siRNA knockdown experiments in animals and sensory neurons in culture which demonstrated efficient knockdown 3 days after siRNA treatments (Altier et al., 2007). CaV2.2 surface expression can also be rapidily decreased (> 50% in 30 min) following G-protein coupled receptor (GPCR) activation (Altier et al., 2006; Kisilevsky et al., 2008; Kisilevsky and Zamponi, 2008a). CaV2.2 is co-internalized along with the GPCR following application of dopamine or nociceptin, which activate dopamine 1/2 and nociceptin receptors respectively, through a direct interaction between CaV2.2 and the GPCR (Altier et al., 2006).

1.1.9. The CaV2.2 interactome

Synaptic transmission requires a diverse complement of proteins to facilitate the proper localization of pre-synaptic Ca^{2+} channels within proximity of vesicle fusion proteins. The formation of an almost autonomous pre-synaptic release site complex containing CaV2.2 along with scaffolding, endocytotic, vesicle fusion, and cell-cell adhesion proteins has been

demonstrated (Khanna et al., 2007a; Khanna et al., 2007b; Weiss and Zamponi, 2012). Key in this CaV2.2-containing release site complex are Soluble NSF Attachment REceptor (SNARE) proteins that facilitate vesicular fusion of neurotransmitter-containing vesicles following calcium influx via CaV2.2.

The first biochemical interaction implicating specific proteins in the formation of a pre-synaptic release complex was observed between CaV2.2 and synaptotagmin (Leveque et al., 1992). Synaptotagmin is a Ca^{2+} binding protein that is localized to synaptic vesicles and has been implicated as *the* Ca^{2+} sensor for synaptic release (Chapman, 2008; Matthew et al., 1981; Perin et al., 1990). The interaction between CaV2.2 and synaptotagmin supported the proposed hypothesis that pre-synaptic Ca^{2+} channels link to synaptic vesicles. Biochemical purification of synaptic vesicles found that CaV2.2 formed a complex with both synaptotagmin and syntaxin, suggesting association of CaV2.2 with both vesicle delimited and membrane-associated SNARE proteins, respectively (Leveque et al., 1994). Later studies, however, found that CaV2.2 was unable to directly bind syntaxin and synaptotagmin concomitantly as they competed for binding (Sheng et al., 1997). Syntaxin and synaptotagmin were determined to bind to the *synprint* region of CaV2.2 (Sheng et al., 1994; Sheng et al., 1997). Subsequently, it was found that the SNARE SNAP-25 also interacts with CaV2.2 in the *synprint* region (Sheng et al., 1996). Adding a level of complexity to this protein complex, it was discovered that binding of synaptic proteins to CaV2.2 is dynamically regulated by protein kinase C (PKC) and Ca^{2+} calmodulin activated kinase II (CaMKII) where phosphorylation of the *synprint* region by these kinases inhibits binding of syntaxin and SNAP-25 (Yokoyama et al., 1997b). Furthermore, both syntaxin and SNAP-25 show bi-phasic Ca^{2+} dependent interactions with the *synprint* such that maximal binding is observed at ~10-30 μM Ca^{2+} and little binding is observed below 5 or above 35 μM Ca^{2+} (Sheng et al., 1996). That the binding between SNAREs and CaV2.2 displays a Ca^{2+} dependence may provide an activity-dependent mechanism to allow for rearrangement of the pre-synaptic complex. Importantly, introduction of exogenous *synprint* peptides inhibited neurotransmitter

release supporting the notion that coupling of synaptic proteins to CaV2.2 at the *synprint* region is required for neurotransmitter release (Mochida et al., 1996). The synprint peptide also reduced the coupling of Ca^{2+} influx to neurotransmitter release suggesting it reduces the spatial localization of vesicles within the mouth of CaV2.2 (Rettig et al., 1997).

Both syntaxin and SNAP-25 regulate biophysical properties of CaV2.2 (Bezprozvanny et al., 1995; Mochida et al., 1995; Wiser et al., 1996). Expression of syntaxin leads to inhibition of CaV2.2 current amplitude, likely due to a hyperpolarizing shift in steady state inactivation. This effect can be reversed by introduction of a *synprint* peptide or by co-expression with CaV2.2 binding target-SNAREs SNAP-25 or Munc18-1 (Chan et al., 2007; Jarvis and Zamponi, 2001). It has been suggested that the relief of syntaxin-mediated inhibition of CaV2.2 by co-expression of other t-SNAREs may be a mechanism for cells to inhibit channels which are not in a complete pre-synaptic complex (Zamponi, 2003). The syntaxin-mediated inhibition of CaV2.2 can also be reversed using strong depolarizing prepulses (Jarvis et al., 2000; Jarvis and Zamponi, 2001).

As synaptic transmission is the basis of communication between neurons, it is not surprising that neurons have developed rapid and efficient mechanisms to regulate transmission. Perhaps the most-well characterized example relating to pre-synaptic Ca^{2+} channels is GPCR-mediated inhibition of CaV2.2 (De Waard et al., 2005; Tedford and Zamponi, 2006). GPCR-mediated inhibition occurs through many different GPCRs as approximately 20 GPCR ligands have been found to induce CaV2.2 inhibition (Dolphin, 2003b; Tedford and Zamponi, 2006). GPCR-mediated inhibition of CaV2.2 is responsible in part for the analgesic efficacy of opioids such as morphine (Rhim and Miller, 1994; Scott et al., 2002). Sympathetic neurotransmitter release through CaV2.2 is inhibited by adrenergic GPCRs among others (Beech et al., 1992; Boehm and Huck, 1996; Zhu and Ikeda, 1994). Mechanistically GPCRs regulate CaV2.2 through direct interaction of G-proteins (G_{α} and $G_{\beta\gamma}$) with several cytosolic regions within CaV2.2 (De Waard et al., 2005; Tedford and Zamponi, 2006). For example, G_{α} interacts with the C-terminus of CaV2.2 whereas $G_{\beta\gamma}$ interacts with the I-II loop and C-terminus of CaV2.2 (Zamponi et al.,

1997). G protein modulation of CaV2.2 is plastic as CaV2.2 splice variants have been identified that can alter GPCR-induced inhibition (Andrade et al., 2010; Raingo et al., 2007).

Studies in the Khanna laboratory (Khanna et al., 2007c) as well as in others (Muller et al., 2010) point to an incredible diversity in the CaV2.2 proteome. To illustrate the diverse nature of these interactions, I next highlight only a limited set of these interactors, focusing on those with a functional impact on CaV2.2:

(i) 14-3-3: 14-3-3 proteins (seven isoforms β, γ, ε, ζ, η, σ, and τ/θ) were originally identified in brain by Moore and Perez in 1967 and are so named due to the method in which they were purified (Carlson et al., 1968). These proteins are very abundant in the brain (~1% of soluble protein) and although they interact with a multitude of proteins (~100), their functions are poorly understood (Berg et al., 2003; Takahashi, 2003). Several 14-3-3 isoforms (ε, η, γ, β, and ζ) are present in synapses suggesting they may interact with synaptic proteins (Martin et al., 1994). This led to the discovery that the C-terminus of CaV2.2 (2121-39) binds to 14-3-3 proteins and that 14-3-3 expression can modulate channel function (Li et al., 2006b). Overexpression of 14-3-3 proteins (β, γ, ε, ζ, and τ/θ) led to slowed inactivation and a depolarizing shift in the voltage-dependence of inactivation culminating in decreased CaV2.2 inactivation. A short follow up study also found that 14-3-3 protein self-dimerization is not required for decreasing CaV2.2 inactivation (Li et al., 2007b). Collectively these two studies have shown 14-3-3 to be an important CaV2.2 regulatory protein that likely aids in proper synaptic function.

(ii) RIM: Rab3a interacting molecule (RIM), is a large protein with many synaptic interactions that have suggested it functions as a scaffolding protein to assist with neurotransmission (Calakos et al., 2004; Wang et al., 1997). In this context, RIM1 was initially observed to interact with CaV2.2 via its synprint region (Coppola et al., 2001). However, there is some controversary as to whether RIM1 and CaV2.2 are present in the same biochemical complex as neither immunohistological nor immunoprecipitations approaches demonstrated co-

localization or interaction of RIM1 with CaV2.2 in the chick ciliary ganglion calyx pre-synaptic terminal (Khanna et al., 2006a; Wong and Stanley, 2010). In support of the latter findings, it was reported the interaction between RIM1 and Ca^{2+} channel was via the β-, not the α- subunits for the CaV2.1 complex (Kiyonaka et al., 2007). Consistent with the involvement of the β-subunit in the interaction, expression of RIM1 led to an ~30-60 mV depolarizing shift (depending on the β-subunit expressed) in the $V_{1/2}$ of inactivation (Kiyonaka et al., 2007; Weiss et al., 2011). Despite the controversy, RIM1 appears to modulate GPCR signaling-mediated inhibition of CaV2.2 as well as enhancing recovery from inhibition (Weiss et al., 2011).

(iii) Munc18: Munc18-1, also referred to as nSec1, was classically identified as a syntaxin binding protein (Hata et al., 1993). Munc18-1 has subsequently been identified as an important player in vesicle priming, docking, and fusion (Deak et al., 2009; Gerber et al., 2008; Voets et al., 2001; Zilly et al., 2006). Munc18-1 was further linked to the pre-synaptic release complex through observations that Munc18-1 interacts directly with CaV2.2 (Chan et al., 2007). It appears that Munc18-1 expression is not limiting, as overexpression does not alter CaV2.2's properties, but siRNA knockdown of Munc18-1 causes a ~10 mV hyperpolarizing shift in steady-state inactivation (Chan et al., 2007). Collectively, these results suggested that Munc18-1 plays a minimal role in CaV2.2 activity but rather may function as a scaffold to link other synaptic proteins to CaV2.2.

In Table 1.1, I summarize the currently known interactome of CaV2.2. To qualify as a CaV2.2-interacting protein, the protein must meet one of the following criteria: (i) biochemical interaction as demonstrated by protein pull downs or immunoprecipitations, or (ii) a functional effect on CaV2.2 function. This section has introduced the CaV2.2 interactome as a web of protein interactions that can regulate synaptic release through modulation of CaV2.2. In addition these proteins identify many possible targets for CaV2.2-related pathology. In Chapter 3 of my thesis, I introduce CRMP-2 as a novel interactor of CaV2.2 and modulator of CaV2.2 activity and relate it to previously identified interactions.

Table 1.1 CaV2.2 interacting proteins

CaV2.2 interaction partner	Validated Biochemical Interaction	Site of Interaction (CaV2.2)	Site of Interaction (CaV2.2)	Reference(s)
14-3-3	Y	C-terminus (2121-2139)	Interaction leads to slowed channel inactivation	(Khanna et al., 2007c; Li et al., 2007b; Li et al., 2006b)
Actin	Y	ND	Interaction with MAP1A LC2 links to CaV2.2 stabilizing it in the synapse	(Khanna et al., 2007b; Khanna et al., 2007c; Leenders et al., 2008)
Adaptin	N	ND	Associates with endocytotic channel complex	(Khanna et al., 2007b; Khanna et al., 2007c; Muller et al., 2010)
AP180	Y	ND	Associates with endocytotic channel complex	(Khanna et al., 2007c)
β_{1-4}	Y	I-II loop (378-396) & C-terminus	Interaction retards proteasomal degradation of CaV2.2, enhances surface expression, modulates biophysical properties	(De Waard et al., 1994; Pragnell et al., 1994)
Clathrin HC-1	Y	ND	Associates with endocytotic channel complex	(Khanna et al., 2007b; Khanna et al., 2007c; Muller et al., 2010)
CaM	Y	C-terminus (1788-1868)	Binds to C-terminus of CaV2.2 to induce CDI	(Liang et al., 2003)
CaMKII	N	ND	Phosphorylates synprint region of CaV2.2 reducing synaptic protein binding	(Yokoyama et al., 1997a)
CASK	Y	C-terminus (2039-2194)	Interaction with CaV2.2 aids in synaptic targeting of the channel	(Khanna et al., 2006b; Maximov and Bezprozvanny, 2002; Maximov et al., 1999)
Catenin α/β	Y	ND	Associates with endocytotic channel complex	(Khanna et al., 2007b; Li et al., 2006b; Maximov et al., 1999)
Cdk5	N	ND	Phosphorylation of CaV2.2 C-terminus leads to enhanced surface expression, current density, and transmitter release	(Su et al., 2012)

CaV2.2 interaction partner	Validated Biochemical Interaction	Site of Interaction (CaV2.2)	Site of Interaction (CaV2.2)	Reference(s)
CSP	Y	Synprint (718-963)	Interaction of CSP along with G-proteins leads to tonic inhibition of CaV2.2	(Magga et al., 2000; Miller et al., 2003a; Miller et al., 2003b)
Dopamine 1/2 receptors	Y	II-III loop and C-terminus	D1/2 receptors display GPCR-mediated inhibition of CaV2.2, but also regulate CaV2.2 surface expression which is reduced upon receptor activation	(Kisilevsky et al., 2008; Kisilevsky and Zamponi, 2008a)
Dynamin	Y	ND	Associates with endocytotic channel complex	(Khanna et al., 2007a; Khanna et al., 2007b; Khanna et al., 2007c; Muller et al., 2010)
ENH	Y	C-terminus	Forms complex with CaV2.2 and PKCε which enhances PKC mediated potentiation of CaV2.2	(Maeno-Hikichi et al., 2003)
G-protein α	Y	C-terminus	Leads to inhibition of CaV2.2 following GPCR activation and subsequent disassembly of trimeric G protein complex	(Furukawa et al., 1998; Simen et al., 2001)
G-protein βγ	Y	I-II loop and C-terminus	Couples GPCR activation to inhibition of CaV2.2 through direct interaction with CaV2.2	(Herlitze et al., 1997; Jones et al., 1997a; Zamponi et al., 1997)
Huntingtin	Y	Synprint	Competes with syntaxin for binding of CaV2.2	(Swayne et al., 2005)
Intersectin	Y	ND	Associates with pre-synaptic CaV2.2 complex	(Khanna et al., 2007b)
MAP 1A/B	Y	C-terminus (2046-2069)	Interacts with CaV2.2 and assists with trafficking and synaptic localization of CaV2.2	(Khanna et al., 2007c; Leenders et al., 2008; Muller et al., 2010)
Mint-1	Y	C-terminus (2336-2339)	Interaction with CaV2.2. aids in synaptic targeting of CaV2.2	(Maximov et al., 1999)
Munc18-1	Y	I-I and II-III loop	Associates with pre-synaptic release complex, knockdown by siRNA leads to a 10mV hyperpolarizing shift in CaV2.2 inactivation	(Chan et al., 2007)

CaV2.2 interaction partner	Validated Biochemical Interaction	Site of Interaction (CaV2.2)	Site of Interaction (CaV2.2)	Reference(s)
NSF	Y	ND	Associates with pre-synaptic release complex	(Khanna et al., 2007a; Khanna et al., 2007c)
ORL1	Y	C-terminus	ORL1 receptor mediates GPCR inhibition of CaV2.2 as well as agonist induced internalization of CaV2.2	(Altier et al., 2006; Beedle et al., 2004)
PKC	Y (PKCε)	C-terminus (PKCε)	Phosphorylates synprint region of CaV2.2 reducing synaptic protein binding, formation of complex with ENH and CaV2.2 allows for enhanced potentiation of CaV2.2 by PKC	(Maeno-Hikichi et al., 2003; Yokoyama et al., 1997b)
PP2Cα	Y	C-terminus	Interacts and dephosphorylates CaV2.2 at synprint site reversing PKC mediated potentiation	(Li et al., 2005)
REM	Y	β-subunt	Co-expression of REM with CaV2.2 α1 and β-subunits leads to tonic inhibition of CaV2.2 currents	(Chen et al., 2005; Finlin et al., 2003; Finlin et al., 2005; Flynn et al., 2008)
RGS12	Y	Synprint	Interacts with synprint phospho-tyrosine likely leading to enhanced G protein modulation of CaV2.2	(Richman et al., 2005; Richman and verse-Pierluissi, 2004)
RIM 1	Y*	Synprint/ β-subunit	Co-expression induce depolarizing shift in CaV2.2 inactivation, also enhances recovery from G-protein inhibition	(Coppola et al., 2001; Kiyonaka et al., 2007; Weiss et al., 2011; Wong and Stanley, 2010)
SNAP-25	Y	Synprint	Associates with CaV2.2 in pre-synaptic release complex	(Sheng et al., 1996; Vance et al., 1999; Wiser et al., 1996; Yokoyama et al., 1997b)
Spectrin-α/β	Y	ND	Associates CaV2.2 with submembrane matrix	(Khanna et al., 2007a; Khanna et al., 2007b; Khanna et al., 2007c)
Synaptobrevin/VAMP	Y	Synprint	Associates with CaV2.2 in pre-synaptic release complex	(el et al., 1995; Khanna et al., 2007a; Sheng et al., 1996)

CaV2.2 interaction partner	Validated Biochemical Interaction	Site of Interaction (CaV2.2)	Site of Interaction (CaV2.2)	Reference(s)
Synaptotagmin	Y	Synprint	Associates with pre-synaptic release complex	(Leveque et al., 1994; Sheng et al., 1997)
Syntaxin	Y	Synprint	Assists with association of synaptic vesicle to CaV2.2 complex, expression leads to tonic inhibition of CaV2.2	(Leveque et al., 1994; Sheng et al., 1994)
TCTEX-1	Y	C-terminus (2090-2164)	Disrupting interaction between CaV2.2 and TCTEX-1 reduces CaV2.2 surface expression	(Lai et al., 2005)
Tubulin	Y	ND	Associates with CaV2.2-cytoskeletal complex	(Li et al., 2006b; Maximov et al., 1999)
Ubiquitin	Y	I-II loop	Ubiquitination of CaV2.2 targets it for proteosomal degradation	(Marangoudakis et al., 2012; Waithe et al., 2011)

AP180, assembly protein 180; CaMKII, Ca^{2+} Calmodulin dependent kinase II; CASK, Ca^{2+} Calmodulin activated serine kinase; Cdk5, Cyclin-dependent kinase 5; CSP, Cysteine string protein; ENH, enigma homolog; microtubule associated protein 1 A/B, MAP1A/B; Munc18 interacting protein 1, Mint1; mammalian uncoordinated 18, Munc18-1; NSF, N-ethylmaleimide-sensitive factor; ORL1, opioid receptor like receptor 1; PKC, protein kinase C; PP2C, protein phosphatase 2 C, REM, Rad and Gem-like GTP-binding protein 1; RGS12, regulator of G protein signaling 12; RIM-1, Rab3a interacting molecule 1; SNAP-25, synaptosomal associated protein 25; TCTEX-1, t-complex testis-expressed 1; VAMP-2, Vesicle-associated membrane protein 2.

*: Biochemical interaction is controversial (Wong and Stanley, 2010)

1.1.10. CaV2.2 and pain

The role of CaV2.2 in pathology and physiology has been gleaned from the use of antagonists and knockout animals. In this section, I focus specifically on CaV2.2 in pain as pain represents a serious medical problem where targeting of CaV2.2 appears to have been successful in the development of novel therapeutics. Following discovery of CaV2.2-specific conotoxins, the biological role of this channel could be observed in animals through the use of thesis specific inhibitors. Specific interest in the role of CaV2.2 in sensation arose from the observation that ω-CTX was able to block transmitter release from sensory neurons and spinal nerve terminals (Gruner and Silva, 1994; Maggi et al., 1990a; Maggi et al., 1990b; Santicioli et al., 1992). The role of CaV2.2 in sensory neuron transmitter release and pain sensation is also supported by studies showing that analgesic opioids and adrenergic agonists inhibit CaV2.2 (Bean, 1989; Schroeder et al., 1991). Furthermore, inhibition of spinal CaV2.2 leads to a marked decrease in tactile hypersensitivity due to peripheral nerve injury and nociceptive behavior in response to formalin (Chaplan et al., 1994; Malmberg and Yaksh, 1994). The delivery of CaV2.2 blocking conopeptides requires direct application to the spinal synapse between sensory neurons and spinal neurons. This method of delivery is accomplished by intrathecal injection of the peptides into the cerebrospinal space. That intrathecal application is required and sufficient for analgesia also supports the notion that presynaptic blockade of CaV2.2 is responsible for targeting pain. More recently, the development of α1B knockout mice has allowed further validation of CaV2.2's role in pain. Several independent α1B knockout mice have been made with each mouse showing reductions in pain responses (Hatakeyama et al., 2001; Kim et al., 2001; Saegusa et al., 2001). Interestingly several CNS effects were also observed in the mice including; decreased anxiety behavior, changes in vigilance, and enhanced aggressive behavior (Beuckmann et al., 2003; Kim et al., 2009; Saegusa et al., 2001). Unlike the peripheral effects on pain, little is known about the role of CaV2.2 in the CNS, although patients treated with the CaV2.2 blocker Ziconotide have a long list of side effects that include dizziness, anxiety, and memory impairment (Rauck et al.,

2009; Schmidtko et al., 2010; Webster et al., 2009). In Chapter 3 of my thesis I will discuss the targeting of the CRMP-2-CaV2.2 interaction as a novel pain treatment without some of the deleterious side effects present with Ziconotide treatment. In the following section I will introduce CRMP-2 as a prelude to my studies investigating the functional and biochemical interactions between CRMP-2 and CaV2.2.

1.2. CRMP-2

1.2.1. Identification of CRMP-2

CRMP-2 was discovered as the linchpin for chicken semaphorin-3A (Sema3A) activated growth cone collapse in sensory neurons. At the time of its discovery it was named CRMP-62 due to its observed molecular weight of 62 kDa (Goshima et al., 1995). While this study was the first to link CRMP-2 to Sema3A signaling, other groups also identified CRMP-2 analogues in several additional species. In a proteomic study aimed at identifying genes responsible for rat mammalian cortical development, CRMP-2 was identified as being upregulated following neurogenesis (Geschwind and Hockfield, 1989). This led these researchers to name the protein turned on after development 64 (TOAD-64), based upon its observed molecular weight being ~64 kDa (Minturn et al., 1995a; Minturn et al., 1995b). While this identification appears to be the first CRMP-2 analogue in mammals, an earlier study identified the nematode analogue in *Caenorhabditis elegans* (*C. elegans*). This occurred during a screen of random mutations in nematodes that led to animals with uncoordinated movements. Analysis of these animals for alterations in axonal structure showed that mutations in the CRMP-2 analogue uncoordinated protein 33 (*Unc*-33) displayed what appeared to be axon guidance malfunction (Hedgecock et al., 1985). In mice, CRMP-2, named *Unc*-33 like phosphoprotein (Ulip) by the discovering group, was found to be upregulated during development and phosphorylated in response to nerve growth factor (NGF) and retinoic acid (Byk et al., 1996; Gaetano et al., 1997). This study was important as it linked the CRMP-2 family of proteins to regulation by growth factors in addition to repulsive

cues such as Sema3A. Finally, another group identified a CRMP-2 analogue in humans through its homology with a liver enzyme dihydropyrimidinase (Hamajima et al., 1996). Probing of the genome has led to identification of a total of five CRMP proteins designated CRMPs 1-5 (Fukada et al., 2000; Wang and Strittmatter, 1996). In an attempt to unify the various naming schemes of CRMP family the TUC (TOAD/Ulip/CRMP) nomenclature was proposed, although few subsequent publications have adopted this nomenclature (Quinn et al., 2003). CRMP-2 is the best studied and understood member of the CRMP family. CRMP-2 exists as two isoforms which arise from alternative splicing occurring in the N-terminus (Quinn et al., 2003). The majority of studies regarding CRMP-2 have focused on the short isoform, sometimes referred to as CRMP-2A or CRMP-2S. The long isoform (CRMP-2B or CRMP-2L) is identical from residues 1-572 with an additional 112 amino acids located on the N-terminus. In this thesis, I will refer to CRMP-2A as CRMP-2, unless otherwise specified. As will be described throughout this introduction, the main function – known prior to this dissertation – of CRMP-2 appears to be aiding in proper formation of neuritic processes leading to synaptic connectivity.

1.2.2. Structure of CRMP-2

CRMP-2 forms both homo- and heterotetramers with other members of the CRMP family (Wang and Strittmatter, 1997). The long (684 amino acids) and short (572 amino acids) forms of CRMP-2 have also been shown to interact suggesting they form tetramers together (Yoneda et al., 2012). This tetrameric structure is similar to the closely related dihydropyrimidinase, although it is important to note that unlike dihydropyrimidinases, CRMP-2 lacks the required residues for enzymatic activity (Holm and Sander, 1997; Wang and Strittmatter, 1997). The structure of CRMP-2 was not solved until 2006, ~10 years following its discovery although the structure of the closely related CRMP-1 was reported earlier (Deo et al., 2004; Stenmark et al., 2007). The crystallization of CRMP-1 revealed a “bilobed lung shaped” configuration that was hypothesized to be shared amongst the CRMP family based upon sequence homology. This hypothesis was

A

B

Figure 1.2 Crystal structure of CRMP-2

(**A**) Crystal structure of tetrameric CRMP-2 at 1.90 Å (Majava et al., 2008). Tetrameric CRMP-2 (14-490) was crystalized in the presence of Mg^{2+}. Each momomer is colored differently for clarity. (**B**) CRMP-2 monomer from same crystal structure as depicted in (**A**). Yellow sequences represents C-terminal region of CRMP-2 (484-490), this will be discussed in detail in Chapter 3.10.

substantiated when the structure of a C-terminally-truncated (missing aa 491-572 to allow for crystallization) version of CRMP-2 was elucidated several years later and found to have the same general shape (Figure 1.2) (Stenmark et al., 2007). The majority of CRMP-2 is packed within this structure although the residues 491-572 are predicted to be unstable and are not included in the structure. Crystallization of CRMP-2 required the presence of a divalent metal (such as Ca^{2+} or Mg^{2+}). This requirement is most likely due to tetramerization of CRMP-2 induced by these metal ions (Majava et al., 2008; Stenmark et al., 2007). Despite early work on CRMP-2 and its tetrameric structure, little is known as to how the tetrameric structure relates to the function of CRMP-2, although one study observed that calmodulin bound nearly exclusively to the monomeric form of CRMP-2 (Zhang et al., 2009). At present, it is not known if any other proteins bind preferentially to one form or the other. It is usually assumed, however, that as CRMP-2 was crystallized as a tetramer and was found as a tetramer when isolated from brain, that a tetramer is the most likely native configuration.

1.2.3. Expression and developmental regulation of CRMP-2

Regulation of axon growth and neuronal polarity support CRMP-2 as an important protein in neuronal development (Arimura et al., 2004; Inagaki et al., 2001; Nishimura et al., 2003; Yoshimura et al., 2005). Furthermore, it appears that CRMP-2 could be a potential marker of neuronal differentiation as neuronal cell lines and primary cells increase their expression of CRMP-2 following differentiation (Byk et al., 1996; Gaetano et al., 1997; Minturn et al., 1995a). This increase following differentiation is also consistent with CRMP-2's role in axonogenesis. Initial studies of CRMP-2 observed wide spread expression of CRMP-2 in neuronal tissues such as brain, retinal ganglia, enteric nerves, spinal cord, and dorsal root ganglia (Goshima et al., 1995; Inagaki et al., 2000; Minturn et al., 1995a). Expression in the chicken brain peaks around embryonic day 7 although there is still substantial expression in the adult animal. CRMP-2 expression in the rat and mouse brains is upregulated slightly later with the peak occurring within

a few days of birth (Byk et al., 1998; Minturn et al., 1995a). While the other CRMPs have similar expression profiles during development, they show minimal expression in the adult compared to CRMP-2 which still has substantial expression (Wang and Strittmatter, 1996). These findings together paint a picture of CRMP-2 protein expression turning on during neurogenesis and staying on, perhaps to assist in plasticity.

CRMP-2 is also expressed in non-neuronal cells within the nervous system such as oligodendrocytes (Fernandez-Gamba et al., 2012; Ricard et al., 2000). Oligodendrocytes are responsible for wrapping neurons in the central nervous system with myelin; this sheath of myelin is imperative for fast nerve impulse conduction (Baumann and Pham-Dinh, 2001). The function of CRMP-2 in oligodendrocytes is unclear although it appears to regulate process retraction in response to Sema3A or the oxidative agent 3-nitropropionic acid (Fernandez-Gamba et al., 2012; Ricard et al., 2000). Despite initial studies that reported minimal expression of CRMP-2 outside of the nervous system, several recent papers have highlighted expression of CRMP-2 in non-neuronal cells (Vincent et al., 2005; Vuaillat et al., 2008; Yoneda et al., 2012). A study found that CRMP-2 is expressed in fibroblasts and regulates proliferation and possibly tumorigenesis (Tahimic et al., 2006). CRMP-2 was also identified as being specifically secreted by colon cancer cell lines and has been proposed as a biomarker (Wu et al., 2008). Outside of the nervous system, CRMP-2 has been most heavily investigated in T-cells were its expression correlates with activation and migration (Varrin-Doyer et al., 2012; Varrin-Doyer et al., 2009; Vincent et al., 2005; Vuaillat et al., 2008). These studies show CRMP-2 expression in a non-neuronal cell that is proliferating rapidly (i.e. an activated T-cell). A very recent study also found ubiquitous expression of CRMP-2 in a multitude of non-neuronal cell lines, further supporting the notion that CRMP-2 is expressed outside of the nervous system (Yoneda et al., 2012).

As mentioned previously, CRMP-2 expression appears to be highest during neurogenesis which is consistent with its role in axon guidance and outgrowth. It is still unclear; however, as to *what* signals are responsible for upregulation of CRMP-2 expression during this time period.

A chromatin-immunoprecipitation screen for targets of the SMAD (a portmanteau of mothers against decapentaplegic (MAD) and small body size (SMA)) family of transcription factors) identified CRMP-2 as a protein whose expression could be regulated by SMAD (Fei et al., 2010). SMAD factors are activated by extracellular bone morphogenetic proteins (BMPs) that are vital cues for proper neuronal differentiation and migration (LaBonne and Bronner-Fraser, 1999). This finding was foreshadowed by a prior report that suggested BMP4 regulates CRMP-2 expression in *Xenopus* (Kamata et al., 1998). Consistent with the role of BMPs in neuronal migration and neurite outgrowth (Guan and Rao, 2003), it was found that CRMP-2 expression is down regulated by BMP exposure which is expected to cause reduced migration and neuritic outgrowth of neurons (Fei et al., 2010). This down regulation is likely due to repression of transcription by the binding of SMAD1 and 4 to the CRMP-2 promoter. This study also found that knockdown of CRMP-2 *in utero* leads to deficiencies in neuronal migration and neurite outgrowth. Conversely, several years earlier it was demonstrated that application of glia-derived growth factor (GDNF) to a neuronal cell line enhances expression of CRMP-2 (Kodama et al., 2004). The exact mechanism(s) leading to the increase in CRMP-2 expression are currently unknown, although GDNF is responsible for differentiation of many different neuronal cell populations (Enomoto, 2005), suggesting CRMP-2 is a common factor in determining neuronal fate.

1.2.4. CRMP-2 signaling

Despite knowing for over 15 years that CRMP-2 is an obligatory signaling molecule in Sema3A-induced growth cone collapse, the exact function served by CRMP-2 in this process remains poorly characterized. Treatment of the neuronal PC12 cell line with nerve growth factor (NGF) leads to a substantial reduction in CRMP-2 phosphorylation (Byk et al., 1996). This finding is interesting as NGF induces neuronal differentiation along with neuritic process growth in PC12 cells suggesting that dephosphorylation of CRMP-2 may be a positive effector of axon outgrowth. Pre-treatment of neurons with neurotrophins, including NGF, also attenuates

Sema3A-induced growth cone collapse (Tuttle and O'Leary, 1998). These findings laid the foundation for subsequent exploration of the role of CRMP-2 phosphorylation in axonal growth.

Sema3A binds to and activates the neuropilin-1/plexin-A receptor complex, which transduces Sema3A binding into intracellular signaling culminating with growth cone collapse (Sasaki et al., 2002; Takahashi et al., 1999). Exploration of the signaling pathways involved in Sema3A-induced growth cone collapsed identified the *Src* family kinase Fyn as an obligatory signaling protein (Sasaki et al., 2002). Following binding of Sema3A to its receptor, Fyn kinase binds to the intracellular portion of the receptor complex and activates cyclin dependent kinase 5 (Cdk5). In addition to activating Cdk5, Fyn also phosphorylates CRMP-2 at Tyr-32 following application of Sema3A and a Y32F CRMP-2 mutant greatly reduces Sema3A-induced collapse (Uchida et al., 2009). Cdk5 was subsequently found to phosphorylate CRMP-2 *in vitro* at Ser-522 (Brown et al., 2004). The phosphorylation of CRMP-2 by Cdk5 is vital for Sema3A-induced collapse as expression of a phospho-null mutant (S522A) shows reduced growth cone collapse in DRG cultures. A previous report found that in addition to Cdk5 and Fyn, Sema3A-induced collapse also relied on activity of glycogen synthase kinase 3 (GSK3β) in the growth cone (Eickholt et al., 2002). Consistent with this finding, GSK3β is able to phosphorylate CRMP-2 at Thr-509, Thr-514, and Ser-518 (Brown et al., 2004; Cole et al., 2004; Yoshimura et al., 2005). The phosphorylation of CRMP-2 by GSK3β is prevented by inhibition of Cdk5 or a phospho-null mutation of the Cdk5 site, implicating Cdk5 in a 'priming' role for subsequent phosphorylation by GSK3β. Furthermore, Sema3A application requires phosphorylation of CRMP-2 by GSK3β to induce growth cone collapse (Uchida et al., 2005). Collectively, Sema3A-induced signaling requires activation and phosphorylation of CRMP-2 by three distinct kinases (Cdk5, Fyn, and GSK3β) encompassing a total of 5 phosphorylation sites. In addition to Cdk5, Fyn, and GSK3β, it has been shown that the Src kinases Fes and Fer are also able to phosphorylate CRMP-2 (Mitsui et al., 2002; Shapovalova et al., 2007). Similar to Fyn, CRMP-2 is phosphorylated by Fes

at Tyr-32 (Uchida et al., 2009). The exact site of phosphorylation and role of Fer phosphorylation of CRMP-2 in growth cone collapse is at present unknown.

Lysophosphatidic acid (LPA) also signals through CRMP-2 for growth cone collapse although the pathway is distinct from that of Sema3A (Arimura et al., 2000; Arimura et al., 2005). Interestingly, while Sema3A relies on multiple phosphorylation events, growth cone collapse in response to LPA requires phosphorylation of only Thr-555 by ras homolog (Rho) associated protein kinase 1 (ROCK I). Also of interest is that its original identification in Sema3A signaling found that CRMP-2 was required for Sema3A induced inward current, but had no effect on LPA-induced current (Goshima et al., 1995). This finding is consistent with Sema3A and LPA working to induce growth cone collapse through diverse pathways. Though both pathways induce growth cone collapse, a divergence in intermediary signaling likely leads to the downstream current observed in response to LPA only. A recent report identified isoform specific interactions between CRMP-2 and ROCKs (Yoneda et al., 2012). Despite previous evidence describing phosphorylation of CRMP-2 by ROCK I (Arimura et al., 2000), it was found that CRMP-2 (both short and long forms) binds to ROCK II but not ROCK I. Furthermore, while both forms bind ROCK II only CRMP-2L inhibits ROCK II-dependent cell migration, suggesting that CRMP-2L has a unique ROCK II interaction site not present in CRMP-2S. Notably, despite several studies showing how kinases can modulate CRMP-2, this is the first study suggesting that CRMP-2 *regulates* kinase activity.

Perhaps the most diverse signaling cascade that CRMP-2 has been found to take part in occurs in T-cells rather than neurons. Through a handful of studies it has become clear that in addition to regulating axon outgrowth, CRMP-2 regulates migration of T-cells (Varrin-Doyer et al., 2012; Varrin-Doyer et al., 2009; Vincent et al., 2005; Vuaillat et al., 2008). The chemo-attractive molecule chemokine C-X-C ligand 12 (CXCL12) induces phosphorylation of CRMP-2 which facilitates migration of T-cells. This finding is a solitary example of phosphorylation as a

positive regulator of CRMP-2 function. A tabular representation of known CRMP-2 phosphorylation sites are shown in Table 1.2.

As phosphorylation of CRMP-2 leads to axon retraction, it is not surprising that dephosphorylation of CRMP-2 (e.g. by phosphatases) leads to enhanced neuritic growth (Astle et al., 2011; Zhu et al., 2010). Protein phosphatase 1 (PP1) dephosphorylates CRMP-2 at the GSK3β sites Thr509/514 (Cole et al., 2008). PP1 seems to work specifically on these sites as the Cdk5 site Ser-522 is resistant to phosphatase activity. Interestingly, NGF treatment leads to activation of Cdk5 which in turn phosphorylates and activates PP1, which despite activating Cdk5 has a net increase in axon outgrowth (Li et al., 2007a). Under these conditions CRMP-2 would be $p522^{+}$ and $p509^{-}/p514^{-}$, which appears to still lead to enhancement of axon growth. This finding reaffirms the assertion that phosphorylation at Ser-522 is functionally significant as a priming kinase for subsequent phosphorylation by GSK3β. In addition to PP1, protein phosphatase 2 A (PP2A) is able to dephosphorylate CRMP-2 at GSK3β sites, resulting in the formation of new axons (Zhu et al., 2010). Collectively, there appears to be an inverse correlation between CRMP-2's phosphorylation state, not considering Tyr-479 which appears to downregulate GSK3β phosphorylation (Varrin-Doyer et al., 2009), and axonogenesis/axon outgrowth. Phosphorylation of CRMP-2 likely regulates axon growth via effects on interactions between CRMP-2 and proteins involved in cytoskeletal rearrangements (for example, see §1.2.6 on tubulin).

1.2.5. CRMP-2: protein interactions

CRMP-2 interacts with a litany of proteins that have diverse functions. Given that CRMP-2 regulates axonogenesis and outgrowth, processes which rely heavily on cytoskeletal proteins (Baas, 1997; Bradke and Dotti, 1999; Bradke and Dotti, 2000; Joshi and Baas, 1993), it is not surprising that the first protein found to bind CRMP-2 was the cytoskeleton protein tubulin (Fukata et al., 2002). CRMP-2's interaction with tubulin has been extensively studied and will be

discussed in §1.2.6. In addition to tubulin, CRMP-2 binds to the cytoskeletal proteins actin and vimentin (Arimura et al., 2005; Vincent et al., 2005). The observed interactions with cytoskeletal proteins support the role of CRMP-2 in regulating axon growth through aiding in cytoskeletal rearrangements. As an extension to interacting with actin, CRMP-2 binds to the actin related complex of Sra-1/WAVE that is an obligatory component of CRMP-2's ability to enhance axon length and axonogenesis (Kawano et al., 2005). CRMP-2 also binds to Numb and α-adaptin and likely facilitates endocytosis through these interactions (Nishimura et al., 2003). CRMP-2 has also been described as a regulator of protein trafficking through interactions with motor proteins. Namely, a biochemical complex containing tubulin and kinesin light chain 1 (KLC1) allows CRMP-2 to transport tubulin to the growing axon (Kimura et al., 2005). The residues of CRMP-2 required for KLC1 binding (aa 440-572) are also required for distal axonal accumulation of CRMP-2, although it is unknown if this interaction is the sole reason for this observation. A complex containing CRMP-2 is also responsible for promoting anterograde transport of tyrosine related kinase B (TrkB) receptors (Arimura et al., 2009b). This complex includes the motor protein dynein along with the adaptor proteins synaptotagmin-like protein 1 and Ras-related in brain 27 (Rab27) which along with CRMP-2 forms a complex linking TrkB to dynein (Arimura et al., 2009a). The sites of interaction of CRMP-2 with dynein (aa 100-150 and aa 348-440) are distinct from those found to bind KLC1.

To serve as a trafficking protein a protein must interact with both motor proteins and endocytotic adapter proteins to facilitate trafficking of membrane proteins from the membrane to a different subcellular compartment. CRMP-2 fits this role through its interactions with the endocytotic vesicle complex microtubule associated monoxygenase, calponin and LIM domain containing -like 1 (MICAL-L1) and the motor protein dynein thereby facilitating retrograde transport of vesicles bound to MICAL-L1 (Rahajeng et al., 2010). While the majority of CRMP-2's characterized interactions make a clear link to its role in axon outgrowth, several other interactions hint at more diverse function. For instance, CRMP-2 interacts in a Ca^{2+}-dependen

Table 1.2. CRMP-2 interacting proteins

CRMP-2 interaction partner	Validation: biochemical	Validation: functional	Effect of interaction	Reference(s)
Abl	N	N	ND	(Varrin-Doyer et al., 2009)
Actin	Y	Y	CRMP-2 regulates actin dynamics	(Arimura et al., 2000; Arimura et al., 2005; Yoneda et al., 2012)
α-actinin	N	N	ND	(Hensley et al., 2010)
AP-2	Y	Y	Binding reduces endocytosis	(Nishimura et al., 2003)
sAPP	Y	N	ND	(Pawlik et al., 2007)
BLK	N	N	ND	(Varrin-Doyer et al., 2009)
CaM	Y	Y	Binding prevents CRMP-2 proteolysis and enhances process growth	(Zhang et al., 2009)
α2-chimaerin	Y	Y	Binding decreases axon growth and neuronal migration	(Brown et al., 2004; Ip et al., 2012)
CLN6	Y	Y	Mutations in CLN6 lead to reduced CRMP-2 expression	(Benedict et al., 2009)
CRMP1	Y	Y	Over-expression of CRMP1 and CRMP-2 opposes the effects of RhoA on neurite retraction	(Leung et al., 2002)
CRMP-5	Y	Y	CRMP-5 may block Sema3A-mediated growth cone collapse by inhibition of CRMP-2 function; CRMP-5 acts a dominant negative in preventing neurite outgrowth promotion induced by CRMP-2	(Brot et al., 2010)
Intersectin	N	N	ND	(Varrin-Doyer et al., 2009)

CRMP-2 interaction partner	Validation: biochemical	Validation: functional	Effect of interaction	Reference(s)
Kinesin-1	Y	Y	Binding regulates Kinesin by linking it to cargo	(Kawano et al., 2005; Kimura et al., 2005)
MICAL-L1	Y	Y	Links to intracellular Dynein motors	(Rahajeng et al., 2010)
MBP	N	N	ND	(Hensley et al., 2010)
NFL/NFM	Y	N	ND	(Hensley et al., 2010)
Neurofibromin	Y	Y	Changes in Neurofibromin expression alters CRMP-2 phosphorylation	(Patrakitkomjorn et al., 2008)
Neuropilin 1	Y	Y	Couples Sema3A to CRMP-2 signaling	(Brown et al., 2004; Deo et al., 2004)
Numb$^{\#}$	Y	Y	Binding regulates endocytosis	(Arimura et al., 2005; Nishimura et al., 2003)
NMDARs	Y	Y	CRMP-2 expression regulates surface expression of NR2B subunit	(Al-Hallaq et al., 2007; Bretin et al., 2006)
PIPP	Y	Y	Binding reduces neurite growth	(Astle et al., 2011)
PI3Kβ	N	N	ND	(Zhang et al., 2009)
PLCγ	N	N	ND	(Varrin-Doyer et al., 2009)
PLD_2	Y	Y	Binding inhibits PLD_2 activity	(Lee et al., 2002)
Plexin-1	Y	Y	Couples Sema3A to CRMP-2 signaling	(Deo et al., 2004)
PP2A	Y	Y	Dephosphorylation of CRMP-2 enhances axon growth	(Zhu et al., 2010)
ROCK II	Y	Y	CRMP-2 prevents ROCK II from aiding in cell migration	(Yoneda et al., 2012)

CRMP-2 interaction partner	Validation: biochemical	Validation: functional	Effect of interaction	Reference(s)
Slp1	Y	Y	Links TrkB to CRMP-2 for TrkB trafficking	(Arimura et al., 2009b)
α- and/or β-Spectrin	N	N	ND	(Hensley et al., 2010)
Sra1	Y	Y	CRMP-2 links Sra1/WAVE complex to kinesin for trafficking	(Kawano et al., 2005)
Tau	Y	N	ND	(Takata et al., 2009)
Thioredoxin	Y	Y	Binding induces CRMP-2 phosphorylation causing growth cone collapse	(Morinaka et al., 2011)
TrkB	Y	Y	Links TrkB to Kinesin for anterograde trafficking	(Arimura et al., 2009b)
α-/β-Tubulin[#]	Y	Y	Binding enhances microtubule formation, in addition CRMP-2 regulates tubulin GTPase activity	(Chae et al., 2009; Fukata et al., 2002; Kimura et al., 2005)
VAV1	N	N	ND	(Varrin-Doyer et al., 2009)
Vimentin	Y	Y	CRMP-2 phosphorylation at Tyr-479 alters vimentin mobilization	(Varrin-Doyer et al., 2009; Vincent et al., 2005)
WAVE1	Y	Y	CRMP-2 links Sra1/WAVE complex to kinesin for trafficking	(Kawano et al., 2005)

Abl, Abelson tyrosine kinase; AP2, Adaptor-related protein 2; sAPP, Amyloid precursor protein secreted form (sAPP) RERMS (328–332) neurotrophic domain; CaM, Calmodulin; CaV2.2, N-type voltage-gated calcium channel; aIN, alpha internexin intermediate filament protein, MICAL1, Molecule interacting with CasL; MBP, myelin basic protein; NFL/NFM, Neurofilament Light chain/Neurofilament middle chain; neurotrophin receptor tyrosine kinase; NMDARs, N-methyl-D-Aspartate receptors PI3Kβ, Phosphoinositide-3-kinase β; PIPP, Proline-rich Inositol Polyphosphate 5-Phosphatase; PP2A, Protein phosphatase 2A; TrkB, neurotrophin receptor tyrosine kinase; VAV1, Vav proto-oncogen; WAVE1, Wiskott–Aldrich syndrome protein family verprolin-homologous protein-1.

[#]*Interaction is decreased following phosphorylation of CRMP-2 by Cdk5/GSK3β/ROCK*

ND: not determined

fashion with the Ca^{2+}-binding protein Calmodulin (CaM) (Zhang et al., 2009). While it is well known that CaM is an important protein in Ca^{2+} signaling, it is unknown whether its interaction with CRMP-2 aids in this signaling. Also although this study did observe changes in cell process length in response to CaM inhibition, their results did not assess if the interaction was responsible for this effect. A comprehensive list of the many other proteins CRMP-2 has been found to interact with biochemically and functionally appears in Table 1.2.2. Proteins which were observed in proteomic studies, but have not been verified by *in vitro* binding are included although they are marked as not having a verified biochemical interaction.

1.2.6. Interaction and modulation of tubulin by CRMP-2

It is fitting that the first characterized protein-protein interaction of CRMP-2 also appears to be one of its most functionally relevant and important interactions. While it was known from the initial discovery of CRMP-2 that it functions to regulate axon growth dynamics, the identified interaction and modulation of tubulin by CRMP-2 revealed its aptitude for cytoskeletal rearrangement. The first hint that CRMP-2 may regulate cytoskeleton as a means to modulating axon growth was through an observation in *C. elegans*. A massive increase in the amount of microtubules was observed in animals with mutations in the *Unc-33* sequence, representing the first reported link between the CRMP family of proteins and microtubule regulation (Hedgecock et al., 1985). A study in 2000 further hinted that CRMP-2 may regulate microtubules (Gu and Ihara, 2000) although it was not until 2002 that a detailed study exclusively looked at this interaction (Fukata et al., 2002). CRMP-2 was found to bind to both α- & β-tubulin in a screen using a CRMP-2 affinity column (Fukata et al., 2002). This appears to not be a CRMP-2–specific interaction, however, as CRMPs -1, -3, and -4 also bound tubulin. Interestingly, the well-known tubulin binding proteins Tau, MAP-1B, and 2 were not found to interact with CRMP-2.

CRMP-2 leads to enhanced tubulin polymerization likely through binding tubulin heterodimers preferentially over longer chain polymerized tubulin. Although both the long and

short splice variants of CRMP-2S/L interact with tubulin, it appears that only CRMP-2S enhances axon outgrowth, whereas CRMP-2L antagonizes this function of CRMP-2S – although this phenomenon has yet to be replicated (Yuasa-Kawada et al., 2003). The CRMP-2 residues responsible for polymerization of tubulin were localized to amino acids 323-381. The exact function of this sequence remains unclear, as a more recent study observed that residues 480-510 of CRMP-2 regulate tubulin polymerization as well (Chae et al., 2009). These latter residues enhance tubulin's GTPase activity, which is an important determinant in polymerization, while the previously reported residues (323-381) had a minimal effect on GTPase activity. In addition to the GTPase enhancer sequence (480-510), it was also found that an inhibitory domain (150-299) antagonizes the activity of the former sequence. Collectively, these studies suggest that CRMP-2 has a complex interaction with tubulin that is regulated by at least three different sequences. Further supporting that the interaction between tubulin and CRMP-2 is important for neuritic growth, phosphorylation of CRMP-2 by either Cdk5 or ROCK leads to reduced binding to tubulin (Arimura et al., 2005; Uchida et al., 2005).

1.2.7. CRMP-2 phosphorylation and function

As it relates to CRMP-2, the term "activity" usually refers to its ability to enhance axon outgrowth. Since phosphorylation of CRMP-2 is a negative determinant of axon growth, phosphorylated CRMP-2 is commonly referred to as inactive while the native unphosphorylated form is considered active. The activity of CRMP-2 likely depends on the biochemical interactions engaged by these two CRMP-2 states. Interestingly, phosphorylation at Thr-555 by ROCK (following LPA application) phenocopies (i.e. displays a similar phenotype) phosphorylation at Ser-509/Thr-514/Thr-518/Ser-522 by Cdk5/GSK3β (following Sema3A application) as it relates to axon growth and collapse. The only observed biochemical reason for these observations currently is that phosphorylation by either the LPA or Sema3A pathway both lead to maintenance of CRMP-2's interaction with actin while simultaneously disrupting the

interactions with tubulin and Numb (Arimura et al., 2005). While CRMP-2 has many biochemical partners, the effect that phosphorylation has on these interactions is currently limited to those mentioned above.

As there has yet to be a published report of a CRMP-2 knockout mouse, the whole animal effects of CRMP-2 are unknown. The role of CRMP-2 in both the LPA and Sema3A growth cone collapse pathway links CRMP-2 to rapid alteration of the cytoskeleton. CRMP-2 also regulates slow more subtle processes in the regulation of neuronal growth. Over expression of CRMP-2 enhances the length of axons and leads to more axons per neuron (Inagaki et al., 2001). Conversely, knockdown of CRMP-2 using siRNA reduces axon outgrowth (Nishimura et al., 2003; Yoshimura et al., 2005). If these findings are grossly oversimplified and applied to a whole animal, the projected outcome would likely involve neuronal connection deficiencies likely resulting is devastating phenotype. A recent study was published where a transgenic mouse was generated in which CRMP-2 was phospho-insensitive at Ser-522 (Yamashita et al., 2012). In theory this mouse should be completely insensitive to Sema3A-induced growth cone collapse and is therefore predicted to display deficiencies in proper axon targeting. This study also characterized the offspring from CRMP-2 522A and CRMP-1 knockout mouse (Su et al., 2007) to minimize possible effects of redundancy. Surprisingly, the animals appeared to have no gross neuronal abnormality or cortical structure aberrations. The only reported atypical finding in these mice was extreme curling of their cortical basal dendrites. This finding phenocopies the $Cdk5^{-/-}$ mice that also showed basal dendrite abnormalities, which was not unexpected as Cdk5 is the primary kinase responsible for phosphorylating Ser-522 of CRMP-2 (Ohshima et al., 2007). A caveat to this CRMP-2 transgenic animal is that the animal should likely show positive increases in axon growth rather than deficiencies and therefore a phospho-mimetic (S522D) or a knockout will likely result in more interesting results. Furthermore, this study suggests that having an always active CRMP-2 does not lead to any deficiencies.

1.2.8. CRMP-2 and neurological diseases

The interest in CRMP-2 grew rapidly following the turn of the century likely due to several studies linking it to neurological disease. The most prominent finding was that CRMP-2 is present in neurofibrillary tangles (NFTs) – a histological hallmark of Alzheimer's disease (AD) (Yoshida et al., 1998). AD patients suffer from cognitive decline that is correlated with increasing neuronal death due to a still highly controversial mechanism. The two pathological hallmarks of AD are the presence of extracellular β-amyloid plaques and intracellular NFTs (Hardy and Selkoe, 2002). Given the importance of NFTs in AD, many studies have further investigated the link between CRMP-2 and AD. Similar to tau that is hyperphosphorylated in NFTs, CRMP-2 present in NFTs was also found to be heavily phosphorylated (Gu et al., 2000). The phosphorylation of CRMP-2 appears to occur early on during the pathogenesis of AD (Cole et al., 2007). The CRMP-2 phosphorylation sites present in NFTs were subsequently found to be the same sites as those involved in Sema3A signaling. In addition, the NFTs were found to contain an enriched complex composed of other components of the Sema3A signaling pathway including Sema3A itself and its receptor dimer (Good et al., 2004). CRMP-2 has also been implicated in β-amyloid processing and plagues, the other hallmark of AD pathology. Incubation of a neuronal cell line with β-amyloid led to an increase in Thr-555 phosphorylation through upregulating ROCK activity (Petratos et al., 2008). Phosphorylation at the GSK3β and Cdk5 sites of CRMP-2 were also significantly increased in animals overexpressing the intracellular domain of β-amyloid precursor protein (Ryan and Pimplikar, 2005). CRMP-2 expression is also down regulated in AD which might phenocopy the effect of phosphorylated CRMP-2 as both have negative effects on axon outgrowth (Lubec et al., 1999).

CRMP-2 has also been linked to recurring seizures with studies reporting a decrease in full length CRMP-2 in epilepsy patients and animal models (Czech et al., 2004; Ryu et al., 2008). Interestingly, the anti-epilepsy medication lacosamide appears to bind to CRMP-2 leading to an as yet undetermined outcome on CRMP-2 function (Beyreuther et al., 2007; Park et al., 2009).

The link between CRMP-2 and neurofibromatosis type 1 (NF1) has also been made as CRMP-2 interacts with neurofibromin (Lin and Hsueh, 2008; Patrakitkomjorn et al., 2008). Mutations in the NF1 gene lead to subsequent truncation of the protein product neurofibromin, where loss of this protein's function leads to NF1. Similar to AD, alteration in phosphorylation of CRMP-2 was observed when neurofibromin protein levels were decreased. Despite the findings linking CRMP-2 to these diseases it is poorly understood whether CRMP-2 contributes to the pathology or if these alterations simply occur as a result of the pathology.

1.2.9. CRMP-2 and neurotrauma

Neurotrauma is a broad term referring to a nerve injury or injury to the nervous system. This encompasses both local injuries such as nerve lesions as well as insults to the CNS such as spinal cord injury and cerebral ischemia. In general (plasticity not withstanding) axons grow during neurogenesis and insult-induced regeneration. While the role of CRMP-2 in axon guidance during development is well characterized, CRMP-2 has also been implicated in injury-induced regeneration. Crushing of the sciatic nerve leads to peripheral axotomy and subsequent axonal regeneration (McQuarrie et al., 1977). One of the first studies on CRMP-2 sought to identify the possible involvement of CRMP-2 in axonal regeneration given the initial findings of its regulation of axon outgrowth in *c. elegans* (Minturn et al., 1995a). This hypothesis was confirmed when CRMP-2 was found to be upregulated in motor neurons of the ventral horn following sciatic nerve crush. Similar results were also observed using a hypoglossal nerve injury model in rats, where it was found that CRMP-2 was upregulated following injury (Suzuki et al., 2003). Interestingly, somewhat opposing results were found in regenerating chicken spinal cord, where CRMP-2 expression was minimally altered, but had an increase in phosphorylation (Gogel et al., 2010).

CRMP-2 was first implicated in CNS neurotrauma by appearance of an atypical molecular weight isoform of CRMP-2 in rat brain tissue following middle carotid artery-

occlusion (MCAO) (Chung et al., 2005). Expression of CRMP-2 was also found to be up-regulated following focal cerebral ischemia (Chen et al., 2007a). The atypical isoform of CRMP-2 was later found to be due to cleavage of CRMP-2 by the protease calpain leading to the observed shift of full length CRMP-2 from 62kD to ~55kD (Bretin et al., 2006; Hou et al., 2009; Jiang et al., 2007; Touma et al., 2007; Zhang et al., 2009; Zhang et al., 2007). Calpain is a Ca^{2+}-activated protease that has been linked to neurotoxic signaling (Vosler et al., 2008). Cleavage of CRMP-2 by calpain has been observed following ischemia (Jiang et al., 2007), neurotrauma (Zhang et al., 2007), excitotoxicity (Bretin et al., 2006), as well as nerve growth factor deprivation induced-neurite degeneration (Touma et al., 2007). The cleavage of CRMP-2 by calpain occurs through activation of N-methyl-D-aspartate receptors (NMDARs) (Bretin et al., 2006). The role of NMDARs in neurotrauma will be explored extensively later (§1.3). Cleavage is not specific to CRMP-2, however, as CRMPs 1, 3, 4, 5 also appear to be cleaved by calpain following neurotoxic insult (Hou et al., 2006; Jiang et al., 2007; Zhang et al., 2007). Despite their high sequence identity, CRMP-1, -2, -4 are cleaved at a distinct location (C-terminus) compared to CRMP-3 (N-terminus) (Jiang et al., 2007; Liu et al., 2009). Interestingly, expression of the calpain cleavage product of CRMP-2 is neuroprotective while the cleavage product of CRMP-3 is neurotoxic (Hou et al., 2006). While it is unknown what affect acute cleavage of CRMP-2 by calpain has on neuronal survival, expression of a CRMP-2 construct mimicking calpain cleavage increases neuronal survival following excitotoxic challenge (Bretin et al., 2006). The proposed mechanism for the neuroprotection conferred by expression of truncated CRMP-2 is reduced surface expression of NR2B containing NMDARs. By reducing surface expression of NMDARs, the number of neurons exposed to toxic Ca^{2+} influx through NMDARs was reduced. The likely mechanism for this neuroprotection is CRMP-2 regulates NMDAR surface expression through a biochemical interaction, which is supported by data showing a biochemical interaction between NMDARs and CRMP-2 (Al-Hallaq et al., 2007). Al-Hallaq and colleagues found that CRMP-2 interacts biochemically with both NR2A and 2B subunits of NMDARs.

Despite the extensive studies linking CRMP-2 phosphorylation to its signaling and role in growth cone collapse, there have been relatively few studies suggesting its phosphorylation in neurotrauma. Using cortical neurons stimulated with glutamate (to mimic conditions of excitotoxicity), it was shown that phosphorylation of CRMP-2 at Thr-555 is upregulated following stimulation (Hou et al., 2009). Notably, this phosphorylation was not due to ROCK, which is known to phosphorylate this site, but rather due to CaMKII. It appears that phosphorylation Thr555 is not important for extent of injury, however, as a T555A mutant showed no neuroprotection. Inhibition of CaMKII enhanced calpain cleavage of CRMP-2. A more recent study found that hypoxic-ischemic brain injury decreased phosphorylation of CRMP-2 at Thr-514 over a 72 hr period following insult (Xiong et al., 2012). The exact ramifications of the changes in Thr-514 phosphorylation and their role in neuronal survival are unclear. Collectively, despite several reports linking CRMP-2 to neuronal survival, little is known about how CRMP-2 functions in neurons that are exposed to glutamate. The only clear functional link is the observation that CRMP-2 is able to modulate NMDARs surface expression, suggesting an interaction between CRMP-2 and NMDAR may be important for neuronal death following neurotrauma. In Chapter 4, I will describe my findings targeting CRMP-2 in NMDAR-mediated glutamate toxicity through the use of a CRMP-2 peptide. In the following section of my dissertation, I will introduce the NMDAR and NMDAR-associated signaling involved in glutamate-mediated toxicity.

1.3. NMDAR introduction

At the time I began my dissertation research, there appeared two reports that seemed to tie CRMP-2 to potential regulation and activity of post-synaptic NMDARs. As these proteins also allow Ca^{2+} influx, albeit on the post-synaptic side of the synapse, I was interested in determining whether this was indeed the case and with the tools that I had developed while studying CRMP-2 mediated regulation of CaV2.2 (see Chapter 3), I wanted to address signaling between the CRMP-2-NMDAR complex (Chapter 4).

1.3.1. Structure and function of NMDARs

Composed of four subunits, the NMDAR is a non-selective, ligand-gated ion channel that is activated by glutamate (Figure 1.3) (Dingledine et al., 1999; Kohr, 2006). NMDARs belong to a family of three classes of ligand-gated ion channels that respond to glutamate; NMDARs, 2-amino-3-(3-hydroxy-5-methylisox-azol-4-yl) propionate receptors (AMPARs), and kainate receptors. These receptors families can be isolated pharmacologically with specific agonists (e.g. NMDA or AMPA) as well as by specific antagonists (described in §1.3.2.). While much controversy surrounds the subunit stoichiometry of NMDARs (Kohr, 2006), they are largely believed to be composed of two NMDAR subtype 1 (NR1) and two NR2 subunits, each with four transmembrane segments (Ishii et al., 1993; Moriyoshi et al., 1991). To date, a single NR1 subunit and four NR2 subunits (NR2A-D) have been identified (Dingledine et al., 1999). These four subunits multimerize to form the functional pore that allows passage of Na^{+}, K^{+} , and Ca^{2+} in response to engagement of extracellular ligand binding sites (Dingledine et al., 1999) (Figure 1.3.1). The rest of this section of the Introduction will focus on the NR2B subunit as this 1484 amino acid long protein is the predominant NMDAR expressed in hippocampal and cortical neurons during the stages of cultures examined in my experiments (see Chapter 4). NMDARs require both glutamate and the co-agonist glycine or D-serine to be activated (Johnson and Ascher, 1987; Kleckner and Dingledine, 1988). The binding site for glycine is contained within

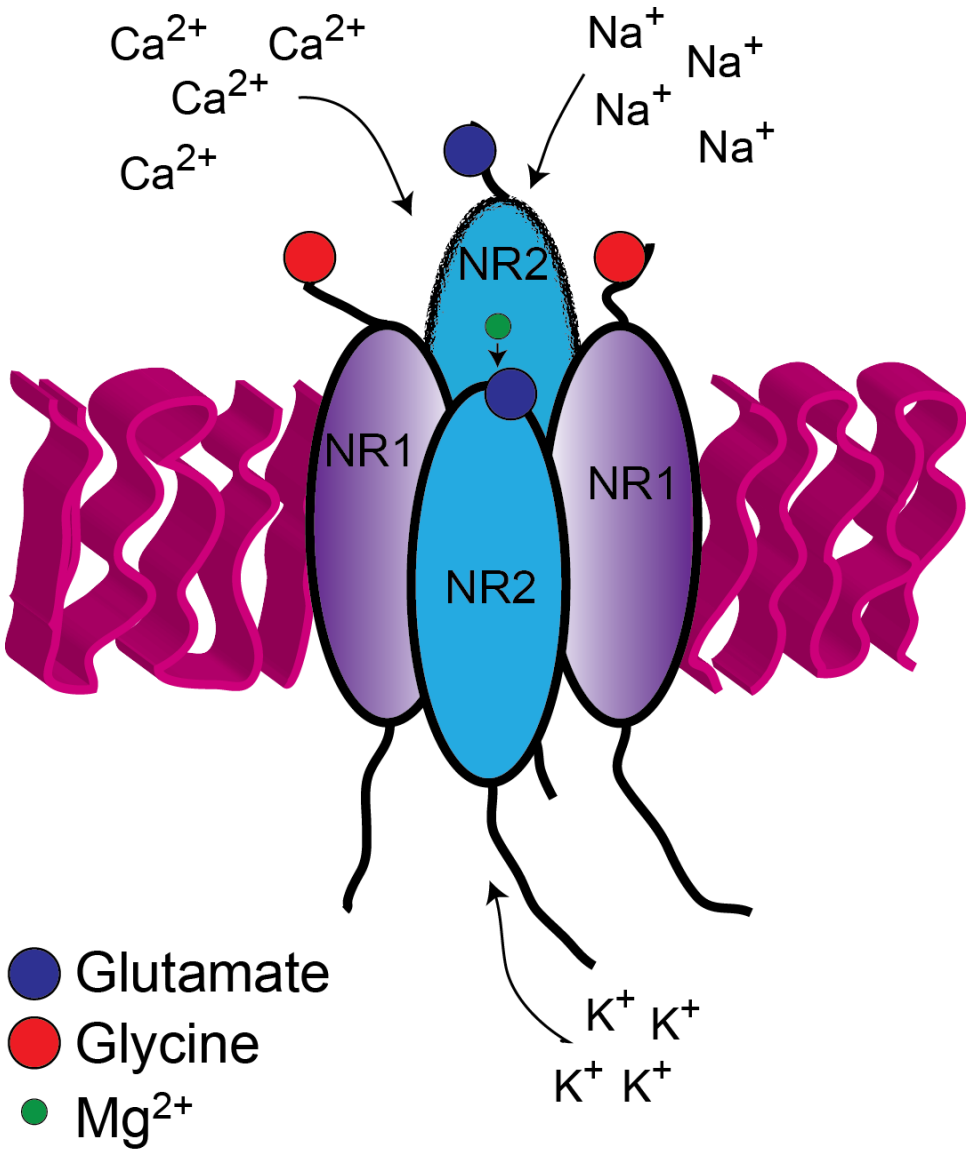

Figure 1.3 NMDARs: subunit composition and stoichiometry

The NMDAR is a tetramer composed of two NR1 and two NR2 subunits. These subunits have extracellular N-termini which are responsible for ligand binding and intracellular C-termini responsible for forming biochemical complexes. Also depicted in the schematic is pore-occlusion by Mg^{2+} under resting conditions and cation permeability assuming normal extra/intracellular cation concentrations.

the extracellular portion of NR1 (amino acids 390, 392, and 466) (Kuryatov et al., 1994), while the glutamate site is present on the NR2 subunit (amino acids 387, 486, 493, and 488) (Laube et al., 1997).

1.3.2. NMDAR agonists and antagonists

There are several inhibitors of NMDARs that have been developed for use in the research laboratory as well as for possible therapeutic potential. Consistent with its function as a glutamate receptor, NMDARs are endogenously activated by L-glutamate and L-aspartate (Dingledine et al., 1999). They are additionally activated by NMDA, which does not activate other ionotropic glutamate receptors. Conversely, NMDARs are endogenously blocked at resting membrane potentials by Mg^{2+} (Nowak et al., 1984). Interestingly, the tonic block by Mg^{2+} confers voltage-gated properties upon the NMDARs wherein a strong depolarization is required to dislodge Mg^{2+} and allow other cations to travel through the channel pore. While several NMDAR inhibitors have been developed, (+)-5-methyl-10,11-dihydro-5H-dibenzo[a,d] cyclohepten-5,10-imine maleate (MK-801) and D-(-)-2-Amino-5-phosphonopentanoic acid (AP-5) are the work horses for most laboratory research on these receptors. MK-801 inhibits NMDARs by binding to and occluding the open pore of the NMDAR in an irreversible manner (Foster and Wong, 1987; Huettner and Bean, 1988) whereas AP5 reversibly binds to the glutamate site and competes with glutamate for NR2 subunit binding (Crunelli et al., 1983; Olverman et al., 1984).

1.3.3. Post-synaptic interactions of NMDARs

Similar to CaV2.2 and the pre-synaptic Ca^{2+} channel complex, NMDARs function as part of a larger multimeric complex with a litany of proteins aiding in their post-synaptic responses (Sheng, 2001). That the NMDAR NR2 subunits harbor a large cytosolic C-terminus (~650 amino acids) is suggestive of their involvement in complex protein interactions (Ishii et al., 1993;

Moriyoshi et al., 1991; Wo and Oswald, 1994). Peter Seeburg's laboratory sought to investigate possible C-terminal interactions by employing a two hybrid screen for potential binding partners of the C-termini of NR2 subunits (Kornau et al., 1995). This screen found that the second PDZ domain of post-synaptic density 95 protein (PSD-95) bound to the last seven amino acids contained in the C-termini of the NR2 subunits (amino acids SSIEDV in NR2B). Introduction of a SSIEDV peptide (commonly referred to as *t*SXV) dissociated NR2 subunits from PSD-95 and has hence been used extensively to study this interaction. PSD-95 is a member of the membrane-associated guanylate kinase (MAGUK) family. Other members of the MAGUK family including synapse associated protein 102 (SAP-102) and post-synaptic density 93 (PSD-93) also binding to NMDARs (Kim et al., 1996; Sans et al., 2000). It was subsequently determined that PSD-95 is able to concomitantly bind NMDARs and neuronal nitric oxide synthase (nNOS) (Christopherson et al., 1999). Furthermore, a complex containing NMDARs, PSD-95, and nNOS was co-precipitated from brain (Christopherson et al., 1999). The existence of this complex answered a quandary in the field of neuroscience as to why NMDAR activation induces NO production while other Ca^{2+} influx pathways do not (Bredt and Snyder, 1990; Kiedrowski et al., 1992). The reason for this selective activation is that the biochemical complex coupling nNOS to NMDARs is required for its activation. Subsequent work supported this conclusion as treatment of cells with a PSD-95–NMDAR interaction disrupting peptide reduced nNOS activation following glutamate exposure (Aarts et al., 2002). The post-synaptic complex containing NMDARs, MAGUKs and their associated proteins are commonly referred to as the NMDAR complex or MAGUK associated signaling complex (MASC) (Husi et al., 2000; Ryan et al., 2008).

NMDARs also interact and are regulated by various kinases (Ryan et al., 2008). The first kinase found to regulate NMDARs was protein kinase C (PKC) (Chen and Huang, 1991). Activation of PKC leads to an increase in open probability which led to increased NMDAR currents (Lan et al., 2001; Liao et al., 2001). Furthermore, PKC phosphorylation has also been shown to regulate NMDAR surface expression (discussed in §1.3.4). NMDARs are also

phosphorylated by protein kinase A (PKA) (Cerne et al., 1993). Activation of PKA leads to enhanced NMDAR currents via an increase in the open probability. PKA is also part of the MASC through complexation with A kinase anchoring proteins (AKAPs) 79/150 that bind to PSD-95 that brings together both the NMDAR and PKA (Klauck et al., 1996; Sanderson and Dell'Acqua, 2011). In addition to PKA, AKAPs also aid in coupling the MASC to protein phosphatases (calcineurin and protein phosphatase 1) (Gomez et al., 2002; Klauck et al., 1996; Westphal et al., 1999). By bringing these kinases and phosphatases in close spatial proximity to the NMDARs, AKAPs serve as a scaffold and allow for rapid phosphorylation/dephosphorylation of NMDARs to regulate their activity (Sanderson and Dell'Acqua, 2011).

Another kinase that has a well delineated interaction with NMDARs is CaMKII. Early work by Mary Kennedy's laboratory identified Ser1303 in NR2B as the phosphorylation site for CaMKII (Omkumar et al., 1996). This site is also a target of PKC, so it is difficult to tease apart the precise contribution CaMKII phosphorylation of NR2B has on receptor function (Liao et al., 2001). Further complicating the matter is the finding that CaMKII binds to NR2B and this binding is enhanced by NMDAR activation (Strack and Colbran, 1998; Strack et al., 2000). Interestingly, phosphorylation of NR2B by CaMKII decreases the affinity of CaMKII for NR2B. This suggests an intricate series of events where CaMKII becomes active and binds to NR2B, but simultaneously reduces its ability to bind NR2B by phosphorylating Ser-1303. The association between CaMKII and NMDARs has been fiercely studied as both are important players in memory and learning (Bear and Malenka, 1994; Malinow et al., 1989).

While the two previously discussed proteins that interact with NMDARs are both serine/threonine kinases, several Src family tyrosine kinases (SFKs) also interact and phosphorylate NMDARs (Chen and Roche, 2007; Salter, 1998). One of the functions served by tyrosine phosphorylation of NMDARs is regulation of trafficking (discussed in detail in §1.3.5). In a seminal study by Michael Salter's laboratory, it was observed that treatment of neurons with the SFK inhibitor genistein led to pronounced inhibition of NMDAR currents (Wang and Salter,

1994). Conversely, addition of immunoprecipitated Src protein to the recording pipette led to a significant enhancement of currents. SFKs functions extend beyond phosphorylating NMDARs to assembling biochemical complexes with MASC that enable a tight coupling between SFK activation and NMDAR phosphorylation (Yaka et al., 2002; Yu et al., 1997). Phosphorylation of NMDARs by SFKs has also been proposed as a molecular mechanism for memory and learning (Grosshans et al., 2002).

As introduced in §1.2.9, Robert Wenthold's group reported CRMP-2 as a putative NMDAR-interacting protein (Al-Hallaq et al., 2007). Specifically, his group isolated CRMP-2 as an interacting protein through mass spectrometric analysis of enriched NR2A/B heteromeric NMDARs. Furthermore, using sequential co-immunoprecipitation methodologies, they observed CRMP-2 in a biochemical complex with NR2A and NR2B. This study was strictly biochemical and reported no functional impact of the interaction. This section has introduced how NMDARs engage in signaling complexes which link their activation to downstream effectors (i.e. kinases). This is in stark contrast to CaV2.2, which interacts with the synaptic vesicle machinery to aid in tight coupling of Ca^{2+} channel activity with neurotransmitter release. The common denominator, however, is that both CaV2.2 and NMDARs use biochemical complexes to link their activity with the next step in neurotransmission. These biochemical complexes are hence vital to their function.

1.3.4. Trafficking, localization, and quality control of NMDARs

Exploration into the molecular determinants of NMDAR trafficking identified the C-terminus of the NR1/2 subunits as paramount in ensuring surface expression of the receptor (Wenthold et al., 2003). This is not surprising as the C-terminus is over 600 amino acids and comprises the majority of intracellular region of the receptor and likewise encompasses the majority of protein interactions. As previously described for CaV2.2, the NMDAR must also pass through ER and Golgi compartments prior to arriving at the membrane (Petralia et al., 2009;

Stephenson et al., 2008). While CaV2.2 has auxiliary subunits and synaptic proteins that aid in proper trafficking, the NMDAR relies on the MASC and associated STKs interactions within the NR2 C-termini. NMDARs must pass ER quality controls prior to exiting the ER which assures that only NMDARs containing NR1 and NR2 are exported from the ER (McIlhinney et al., 1998). Following exit from the ER, NMDARs are modified in the Golgi before reaching their final destination.

NMDARs must hitch a ride with adapter proteins (e.g. MAGUKs) linking their transport out of the Golgi to endosomes and beyond. The MAGUK SAP-102 links the NMDAR to the exocyst complex which is associated with transport out of the Golgi (Bowser et al., 1992), and appears to aid in transport of NMDARs from the Golgi to intracellular transport vesicles (Sans et al., 2003). NMDARs are present in mobile clusters along dendritic processes which allow for rapid movement of receptors along dendrites (Washbourne et al., 2002). The NMDAR is then transported to the membrane along microtubules (Washbourne et al., 2002) with the assistance of kinesin motor proteins (Guillaud et al., 2003; Setou et al., 2000). To localize to the synapse, the NR2 subunit must bind to either PSD-95 or SAP-102 (Prybylowski et al., 2005; Sans et al., 2003). The translocation of the clustered receptors from intracellular compartments to the plasma membrane occurs through interaction with the post-synaptic SNAREs SNAP-23/25 (Lan et al., 2001; Suh et al., 2010; Washbourne et al., 2004). This transport from intracellular stores to the membrane can be initiated by PKC activation which leads to subsequent activation of SFKs (Huang et al., 2001; Lu et al., 1999). The rapid insertion of NMDARs into the membrane requires both PKC and SFK activation and represents a mechanism whereby cells can add receptors to the membrane promptly following stimulation (Grosshans et al., 2002). As discussed previously in §1.2.9, CRMP-2 has also been suggested to be involved in the trafficking of NMDARs (Bretin et al., 2006), although these findings have yet to be substantiated and are controversial. The current consensus is that NMDARs are present in clusters along dendrites

where they can rapidly move in and around dendritic membranes to facilitate changes in NMDAR responses.

Following trafficking of the NMDAR to the surface, there are multiple pathways that have been identified that can reduce surface expression of the receptor, most notably via receptor internalization. Interestingly, unlike synaptic AMPARs which are recycled vigorously, NMDARs are rather stable in the post-synaptic terminal (Luscher et al., 1999). Nevertheless, NMDARs still undergo internalization as was initially observed in experiments expressing NR1/NR2B in a heterologous cell line (Roche et al., 2001). This internalization relied on a sequence (amino acids YEKL) just N-terminal to the PDZ binding peptide of NR2B. Internalization of NR2B occurs through dynamin-dependent endocytosis and appears to be developmentally regulated with immature (DIV 7) hippocampal neurons exhibiting significantly more internalized receptors than mature (DIV 18) neurons (Roche et al., 2001). This internalization can be prevented by co-expression of PSD-95 (Lavezzari et al., 2003). This is consistent with PSD-95 binding to the PDZ domain and stabilizing NMDARs while interfering with YEKL mediated-internalization (Roche et al., 2001). Preventing AP-2 binding to NR2B reversed loss of synaptic receptors in response to mutation of the NR2B PSD-95 binding site, suggesting that synaptic internalization occurs via binding of the adaptin protein 2 (AP-2) complex which links NR2B to the clathrin-mediated internalization machinery (Lavezzari et al., 2003; Prybylowski et al., 2005). This finding further suggests that, under normal conditions, AP-2 actively removes channels which are not associated with PSD-95 (Prybylowski et al., 2005). Additionally, phosphorylation of NR2B Tyr-1472 (YEKL) by the SFK Fyn leads to enhanced currents consistent with the observed reduction in AP-2 binding of NR2B following Tyr-1472 phosphorylation. Phosphorylation of Tyr-1472 can also be upregulated by inhibition or loss of Cdk5 activity (Zhang et al., 2008). This occurs as phosphorylation of PSD-95 by Cdk5 reduces the affinity of SFKs for PSD-95 and therefore leads to reduced Tyr-1472 phosphorylation. The net result of Cdk5 inhibition is an increase in surface expressed NR2B due to reduced NR2B–AP-

2 interactions (Zhang et al., 2008). NMDAR internalization can also be initiated by activation of CaMKII (Chung et al., 2004). Following activation CaMKII phosphorylated and activated casein kinase 2 (CK2) which in turn phosphorylates Ser-1480. This phosphorylation reduces NR2B-PSD-95 interactions leading to NR2B internalization. Finally, it has also been shown that GSK3β activity can regulate NR2B surface expression (Chen et al., 2007b). While it was observed that Cdk5 inhibition leads to reduced NR2B internalization, the converse was found to be true for GSK3β. The use of GSK3β inhibitors or siRNA led to a sharp decline in NMDAR currents (~30% of peak within 5 minutes). This decline was dynamin dependent and accompanied by a decrease in NMDAR-PSD-95 interactions. Collectively then, it appears that internalization of NR2B containing receptors is dependent upon the phosphorylated state of Tyr-1472 and Ser-1480. These phosphorylation sites in turn regulate interactions between NR2B and PSD-95/AP-2 where PSD-95 favors membrane NR2B and AP-2 binding favors internalization of NR2B.

1.3.5. Excitoxicity and role of NMDAR in glutamate-induced neuronal death

The death of neurons due to toxic excitation is a phenomenon known as excitoxicity (Choi, 1992). Excitotoxic death of neurons occurs due to excessive Ca^{2+} influx leading to activation of neurotoxic cascades (Choi, 1985). Neuronal insults such as a stroke or traumatic brain injury induce localized cell death around the insult leading to dumping of glutamate from neuronal stores (Bullock et al., 1995; Katayama et al., 1990). The excess of extracellular glutamate activates a variety of glutamate receptors including glutamate ligand-gated ion channels, which are the most commonly implicated receptors in glutamate toxicity (Sattler and Tymianski, 2001). Ca^{2+} influx through NMDARs in particular is thought to be a key mediator of excitotoxicity as antagonists of these receptors are neuroprotective in animal models of traumatic brain injury and ischemia-induced excitotoxicity (Faden et al., 1989; Grotta et al., 1990; Park et al., 1988; Steinberg et al., 1989). However, the majority of human trials using NMDAR antagonists did not replicate the effectiveness seen in animal models and alarmingly found

NMDAR antagonists to be toxic (Ikonomidou et al., 2000; Ikonomidou and Turski, 2002; Muir, 2006). In contrast, the non-competitive NMDAR antagonist memantine has shown early promise in various models of excitotoxicity (Sonkusare et al., 2005; Volbracht et al., 2006) and appears to be clinically well-tolerated (Jain, 2000; Parsons et al., 1999).

NMDAR activation causes a deregulation of Ca^{2+} homeostasis initiating a variety of pathways culminating in neuron cell death (Choi, 1985). One such pathway that is activated during excitotoxicity is production of the free radical NO by nNOS (Dawson et al., 1991). Not only is the Ca^{2+} influx through NMDARs responsible for nNOS activation, but the direct coupling of nNOS to NMDARs facilitates NO production (Aarts et al., 2002; Sattler et al., 1999). The production of NO and other free radicals leads to modification of proteins, DNA, and lipids resulting in cell death (Sattler and Tymianski, 2000). As previously mentioned, nNOS interacts with NMDARs by binding to PSD-95 and hence disruption of the NR2B–PSD-95 interaction displaces nNOS from the MASC. Disruption of the NR2B-PSD-95 interaction using a peptide containing the last 9 amino acids of NR2B (NR2B9c) is therefore neuroprotective and has been used to prevent neuronal death following stroke (Aarts et al., 2002). As many proteins interact with the NMDAR through PSD-95, it is difficult to attribute neuroprotection to a single protein and therefore the mechanism of NR2B9c remains enigmatic and controversial.

NMDAR-mediated Ca^{2+} influx can also activate the Ca^{2+} activated protease calpain (del Cerro et al., 1994), which has been heavily linked to neurotoxic signaling (Vosler et al., 2008). Calpain is a cytosolic cysteine protease consisting of calpain I and II. Inhibition of calpains has been shown to be neuroprotective *prior* to excitoxicity, suggesting that its activation aids in neuronal death (Bevers et al., 2009; Hong et al., 1994). The prototypical calpain substrate is the cytoskeletal protein spectrin, where calpain activity is commonly monitored through the predictable cleavage pattern of spectrin (Czogalla and Sikorski, 2005). Dozens of additional calpain substrates in the nervous system are known including cytosolic, mitochondrial, nuclear, and membrane bound proteins. Pertinent to my dissertation, calpain cleaves both CRMP-2

(Bretin et al., 2006; Chung et al., 2005) and NR2B (Simpkins et al., 2003). Another interesting substrate of calpain is p35 (activator of Cdk5), where cleavage of p35 to p25 occurs during neurotoxic stimulation and leads to activation of Cdk5 (Lee et al., 2000). Cleavage of CRMP-2 has previously been discussed in detail in § 1.2.9. Stimulation of hippocampal neurons with NMDA for 5 min leads to a pronounced (~35%) decrease in NMDAR currents (Wu et al., 2005). Inhibition of calpain completely prevents the decrease, suggesting that cleavage reduces the amount of functional receptors. Despite many prior studies showing calpain inhibition to be neuroprotective, a recent study found that neuroprotection by disrupting the NR2B–PSD-95 interaction relied on calpain *activation* (Yuen et al., 2008). This study suggests that by disrupting the NR2B–PSD-95 interaction, the NR2B subunit becomes susceptible to cleavage and therefore sparing the cells from NMDAR-mediated cell death.

In addition to the negative signaling initiated by NMDAR activation, there is also pro-survival signaling that occurs via NMDAR activation. One theory behind the failure of NMDAR antagonists in clinical trials is that inhibition of NMDARs prevents both pro-survival as well as neurotoxic NMDAR signaling. In other words, although the neurotoxic effects of NMDARs are blocked, neurons also lose the positive survival signaling that in turn leads to toxicity. Work performed using both *in vivo* and *in vitro* models found that pre-incubation with low concentrations of NMDA reduced excitotoxicity (Jiang et al., 2005; Lee et al., 2005; Marini and Paul, 1992; Ogita et al., 2003). This pro-survival signaling appears to be through a cyclic-AMP response element binding protein (CREB). Following activation of NMDARs, CREB is rapidly phosphorylated which in turn induces release of the pro-survival brain-derived neurotrophic factor (Jiang et al., 2005). While these results suggest that NMDARs possess the capability to be both pro-survival and neurotoxic, it is unknown what property of an NMDAR determines it role in neuronal survival. Some studies have hypothesized that synaptic versus extrasynaptic NMDARs couple differently to these two distinct signaling pathways (Hardingham and Bading, 2002; Hardingham et al., 2002). The role of these receptors in cell viability has been linked to

CREB signaling, which is enhanced via synaptic NMDARs and reduced via extrasynaptic NMDARs (Hardingham et al., 2002). These findings position NMDARs not only as a target for neuronal death but also for survival. Recent findings suggest that the NMDAR interacting protein CRMP-2 may be neuroprotective by altering NMDAR receptor function (Al-Hallaq et al., 2007; Bretin et al., 2006). However, nothing is known about ***how*** the NMDAR-CRMP-2 interaction is neuroprotective. In Chapter 4, I will explore CRMP-2 and the role that a CRMP-2 peptide plays in preventing NMDAR-mediated neuronal death.

THESIS AIMS:

1. To determine if CRMP-2 interacts functionally and biochemically with CaV2.2.
2. To determine if phosphorylation of CRMP-2 by Cdk5 is an important determinant of CaV2.2 modulation.
3. To determine if disruption of CaV2.2-CRMP-2 interaction prevents CRMP-2-mediated modulation of CaV2.2.
4. To determine if TAT-CBD3 is neuroprotective.
5. To determine the mechanism of TAT-CBD3 neuroprotection.

CHAPTER 2. MATERIALS AND METHODS

2.1. Synaptosome isolation

Synaptosomes are biochemically isolated preparations enriched with pre-synaptic structures and post-synaptic densities. Synaptosomes were prepared as described (Carlin et al., 1980; Huttner et al., 1983) with modifications. Brains from PN1-2 Sprague Dawley rats (Harlan Labs) were dissected into 10 volumes ice-cold homogenization buffer A (see Table 2.1 for buffer compositions) and homogenized using 10-15 strokes of a glass Teflon hand-held homogenizer. The homogenate (H) was spun for 10 min at 1400x g 4°C and the supernatant was saved. The pellet (P1) from this spin was re-homogenized in buffer A and spun as before. Both low-speed spin supernatants were combined and spun for 10 min at 13,800x g 4°C yielding a supernatant cytosolic fraction (S2) and a pellet consisting of a crude synaptosomal fraction (P2). The P2 fraction was homogenized in sucrose buffer B and layered onto a sequential gradient of 1M and 1.4M sucrose (buffered with 0.5 mM HEPES/KOH pH 7.4) and centrifuged at 82,500x g (4°C) for 90 min in a swinging bucket rotor with slow acceleration and deceleration. The gradient interphase contained intact synaptosomes (P2'), which were used for depolarization experiments within 2 h of isolation or lysed in modified RIPA buffer; filtered through a 0.22 μm syringe filter and fractions stored at –80°C until use. Protein concentrations were determined for all lysates using a BCA protein assay (Thermo Scientific).

2.2. Sucrose density gradient centrifugation

To assess the sub-cellular distribution of CRMP-2 and CaV2.2 proteins, sucrose density gradients were prepared from PN1 rat brains. Rat brains (~2 mg) were solubilized in 2 ml 1% Triton X-100 (Sigma) in MBS (2-morpholinoethanesulfonic acid (MES)-buffered saline). Following homogenization using 10-15 strokes of a glass Teflon hand-held homogenizer, the homogenates were adjusted to 45% with sucrose and overlaid with 4 ml of 30% sucrose in MBS

Table 2.1. Buffers used in this thesis

Buffer Name	Contents
(protease inhibitors)	1 µg/ml pepstatin, 1 µg/ml leupeptin, 2 µg/ml aprotinin, 1 mM PMSF (Sigma) together with Protecease inhibitor cocktail
DEAE buffer	25 mM sodium phosphate (pH 7.8) containing 10 mM 2-mercaptoethanol and 1 mM phenylmethylsulfonyl fluoride
Excitatory Tyrode's buffer	32 mM NaCl, 90 mM KCl, 2 mM $CaCl_2$, 2 mM $MgCl_2$, 25 mM HEPES pH 7.5, 30 mM Glucose
Extracellular solution	140 mM NaCl, 5 mM KCl, 1 mM $MgCl_2$, 2 mM $CaCl_2$, 10 mM HEPES, pH 7.4, 10 mM glucose
GST lysis buffer	20 mM Tris pH 7.5, 200 mM NaCl, 0.1 mM EDTA, 1 mM DTT, and protease inhibitors
HA buffer	10 mM potassium phosphate (pH 7.0) containing 10 mM 2-mercaptoethanol
HBS-EP buffer	10 mM HEPES, pH 7.4, 10 mM M NaCl, 3 mM EDTA, and 0.005% surfactant P20
Heparin extraction buffer	5% SDS, 20 mM DTT, 125 mM Tris-HCl, pH 6.8, 10% sucrose, 20 mM EDTA
His elution buffer	50 mM HEPES pH 7.4, 150 mM NaCl, 100 mM Imidazole
His lysis buffer	50 mM HEPES pH 7.4, 150 mM NaCl
His storage buffer	10 mM HEPES, pH 7.4, 100 mM M NaCl, and 20 mM $CaCl_2$
His wash buffer	50 mM HEPES pH 7.4, 150 mM NaCl, 10 mM Imidazole
Homogenization buffer A	0.32 M sucrose, 10 mM HEPES pH 7.4, 2 mM EDTA, with protease inhibitors
Kinase assay buffer	100 mM HEPES pH 7.2, 20 mM $MgCl_2$, 2 mM MgATP, 2 mM DTT
MBS	25 mM MES pH 6.5, 150 mM NaCl
Mild lysis buffer	20 mM HEPES pH 7.2, 150 mM NaCl, 2 mM $MgCl_2$, 1 mM DTT, 0.5% (v/v) Triton X-100,
PBS	137 mM NaCl, 2.7 mM KCl, 4.3 mM Na_2HPO_4, 1.47 mM KH_2PO_4
Protein binding buffer	20 mM HEPES pH 7.2, 1 mM EDTA, 150 mM NaCl, 5 mM $MgCl_2$, 0.1 % NP-40 with protease inhibitors
RIPA #1	50 mM Tris-HCl, pH 8, 1% NP-40, 150 mM NaCl, 0.5% Na deoxycholate, and 1 mM EDTA with protease inhibitors
S buffer	25 mM sodium phosphate (pH 6.0) containing 10 mM 2-mercaptoethanol
Standard bath solution	139 mM NaCl, 3 mM KCl, 0.8 mM $MgCl_2$, 1.8 mM $CaCl_2$, 10 mM NaHEPES, pH 7.4, 5 mM glucose
Sucrose buffer B	0.32 M sucrose, 0.5 mM HEPES/KOH pH 7.4 and protease inhibitors

Sucrose homogenization buffer	320 mM Sucrose, 10 mM Tris-HCl pH 7.5, 1 mM EDTA, 1 mM EGTA pH 7.5 and protease inhibitors
TAE buffer	40 mM Tris Acetate, 1 mM EDTA
TBST	25 mM Tris-Cl, pH 8.0, 125 mM NaCl, 0.1% to 2% Polyoxyethylene Sorbitan Monolaurate (Tween-20)
TE SDS buffer	1% SDS, 100 mM Tris-HCl pH 7.5, 10 mM EDTA
Triton X100 extraction buffer	Sucrose homogenization buffer with 0.5 % Triton X100
Tyrode's buffer	119 mM NaCl, 2.5 mM KCl, 2 mM $CaCl_2$, 2 mM $MgCl_2$, 25 mM HEPES pH 7.5, 30 mM Glucose

and 4 ml of 5% sucrose in MBS. The sucrose gradient was formed by centrifuging at 200,000x *g* for 18 h at 4°C using a Beckman SW41 rotor (Beckman Coulter). Twelve 1 ml aliquots were removed, beginning at the top. The high density membrane fractions (9–12) at the bottom of the gradient contain proteins like the Na^+/K^+ ATPase and voltage-gated ion channels(Wong et al., 2002), fractions 5 and 6 are rich in cholesterol and sphingolipids, confirming the ability of this centrifugation method in separating membrane and cellular components.

2.3. Preparation of synaptic and extrasynaptic brain fractions

Protocol was modified from a previously published study (Goebel-Goody et al., 2009). Freshly removed E19 rat cortices were homogenized in sucrose homogenization buffer. Homogenates were then spun for 10 min at 1000 x g to remove insoluble debris and the nuclear fraction (P1). The supernatant (S1) was then spun at 10,000 x g for 10 min producing a crude synaptosomal pellet (P2) and a cytosolic fraction (S2). S2 was then further spun at 100,000 x g for 60 min producing an intracellular membrane fraction (LP1) and a nonmembrane cytosolic fraction (LP1). P2 was then resuspended in Triton X100 extraction buffer and agitated gently by continual rotation at 4°C for 30 min. The resuspended pellet was then centrifuged at 32,000 x g for 30 min producing a pellet containing an enriched synaptic fraction (TxP) and a supernatant containing an enriched extrasynaptic fraction (TxS). TxP and LP1 fractions were resuspended in SDS TE buffer along with sonication and boiling. All samples were quantified for total protein and equal protein from each fraction was separated by SDS-PAGE before immunoblotting was performed.

2.4. Co-immunoprecipitations and western blotting

Rat brain synaptosomes were pre-cleared by a 1 h incubation with 20 µl of a 50% slurry of protein A/G beads (Pierce). The cleared lysate was then incubated overnight with various primary antibodies (see Table 2.2) or rabbit or mouse isotype-specific IgGs (Sigma or Jackson

Table 2.2. Antibodies used in this thesis

Protein	Dilution	Species	Source	Epitope	Applications	Company	Cat #
Akt	1:500	Mouse	Rabbit	C-terminal peptide	WB	Cell Signaling	C67E7
CaV2.2	1:500	Rat	Rabbit	851-867	WB, IP	Calbiochem	681505
CaV2.2	1:500	Human	Rabbit	2013-2169	WB	Origene	TA308673
CRMP-1	1:750	human	Rabbit	unknown	WB	Sigma	AV41932
CRMP-2	1:1000	Human	Rabbit	unknown	IC, WB, IP	Cell Signaling	9393
CRMP-2	1:1000	Rat	Rabbit	unknown	IC, WB, IP	Chemicon	AB9218
CRMP-2	1:1000	Human	Mouse	C-terminal peptide	WB	Abcam	AB62539
CRMP-2	1:1000	Human	Rabbit	476-493	WB	Sigma	C2933
CRMP-2 (C4G)	1:1000	Human	Mouse	C-terminus	WB, IP	Immuno-Biological Laboratories	11096
CRMP-2 (p522)	1:1000	Human	Rabbit	Phospho-peptide	WB	ECM Biosciences	CP2191
CRMP-3	1:500	Human	Mouse	unknown	WB	Abcam	AB36217
CRMP-4	1:500	Human	Rabbit	499-511	WB	Chemicon	AB5454
CRMP-5	1:500	Human	Rat	whole protein	WB	Chemicon	MAB5442
Kv2.1	1:500	Rat	Mouse	837-853	WB	NeuroMab	K89/34

Protein	Dilution	Species	Source	Epitope	Applications	Company	Cat #
GFP	1:20,000	Jellyfish	Mouse	whole protein	WB	Clontech	632375
Glu Tag	1:500	peptide	Mouse	Glu peptide	WB, IP	Dr. Clark Well's (IUSM)	N/A
GluR2	1:250	Rat	Mouse	834-883	WB	NeuroMab	L21/32
Munc18	1:500	Rat	Mouse	381-567	WB	BD Biosciences	610336
NR2B	1:1000	Rat	Mouse	892-1051	WB ,IP	BD Biosciences	610417
NR2B	1:1000	Mouse	Rabbit	1437-1456	WB, IP	Millipore	06-600
NR2B	1:200	Rat	Mouse	20-271	IP	NeuroMab	N59/20
PSD-95	1:1000	Human	Mouse	77-299	WB	Neuromab	K28/43
Tubulin (βIII)	1:2000	Human	Mouse	373-378	WB	Promega	G7121
WB: western blot, IP: immunoprecipitation, IC: Immunocytochemistry							

Immunoresearch) as controls. The antibody-captured complexes were recovered with fresh protein A (for rabbit polyclonal antibodies) or protein A/G (for mouse monoclonal antibodies) agarose beads (15-30 µl original bead slurry per sample) by incubation with lysate-antibody mixture at 4°C for 2 h. The beads were then washed three times with lysis buffer. Prior to electrophoresis on SDS polyacrylamide gels, protein samples were boiled in Laemmli sample buffer for 5 minutes. Proteins were fractionated on 5%, 7.5%, 10% or 4-15% separating gels with 4% stacking gels. Apparent molecular weights were determined using broad range standards (Fermentas). Following electrophoresis, proteins were transferred to PVDF membranes (Invitrogen) for immunoblotting and stained with Amido black or ponceau (BioRad) to monitor transfer efficiency. The membranes were blocked for 1 h in 5% skim milk powder in TBST at RT. Primary antibody incubations were for 2 h at RT or overnight at 4°C. Following incubations with primary antibody and secondary antibody (goat anti-rabbit or anti-mouse IgG horseradish peroxidase (1:10,000 or 1:20,000; Stressgen)), blots were washed extensively in TBST and probed with Enhanced Chemiluminescence Western blotting substrate (Thermo Scientific) before exposure to photographic film. Blots were exposed for a range of durations to ensure the generation of a print in which the film is not saturated. Films were then scanned, digitized and quantified using Un-Scan-It gel V6.1 scanning software (Silk Scientific Inc., Orem), limiting our analysis to the linear range.

2.5. Isolation and culture of hippocampal or cortical neurons

Rat hippocampal and cortical neuron cultures were prepared from hippocampi or cortices dissected from PN1 or embryonic day 19 (E19) rats respectively as described(Goslin and Banker, 1989). Briefly, rat hippocampi were dissected out of PN1 rats, and cells were dissociated enzymatically and mechanically (trituration through Pasteur pipette) in a Papain solution (12 U/ml; Worthington) containing Leibovitz's L-15 medium (Invitrogen), 0.42 mg/ml cysteine (Sigma), 250 U/ml DNase 1 (type IV; Sigma), 25 mM $NaHCO_3$, penicillin (50

U/ml)/streptomycin (50 µg/ml), 1 mM sodium pyruvate, and 1 mg/ml glucose (Invitrogen). After dissociation, the cells were gently washed by sequential centrifugation in Neurobasal medium containing either 2 mg/ml or 20 mg/ml BSA and Pen/Strep, glucose, pyruvate, and DNase1 (as above) and then plated on poly-D-lysine-coated Aclar coverslips at high density (~2000 cells/mm^2). Growth media (1 ml/well) consisted of Neurobasal medium continaing 2% NuSerum, 2% B27 or NS21 (Chen et al., 2008), supplemented with penicillin/streptomycin (100 U/ml; 50 µg/ml), 0.1 mM L-Glutamine and 0.4 mM L-glutamax (Invitrogen). Cytosine β-D-arabinofuranoside (5 µM; Sigma) was added 24 h after plating to reduce the number of non-neuronal cells. After 4 d in culture and 2× each week thereon, half of the growth medium was replaced with medium without cytosine β-D-arabinofuranoside.

2.6. Immunocytochemistry, confocal microscopy and iterative deconvolution deblurring

DIV 10 hippocampal cultures were fixed with 4% paraformaldehyde (diluted in 0.1 mM PBS) for 10 min at room temperature, permeabilized with 0.2% Triton X-100 for 10 min, and then washed three times with 0.1 mM PBS. Neurons were then pre-incubated with 10% bovine serum albumin (diluted in 0.1 mM PBS) for 1 h at RT to block nonspecific binding with the primary antibody. Primary antibodies for monoclonal CRMP-2 (Abcam) and rabbit polyclonal N-type/CaV2.2 (Calbiochem) were diluted 1:100 (in 0.1 mM PBS) and applied to the cells. After incubation at 4°C overnight, the neurons were washed again with PBS and secondary antibodies (goat anti-mouse Alexa 488 or anti-rabbit Alexa 594, 1:1000; Molecular Probes, Eugene, OR) were incubated in blocking solution for 45 min at RT. Coverslips were mounted in Prolong Gold Antifade mounting media (Molecular Probes). The hippocampal neurons were imaged on a Nikon Ti swept-field confocal microscope using a 60X, 1.4 NA lens and standard FITC/Texas red fluorescence cubes with a cooled Cascade 512B digital camera (Photometrics, Tucson, AZ). Z stack image pairs were captured at an inter-plane distance of 200 nm through the sample. Images

were deblurred off line by an iterative deconvolution protocol (Nikon Elements v3.0) using a theoretical point-spread function and pseudocolored for presentation.

2.7. Intensity correlation analysis (ICA)/Intensity correlation quotient (ICQ)

Developed by Dr. E. F. Stanley (Toronto Western Research Institute, Toronto, Canada), this analysis was completed as previously described with modifications (Khanna et al., 2006b). ICA/ICQ analysis was carried out by means of an automated graphic plugin (Khanna et al., 2006b) for the public domain image analysis software ImageJ (Wayne Rasband; National Institutes of Health, Bethesda MD). For the intensity correlation analysis (ICA) the function was calculated $(Ai–a)(Bi–b)$, where a and b are the means of each pixel staining pair intensity values Ai and Bi. Ai or Bi was graphed in separate scatter plots against their respective $(Ai–a)(Bi–b)$ value. Distributions that skew to the right reflect dependent staining patterns (where the two pixel staining intensity values vary in synchrony); distributions that are symmetrical about the 0 axis indicate random staining, while those that skew to the left reflect independent staining patterns, where the pixel staining intensity values vary inversely. Analysis for each stain was performed separately so that a dependence of stain A on B but a lack of dependence of B on A can be identified and, further, that the plots permit detection of complex or mixed staining relations. The intensity correlation quotient (ICQ) reflects the ratio of the number of positive $(Ai–a)(Bi–b)$ values to the total number of pixels in the ROI, corrected to a -0.5 (independent staining) to +0.5 (dependent staining) range by subtracting 0.5. The ICQ provides a single value parameter that is used for statistical comparisons. Typically, with $N>6$ ROIs, a mean ICQ value of -.05 to +.05 indicates random staining, +.05 to +.10, indicates a moderate covariance and >.1 a strong covariance. Images shown in Figure 3.3C were enhanced using the smart sharpen mask filter, high pass, and brightness-contrast adjustment functions in Adobe Photoshop. Images were processed with Nikon Elements v3.0 and all figures were constructed in Adobe Illustrator CS5 (Adobe Systems).

2.8. Cloning CRMPs and CaV2.2 channel fragments into pGEX-Glu vectors

Constructs containing full length and truncated CRMP-2 in the pGEX-5X-3 vector were generously provided by Dr. Akihiro Kuramasa (Tahimic et al., 2006). The intracellular loops of CaV2.2 were cloned into the dual-tagged pGEX3X-GST-Glu (a kind gift of Dr. Andy Hudmon) vector for expression of recombinant proteins. Using Vector NTI (v. 11; Invitrogen) or GENtle software, primers were designed to amplify regions corresponding to intracellular loops of rat CaV2.2 cDNA from P3 rat brain cDNA. The primers (Table 2.3) harbored restriction sites (*Bam*HI or *Bgl*II (5') and *Eco*RI or *Mfe*I (3')) to facilitate cloning into the plasmid. In addition to the GST-tag, this vector contains the Glu tag, a sequence of six amino acids (EYMPME).

2.9. Polymerase chain reaction (PCR)

A vector containing full length CaV2.2 cDNA was used as a template for amplification of the CaV2.2 cytosolic regions by PCR. PCR reactions consisted of 0.4 mM dNTPs, 0.4 mM of each primer, 1-5 units of *Taq* polymerase, and 50-100 ng of template. The reaction was run using a standard heated lid thermocycler (Eppendorf, Hamburg, Germany). Samples were heated to 95°C for 2 min to denature the cDNA and primers before cooling to 55°C to allow for annealing of the primers to the cDNA. Samples were then warmed to 72°C for 1 min/kb of desired product to promote elongation of the product by *Taq* polymerase. The samples were then cycled between denaturing, annealing, and elongation (using only a 30 sec denaturing) for a total of 30 cycles before a 10 min long elongation period to finish elongation on any incomplete strands. The thermocycler was then cooled to 4°C until the samples were removed.

2.10. Restriction digestion, gel purification, and ligation.

Correctly-amplified PCR products and parent pGex-3x-Glu vector were digested in the appropriate buffer for the selected restriction enzymes (as indicated by the provider of the enzyme) by incubating at 37°C for 4-6 hours. The digested DNA was then separated on a 1%

agarose gel in TAE buffer and visualized using SybrSafe™ (Invitrogen). DNA bands at the predicted sizes were excised using a scalpel and the DNA was extracted using the GeneJET™ Gel Extraction Kit (Fermentas, Vilnius, Lithuania). The extracted DNAs were quantified (Nanodrop 1000, Thermo Scientific), and ligations were performed using 6:1 and 3:1 insert to vector molar ratios. The ligations were transformed into XL-10 or DH5α *Escherichia Coli* (*E. Coli*) and colonies were screened using colony PCR. Those colonies with the correct-sized inserts were further verified by dideoxy sequencing (Cogenics, Houston, PA).

2.11. Recombinant GST protein production

DNA encoding verified pGex-CaV2.2-Glu-type channel fragments, GST-Glu, Munc18-1-GST, CRMP-2-GST, p25-GST, Cdk5-GST, and GSK3β-GST constructs were transformed into the BL21 (DE3) *E. Coli* for protein expression. CRMP-2-GST fusion constructs were generously provided by Dr. Akihiro Kurimasa (Tottori, Japan) (Tahimic et al., 2006) and a Munc18-1-GST fusion vector was provided by Dr. Debbie Thurmond (IUSM). Expression of fusion proteins was induced with 1 mM isopropyl-β-d-thiogalactopyranoside (IPTG). For purification, following overnight growth at 16°C, transformed bacteria were pelleted at 5,000 x g for 20 min at 4°C and lysed in GST lysis buffer using a M-110L Microfluidizer (Microfluidics Corp., Newton, MA). The microfluidized lysate was adjusted with Triton-X100 (1% final for CaV2.2 constructs only) and the cells were incubated on ice for 30 min followed by centrifugation at 30,000 x g for 45' at 4°C. The high-speed supernatant was then incubated with either Glutathione-cellulouse beads or protein G agarose beads (for GST-Glu proteins) conjugated with mouse monoclonal Glu primary antibody (gift from Dr. Clark Wells, IUSM). Alternatively proteins were loaded on a glutathione-cellulouse column, washed extensively with GST lysis buffer, and eluted with glutathione using a stepwise gradient from 0 to 100 mM glutathione. Purified protein concentration was determined using a bovine serum albumin curve on a SDS-PAGE stained by comassie. The Coomassie

Table 2.3. Primers used to generate GST-CaV2.2-Glu fusion constructs

Construct	***Nucleotides***	***Primer Sequence 5′ → 3′***	***Restriction site***
N-terminus (Nt)	46-330	TAG GAT CCT TAT GGT CCG CTT CGG GGA CGA GCT A	***BamHI***
		TAT GAA TTC GGC CAT TCG GTG ATG CGC TTA	***EcoRI***
I-II loop (L1)	1111-1494	TAG GAT CCC ATC AGG AGA GTT TGC CAA AGA G	***BamHI***
		TAT GAA TTC CCG CTC TGT GCT TTC ACC ATA CGA	***EcoRI***
II-III loop proximal region (L2-p)	2176-3000	CTA GAT CTT GGA AGA GGC AGC CAA TCA GAA GC	***BglII***
		TAT GAA TTC CCT GCA CGG TGC CTG CGT GTG	***EcoRI***
II-III loop distal region (L2-d)	2914-3471	TAC TAG ATC TTG GGC GAG CGT CGC GCA AGA CAT	***BglII***
		TAT GAA TTC CCG TAA TGG CAG AAG CGA CGG AG	***EcoRI***
III-IV loop (L3)	4276-4467	TGG GAT CCC CTT GAT CAT CAT CAC CTT CCA G	***BamHI***
		CCG GAA TTC CCA ATG AAG TAC TCA AAG GGT GG	***EcoRI***
C terminus proximal (Ct-p)	5116-5793	TGG GAT CCT CTG TTC CTT TCT GAT GCT GAA	***BamHI***
		TGA CCG CAA TTG GAA GTT GCA CTC TTT TGT C	***MfeI***
Ct-medial (Ct-m)	5683-6429	TAG GAT CCA GAT GGG TCC TGT TTC CCT GTT	***BamHI***
		CTG GAA TTC CCA AAG CGG TCA CAG GAA TA	***EcoRI***
Ct-distal (Ct-d)	6400-7044	TGG GAT CCA GCG CTT CTA TTC CTG TGA C	***BamHI***
		TTA TCC CAA TTG CAC CAG TGA TCC TGG TCT	***MfeI***

stained gels were then scanned and bands were quantified by UN-SCAN-IT gel (Silk Scientific Inc, Orem, Utah).

2.12. Endogenous CRMP-2 purification

This was performed as described previously with slight modifications (Wang and Strittmatter, 1997). Adult rat brains (~10g) were homogenized in 3 volumes of DEAE buffer with a Teflon/glass homogenizer. The homogenate was centrifuged at 200,000 *g* for 40 min at 4°C and the supernatant was applied to a 1 mI DEAE-Sephacel column (Sigma) equilibrated with DEAE buffer. The column was washed thoroughly with DEAE buffer, and bound proteins were eluted with 100, 200, and 300 mM NaCI step gradients in DEAE buffer. Two ml fractions were collected at each salt concentration. Peak CRMP-2-containing fractions (as monitored by Western blot with a polyclonal CRMP-2 antibody) in the 200 mM NaCI elution was diluted 10-fold with S buffer, and applied to a 2 ml S-Sepharose (GE Healthcare/ Amersham) column equilibrated with S buffer. After washing, proteins were eluted in 150 mM NaCI in S buffer. One 3 ml fraction was collected, diluted fivefold with HA buffer. The diluted sample was applied to a 1 ml hydroxyapatite column (Bio-gel HTP; Bio-Rad) and eluted with 100 mM potassium phosphate (pH 7.0) containing 10 mM 2-mercaptoethanol. Six fractions of 0.5 ml each were collected. At this step, Coomassie Blue staining and Western blot analysis was performed to verify CRMP-2 purification at the predicted molecular mass of 65 kDa. An identical procedure was used to purify CRMP from rat brains at several ages.

2.13. *In vitro* protein-binding assay

For binding studies, the cytoplasmic loops of CaV2.2 and full-length (as well as truncated) CRMP-2 proteins were purified as GST or GST-Glu-tagged proteins, respectively. Binding reactions were performed in protein binding buffer. Monoclonal Glu antibody-saturated Protein G beads (GE Healthcare) carrying various CaV2.2 cytoplasmic loop constructs or GST-

Glu were incubated with rat brain purified CRMP-2 protein in a total reaction volume of 100 µl. For binding assays using synaptosomes the purified proteins were added to synaptosomes. Reactions were incubated end-over-end for 4 h at 4°C, washed three times with a 10-fold excess of binding buffer, and the proteins were eluted in 60 µl of SDS gel buffer and boiled for 5 min, after which 20 µl of each assay was run on SDS-PAGE and analyzed by immunoblotting with CRMP-2. To determine binding affinity (K_d), experiments were performed using a fixed amount of rat brain purified CRMP-2 protein and increasing CaV2.2-GST-Glu fusion proteins.

2.14. Transfection/Infection of Hippocampal neurons

Adherent hippocampal cultures were transfected with cDNAs using Lipofectamine 2000 (Invitrogen) as per the manufacturer's instructions or infected with lentivirus expressing CRMP-2 or scrambled shRNAs. I routinely achieve about 10–15% transfection efficiencies in hippocampal neurons transfected with this method. With lentiviral infections, I have observed up to 95% infection in ≤7 days. Typically, cultured neurons were transfected with equal amounts of different cDNA constructs at 10-12 DIV, and electrophysiology experiments performed two days later.

2.15. Construction of pLL3.7-CRMP-2 shRNA, pLL3.7 CaV2.2 shRNA, and control shRNA lentiviral shuttle vectors

Primers were designed containing the published target sequence against rat CRMP-2 [5′-GTAAACTCCTTCCTCGTGT-3′] (Uchida et al., 2005) or the novel CRMP-2 target sequence

Table 2.4 Primers used to generate shRNA constructs and CRMP-2 mutants

Primer name	Sequence (5'→3')	Restriction Enzyme
CRMP-2 shRNA 1	TGTAAACTCCTTCCTCGTGTTTCAAGAGAACACGAGGAAGGAGTTTACTTTTTTC	*Hpa I* and *Xho I*
	TCGAGAAAAAAGTAAACTCCTTCCTCGTGTTCTCTTGAAACACGAGGAAGGAGTTTACA	
CRMP-2 shRNA 2	TGCCTATTGGCAGCCTTTGATTCAAGAGATCAAAGGCTGCCAATAGGCTTTTTTC	*Hpa I* and *Xho I*
	TCGAGAAAAAAGCCTATTGGCAGCCTTTGATCTCTTGAATCAAAGGCTGCCAATAGGCA	
Scramble shRNA	TGACTTCGATCCTCGTACTTTTCAAGAGAAAGTACGAGGATCGAAGTCTTTTTTC	*Hpa I* and *Xho I*
	TCGAGAAAAAAGACTTCGATCCTCGTACTTTCTCTTGAAAAGTACGAGGATCGAAGTCA	
CRMP-2 KDR	CCACGGGGTAAATAGCTTCCTCGTGTAC	NA
	GTACACGAGGAAGCTATTTACCCCGTGG	
CRMP-2 S522A	CATCAGCTAAGACAGCCCCTGCCAAGCAG	NA
	CTGCTTGGCAGGGGCTGTCTTAGCTGATG	
CRMP-2 S522D	CATCAGCTAAGACAGACCCTGCCAAGCAG	NA
	CTGCTTGGCAGGGTCTGTCTTAGCTGATG	
CRMP-2 T555A	CCCGCCGCACCGCCCAGCGCATC	NA
	GATGCGCTGGGCGGTGCGGCGGG	
CRMP-2 T555E	CCCGCCGCACCGAACAGCGCATC	NA
	GATGCGCTGTTCGGTGCGGCGGG	

For shRNA sequences: blue = target/scramble sequence, green = loop sequence, red = poly A terminator, black = restriction site mimic
NA = not applicable for the sequence (i.e. mutagenic primer)

[5'-GCCTATTGGCAGCCTTTGA-3'] and harboring *Hpa I* and *Xho I* restriction sites. Primers (sense and antisense) were annealed, by heating to 90°C then slowly cooling to RT, and then ligated into the previously digested pLentilox3.7 (pLL3.7; generous gift of our collaborator, Dr. Michael R. Vasko, IUSM) to create the pLL3.7-CRMP-2-v1 and pLL3.7-CRMP-2-v2 expression vectors. Scrambled shRNA sequences with the same percentage of GC but no sequence homology were used to create control lentiviral vectors. Primers are shown in Table 2.3.

2.16. Recombinant lentivirus production

Self-inactivating LV vectors were packaged as described (Zufferey, 2002). Human embryonic kidney (HEK) 293T cells were transfected with a 4-plasmid vector system, *i.e.*, the shuttle plasmid (LV-CRMP-2 shRNA-v1-CMV-EGFP, LV-CRMP-2 shRNA-v2-CMV-EGFP or LV-Scrambled shRNA-CMV-EGFP) and the packaging plasmids pMDMg/pRRE, pRSV-Rev, and pCMV-VSV-G, to provide the VSV-G envelope. Two days post-transfection, the virus-containing medium was collected, and debris removed by centrifugation. Virus was concentrated by ultracentrifugation, and the viral pellet was suspended in DMEM supplemented with 10% FBS, passed through a 0.45 μm filter and frozen at -80°C. The viral titer, as determined by analysis of the virus-associated p24 core protein (QuickTiter Lentivirus Quantification Kit (Cell Biolabs)), was above 2×10^8 TU/ml for all viruses used in this thesis. Virus particles were produced in the SNRI's Viral Production Core Facility staff.

2.17. Electrophysiological recordings of whole cell Ca^{2+} currents from hippocampal neurons

Whole-cell calcium currents were isolated using the following solutions: external (bath) medium (in mM): NaCl 128, KCl 5, $MgCl_2$ 1, $BaCl_2$ 10, D-glucose 10, HEPES-Na 10, and tetraethylammonium-Cl 10; with an osmolarity of 300 mosm/l and pH 7.3; patch electrode intracellular solution: $CsCl_2$ 110, EGTA 10, $MgSO_4$ 1, HEPES(Cs) 25, ATP 2, and GTP 0.2; osmolarity 305 mosm/l, pH 7.4. Tetrodotoxin (1 μM; Alomone Laboratories) and nifedipine (1

μM; Calbiochem, La Jolla, CA) were added in the bath solution to block Na^+ and L-type Ca^{2+} channels. Under these conditions, the primary Ca^{2+} current component should be of N- and P/Q-type with some R-type Ca^{2+} current (Zhang et al., 1993). Cells were held at a holding potential of –80 mV. Current to voltage relations were assessed using a standard, incrementing 10 mV step depolarizing pulses at 1 sec intervals. Leak currents were subtracted on line using a -P/5 procedure. Data was acquired using an EPC-10 amplifier (HEKA Electronics) and analyzed using Pulsefit (v8.5, HEKA) and Origin 7.0 software (Microcal, Northampton, Mass., USA). All experiments were performed by Drs. Cummins, Wang, and Piekarz.

2.18. Cell surface biotinylation of hippocampal and cortical neurons

Hippocampal neurons grown for 10 DIV were transfected with EGFP or CRMP-2–EGFP for 2 days and then processed for biotinylation experiments. Cortical neurons were grown for 7 DIV before being exposed to TAT peptides +/- glutamate/ glycine stimulation. Live cells were incubated with sulfosuccinimidyl 2-(Biotinamido) Ethyl-1,3'Dithiopropionate (EZ-link Sulfo NHS-SS-biotin; 1 mg/mg protein, Pierce) for 30 min at 4°C in cold PBS, pH 8.0. Excess biotin was quenched with PBS containing 100 mM glycine, washed 3× with ice-cold PBS and the pellet was resuspended in RIPA lysis buffer. The resuspended pellet was triturated 10× (25-gauge needle) and centrifuged at 100,000 x g for 20 min. The biotinylated proteins were separated from clear solubilizate by adsorption onto Streptavidin agarose beads (Novagen) for 2–4 h at 4°C. Beads were washed 3–5× with RIPA buffer, and bound biotinylated proteins were gently eluted off the beads with RIPA buffer containing 2% Triton X-100 and 650 mM NaCl by end-over-end incubation for 1 h at 30°C. The biotinylated fraction was subjected to immunoblotting with CRMP-2 and CaV2.2 antibodies. To ensure that the cells remained intact throughout the surface labeling, biotinylation of β-tubulin, a cytosolic protein, was analyzed by immunoblotting.

2.19. glutamate release assay – HPLC

glutamate released into the cytosol in CRMP-2-overexpressing or ablated hippocampal neurons was measured by HPLC separation and electrochemical detection of the o-phthaldialdehyde-mercaptoethanol derivative using modifications of the methods of Donzanti & Yamamoto (Donzanti and Yamamoto, 1988). Using this method, the minimal detectable amount of glutamate is ~2.5 pmol. Following a series of washes in phosphate buffered saline, and a 1 h incubation in normal Tyrode's buffer, 400 µl samples were sequentially collected every 10 min from the cytosol: (1) bathed in Tyrode's buffer, (2) bathed in Tyrode's buffer in the absence or presence of drug, (3) in high K^+ Tyrode's, and (4) re-bathed in Tyrode's buffer. These samples were collected on ice, filtered with 0.22 µm filters (Millipore), and processed for HPLC analyses. The resulting four values represent basal 1, +drug, stimulated, and basal end for each sample. Samples were processed in triplicate and averaged to yield a single value.

Several measures were used to ensure that comparable numbers of viable cells were present in all wells within a dish. The average basal releases of neurotransmitter from each treatment group (in the absence of drug) in an experiment were within 20% of each other. The cells exhibited robust KCl-stimulated neurotransmitter release at least three-fold over the basal levels. Post-treatment basal release (in the absence of drug) was measured in some glutamate assays and was not more than 50% higher than initial basal levels indicating that the release assay did not damage the cells or induce cell lysis. These observations when taken together indicate that similar numbers of neurotransmitter releasing cells were present in all wells within an experiment.

2.20. Culturing Catecholamine A Differentiated (CAD) cells

CAD cells were grown at 37°C and in 5% CO2 (Sarstedt) in Ham's F12/EMEM medium (GIBCO), supplemented with 8% fetal bovineserum (FBS; Sigma) and 1% penicillin/streptomycin (100% stocks, 10,000U/ml penicillin G sodium and 10,000 µg/ml

streptomycin sulfate) (Wang and Oxford, 2000). Cells were passaged every 6-7 days at a 1:25 dilution.

2.21. Generation of CRMP-2 DsRed and CRMP-2 mutants

Mouse CRMP-2 cDNA (*mus musculus* accession # NM_009955.3) was cloned into pDsRed2-N1 using PCR amplification followed by restriction digest and ligation. All mutations were made as previously described using Quikchange II XL (Agilent Technologies, Santa Clara, CA) using primers as listed in Table 2.3 and verified by DNA sequencing.

2.22. Knock-down of gene expression by siRNA

Validated siRNAs against the rat CRMP-2 [5′-ACTCCTTCCTCGTGTACAT-3′] sequence and controls (scrambled sequence with approximately the same percentage of GC but no sequence homology) were used for CRMP-2 knockdown (Invitrogen, Carlsbad, CA). Cells were incubated for 2-4 days with vector-siRNA or scrambled siRNA (50-1000 nM optimized for each condition) and assessment of knock-down was performed by western blot.

2.23. Treatment of hippocampal neurons with kinase inhibitors

P2 hippocampal neurons DIV 9 were treated with either vehicle (0.1% Methyl-2-pyrrolidone; MPL), 10 μM Purvalanol A, or 10 μM Y27632. Purvalanol A is a Cdk5 specific inhibitor where a dose of 10 μM has been previously shown to reduce phosphorylation of CRMP-2 in culture (Cole et al., 2006; Gray et al., 1999; Patrakitkomjorn et al., 2008). Y27632 is a ROCK specific inhibitor with an IC_{50} = 0.7 μM, which was used at 10 μM to ensure complete inhibition (Uehata et al., 1997). Neurons were treated for 1, 2, or 18 hours with the drugs before being washed in PBS and removed from the culture dishes using a cell scrapper. Cells were then lightly spun at 10,000x g for 2 min to pellet the cells, which were subsequently resuspended in mild lysis buffer by gentle pipetting before incubating at 4°C for 10 min with continual agitation.

Lysates were then spun at 10,000x g for 20 min to remove and insoluble material. The supernatant was saved and used in subsequent immunoblotting analysis.

2.24. Fura-2 Ca^{2+}imaging of transfected cortical neurons

E18 cortical neurons were plates on poly D-Lysine coated glass bottom 35 mm dishes (World Precision Instruments). At 7-8 DIV cells were co-transfected with pDsRed-CRMP-2 KDR constructs (WT, S522A, S522D, T555A, T555E) and/or 200 nM CRMP-2 siRNA using Lipofectamine 2000 (Invitrogen). Two days following transfection Ca2+ imaging experiments were performed. Neurons were loaded with 3 μM Fura-2AM (Invitrogen) in Tyrode's buffer (119 NaCl, 2.5 KCl, 2 $CaCl_2$, 2 $MgCl_2$, 25 HEPES pH 7.5, 30 Glucose, concentrations in mM) for 25 min at RT in the dark. Neurons were then washed 3x with Tyrode's buffer and transferred to the imaging stage. Changes in intracellular calcium was measured by digital video microfluorometry with an intensified CCD camera coupled to a microscope and monitored using Nikon Elements Software (Nikon Instruments Inc., Melville, NY). Cells were illuminated with a Lamda DG-4 175 W xenon lamp, and the excitation wavelengths of the fura-2 (340/380 nm) were selected by a filter changer. Cells were observed using DIC prior to beginning experiments to verify cells were healthy and intact. Fura-2AM fluorescence (F340/F380) was measured every 10 seconds in order to minimize photo-bleaching. After a baseline of at least 6 images was obtained, neurons were stimulated by addition of Excitatory Tyrode's buffer to a final concentration of 46.25 mM KCl. Neurons were then imaged for an additional 7 minutes following stimulation. Cells which had either F340 or F380 drop below that of background (an area without any cells present) were disregarded from the analysis.

2.25. Purification of CRMP-2-6xHis

The vector pET28B containing CRMP-2-His, a kind gift from Dr. Rihe Liu (University of North Carolina) was used to express CRMP-2-6xHis in bacteria. CRMP-2-His protein was

grown as previously described for GST-fusion proteins except the bacterial pellet was resuspended in His lysis buffer. The resuspended pellet was then lysed using the microfluidizer and clarified by spinning at 30,000 x g for 45' at 4°C. The supernatant was then filtered through a 0.45 μm syringe filter. The filtered supernatant was loaded onto a Talon™ metal affinity resin (Clontech, Mountain View, CA) column pre-equilibrated with His wash buffer. Column was washed with 2x column volumes of His wash buffer and the eluted with His elution buffer. Elution fractions were separated by SDS-PAGE and fractions containing CRMP-2 were combined. The combined elution fractions were then dialyzed against protein storage buffer. Purified protein concentration was determined using a bovine serum albumin curve on a SDS-PAGE stained by comassie and protein identity was verified by immunoblotting.

2.26. *In vitro* phosphorylation of CRMP-2-His by Cdk5/GSK3β

CRMP-2-6xHiswas phosphorylated *in vitro* as previously described with minor modifications. Purified Cdk5-GST (1 μM) and its cofactor, p25-GST (1 μM) were incubated at room temperature for 2 hours to activate the kinase. CRMP-2-6xHis was then incubated in Kinase assay buffer (100 mM HEPES pH 7.2, 20 mM $MgCl_2$, 2 mM MgATP, 2 mM DTT) along with 200 nM activated Cdk5/p25 and/or 200 nM GSK3β for 1 h at 30°C.

2.27. Co-immunoprecipitation and western blotting using phosphorylated CRMP-2-6xHis

Rat brain lysates were generated by homogenization and gentle sonication in a detergent free modified RIPA buffer (50 mM Tris-HCl, pH 8, 150 mM NaCl, and 1 mM EDTA with protease inhibitors). Lysates were incubated with CRMP-2-6xHis, following phosphorylation, and immunoprecipitated with a 6x-His ab (UC Davis/NIH NeuroMab Facility, clone N144/14) O/N at 4°C with gentle rotation. Samples were then incubated with Protein G-agarose for 2 hr at 4°C before being processed by immunoblotting for CaV2.2 (Origene).

2.28. Purification/enrichment of Ca^{2+} channels from synaptosomes

To prepare a rich source of CaV2.2 for the far-Western analyses (see below), synaptosomes from P1 neonatal rat brains were solubilized with digitonin and enriched by chromatography on WGA-Sepharose as described previously (Westenbroek et al., 1992; Westenbroek et al., 1995). Briefly, 30 PN1 neonatal rat brains were homogenized in 180 ml of 320 mM sucrose with a glass-Teflon homogenizer. After a short centrifugation (5000 rpm, 2 min), the supernatant (SN) was centrifuged (42,000 rpm, 60 min). The membranes were solubilized with 1.2% digitonin, 80 mM sodium phosphate buffer, pH 7.4 for 20 min. Unsolubilized material was removed by the centrifugation as before, and the supernatant (S3) was poured over a 40 ml WGA-Sepharose column (50 ml/h). After incubation for 1 hr at 4°C, the column was washed with 10 column volumes of WGA-column buffer at a flow rate of 50 ml/hr. The glycoproteins bound to the WGA-Sepharose column were eluted with 100 mM N-acetyl-D-glucosamine (Sigma, St. Louis, MO) in the same buffer at a flow rate of 50 ml/hr. Three milliliter fractions were collected and the protein concentration of each fraction was determined by BCA protein assay kit (Thermo Fisher Scientific, Shelbyville, IN). To further enrich for Ca^{2+} channels, WGA-column fractions were incubated for 4 hr on ice with 200 µl of heparin-agarose 85. The resin was washed four times with 0.2% CHAPS, 10 mM Tris-HCl, pH 7.4, and once with 10 mM Tris-HCl, pH 7.4. Ca^{2+} channels were gently extracted for 30 min at 50°C with100 µl of Heparin extraction buffer.

2.29. Peptide spots arrays and Far Westerns

Peptide arrays (10-15 mers) spanning the entire length of rat CRMP-2 were constructed using the SPOTS-synthesis method (Edmondson and Roth, 2001; Hall, 2004; Schechtman et al., 2003; Wu et al., 2007). Standard 9-fluorenylmethoxy carbonyl (Fmoc) chemistry was used to synthesis the peptides on cellulose membranes prederivatized with a polyethylene glycerol spacer (Intavis AG). Fmoc protected and activated amino acids (Intavis) were spotted in 20-30 arrays on

150 mm by 100 mm membranes using the Intavis MultiPep robot. Membranes were probed in a far-Western manner with an antibody against CaV2.2 (Calbiochem Inc, La Jolla, CA). Briefly, Peptides (10-15–mers) were immobilized to nitrocellulose membrane which was then soaked in 10 mM CAPS pH 11.0 and 20% methanol for 30 min, washed once with TBST, and then blocked for 1 h at RT with gentle shaking in TBST containing 5% non-fat milk and finally incubated with a purified synaptosome fraction enriched in Ca^{2+} channels for 1 h at RT with gentle shaking. Next, the membrane was incubated in primary antibody for CaV2.2 for 2 h at RT with gentle shaking, followed by washing with TBST. Finally, the membrane was incubated in secondary antibody (horseradish peroxidase-conjugated goat anti-rabbit; 1:10,000) for 45 min, washed for 30 min in TBST and developed using enhanced chemiluminescence.

2.30. Peptides

TAT-Control (YGRKKRRQRRRWEAKEMLYFEALVIE (TAT sequence denoted in underlined text); a random sequence with no homology to any known sequence) TAT-CBD3 (YGRKKRRQRRRARSRLAELRGVPRGL) were synthesized by Antagene Inc. (Sunnyvale, CA).

2.31. Surface plasmon resonance (SPR)

Binding analyses between TAT-CBD3 or TAT-Control peptides and CaV2.2 L1- or Ctdis-GST fusion proteins was determined by surface plasmon resonance using a BIAcore3000 instrument (Biacore AB, Uppsala, Sweden)(Richman et al., 2005). Briefly, binding assays were performed using HBS-EP buffer as the running buffer. The CaV2.2 L1- and Ct-dis GST fusion proteins were diluted in HBS-EP buffer and injected at a 10 μl/min flow rate over four flow cell surfaces simultaneously using the KINJECT command. Surface regeneration was performed by 10-μl injections of 0.05% SDS in HBS-EP buffer at a 20 μl/min flow rate. Background binding to a negative control peptide surface (control) was subtracted from all binding curves using

BIAevaluation software version 3.0 (BIAcore Inc.) and plotted using GraphPad Prism version 4.0 (Graph-Pad Software Inc.).

2.32. Isolation and maintenance of sensory neurons for electrophysiology

DRG from young adult rats (~150g) were dissociated and cultured as described previously (Koplas et al., 1997). Spinal cords were rapidly removed from rats before DRGs were visually identified and isolated, and then dissociated by a combination treatment with a dispase/collagenase cocktail and mechanical disruption through a series of fire-polished glass pipettes with a decreasing inner tip diameter. The resulting suspension of single cells was plated on poly-D-lysine-coated coverslips and maintained in Dulbecco's modified Eagle's medium (DMEM) (Gibco, Invitrogen) supplemented with 10% fetal bovine serum (FBS) (Hyclone) and 100 units/ml penicillin and 100 μg/ml streptomycin for 12-16 hours at 37°C under 5% CO_2.

2.33. Whole-cell patch-clamp recordings from sensory neurons

Whole-cell voltage recordings were performed at room temperature on primary sensory neurons using an EPC 10 Amplifier (HEKA Electronics, Germany). Electrodes were pulled from thin-walled borosilicate glass capillaries (Warner Instruments, Hamden, CT) with a P-97 electrode puller (Sutter Instrument, Novato, CA) such that final electrode resistances were 2–3 MΩ when filled with internal solutions. The internal solution for recording Ca^{2+} currents contained (in mM): 150 $CsCl_2$, 10 HEPES, 5 Mg-ATP, and 5 BAPTA (pH 7.2 with KOH). The external solution contained (in mM); 110 N-methyl glucamine (NMG), 2 $CaCl_2$, 30 TEA-Cl, 10 HEPES, and 10 glucose; 1 μM TTX and 1 μM Nifedipine were added just before use to block voltage-gated Na^+ and L-type Ca^{2+} channels, respectively. Whole-cell capacitance and series resistance were compensated with the amplifier. Series resistances compensation (70–80%) was routinely applied. Cells were considered only when the seal resistance was more than 1G Ω and the series resistance was less than 10 MΩ. Linear leak currents were digitally subtracted by P/4.

Signals were filtered at 10 kHz and digitized at 10-20 kHz. Analysis was performed using Fitmaster and origin8.1 (OriginLab Corporation, MA, USA). For activation curves, conductance (G) through ion (Ca2+) channels was calculated using the equation G= I/(Vm −Vrev), where V_{rev} is the reversal potential, V_m is the membrane potential at which the current was recorded and I is the peak current. Activation and inactivation curves were fitted to a Boltzmann function G/Gmax = $1/\{1+\exp[(V-V_{50})/k]\}$, where G is the peak conductance, Gmax is the fitted maximal G, V_{50} is the half-activation voltage, and k is the slope factor. All experiments were performed by Drs. Zhu and Wang.

2.34. Release of iCGRP from rat spinal cord slices

The release of iCGRP from spinal cord slices was performedby Dr. Duarte using a modification of the technique previously described (Chen et al., 1996). Briefly, rats were sacrificed using CO_2 asphyxiation and decapitation and the spinal cord from each animal was removed and a 2 cm section of the lumbar enlargement was weighed and chopped parasagitally and transversely into 300 μm cross-sections using a McIllwain Tissue Chopper. The sections from each spinal cord were placed into individual chambers and perfused at a flow rate of 0.5ml/min with a HEPES buffer, consisting of HEPES 25 mM, NaCl 135 mM, KCl 3.5 mM, $MgCl_2$ 1 mM, $CaCl_2$ 2.5 mM, dextrose 3.3 mM, bovine serum albumin 1%, ascorbic acid 200 μM, phe-ala 100 μM, phenylmethanesulfonyl fluoride (PMSF) 10 μM and bacitracin 20 μM, aerated with 95% O_2–5% CO_2, pH 7.4–7.5, and maintained at 36–37°C. After 30 min, 1.5 ml samples were collected into test tubes containing 75 μl of 1 M MES buffer (pH 6.7–6.9) every 3 min. Basal release was established by first perfusing the tissue with HEPES buffer for 9 min and then with HEPES buffer containing 10 or 20 μM of the TAT-Control peptide or TAT-CBD3 for 9 min. To evoke iCGRP release, tissue was then perfused for an additional 9 min with HEPES buffer containing 500 nM capsaicin with 10 or 20 μM of the TAT-Control or TAT-CBD3. To demonstrate a return to basal release after stimulation, the tissue was perfused with HEPES buffer

alone for another 15 min. Evoked release is determined by subtracting the values obtained for stimulated release from those obtained for basal release. After the release protocol was complete, the spinal cord tissue was recovered and homogenized in 4 ml 0.1 N HCl. The homogenate was centrifuged at 3000 x g for 20 min at 4°C and the supernatant was serially diluted with HEPES buffer and assayed for iCGRP by RIA, as previously described (Chen et al., 1996). The total peptide content was the amount of iCGRP released during the perfusion and the amount remaining in the tissues. This value was used to determine the amount of release as % of total content.

2.35. ddC model of peripheral neuropathy

Hyperalgesia and allodynia were established by a single injection (25 mg/kg) of the antiretroviral drug 2′,3′ -dideoxycytidine (ddC, Sigma) given i.p. A single administration of ddC produced a significant bilateral decrease in paw withdrawal threshold to von Frey hair stimulation from post-injection day (PID) 3 through the last day of testing at PID42 58. The von Frey test was performed on the area of the hind paws as previously described (LaMotte et al., 1998; Ma et al., 2003; Song et al., 1999; Zhang et al., 1999). Briefly, the rat was placed on a metal mesh floor and covered with a transparent plastic dome where the animal rested quietly after an initial few minutes of exploration. Animals were habituated to this testing apparatus for 15 minutes a day, two days prior to pre-injection behavioral testing. Following acclimation, each filament was applied to six spots spaced across the glabrous side of the hind paw; two distinct spots for the distribution of each nerve branch (saphenous, tibial and sural). Mechanical stimuli were applied with seven filaments, each differing in the bending force delivered (10, 20, 40, 60, 80, 100, and 120 mN), but each fitted a flat tip and a fixed diameter of 0.2 mm. The force equivalence of mN to grams is: 100 mN=10.197 grams. The filaments were tested in order of ascending force, with each filament delivered for 1 second in sequence from the 1st to the 6th spot alternately from one

paw to the other. The interstimulus interval was 10-15 seconds. A cutoff value of 120 mN was used; animals that did not respond at 120 mN were assigned that value.

Measurements were taken on 3 successive days before rats were subjected to either TAT-Control or TAT-CBD3. Stimuli were applied randomly to left and right hind paws to determine the stimulus intensity threshold stiffness required to elicit a paw withdrawal response. The incidence of foot withdrawal was expressed as a percentage of six applications of each filament as a function of force. A Hill equation was fitted to the function (Origin version 6.0, Microcal Software) relating the percentage of indentations eliciting a withdrawal to the force of indentation. From this equation, the threshold force was obtained and defined as the force corresponding to a 50% withdrawal rate. A threshold that exhibits at least a -20 mN difference from the baseline threshold of testing in a given animal is representative of neuropathic pain. Threshold values were statistically analyzed for each foot separately and the significance of differences between the average of at least two pre-injection tests and the mean obtained for each post-injection test. In all tests, baseline data were obtained for the ddC-treated and sham-treated groups before drug or vehicle administration. Within each treatment group, post-administration means were compared with the baseline values by repeated measures analyses of variance (RMANOVA) followed by post hoc pairwise comparisons (Student-Newman-Keuls Method). A probability level of $p < 0.05$ indicates significance. These experiments were performed by Matt Ripsch.

2.36. Rotarod test for motor coordination

The rotarod test was performed as described previously (Nakamura et al., 1999; Onyszchuk et al., 2008) with slight modifications. The latency to fall off a rotating rod was measured at two different rotational accelerations (fast and slow). The rotarod device (IITC Life Science, Inc., Woodland Hills, CA, USA) consists of a metal rod with hard plastic drums (diameter: 1.25 in) in each of five individual lanes. For slow acceleration, the device was

accelerated from 1 rpm to 18 rpm over 90 seconds, with each trial lasting a maximum of 120 seconds. For fast acceleration, the device was accelerated from 1 rpm to 30 rpm over 90 seconds, with each trial lasting a maximum of 120 seconds. The trials ended when the mouse (C57BL6) either fell off the rod or clung to the rod as it made one complete rotation. The rotarod tests were performed before the injection to score the baseline latencies for each animal. These trials also served to acclimate the animals to the test paradigm. Four trials each of the fast and slow acceleration paradigms were performed, and the average of the two middle latencies was taken as the baseline. Following intraperitoneal (i.p.) injection of vehicle or peptides (10mg/kg or 50mg/kg), the mice were tested with three trials each of fast and slow acceleration. All experiments and analyses were done in a double-blind manner by Dr. Liu.

2.37. Morris water maze test of spatial/reference memory

The Morris water maze test was used to test spatial memory(D'Hooge and De Deyn, 2001). The maze consisted of a plastic pool (100 cm in diameter and 60 cm in depth) filled with water to a depth of 26.5 cm, with a clear Plexiglas stand (10 cm in diameter and 26 cm in height [i.e., 0.5 cm below the water's surface]) used as the hidden goal platform. The mice were trained prior to the injection for 4 consecutive days (4 trials/day). For each daily block of four trials, the mice were placed in the pool facing the wall. Trials were initiated from each of the four possible start locations (north, east, south, west) in a randomized manner. A maximum of 60 sec was allowed for each mouse to find the hidden platform. If the mouse failed to find the platform within the allotted time, it was placed on the platform by the experimenter where it remained for 30 sec before being placed in a heated incubator between trials (4-min inter-trial interval). Mice were excluded from the study if their average latency to locate the platform on day 4 of the trials was greater than 50 sec. As a control for nonspecific deficits such as visual processing and motivation, additional trials were performed with the hidden platform positioned below a ball,

which served as a marker. All experiments and analyses were done in a double-blind manner by Dr. Liu.

2.38. Excitotoxic stimulation by glutamate + glycine/D-serine

E18-19 cortical neurons (7-8 DIV) grown in 96, 12, or 6 plates were stimulated for 30 minutes in serum free media in a final volume of 100, 1000, or 2000 μL respectively. The excitotoxic insult was achieved by addition of 200 μM L-glutamate and 20 μM glycine or 100 μM D-serine (an NMDAR co-agonist (Mothet et al., 2000)). Following stimulation, all media was removed from neurons and replaced with fresh complete media. For biochemical experiments cells were harvested at the time point indicated. For cell viability experiments cells were grown for 24 hours under normal growth conditions before cell viability was measured. The cell viability of cultured neurons was quantified using the CellTiter 96® AQ_{ueous} One Solution Cell Proliferation Assay (MTS) from Promega. Following the 24 hour growth period MTS reagent was added to each well and incubated for 1 hour at 37°C. MTS is a tetrazolium analog that is converted to the water-soluble blue absorbing formazan by the endogenous reductases of living cells (Hansen et al., 1989). The formation of formazan following incubation with MTS reagent was then measured (*Viktor3v*, Perkin Elmer) by recording the absorbance at 490 nm. Control wells containing media only (no cells) were used to subtract the background absorbance from the neuronal culture media.

2.39. *In vitro* calpain cleavage

Lysates were freshly prepared from E18-19 brains using a mild lysis buffer. Rat brains were homogenized then allowed to lyse for 30 minutes before clarifying by centrifugation at 15,000 x g for 20 minutes. The soluble protein fraction was removed and used the same day for cleavage experiments. Lysates were incubated with TAT-CBD3 or MDL28170 for 10 minutes prior to addition of 20 mM $CaCl_2$. Lysates were then incubated at RT for 30 minutes to allow for

proteolytic cleavage. Reactions were stopped by addition of SDS loading buffer and then processed for immunoblotting.

2.40. *In vitro* measurement of calpain activity

Lysates were prepared as described above and incubated for 10 minutes with vehicle (0.2% DMSO), TAT-CBD3 (10 μM) or MDL-28170 (50 μM) prior to addition of 20 mM $CaCl_2$. The fluorogenic calpain substrate *t*-Boc-Leu-Met-CMAC (*t*-Boc, 10 μM) was then added to the lysates. Samples were then transferred to a 96 well plate and incubated for 30 minutes at 37°C. Cleavage of *t*-Boc was assayed by measuring fluorescence using a plate reader (*Viktor3v*, Perkin Elmer, Covina, CA) with a 355 nm excitation filter and a 460 nm emission filter (Kennett et al., 2004). Wells containing t-Boc alone were used to subtract background fluorescence. Background subtracted values were then normalized to vehicle treated samples.

2.41. Calcium imaging of glutamate and NMDA evoked Ca^{2+}-fluxes

Cortical neurons were loaded at 37°C with 2.6 μM Fura-2FF-AM (Kd=25 μM, λ_{ex} 340, 380 nm/λ_{emi} 512 nm) or Fura-2-AM (Kd=224 nM) to follow changes in $[Ca^{2+}]_c$ in standard bath solution. Fluorescence imaging was performed with an inverted microscope, Nikon Eclipse TE2000-U, using objective Nikon Super Fluor 20× 0.75 NA and a Photometrics cooled CCD camera $CoolSNAP_{HQ}$ (Roper Scientific, Tucson, AZ) controlled by MetaFluor 6.3 software (Molecular Devices, Downingtown, PA). The excitation light was delivered by a Lambda-LS system (Sutter Instruments, Novato, CA). The excitation filters (340±5 and 380±7) were controlled by a Lambda 10-2 optical filter change (Sutter Instruments, Novato, CA). The excitation filters (340±5 and 380±7) were controlled by a Lambda 10-2 optical filter change (Sutter Instruments, Novato, CA). Fluorescence was recorded through a 505 nm dichroic mirror at 535±25 nm. To minimize photobleaching and phototoxicity, the images were taken every 15 seconds during the time-course of the experiment using the minimal exposure time that provided

acceptable image quality. The changes in $[Ca^{2+}]_c$ were monitored by following a ratio of F340/F380, calculated after subtracting the background from both channels. $[Ca^{2+}]_c$ was calculated using the Grynkiewicz equation using K_D= 25 μM for Fura-2FF and K_D= 224 nM for Fura-2 (Grynkiewicz et al., 1985). All of these experiments were performed by Tatiana Brustovetsky.

2.42. SEP fluorescent microscopy

E18-19 cortical neurons, transfected with NR2B-SEP DNA using lipofectamine 2000, were imaged on a Nikon Ti swept-field confocal microscope using a 60x, 1.4 numerical aperture lens and a standard fluorescein isothiocyanate cube with a cooled Cascade 512B digital camera (Photometrics, Tucson, AZ). Neuronal somatic fluorescence was measured by digital video microfluorometry with an intensified CCD camera coupled to a microscope and Nikon Elements Software (Nikon Instruments Inc., Melville, NY). Cells were bathed and all drugs were diluted in extracellular solution. Experiments were completed at room temperature and images were taken every 15 (spines) or 10 (soma) seconds to prevent photo-bleaching. After completing each imaging experiment SEP fluorescence was quenched by the addition of acetic acid (final pH 5.5). Finally cellular integrity was verified by differential image contrast microscopy.

2.43. Hippocampal neuron whole cell voltage-clamp electrophysiology of NMDA Ca^{2+}-currents

Whole-cell voltage-clamp recordings were performed on rat hippocampal neurons (DIV7-11) days in culture (Khosravani et al., 2008), at room temperature using an Axopatch 200B amplifier (Axon Instruments, Union City, CA), with a holding potential of -60 mV. The NMDAR external solution contained (in mM): 140 NaCl, 5 KCl, 1 $CaCl_2$, 25 HEPES and 33 D-glucose, pH adjusted to 7.4 with NaOH. The external solution was supplemented with 0.5 μM TTX (Tocris Bioscience, UK), 100 μM picrotoxin, 100 μM glycine. The internal pipette solution was composed of (in mM): 120 CsCl, 35 CsOH, 11 EGTA, 1 $CaCl_2$, 2 $MgCl_2$ and 10 HEPES, 4

ATP (tris salt) and 20 phosphocreatine (tris salt) and creatine phosphokinase 50 U/ml, pH adjusted to 7.3 with CsOH.

Drug delivery was controlled by a Valvelink8.2 perfusion system (Automate Scientific Inc., Berkeley, CA) with a pressurized superfusion device to achieve fast switching of solution. NMDA current was evoked by application of NMDA (50 μM, Tocris Bioscience) for 2 s every 30 s. During experiments, control NMDA current was stabilized for 5 mins (10 traces, with peak current fluctuation within 5%) before TAT-CBD3 application. Data were analyzed using Clampfit (Axon Instruments), Origin 7 (OriginLab) and Prism 5 (GraphPad Software Inc.). All of these experiments were performed by Dr. Haitou You.

2.44. Co-immunoprecipitations with CRMP-2 and NR2B

Co-immunoprecipitations were performed on freshly prepared or flash frozen lysates. For co-immunoprecipitations in the presence of TAT peptides, lysates were incubated with 100 μM TAT-Control or TAT-CBD3 or an equal volume of vehicle (DMSO) for 1 hour at 37°C prior to addition of the primary antibody. Lysates were incubated with the primary antibody of interest under gentle agitation for 2 hours or overnight at 4°C. Samples were then clarified to remove any additional precipitate and incubated with Protein A/G Plus for rabbit primary antibodies or Protein G Plus agarose for mouse primary antibodies (Santa Cruz Biotechnology) for 2 hours at 4°C. The immune-captured complexes were then washed three times with lysis buffer before being boiled in equal volumes of SDS loading dye (Invitrogen). Samples were then processed by immunoblotting.

2.45. P2 membrane preparation from Rat brains

Enrichment for the plasma membrane fraction of rat brains was performed as previously described (Aarts et al., 2002). Approximately 10 PN2 rat brains were homogenized in Sucrose homogenization buffer with 2 mM $NaOV_4$. The homogenate was spun at 800x g for 10 min to

remove any insoluble homogenate. The supernatant was then spun at 11,000x g for 20 min producing a pellet consisting of enriched plasma membranes. The pellet was resuspended in Sucrose homogenization buffer and quantified. The resuspended pellet was then diluted and 200 µg/90 µl at a final concentration of 1% sodium deoxycholate and 0.1 % Triton X-100 before incubating at 37°C for 30 min. The lysates was then spun at 100,000x g for 10 min to clarify the lysates. Aliquots of 200 µl were then flash frozen on dry ice and stored at -80°C.

2.46. Statistical Analyses

Differences between means were compared by either paired or unpaired two-tailed Student's *t*–tests or an analysis of variance (ANOVA) when comparing multiple groups. With the ANOVA, if a significant difference is determined, then either Tukey's or Dunnett's post-hoc was performed unless otherwise noted. Data is expressed as mean±S.E.M, with $p < 0.05$ considered as the level of significance. Imaging (ICA/ICQ) values were either tested for two means between conditions (P) or for one mean for a difference from 0 ($P_{=0}$). Each hippocampal ICQ value reflects the mean of two determinations from image planes at least 400 nm apart (two *z* axis increments). The normal approximation to the sign test was used for statistical tests of ICQ values for single experiments.

2.47. Accession numbers

Accession numbers for the clones used in this thesis are: NM_147141 for α1B (CaV2.2), NM_009955.2 for CRMP-2, AB012697.2 for Munc18-1, and NM_012574 for NR2B.

CHAPTER 3. REGULATION OF CaV2.2 BY CRMP-2

3.1. Introduction

The role of CRMP-2 in synaptic regulation has yet to be properly explored. It is known that CRMP-2 is important for axon path finding and neuronal polarity (Arimura et al., 2004; Schmidt and Strittmatter, 2007). By inference then, it is possible that CRMP-2 may be important for proper synapse formation given that neurons must polarize and send their axons to the proper dendritic fields to form intended synaptic connections. In Chapter 4, I will focus on CRMP-2 and the post-synaptic NMDAR which has been proposed to be modulated by CRMP-2 (Al-Hallaq et al., 2007; Bretin et al., 2006), which, at the time I began my dissertation work, was the only report that provided a potential link between CRMP-2 and modulation of synaptic function. One additional study reported the presence of a closely related CRMP-4L (long isoform) homolog in synaptic vesicles (Quinn et al., 2003). Thus, a goal of my thesis work was to focus on the potential role of CRMP-2 in synaptic biology.

Proteomic studies conducted by Dr. Khanna's laboratory and others had identified CRMP-2 as a putative interacting partner of CaV2.2 (Khanna et al., 2007c; Muller et al., 2010). Enriched at functional release sites, CaV2.2 forms part of a large macromolecular complex, which facilitates efficient neurotransmitter release. Identification and analyses of a litany of protein-protein interactions within the nerve terminal have demonstrated a functional coupling between presynaptic Ca^{2+} channels and the transmitter release machinery (Catterall and Few, 2008; Davies and Zamponi, 2008; Kisilevsky and Zamponi, 2008b; Stanley, 1997). Although neurotransmission was not affected in CRMP-1 knockout mice (Su et al., 2007), long-term potentiation, spatial learning and memory were affected in both CRMP-1 and CRMP-3 knockout mice (Quach et al., 2008; Su et al., 2007), suggesting a role for CRMPs in neurotransmission as well as synaptogenesis. As potential binding partners, CRMPs could affect neurotransmission by either a physical interaction with the synaptic machinery or CaV2.2 itself. Therefore, in this Chapter I sought out to confirm that CRMP-2 was indeed a *bona fide* binding partner of CaV2.2, determine the functional consequence of this interaction, determine how

signaling between the two proteins occurred and if it affected release of neurotransmitter. Given the unequivocal ties between CaV2.2 and chronic pain treatments (see §1.1.10), I also sought to target the interaction between CRMP-2 and CaV2.2 with the idea that disruption of this interaction could be an alternative approach to discovering useful tools for pharmacological investigations of calcium channels as well as potential pharmacotherapeutics for management of chronic pain. Part of the work in this Chapter has been previously presented in several publications (Brittain et al., 2011b; Brittain et al., 2009; Brittain et al., 2012b).

3.2. Subcellular and synaptic localization of CRMP-2 and CaV2.2

CRMP-2 is extensively expressed in neurons, although the exact subcellular localization as it relates to the synapse has not been described (Wang and Strittmatter, 1996; Wang and Strittmatter, 1997). Therefore, in order to determine if CRMP-2 is able to interact with CaV2.2 I first sought to determine if it is present in the proper subcellular domains. Synaptic structures can be enriched from brain tissue using differential centrifugation and a discontinuous sucrose gradient yielding a so-called "synaptosome" (Huttner et al., 1983; Takamori et al., 2006). As expected the synaptosome fraction (P2') isolated from neonatal PN1 rat brain contained synaptic proteins including CaV2.2, the AMPAR subunit GluR2, and Munc18 (Figure 3.1A). All five CRMP proteins were present in synaptosomes, with CRMP-2 being relatively more abundant than the other CRMPs. This finding shows that CRMP-2 is present in the synaptosome and therefore in the same subcellular compartment as CaV2.2. Next, sucrose density gradient fractionation of PN1 rat brains revealed co-sedimentation of CRMP-2 and CaV2.2 in both cholesterol rich/cytosolic (*lanes 5–8*, Figure 3.1B, C) and membrane fractions (*lanes 9–12*, Figure 3.1B, C), consistent with cytosolic and membrane distribution of both proteins.

Now having shown that CRMP-2 is present in some of the same subcellular fractions as CaV2.2 I wanted to further delve into its localization within the synapse. In order to study this I employed a technique to separate the synaptic and extrasynaptic regions of the synaptosome.

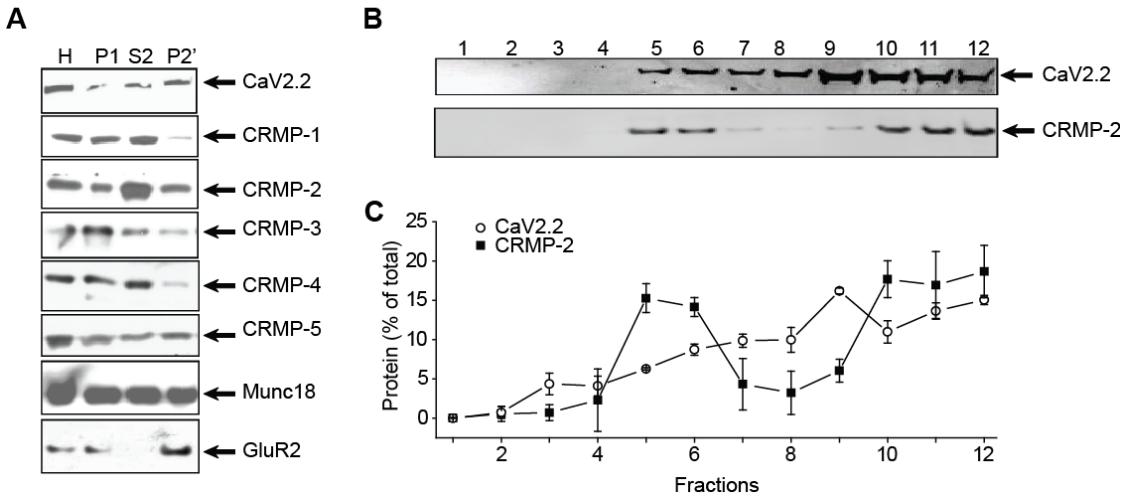

Figure 3.1. Neuronal subcellular localization of CRMP-2

(**A**) Western blots of CaV2.2, CRMPs 1-5 and synaptic proteins Munc18 and the glutamate receptor 2 subunit (GluR2) in homogenate (H), pellet (P1), supernatant (S2) and synaptosomes (P2') of PN1 rats. (**B, C**) CRMP-2 and CaV2.2 are present in both cytosolic (lanes 5–8) and membrane (lanes 9–12) fractions in sucrose density gradients from PN1 rat brain synaptosomes. Summary of fractionation data represents mean ± SEM of four experiments.

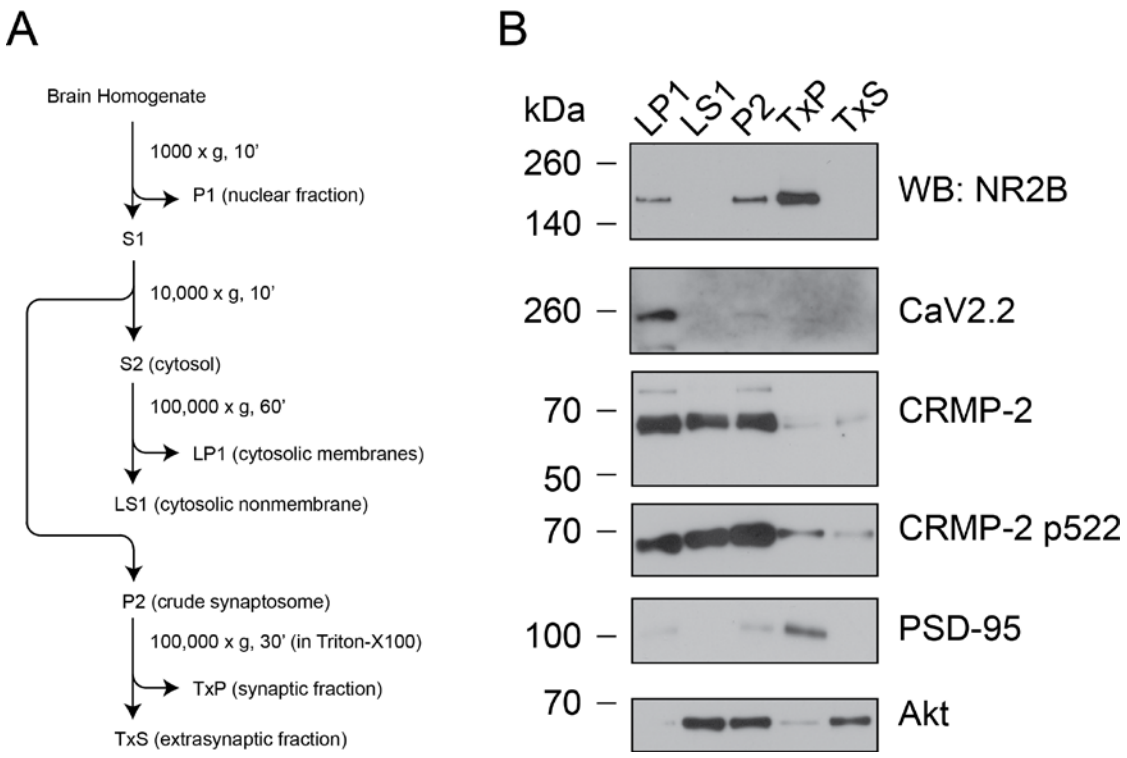

Figure 3.2. Synaptic and Extrasynaptic localization of CRMP-2

(**A**) Synaptic and extrasynaptic fractions of PN1 rat brains were isolated using differential centrifugation along with the Triton-X100 insolubility property of synaptic PSD-95. (**B**) Immunoblots display protein localization to the various neuronal fractions. An equal amount of protein from each fraction was loaded to compare the relative amount of protein present in the various fractions. Fractions and percent loaded are as follows: LP1 (~0.8%): intracellular membranes, LS1 (~0.1%): cytosol non-membrane, P2 (~0.3%): Synaptosome, TxP (~1.2%): synaptic fraction, TxS (~0.4%): extrasynaptic, kDa: kilo-Daltons.

Using differential centrifugation and detergent selective sedimentation the PSD-95 associated synaptic fraction can be isolated. PSD-95 is known to be insoluble in Triton-X100 that can be used to isolate the extrasynaptic fraction from the synaptic (Cotman and Taylor, 1972; Matus and Taff-Jones, 1978). This method was verified by the selective presence of PSD-95 in the Triton X100 insoluble pellet (TxP) otherwise known as the synaptic fraction (Figure 3.2). The NR2B subunit of the NMDAR was also found primarily in the synaptic fraction. As would be expected given its role in synaptic transmission, CaV2.2 was found in the synaptic fraction. Both of these Ca^{2+} channels were not present in the cytosolic light soluble fraction (LS1), but were in the light pellet fraction (LP1) that is composed of intracellular membranes. Interestingly, CRMP-2 was present, in varying degress, in all fractions including the membrane and cytosolic fractions as well as the synaptic and extrasynaptic fractions although at much lower quantities.

3.3. Biochemical complex containing CaV2.2 and CRMP-2

Finally, to confirm that CRMP-2 has a *bona fide* interaction with CaV2.2, standard co-immunoprecipitations and immunoblotting were performed. Precipitation of CaV2.2 with a polyclonal CaV2.2 antibody or a polyclonal CRMP-2 antibody from PN1 rat brain synaptosomes reliably precipitated the associated protein (Figure 3.3A). No proteins were observed in control immunoprecipitations using rabbit isotype-specific IgG antibodies. The interaction of CaV2.2 and CRMP-2 was also observed in hippocampal neurons cultured for 14 DIV (Figure 3.3B). Thus, biochemical evidence clearly shows that CRMP-2 and CaV2.2 co-exist in a complex.

Immunocytochemistry on PN1 rat hippocampal neurons revealed the presence of CRMP-2 in soma, dendrites, neurite shafts, as well as in punctate structures. An overlap was observed in the staining patterns for CRMP-2 and CaV2.2 in the soma as well as in presynaptic varicosities (Figure 3.3C). ICA was used to quantitatively assess the colocalization (Khanna et al., 2007a; Khanna et al., 2007b; Khanna et al., 2006a). This method tests if staining for two proteins co-vary, as they should if the two proteins are part of the same complex. This test generates an ICQ,

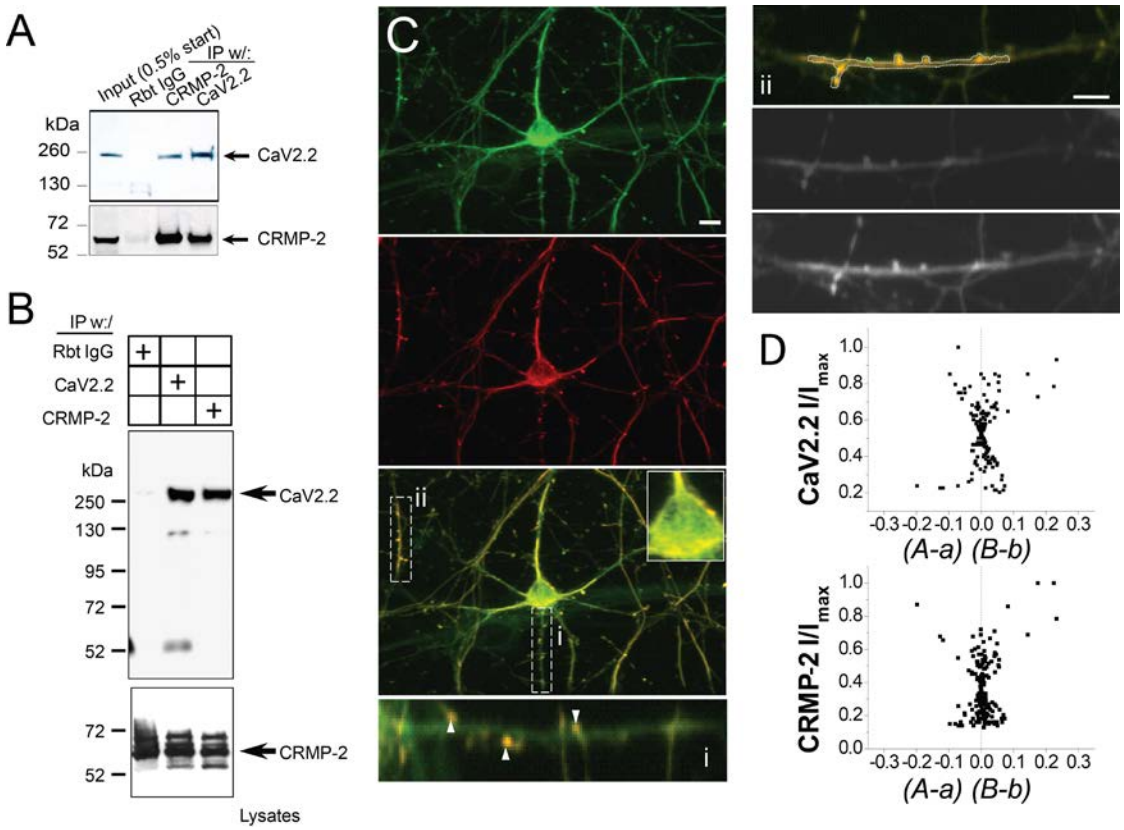

Figure 3.3. CRMP-2 is in the same biochemical complex as CaV2.2

(**A**) CRMP-2 and CaV2.2 co-immunoprecipitate reciprocally from purified synaptosomes. (**B**) Immunoblot with CaV2.2 antibody showing that CRMP-2 and CaV2.2 co-immunoprecipitate from purified hippocampal neurons grown for 14 days *in vitro* (DIV). The bottom blot, probed with CRMP-2 antibody, represents 10% of the lysates used in the IPs. (**C**) Double labeling of endogenous CRMP-2 (green) and CaV2.2 (red) in cultured hippocampal neurons. Enlarged regions show co-localization of both proteins at the cell surface of the soma and in punctate structures along neurites (i, ii). (**D**) Merged and black and white confocal images of region ii from a. Quantitative co-localization analysis shows a moderate to strong skew in the intensity correlation analysis (ICA) plots for CaV2.2 and CRMP-2, indicative of staining pairs that vary in synchrony. The intensity correlation quotient (ICQ) of the region in ii was 0.178. Rbt IgG, isotype-specific rabbit IgG (control) antibody.

which ranges from –0.5 to +0.5 and can be used for statistical comparison. ICA plots of CaV2.2 and CRMP-2 staining of the soma cell surface, in the axons, and in boutons/dendritic spines (see examples in Figure 3.3 C, D) exhibited varying degrees of positive skews, suggesting strong to moderate levels of covariance. The mean ICQ values were 0.078±0.017 (axons, n=12, $P_{=0}$ <0.001), 0.038±0.052 (surface of soma, n=7, $P_{=0}$ <0.001), and 0.245±0.073 (boutons/dendritic spines, n=9, $P_{=0}$ <0.001).

3.4. CaV2.2 and CRMP-2 regions responsible for CaV2.2-CRMP-2 complex

To identify regions of CRMP-2 and CaV2.2 that are responsible for the interaction between CRMP-2 and CaV2.2, *in vitro* pull down assays were performed to assess binding. First, I purified bacterially expressed GST-fusion proteins of full length CRMP-2 or fragments and incubated them with PN1 rat synaptosomes. To ensure that the synaptosomes contained a sufficient amount of CaV2.2, the channels were partially purified with wheat-germ agglutinin as described by Catterall and colleagues (Westenbroek et al., 1992) followed by enrichment with heparin-agarose. The *in vitro* complexes were recovered by incubation with glutathione sepharose beads, washed extensively and immunoblotted with a CaV2.2 antibody. CaV2.2 bound to full-length CRMP-2 (Figure 3.4A, B). Within CRMP-2, three regions of interactions were determined: a region in the CRMP-2 N-terminus (residues 94-166), a region in the middle of the protein (residues 212–297), and one near the C-terminus of the CRMP-2 protein (residues 479-500), proximal to the microtubule binding domain ((Figure 3.4B). These regions, designated CaV binding domains (CBDs) 1–3 are identified in the crystal structure of CRMP-2 tetramer (RCSB databank PDB code: 2GSE; Figure 3.4C) (Deo et al., 2004); for clarity, the CBDs are identified only on monomer 1. Interestingly, the CBD3 interaction lies near the oligomerization domain of the tetrameric CRMP-2 protein (Figure 3.4C). A large portion of CBD2 appears to be buried within the CRMP-2 tetrameric structure and may interfere with binding of the other CBDs

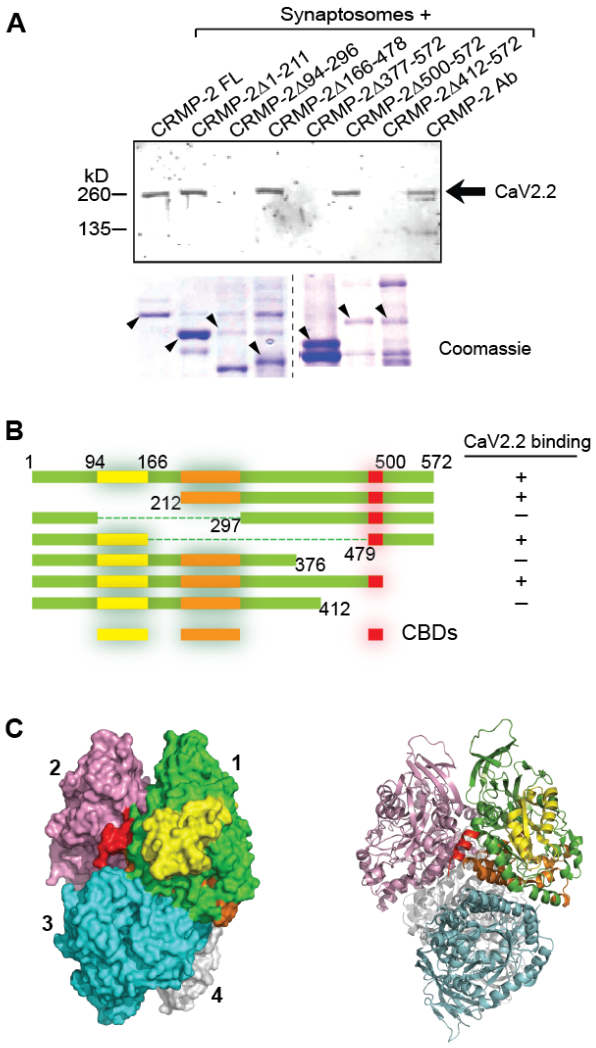

Figure 3.4. Mapping binding sites between CRMP-2 and CaV2.2

(**A**) Binding experiments pulling down CaV2.2 from synaptosomes using CRMP-2 GST truncation mutants. Bound proteins were analyzed by Western blotting with an antibody for CaV2.2 and CRMP-2 GST mutants visualized by coomassie staining. (**B**) Three CaV binding domains (CBDs) on CRMP-2 were observed – residues 94-166, designated CBD1; yellow, residues 212-297, CBD2; orange, residues 479-500, CBD3; red). (**C**) These regions (CBD1, CBD2, and CDB3) are identified in the crystal structure of CRMP-2, regions present in monomer 1 only (RCSB databank PDB code: 2GSE). Images were rendered using PyMol (v. 0.99).

A

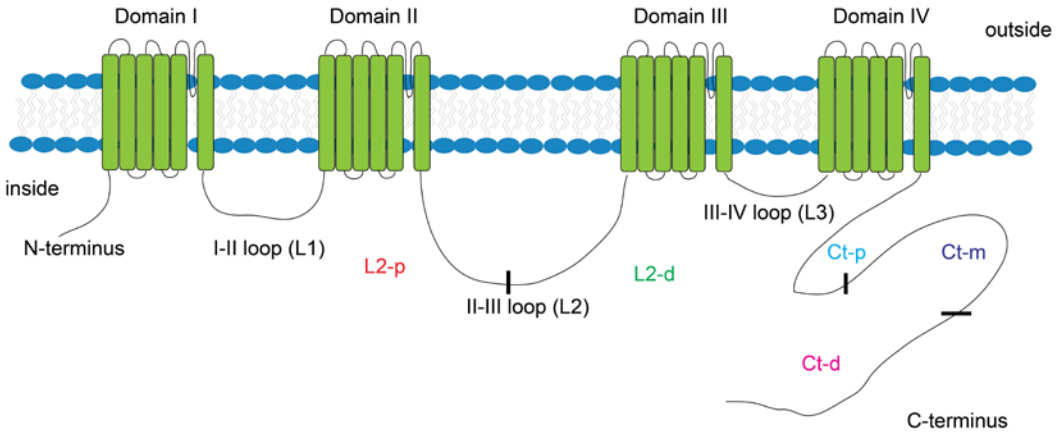

B

Construct	Nucleotides	DNA length	Amino Acids	Protein length	predicted kD	predicted kD with GST-Glu
N-terminus	46-330	285	1-95	95	9.9	37.7
L1	1111-1494	384	356-483	128	14.9	42.7
L2-proximal	2176-3000	825	711-984	274	31.0	58.8
L2-distal	2914-3471	558	957-1142	186	20.6	48.4
L3	4276-4467	192	1411-1474	64	7.2	35.0
C-terminus proximal	5116-5793	678	1691-1916	226	25.5	53.3
C-terminus medial	5683-6429	747	1880-2128	249	27.1	54.9
C-terminus distal	6400-7044	645	2119-2333	215	23	50.8

Figure 3.5. Details of the boundaries for the intracellular regions of CaV2.2

(**A**) Diagram depicting the protein sequence of CaV2.2 as it relates to the transmembrane and intracellular regions and the nomenclature used for these regions. (**B**) Table displaying the specific nucleotides and amino acids of the intracellular regions and the subdivisions used for cloning of these intracellular regions. Nucleotides are from the rat cDNA sequence accession #NM_147141.

by an as yet unclear mechanism. This is consistent with the demonstration of large segments of the CRMP protein being involved in oligomerization (Wang and Strittmatter, 1997).

The alpha subunit of CaV2.2 is 2399 amino acids long and has 4 domains with each of domains containing 6 transmembrane regions (Figure 3.5A). The majority of biochemical interactions with CaV2.2 occur not within these regions but rather with the intracellular regions where the majority of cytosolic proteins have access (Sheng et al., 1994; Sheng et al., 1997; Vance et al., 1999; Zamponi, 2003). I therefore worked under the assumption that CRMP-2 interacted with CaV2.2 in an intracellular region. In order to determine which intracellular region(s) are responsible for the interaction with CRMP-2 bacterially expressed constructs of these regions were generated (Figure 3.5B). These regions were cloned using a PCR-based approach. Primers were made so that each region could be cloned into the bacterial expression vector pGex3x-Glu. This vector was used as it would produce proteins with two protein tags; glutathione S-transferase (GST) and Glu (amino acids EYMPME) (Figure 3.6A). The primer sequence and restriction enzymes used for the cloning are included in Table 2.3. The CaV2.2 region of interest for each construct was amplified from rat CaV2.2 cDNA before being digested using the listed restriction enzymes (Figure 3.6B). The digested PCR product was then ligated into the Gex3x-Glu vector that had previously been digested with *Eco*RI and *Bam*HI. Ligations were screened by colony PCR and positive clones were grown up in *E-coli* and DNA was subsequently isolated (Figure 3.6C). The potential constructs were then verified by DNA sequencing. Properly sequenced constructs were transformed into BL21(DE3)p*Lys*E for expression. Proteins were grown in large 1 L cultures and then lysed and purified using glutathione cellulose (Figure 3.7). The purified proteins were visualized by comassie-stained SDS-PAGE. In addition to verifying proper purification by SDS-PAGE the CaV2.2 constructs were tested by immunoblotting using an anti-Glu antibody (Figure 3.8A). This was used specifically as the Glu tag is on the C-terminal end of the protein and therefore will only detect full-length proteins.

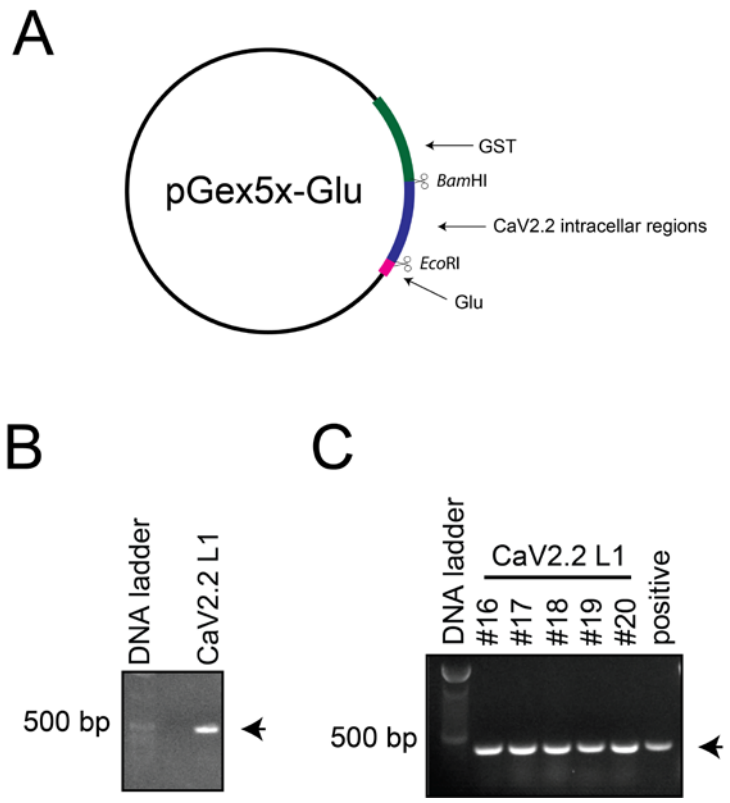

Figure 3.6. Cloning of CaV2.2 intracellular regions into pGex-3x-Glu

The intracellular regions of CaV2.2 were cloned into pGex-5x-Glu using standard molecular biology techniques. (**A**) Vector map of pGex-5x-Glu displaying the 5'- GST protein flanked by a 3'- Glu tag. All CaV2.2 constructs were inserted using restrictions site located between these protein coding sequences. (**B**) DNA gel stained with SYBR® Safe of CaV2.2 L2 amplified from full length CaV2.2 DNA using PCR. The PCR product was then gel purified before being digested with *Bam*HI and *Eco*RI and gel purified again. The digested PCR product was then ligated into a previously digested pGex-5x-Glu vector and transformed. (**C**) Transformed colonies were screened for insertion using colony PCR along with a positive control of a PCR product amplified from CaV2.2 DNA. Positive colonies were then grown and the subsequently isolated DNA was verified by sequencing.

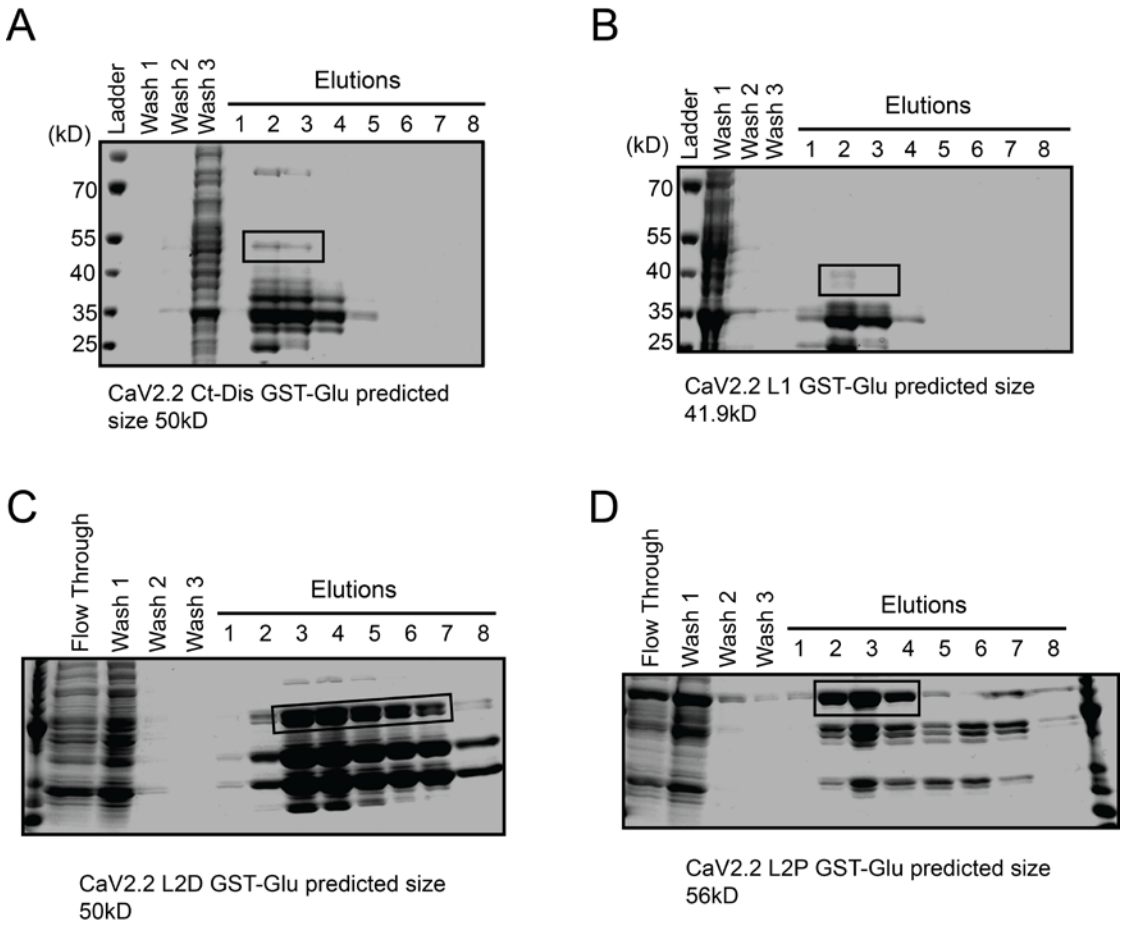

Figure 3.7. Purification of CaV2.2 intracellular regions fusion proteins

(**A**) The cloned CaV2.2 intracellular regions constructs were transformed into *E-coli* and the subsequent protein was purified using glutathione cellulose and eluted using glutathione. Proteins were identified based upon identifying the protein by comassie stained SDS-PAGE as shown. The box highlights the GST-L1-Glu protein at approximately the predicted size. (**B**,**C**,**D**) Additional example comassie stained SDS-PAGE showing purification with a box highlighting the protein at the predicted size.

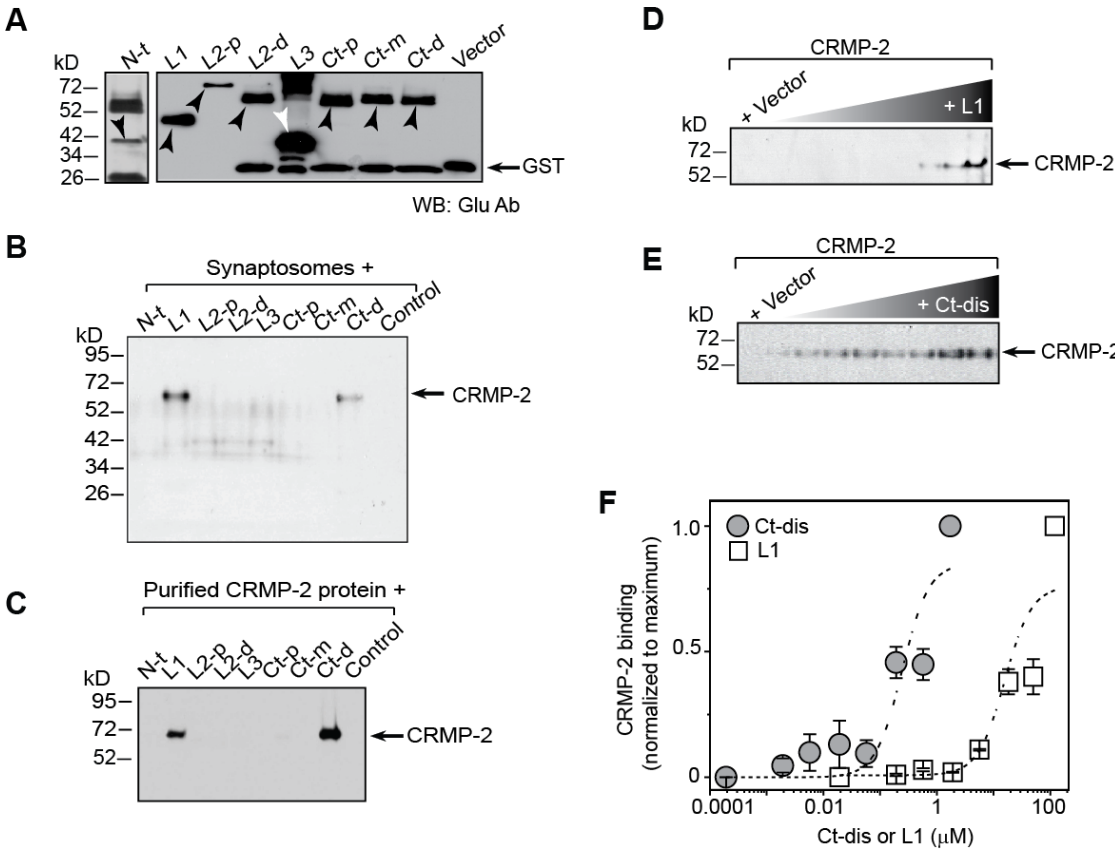

Figure 3.8. CRMP-2 binds to two cytoplasmic regions within CaV2.2

(**A**) Western blot with Glu antibody of GST- and Glu-tagged calcium channel fragments used in the binding experiments. Pulldown assays with GST-Glu fusion CaV2.2 constructs from synaptosomes (**B**) or brain purified CRMP-2 (**C**). Bound proteins were analyzed by immunoblotting with CRMP-2 antibody. GST-Glu-L1 (**D**) or GST-Glu-Ct-d (**E**) proteins at increasing concentrations, incubated with CRMP-2 (~500 nM), were captured by protein A Sepharose beads. Captured CRMP-2 proteins were identified by immunoblotting with CRMP-2 antibodies. Quantitative densitometry was performed on the bands shown in panels **D** and **E**. (**F**) Data representing the normalized average band intensity ± SEM (n=3) were subjected to a Sigmoidal curve-fitting method to evaluate the apparent dissociation constant (K_d). The CaV2.2–CRMP-2 K_ds were: L1 ~24.1 ± 7.1 μM; Ct-d ~0.31 ± 0.09 μM.

Synaptosomes or CRMP-2 protein purified from rat brains using a three-step affinity chromatography method (Wang and Strittmatter, 1997) were used for binding assays. Synaptosomes were incubated with equimolar amounts of glutathione beads saturated with GST-CaV2.2-Glu fusion proteins or GST-Glu protein alone for 2h at 4°C with gentle agitation. After washing, the in vitro complexes were eluted from the beads, resolved by SDS-PAGE and immunoblotted for CRMP-2 protein. CRMP-2 bound two regions on CaV2.2: loop 1 (L1) and the distal part of the C-terminus (Ct-d). Next, the strength of the binding of the CaV2.2 L1 and Ct-d regions was measured using an in vitro binding assay (Figure 3.8B, C). A fixed amount of CRMP-2 protein was incubated overnight at 4°C with increasing amounts of protein G beads saturated with L1 or Ct-d fusion proteins. The bound complexes were washed, resolved by SDS-PAGE and subjected to immunoblotting with CRMP-2 antibody as above (Figure 3.8D,E) . The intensities of the CRMP-2 band were quantified, normalized to the maximum intensity within an experiment (n=3) and plotted against the concentration of the fusion protein. The CaV2.2–CRMP-2 binding affinity (Kd) values were: L1= 24.1 ± 7.1 μM (n=3) and Ct-d = 0.31 ± 0.09 μM (n=3) (Figure 3.8F). As a control, the Kd of interaction between the presynaptic protein Munc 18 (Chan et al., 2007) and Loop 2 (L2-p) of CaV2.2 was found to be ~32 ± 8.5 nM (n=3; data not shown), consistent with the value of ~13.8 ± 4 nM as previously reported (Chan et al., 2007). Thus, CRMP-2 binds directly to CaV2.2 via a moderate affinity (Ct-d) and a low affinity (L1) binding site.

3.5. Activity and Ca^{2+} dependence of CRMP-2-CaV2.2 interaction

Having established that CRMP-2 binds to CaV2.2 and that CRMP-2 is present in synaptic fractions, I next asked if changes in synaptic activity could affect the interaction. To address if the CRMP-2–CaV2.2 interaction was dynamic, neonatal synaptosomes were used. These were chosen since a majority of the Ca^{2+} uptake in neonatal synaptosomes is dependent on CaV2.2 activity (Yamaguchi et al., 1998); this differs dramatically from adult synaptosomes in which

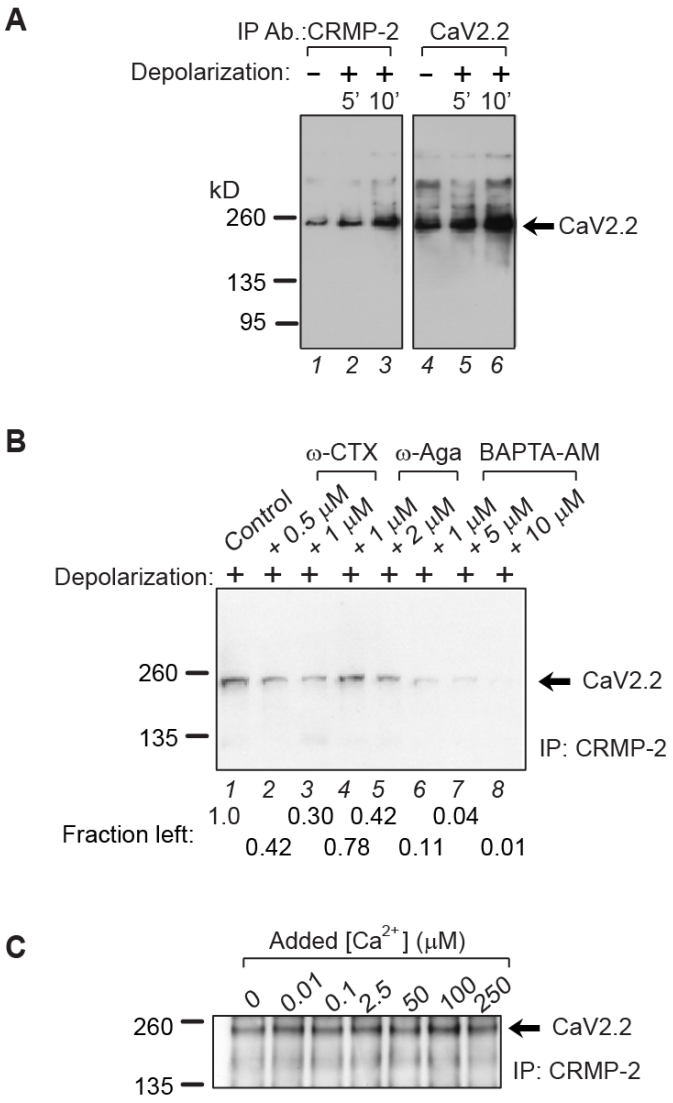

Figure 3.9. Activity-dependent regulation of CRMP-2–CaV2.2 interaction

(**A**) Intact synaptosomes were depolarized with 90 mM KCl for 5 or 10 min, then lysed and immunoprecipitated with CRMP-2 or CaV2.2 antibodies. (**B**) Experiments as completed in **B** were performed with the addition of: ω-CTX; ω-Agatoxin (ω-Aga); and the Ca^{2+} chelator BAPTA-AM. Following lysis, the synaptosomes were IP'ed with CRMP-2 antibody and immunoblotted with CaV2.2. Fraction left denotes the density of the CaV2.2 protein relative to control. (**C**) Synaptosomes were incubated with increasing amount of Ca^{2+} and IP'ed with CRMP-2 antibody followed by immunoblotting with CaV2.2. Representative blots from two to four experiments are shown.

CaV2.2 blockade has little to no effect on uptake. In order to study how synaptic activity may affect the interaction between CaV2.2 and CRMP-2, freshly prepared, unsolubilized synaptosomes were depolarized with 90 mM KCl for 5 or 10 min, and then lysed in RIPA buffer and immunoprecipitated with CRMP-2 or CaV2.2 antibodies and immunoblotted with either antibody. The interaction between CRMP-2 and CaV2.2 was increased upon depolarization (Figure 3.9A). Interestingly, there was relatively more CaV2.2 and CRMP-2 in the depolarized versus non-depolarized immunoprecipitations (Figure 3.9A, compare lanes 3 to 1 and 6 to 4). This result suggests that depolarization may cause changes in the conformations of the interacting proteins which could lead to unmasking of the antigenic sites for either antibody, thereby facilitating greater recovery in the immunoprecipitations and thus greater association. This increase in CRMP-2–CaV2.2 interaction was dependent on Ca^{2+} influx via CaV2.2 as incubation of synaptosomes with ω-CTX for 15 min prior to depolarization decreased the association (Figure 3.9B, compare lanes 2 or 3 to 1). Incubation of the synaptosomes with the CaV2.1 blocker ω-Agatoxin IVA also partially affected the CRMP-2–CaV2.2 interaction (Figure 3.9B). Incubation with increasing amounts of the membrane-permeable Ca^{2+} chelator BAPTA-AM (Nichols and Suplick, 1996) caused a dose-dependent decrease in CRMP-2–CaV2.2 association (Figure 3.9B, lanes 6-8). The interaction exhibited maximal binding at around 100 μM added Ca^{2+} and declined at higher concentrations (Figure 3.9C). Collectively, these results suggest an activity-dependent regulation of the interaction between CRMP-2 and CaV2.2.

3.6. Effect of altering CRMP-2 expression on CaV2.2 function

The biochemical interaction between CRMP-2 and CaV2.2 appear to be both direct and activity dependent which is interesting in its own right. These findings importantly lead to perhaps a more interesting question regarding the relationship between CRMP-2 and functional effects on CaV2.2. In order to test if CRMP-2 regulates CaV2.2 activity I wanted to develop a method to reduce expression of CRMP-2, already having a CRMP-2 overexpression vector that

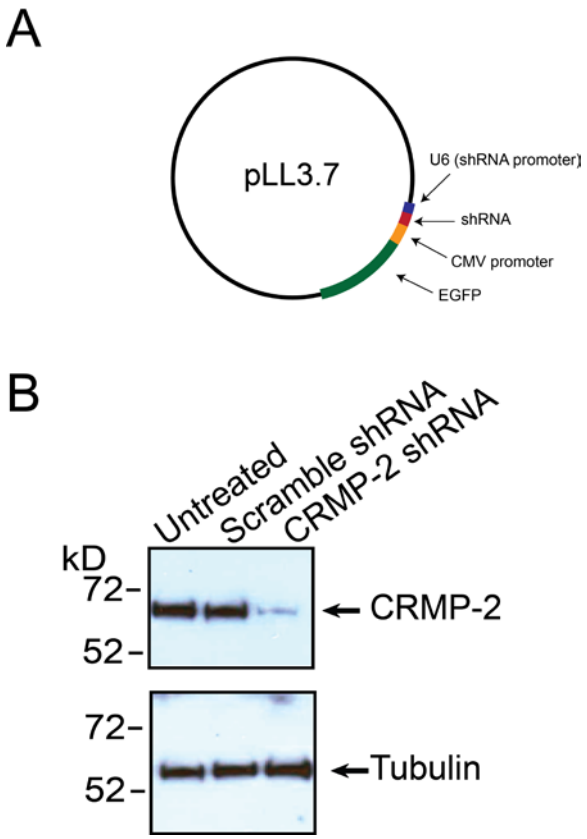

Figure 3.10. Construction and validation of lentiviral CRMP-2 shRNA

(**A**) Lentiviral shRNA vectors were made using the pLL3.7 vector. I used an oligo-cloning approach to insert the shRNA sequences into the vector. Following verification of proper insertion of the shRNA sequences into the pLL3.7 vector, lentiviral particles were generated and purified by expressing the vector along with viral packaging plasmids (pMDMg/pRRE, pRSV-Rev, and pCMV-VSV-G) in HEK293T cells. (**B**) Hippocampal neurons grown in culture for 5 days were treated with equal infectious titers (determined by infection of HEK293 cells) of scrambled or CRMP-2 shRNA lentiviral particles. Western blot analysis with a CRMP-2 monoclonal antibody showing successful (>90%) knockdown of CRMP-2 protein in neurons treated with CRMP-2 shRNA or scrambled shRNA lentiviruses for 7 days. Under the same conditions, expression of the neuronal protein β-III-tubulin was unchanged.

could be used to enhance expression. I decided to develop a lentiviral short hairpin RNA (shRNA) construct to mediate CRMP-2 knockdown. Another requirement would be that the infected cells would express a fluorescent protein to identify cells that were successfully infected. This is particularly important for electrophysiology experiments. The pLL3.7 vector (a generous gift from Dr. Michael Vasko) meets these requirements as it contains a U6 promoter t to drive expression of shRNA and a cytomegalovirus (CMV) promoter driving expression of enhaced green fluorescent protein (EGFP) (Figure 3.10A). The desired shRNA sequences (Table 2.4) were inserted in the pLL3.7 vector using direct ligation of the annealed shRNA oligonucleotides into pLL3.7 previously digested with *Xho*I and *Hpa*I. Lentiviral particles were then grown up after the vector was verified by DNA sequencing. Treatment of cultured neurons with CRMP-2 shRNA lentiviral particles led to a ~90% reduction in CRMP-2 proteins levels compared to scramble shRNA (Figure 3.10B).

In collaboration with Dr. Theodore Cummins' laboratory and using whole cell voltage-clamp electrophysiology, the potential modulation by CRMP-2 on Ca^{2+} currents was examined in primary hippocampal neurons. Drs. Cummins, Yuying Wang (Khanna Laboratory), and Andrew Piekarz recorded whole cell Ca^{2+} currents from EGFP- and CRMP-2-EGFP-overexpressing cells. Whole-cell Ca^{2+} currents were elicited from a holding potential of –80 mV to depolarizing test potentials (ranging from –80 to +70 mV) for 200 ms using Ba^{2+} as the charge carrier (for simplicity, these currents are referred to as Ca^{2+} currents). Figure 3.11A shows representative voltage-dependent inward currents (I_{Ba}) from an EGFP- and a CRMP-2-EGFP expressing neuron. Nifedipine (1 μM) was included in the bath solution to block CaV1 (i.e. L-type) channels. Forty-eight hours after transfection, the Ca^{2+} current density was significantly higher in CRMP-2-EGFP-transfected neurons than in EGFP neurons (Figure 3.11). On average, the Ca^{2+} current density was increased by about 60%, from 12.8 ± 2.2 (n=15) to 20.4 ± 2.5 (n=24) pA pF^{-1} (V_t= 0 mV, p <0.001, One-way ANOVA), consistent with the values of 14.6 ± 1.0 pA pF^{-}reported previously for control hippocampal neurons (Lai et al., 2005). Expression of CRMP-2-EGFP did

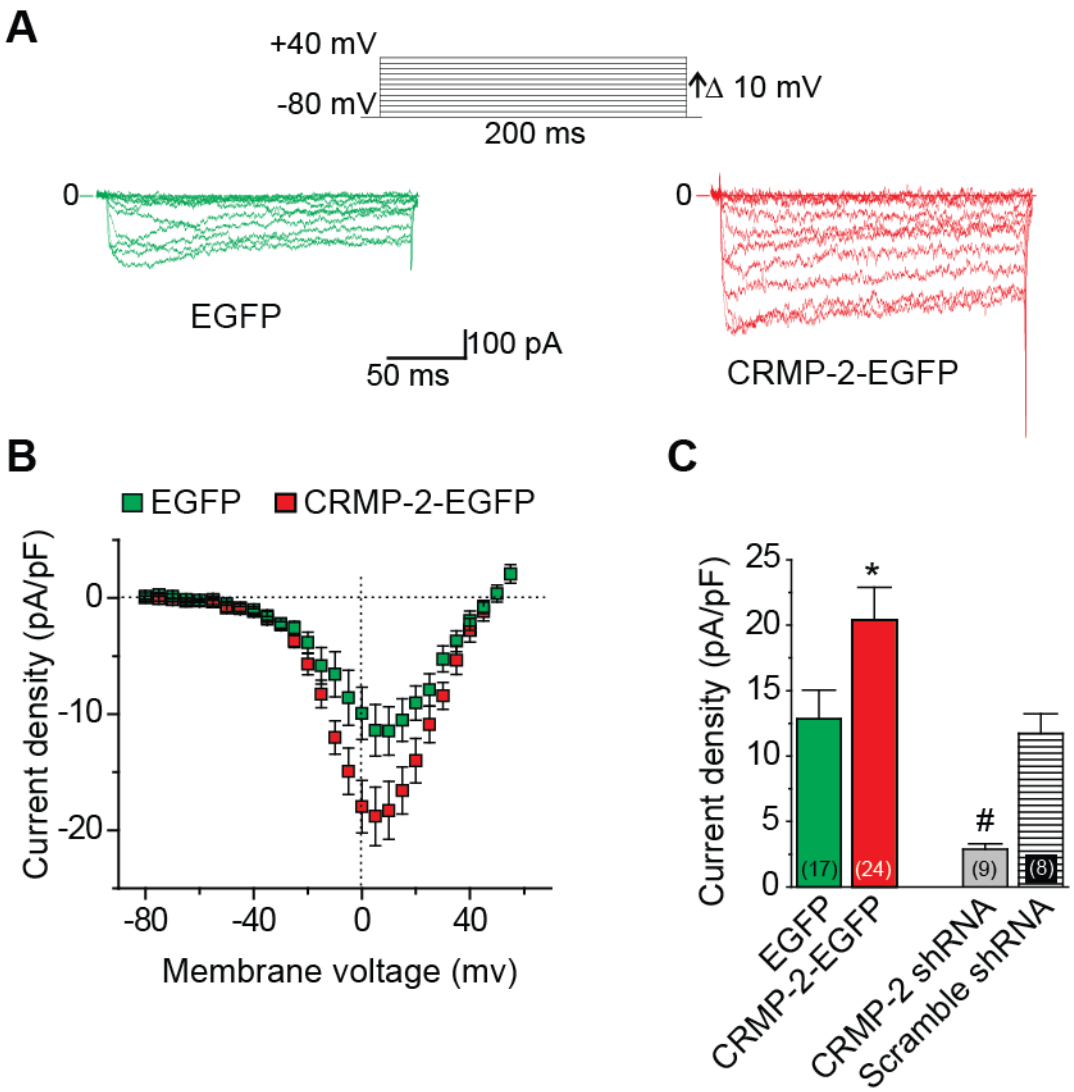

Figure 3.11. CRMP-2 regulates Ca^{2+} current density in hippocampal neurons

(**A**) Exemplar current traces obtained from a cell transfected with EGFP and CRMP-2–EGFP recored using the voltage protocol displayed above the traces. Lines labeled 0 indicate the zero current level. (**B**) *I-V* relationships for the currents shown in **A**. Peak currents were normalized to the cell capacitance. (**C**) Peak current density (pA/pF) measured at + 10 mV for EGFP, CRMP-2–EGFP transfected neurons and CRMP-2 shRNA and scrambled shRNA infected neurons. Numbers in parentheses represent numbers of cells tested, */# indicated $p<0.05$ versus all other conditions (One-way ANOVA). Electrophysiology experiments were performed by Drs. Theodore Cummins, Andrew Piekarz, Yuying Wang.

not alter the size of the transfected neurons' cell bodies, as the cell capacitance was identical in CRMP-2–EGFP (21.8 ± 1.8 pF, n=24) and EGFP (20.2 ± 1.7 pF, n=17, p >0.56) transfected neurons. This result rules out changes in cell size as a potential contributing factor for the increased Ca^{2+} current density.

To further confirm that CRMP-2 manipulation affected Ca^{2+} current density, I asked if CRMP-2 knockdown using lentiviral-mediated delivery of CRMP-2 shRNA would decrease Ca^{2+} current density. Interestingly, infection of 12 DIV hippocampal neurons with CRMP-2 shRNA lentivirus for seven days reduced Ca^{2+} currents to 2.9 ± 0.4 pA/pF (n=9); an ~80% reduction compared to CRMP-2–EGFP over-expressing neurons (Figure 3.11C). Scramble shRNA lentivirus did not affect Ca^{2+} currents; currents were 11.7 ± 1.5 pA/pF (n=8; Figure 3.11C).

3.7. Effect of CRMP-2 expression on CaV2.2 expression

The observed modulation of CaV2.2 current can occur by a change in channel present on the membrane or by differences in open probability. While it is possible that CRMP-2 alters open probability of CaV2.2, direct testing of this would require technically difficult single channel recordings. In addition previous reports linking CRMP-2 to kinesin mediated transport of proteins down axons suggests that CRMP-2 could be an important determinant of CaV2.2 surface trafficking (Kawano et al., 2005; Kimura et al., 2005). Therefore I choose to examine if surface trafficking could account for observed increasd in Ca^{2+} currents. To test if there is a change in surface CaV2.2 following manipulation of CRMP-2 levels, cell surface biotinylation of hippocampal neurons was performed. Immunoblotting with CaV2.2 for streptavidin-enriched complexes from biotinylated neurons showed increased CaV2.2 surface expression in CRMP-2-EGFP expressing neurons compared to EGFP neurons (Figure 3.12Ai, biotinylated (B) fractions). The surface levels of an unrelated membrane protein, the voltage-gated Na^{+} channel, were not affected by CRMP-2 overexpression (Figure 12Aii, *compare lane 3 to 5*). As a control for the biotinylation assay, no surface proteins were detected in samples in which the biotinylation

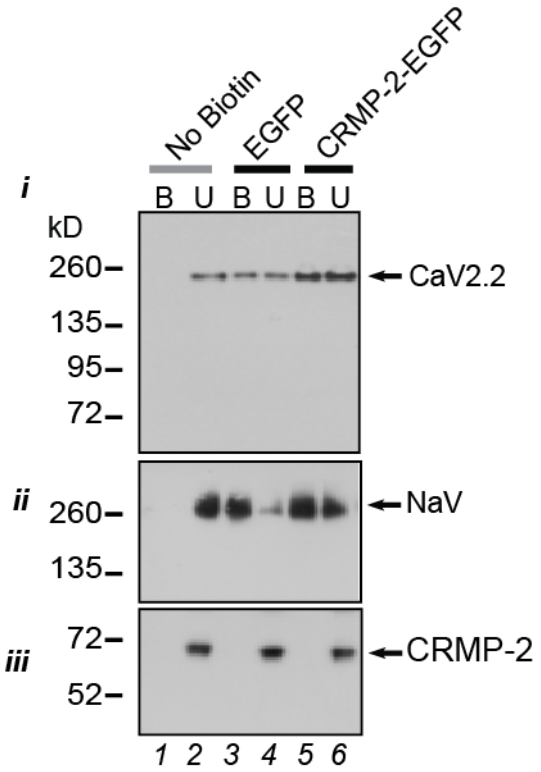

Figure 3.12. CRMP-2 enhances surface expression of CaV2.2

Cell–surface expression of CaV2.2 and CRMP-2 was monitored using a biotinylation assay. Hippocampal neurons expressing EGFP or CRMP-2–EGFP were biotinylated, the cell-surface proteins were harvested from the cell lysates, and the precipitates were analyzed by immunoblotting with CaV2.2 (*i*), Na^+ channel (*ii*) and CRMP-2 (*iii*) antibodies. Equal amounts of samples were used for the precipitation of biotinylated proteins. Of these samples, the entire biotinylated fraction (B) and 10% of the non-biotinylated (U) fraction were loaded. CRMP-2-EGFP overexpression increased the amount of CaV2.2 at the cell surface compared to EGFP transfected cells. Representative blots from three experiments are shown.

reagent was omitted prior to the streptavidin precipitation (Figure 3.12Ai, ii, *lane 1*). Thus, these results suggest that the increased Ca^{2+} current density in CRMP-2 overexpressing neurons likely occurs via increased cell surface trafficking of CaV2.2.

3.8. Effect of CRMP-2 expression on glutamate release

At this point I have observed that CRMP-2 can bind directly to the CaV2.2 channel and can enhance Ca^{2+} current density in hippocampal neurons, but do these events translate into an increase in transmitter release? This question is particularly important as CaV2.2 regulates neurotransmitter release (Wheeler et al., 1994; Wu et al., 1999). To answer this question, glutamate release was measured from hippocampal neurons over-expressing EGFP or CRMP-2-EGFP using high pressure liquid chromatography. At 10 DIV, hippocampal neurons were transfected with EGFP or CRMP-2-EGFP and release experiments were performed 48 h later. Representative chromatographs are shown in Figure 3.13A, B with a typical retention time of glutamate at about 3 min. Exposing hippocampal neurons transfected with EGFP to 30 mM KCl stimulated glutamate release by about 3.5-fold from a basal level of 3.8 ± 1.0 μM/well/10 min to 13.3 ± 0.9 μM/well/10 min. In CRMP-2-EGFP over-expressing neurons, 30 mM KCl stimulated glutamate release by about 8-fold from a basal level of 3.7 ± 0.9 μM/well/10 min to 29.5 ± 1.9 (p<0.001 vs. EGFP). This shows that CRMP-2 can augment glutamate release by 2.3-fold over control EGFP-transfected cells. Although the CRMP-2-mediated glutamate release is smaller than the 2.7- to 12-fold increase in glutamate release that is predicted based on a ~65% increase in Ca^{2+} current density, it is important to note that not every neuron overexpresses CRMP-2 due to incomplete transfection efficiency (<5-15%).

Importantly, the addition of 1 μM ω-CTX, the CaV2.2 blocker, decreased the magnitude of the potassium-stimulated glutamate release from CRMP-2-EGFP expressing neurons by ~77% (to 8.9 ± 1.9 μM/well/10 min) compared to potassium-stimulated glutamate release in the absence of blocker (Figure 3.13C, $p < 0.05$). Block of Ca^{2+} channels did not affect the basal release of

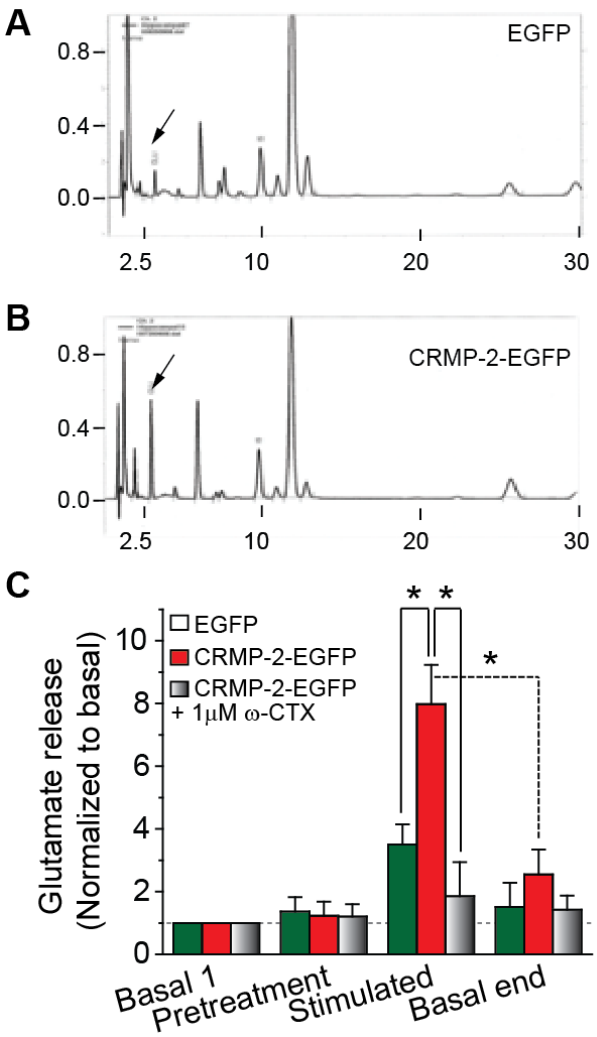

Figure 3.13. CRMP-2 enhances hippocampal glutamate release

Representative HPLC chromatographs of glutamate from hippocampal neurons transfected with EGFP (**A**) or CRMP-2–EGFP (**B**) in response to a depolarizing (30 mM KCl) stimulus. The neurons were incubated with HEPES buffer at 37°C for 1 h and then exposed to successive 10 min incubations for basal 1, pretreatment, stimulated (KCl), and basal end. (**C**) CRMP-2 overexpressing neurons vs. controls (EGFP; $p < 0.05$, Student's t-test; n=9). The addition of 1 μM ω-conotoxin GVIA, the CaV2.2 blocker, completely attenuates the CRMP-2 mediated increase in glutamate release.

glutamate. These results suggest that, in hippocampal neurons at 12 DIV, CaV2.2 supports most, if not all, of the CRMP-2 enhanced, depolarization-associated glutamate release.

3.9. Effect of Cdk5-mediated phosphorylation of CRMP-2 on CaV2.2 function

Phosphorylation of CRMP-2 in the C-terminus regulates its axon growth activity. When CRMP-2 is phosphorylated specifically by Cdk5 or ROCK this leads to a cascade of still unknown signaling leading to halting of neuritic growth (Arimura et al., 2000; Arimura et al., 2005; Brown et al., 2004; Cole et al., 2006). Based upon the important role of phosphorylation in modulating CRMP-2's activity I hypothesized that phosphorylation may also modulate its regulation of CaV2.2. This is likely as well given that the CBD3 region of CRMP-2 is located in the C-terminus near these phosphorylation sites. While there are many kinases involved in modulating CRMP-2 activity Cdk5's phosphorylation of Ser-522 is perhaps the most important due to its role in sema3A-induced growth cone collapse and as a priming kinase for subsequent phosphorylation of CRMP-2 by GSK3β. I first verified that Cdk5 was active in my P2 hippocampal neuron cultures by treating neurons with the Cdk5 inhibitor purvalanol A (10 μM) (Villerbu et al., 2002). As a negative control I also treated neurons with the ROCK inhibitor Y-27632 (10 μM) which should not affect phosphorylation of CRMP-2 at Ser-522. A time-dependent decrease in phosphorylation of CRMP-2 at Ser-522 was detected using a Ser-522 phospho-specific antibody (Figure 3.14). As expected, treatment with Y-27632 did not lead to a significant change in the phosphorylated state of Ser-522. This series of experiments demonstrates that my neuronal cultures have a basal level of Cdk5 activity and supports investigation into the role that phosphorylation of CRMP-2 by Cdk5 plays in its interaction and regulation of CaV2.2.

Despite the effectiveness of purvalanol A in reducing CRMP-2 Ser-522 phosphorylation, the use of a Cdk5 inhibitor to study CaV2.2 function may show complicating factors as other Cdk5 substrates in addition to CRMP-2, including CaV2.2 itself, can regulate CaV2.2 funnction

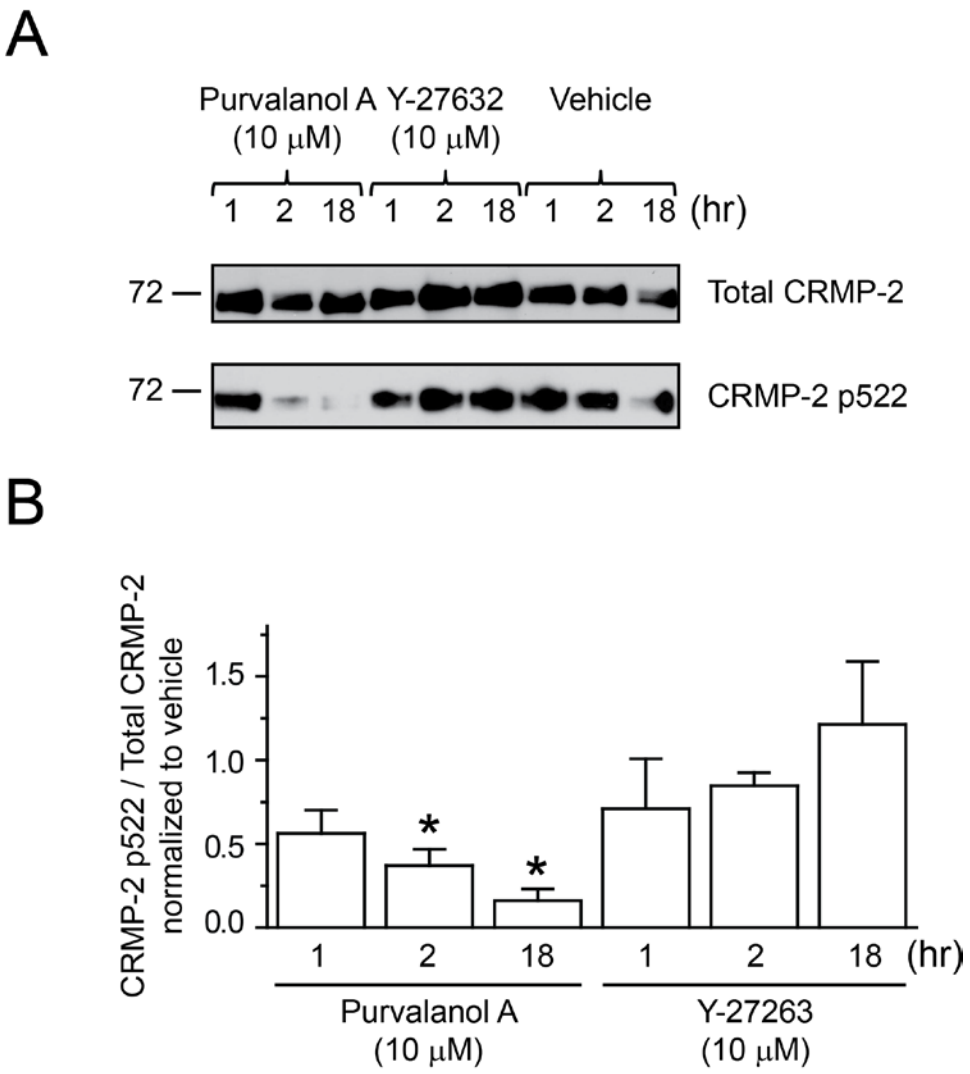

Figure 3.14. Phosphorylation of CRMP-2 in cortical neurons by Cdk5

(**A**) Lysates from neurons exposed to Cdk5 inhibitor Purvalanol, the ROCK inhibitor Y-27632, or vehicle (0.1% DMSO) for the indicated times were immunoblotted with the indicated antibodies. (**B**) Summary data of ratio CRMP-2 p522 to total CRMP-2 and then normalized to vehicle-treated neurons (n= 5-6 from two separate experiments, *, $p<0.05$, one-way ANOVA with Dunnett's post-hoc compared to vehicle).

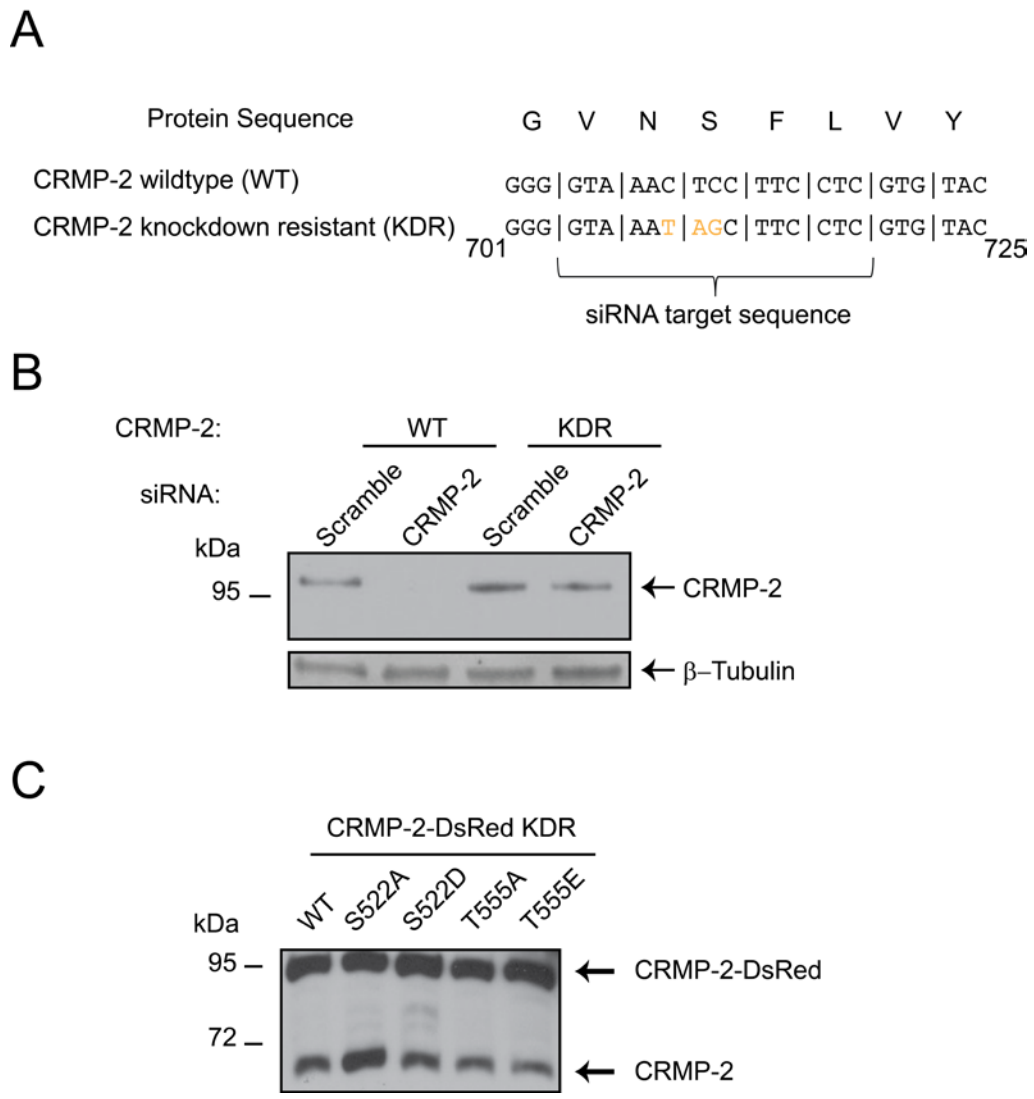

Figure 3.15. Generation of knockdown resistant CRMP-2 and expression of CRMP-2 mutants

(**A**) Alignment of the protein (top) and nucleotide sequences (bottom) within a validated siRNA region targeting CRMP-2 (mouse, GenBank Accession # NM_009955.3) highlighting the silent mutations (underlined nucleotides) used to generate a knockdown resistant (KDR) CRMP-2. (**B**) Lysates from CAD neuronal cells co-transfected with wildtype (WT) CRMP-2-DsRed and scramble or CRMP-2 siRNAs or KDR CRMP-2-DsRed and scramble or CRMP-2 siRNAs. (**C**) Phospho–mimetic or –null mutations engineered into the CRMP-2-KDR-DsRed construct express robustly.

(Samuels et al., 2007a; Su et al., 2012). Based upon this I chose to use a direct approach to investigate the role of CRMP-2 phosphorylation in regulation of CaV2.2. This was accomplished first by generating a CRMP-2 construct that was resistant to knockdown (KDR) by siRNA through site-directed mutagenesis of the siRNA target sequence (Figure 3.15A). Mutation of three nucleotides within the siRNA target sequence, without alteration of the amino acid sequence, prevented knockdown by CRMP-2 targeted siRNA when co-transfected with CRMP-2-KDR in CAD cells, a neuronal cell line (Figure 3.15B). The CRMP-2 KDR construct was then used for subsequent generation of Ser-522 and Thr-555 phosphorylation mutants. The phospho-mimetic mutants (S522D & T555E) and phospho-null mutants (S522A & T555A) along with CRMP-2 wildtype (WT) displayed equal expression when transfected into CAD cells suggesting that the mutations did not alter expression of CRMP-2 (Figure 3.15C). The constructs were then transfected into DIV 7-8 P1 hippocampal neurons along with 200 nM CRMP-2 siRNA. Two days following transfection, Ca^{2+}-channel function was measured by monitoring KCl depolarization-induced Ca^{2+}-influx with the Ca^{2+}-sensitive dye Fura-2. Transfected cells were visualized using DsRed, which is fused to the CRMP-2 constructs. The microscope was then switched to visualize Fura-2 (F340 nm /F380 nm) and stimulated with KCl. Stimulation with KCl led a sharp increase in the Fura-2 ratio which is indicative of an increase in $[Ca^{2+}]_i$ (Figure 3.16A). The peak change in the ratio was then compared between the various conditions. The dotted line represents the average value obtained for neurons transfected with CRMP-2 siRNA alone (Figure 3.16B). While the phospho-mimetic and phospho-null mutants for Thr-555 were not significantly different from WT, mutation of the Cdk5 site of CRMP-2 caused a significant decrease in Ca^{2+}-influx. Interestingly both phospho-mutants of Ser-522 led to a decrease suggesting that both the phosphorylated and unphosphorylated form of CRMP-2 is required to enhance Ca^{2+}-channel function. Alternatively it is possible that CRMP-2 S522D does not function as a phospho-mimetic. Furthermore the regulation of CRMP-2's interaction with

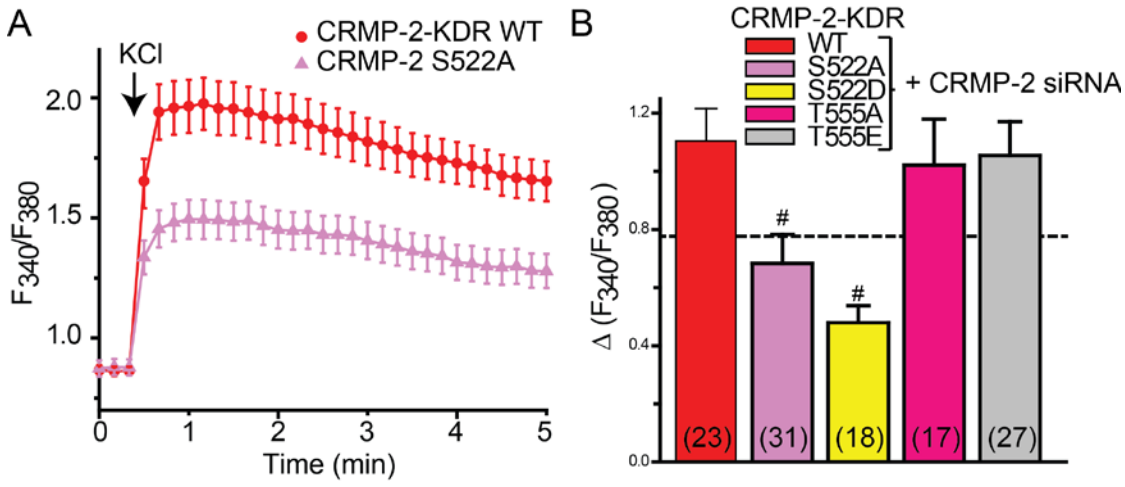

Figure 3.16. Phosphorylation of CRMP-2 at Ser-522 is an important determinant for modulation of Ca^{2+} influx

Cortical neurons (DIV 10-12) were co-transfected with KDR CRMP-2-DsRed constructs and CRMP-2 siRNA and Ca^{2+} influx was monitored 2 days later with Fura-2AM. (**A**) Time course illustrating that a brief stimulation of neurons with 46.5 mM KCl led to a sharp increase in the 340nm/380nm ratio that diminished over the course of the 5 min of the experiments. (**B**) Summary of average peak change ± SEM in Ca^{2+} influx from neurons transfected with CRMP-2-KDR-DsRed constructs as indicated. The dotted line represents mean peak response for neurons transfected with CRMP-2 siRNA only. Number in parentheses represent numbers of cells per condition (#, $p < 0.05$ one-way ANOVA with Dunnett's post-hoc test compared to CRMP-2-WT-KDR).

CaV2.2 is specific to Ser-522 phosphorylation as the Thr-555 sites showed no change in Ca^{2+}-influx.

3.10. Effect of Cdk5-mediated phosphorylation of CRMP-2 on CRMP-2-CaV2.2 interactions

As the basis for regulation of CaV2.2 by CRMP-2 appears to be through a biochemical interaction, I next sought to determine if phosphorylation of CRMP-2 regulated this interaction. To investigate this interaction I wanted to obtain a highly pure source of CRMP-2 that could be phosphorylated *in vitro* and used for binding assays. A CRMP-2 fused to a 6 histidines (CRMP-2-6xHis) was used for this purpose. CRMP-2-6xHis (using the vector pET28B- CRMP-2-6xHis) was purified from BL21(DE3) *E-coli* using a Talon^{TM} metal affinity resin column and eluted by 100 mM Imidazole which was collected over eight fractions (Figure 3.17A). The fractions with the highest concentration of CRMP-2-6xHis were pooled and then dialyzed O/N into His storage buffer. The final dialyzed protein was quantified by SDS-PAGE by comparing to a bovine serum albumin protein standard curve (Figure 3.17B). The final concentration of CRMP-2-6xHis was found to be ~30 µM. I then purified the necessary kinases and accessory proteins to phosphorylate CRMP-2 *in vitro*. Cdk5-, p25-, and GSK3β-GST were purified as previously described in this thesis for other GST fusion proteins (Figure 3.18). Cdk5 is not natively active and therefore must be activated by co-incubation with its activator p25 (Patrick et al., 1999). Purified CRMP-2-6xHis was incubated with Cdk5/p25 and/or GSK3β *in vitro* and phosphorylation was monitored by probing with anti-CRMP-2 p522 (Figure 3.19A). The *in vitro* phosphorylated CRMP-2 was then incubated with P2 synaptosomes and immunoprecipitated with anti-CaV2.2. Immunoprecipitations were then immunoblotted for CRMP-2 and CaV2.2 (Figure 3.19B, n = 5). Interestingly it appears that phosphorylation of CRMP-2 leads to a significant increase in the amount of CaV2.2 bound to the immunoprecipitated CRMP-2 (Figure 3.19C). This finding is consistent with the Ca^{2+}-imaging results supporting phosphorylation of Ser-522 as an important determinant of CRMP-2's modulation of CaV2.2 function.

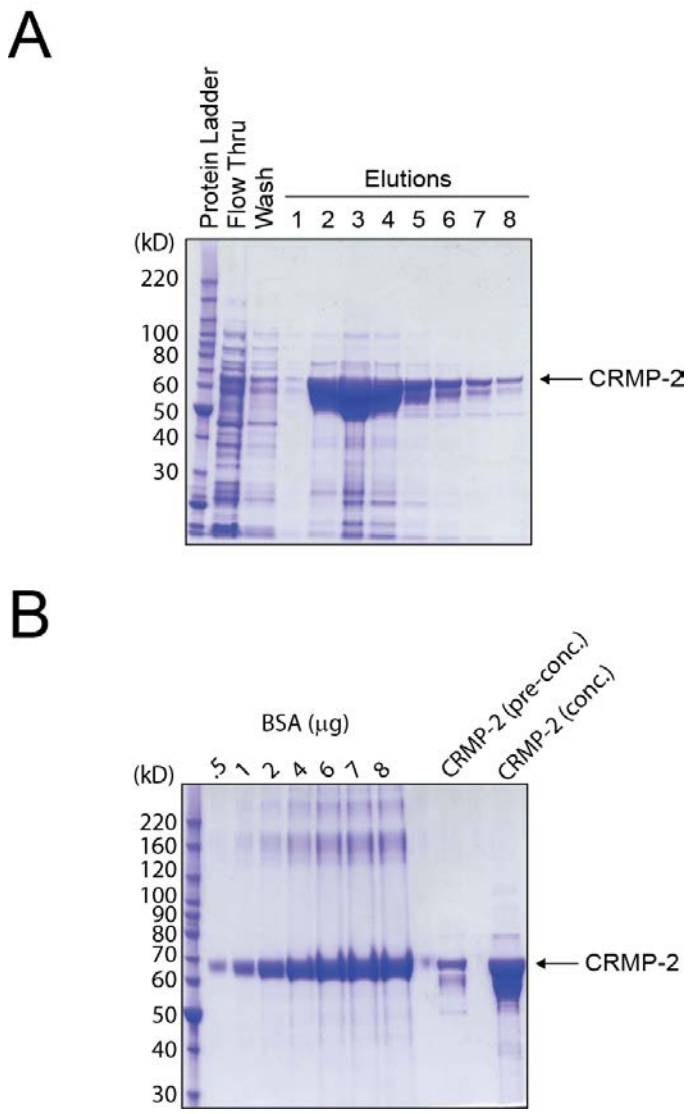

Figure 3.17. Purification of CRMP-2-6xHis

(**A**) CRMP-2-6xHis was purified from *E-coli* using Nickel-agarose and eluted by a grade flow of increasing concentration of Imidazole. The proteins samples were then run on a SDS-PAGE which was subsequently comassie stained to visualize proteins. Elution fractions 2-5 were pooled and then dialyzed into an Imidazole-free buffer. The dialyzed fraction was then concentrated using centrifugation concentrating filters with a cut-off of 30 kDa. (**B**) Comassie stained SDS-PAGE showing final concentrated CRMP-2-6xHis and comparing it to the pre-concentrated protein.

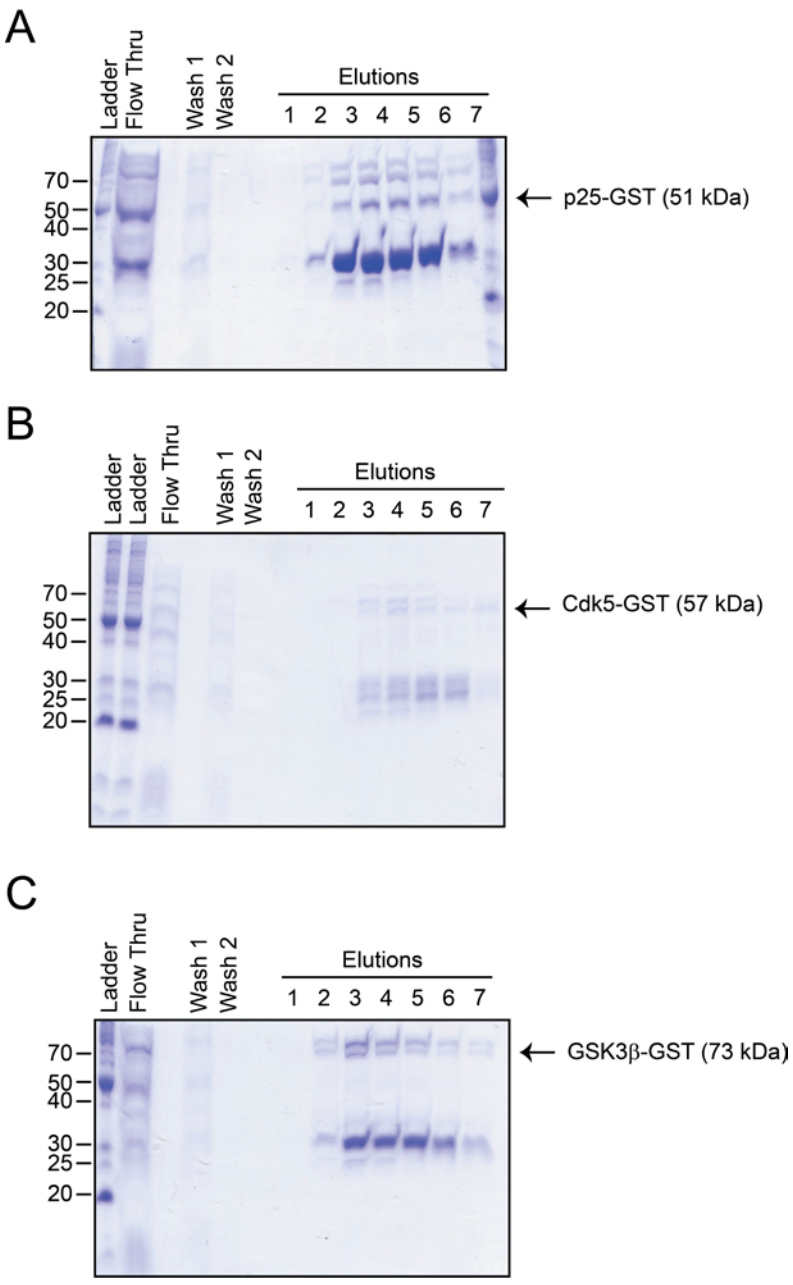

Figure 3.18. Purification of GST-Cdk5, GST-p25, and GST-GSK3β

(**A**) GST-Cdk5 was grown up in *E-coli* and purified using a glutathione cellulose column before elution with glutathione. (**B**, **C**) GST-p25 and GST-GSK3β were purified using the same protocol as Cdk5. Elutions 3-5 were pooled for each protein and then dialyzed against a buffer without glutathione before being concentrated using a centrifugation concentrator.

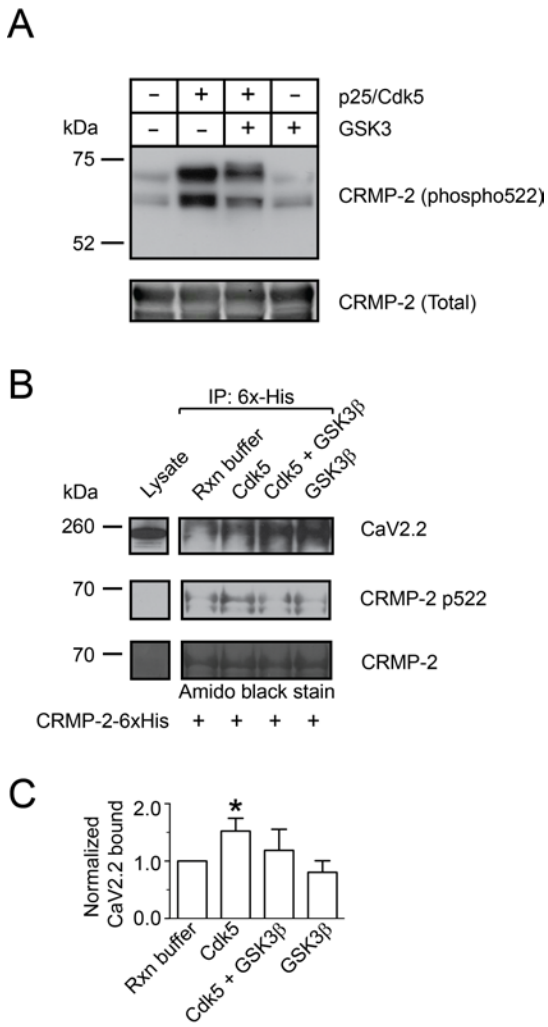

Figure 3.19. Phosphorylation of CRMP-2 by Cdk5 enhances its interaction with CaV2.2 (**A**) Purified CRMP-2-6xHis was phosphorylated *in vitro* by incubation with Cdk5/p25 and/or GSK3β. (**B**) Cdk5-phosphorylated CRMP-2-6xHis was incubated with E19 cortical neuron lysates and then immunoprecipitated for CaV2.2–CRMP-2 protein complexes with an anti-6xHis antibody. The amido black stain demonstrates equal amounts of protein across all lanes. In the example shown, the increases in CaV2.2 recovered by CdK5 + GSK3β- or GSK3β-phosphorylated CRMP-2, compared to without added Cdk5, were *atypically* greater than the average. (**C**) Graph bar depiction of CaV2.2 bound to immunoprecipitated CRMP-2 normalized to rxn buffer condition (no added kinases). Asterisk indicates $p < 0.05$ by Student's t-test where $n = 5$.

3.11. Discovery and characterization of CaV2.2 binding domain 3 (CBD3)

While it has been observed that changes in CRMP-2 expression or phosphorylation lead to correlative changes in CaV2.2 activity and downstream effectors it is unknown whether a direct interaction is responsible for these occurrences. Answering this question may also lead to a way to disrupt the interaction for applications where reduction of CaV2.2 activity may be favorable. To develop a reagent to disrupt the interaction of CRMP-2 with the CaV2.2 complex *in vivo*, a series of overlapping 15-amino-acid peptides were synthesized covering the entire length of CRMP-2 using a robotic peptide spotter (Figure 3.20A). The peptides synthesized included the three CaV2.2 binding domains (CBDs1–3) identified in vitro as crucial for the CRMP-2–CaV2.2 interaction (Figure 3.4). The peptides were spotted onto a membrane which was then overlaid with synaptosomes enriched for Ca^{2+}-channels. Following this incubation the membrane was probed for CaV2.2 using a far western approach (Edmondson and Roth, 2001; Hall, 2004). The binding of CaV2.2 to the peptides was quantified by densitometry of the spots and is depicted as CaV2.2 binding to CRMP-2 normalized to max. The peptide found to have the highest binding potential for CaV2.2 was a 15 amino acid portion of the previously identified CBD3 sequence (Figure 3.20B). This sequence is mildly conserved amongst CRMPs1-5 with CRMP-3 showing highest homology with 12 out of 15 residues being identical (Figure 3.20C). Interestingly the CBD3 peptide sequence is completely conserved from Humans all the way to Zebrafish (Figure 3.20D). This conservation further supports the physiological importance of this sequence.

I next wanted to validate the binding of the CBD3 peptide to CaV2.2 using a different approach. In order to facilitate the penetrance of the CBD3 peptide inside of cell for future studies the CBD3 peptide along with a control peptide having no homology to CBD3 were fused to the transduction domain of the HIV protein TAT (Schwarze et al., 1999). This yielded the cell penetrating peptides TAT-Control and TAT-CBD3. Surface plasmon resonance (SPR) was performed using a BIAcore3000 instrument to observe binding between the TAT-peptides and

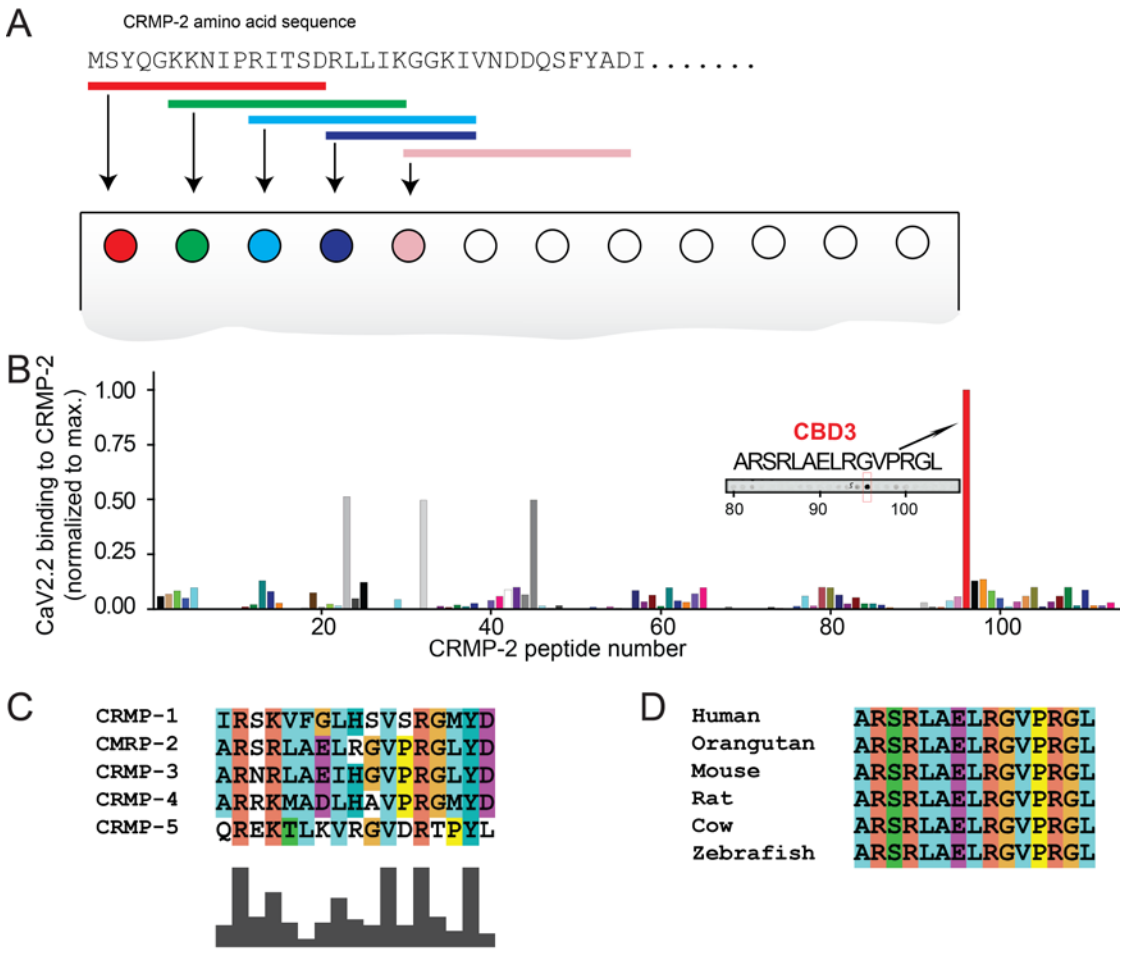

Figure 3.20. CRMP-2 peptides with binding affinity to CaV2.2

(**A**) Diagram describing method for peptide spotting, 15 amino acid long peptides comprising the entire CRMP-2 sequence with 5 amino acids overlapping between peptides were spotted onto a membrane. The membrane was subsequently incubated with synaptosomes enriched for CaV2.2 before being probed for CaV2.2 by immunoblotting. (**B**) Bar graph depicting binding of CRMP-2 peptides to CaV2.2 normalized to max. Small strip shows region of immunoblot containing peptide with the max binding, this peptide was designated Ca^{2+}-channel binding domain 3 (CBD3). (**C**) Alignment of CBD3 peptide between *rattus norvegicus* CRMPs1-5. Alignment was performed using ClustalX 2.1. (**D**) Alignment of CBD3 peptide in CRMP-2 across species. Spots blots were made by Dr. Andy Hudmon.

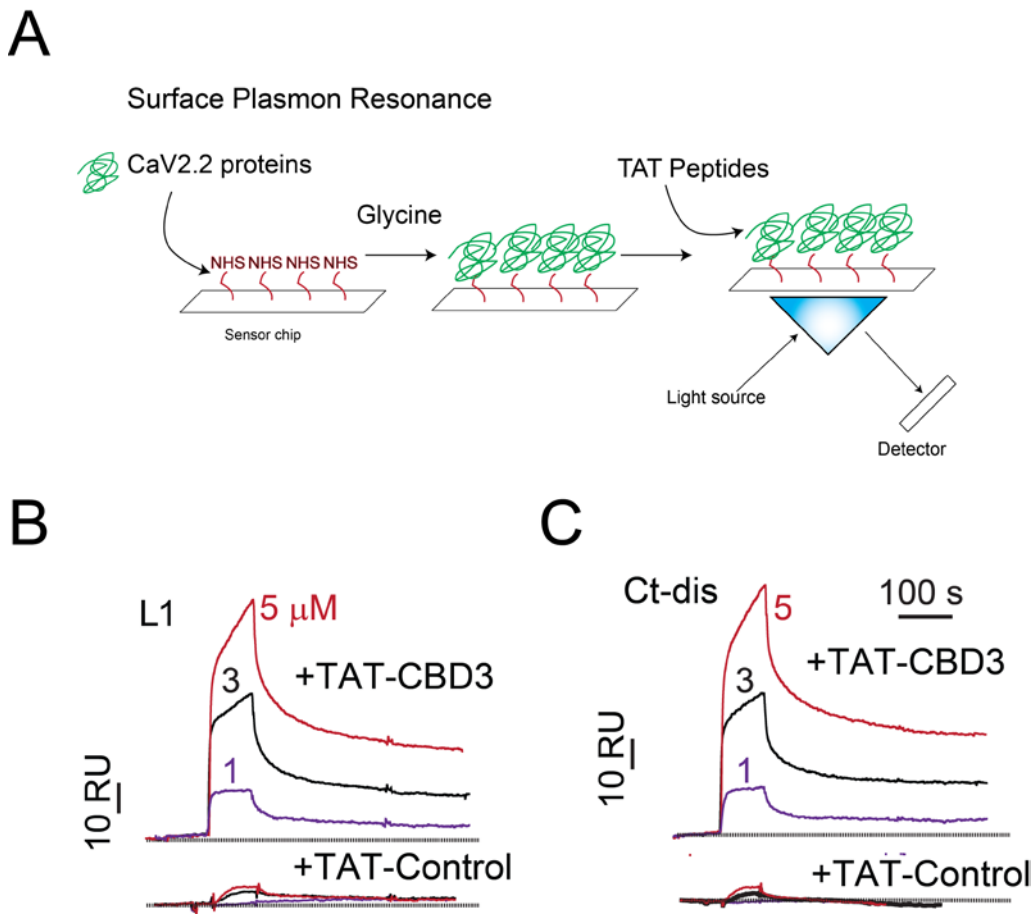

Figure 3.21. TAT-CBD3 binds to both CaV2.2 L1 and Ct-Dis

(**A**) Surface plasmon resonance was used to detect binding of TAT peptides to CaV2.2 regions by adhering the CaV2.2 regions to a sensor chip and then flowing the TAT peptides over the chip. An increase in the observed resonance units (RU) of the light diffracted through the prism and angled at the sensor chip is indicative of association between the proteins on the chip and the peptides. (**B**) Sensorgram displaying binding of TAT-CBD3 to CaV2.2 L1, below shows sensorgrams of TAT-Control in response to interacting with CaV2.2 L1. (**B**) Sensorgram of TAT-CBD3 binding to CaV2.2 Ct-dis, below shows TAT-Control in same experiment. Red traces: 5 µM, Black traces: 3 µM, Purple traces: 1 µM. Traces represent typical result of what was observed from 3 separate runs. SPR traces were generated by Dr. May Khanna from my experimental data collection.

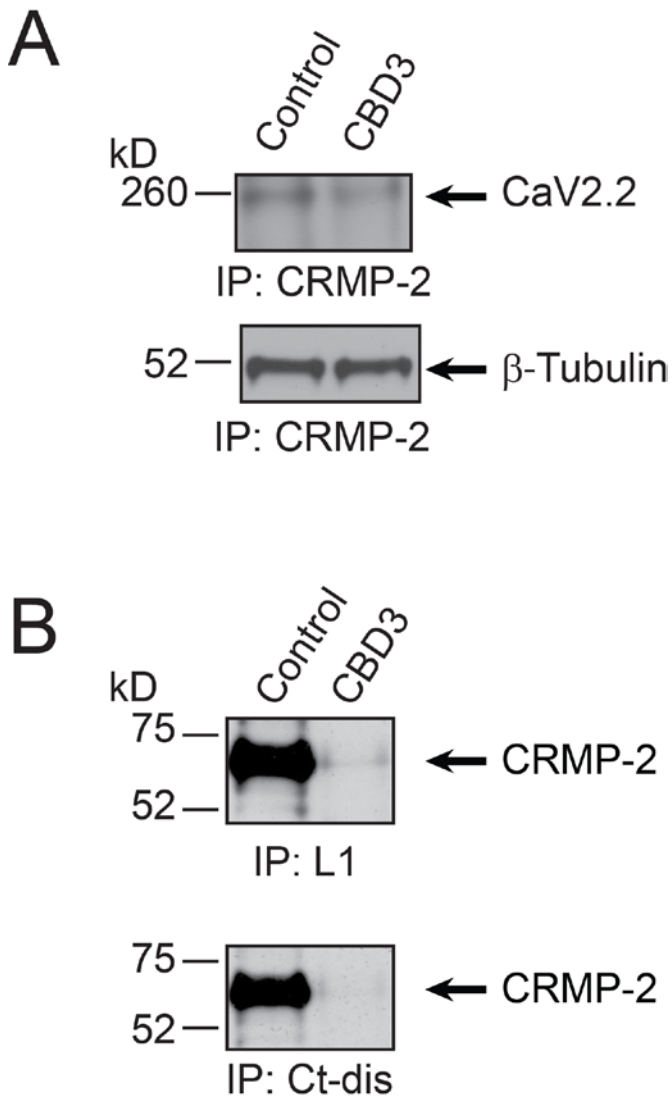

Figure 3.22. TAT-CBD3 disrupts the interaction between CRMP-2 and CaV2.2

(**A**) Immunoprecipitation with recombinant CRMP-2-6xHis in the presence of TAT-CBD3 or TAT-Control, immunoblots are shown for both CaV2.2 and β-tubulin. (**B**) Similar experiments were completed using recombinant CaV2.2 L1-GST and Ct-dis-GST with TAT-CBD3 and TAT-Control with blots for CRMP-2 shown.

CaV2.2 L1 and CaV2.2 Ct-d proteins (Figure 3.21). An upward deflection in the resonance is indicative of binding between the bound protein (CaV2.2 fragments) and the ligand being tested (TAT-peptides). Binding of TAT-CBD3 peptide to both CaV2.2 fragments was observed while no binding was observed for TAT-Control. This result supports CBD3 as a binding partner of CaV2.2 and further shows that attachment of the TAT sequence does not prevent this binding.

Now that the interaction between CBD3 and CaV2.2 has been established I sought to determine if CBD3 was able to disrupt the interaction between CRMP-2 and CaV2.2. Lysates (either E19 brains or PN1 synaptosomes) were pre-cleared with protein-A agarose beads prior to incubation with 10 μM of TAT-CBD3 or TAT-Control for 15 min at 4°C. Lysate were then incubated with a CRMP-2 antibody at 4°C O/N with gentle agitation. Samples were then incubated with protein-A agarose beads for 2 hr before washing three times in RIPA buffer. The samples were then separated by SDS-PAGE and probed by immunoblotting for CaV2.2 and the known CRMP-2 interacting protein β-Tubulin (Figure 3.22A). The addition of TAT-CBD3 reduced the interaction between CRMP-2 and CaV2.2 without affecting the interaction with β-Tubulin. I additionally wanted to test the interaction using specific pieces of CaV2.2. Using a similar protocol lysates were pre-cleared with glutathione-cellulose beads and then incubated with TAT-peptides prior to addition of CaV2.2 L1- or Ct-d-GST-glu fusion proteins. As I previously observed both L1 and Ct-d interact with CRMP-2 and the addition of TAT-CBD3 prevents the pulldown of CRMP-2 by either of these cytoplasmic regions of CaV2.2 (Figure 3.22B). These results show that TAT-CBD3 disrupts the interaction between CaV2.2 and CRMP-2 and can therefore be used to study how disruption of this interaction affects CaV2.2 function.

3.12. Effects of CBD3 on CaV2.2 currents

To determine if CBD3 is able to prevent CRMP-2-mediated enhancement of CaV2.2 function hippocampal neurons were transfected with vector, CRMP-2, or CRMP-2 +CBD3 and whole Ca^{2+} currents were recorded by Dr. Wang 2-3 days following transfection (Figure 3.23A). As observed previously CRMP-2 overexpression cause a significant increase in peak current density compared to vector alone. Co-expression of CBD3 completely abrogated the increase in current density due to over-expression of CRMP-2 (Figure 3.23B). This finding indicates that CBD3 is able to prevent CRMP-2's upregulation of current and therefore suggests that disrupt of the interaction between CRMP-2 and CaV2.2 is responsible for this enhancement of current density. Having shown that co-expression of CBD3 prevents CRMP-2-mediated increased in current density I sought to determine if TAT-CBD3 could be used to reduce current density. The long-term goal of developing TAT-CBD3 was to use it to treat CaV2.2-related pathology. Therefore, the ability of TAT-CBD3 to reduce currents was tested in sensory neurons as CaV2.2 function in sensory neurons has been heavily implicated in pain (Bowersox et al., 1996; Malmberg and Yaksh, 1994; Nebe et al., 1998; Neugebauer et al., 1996). The cell penetrating ability of TAT-CBD3 was verified by using a TAT-CBD3 fused to fluorescein isothiocyanate (FITC) generating TAT-CBD3-FITC. Primary sensory neurons isolated from rat DRG were incubated with TAT-CBD3-FITC for 10 minutes and then fixed in a DAPI containing fixative. TAT-CBD3 showed robust penetrance in neurons within this short time (Figure 3.24A). Next whole cell Ca^{2+}-currents were measured by Drs. Wang and Weiguo Zhu (in collaboration with Dr. Gerry Oxford's laboratory) from sensory neurons after a 15 min application of TAT-CBD3. This application led a ~60% reduction in peak current density compared to TAT-Control treated neurons (Figure 3.24B-D). Current density was not significantly reduced by the addition of the CaV2.2 specific inhibitor ω-CTX suggesting that TAT-CBD3 attenuated the majority of CaV2.2-mediated current.

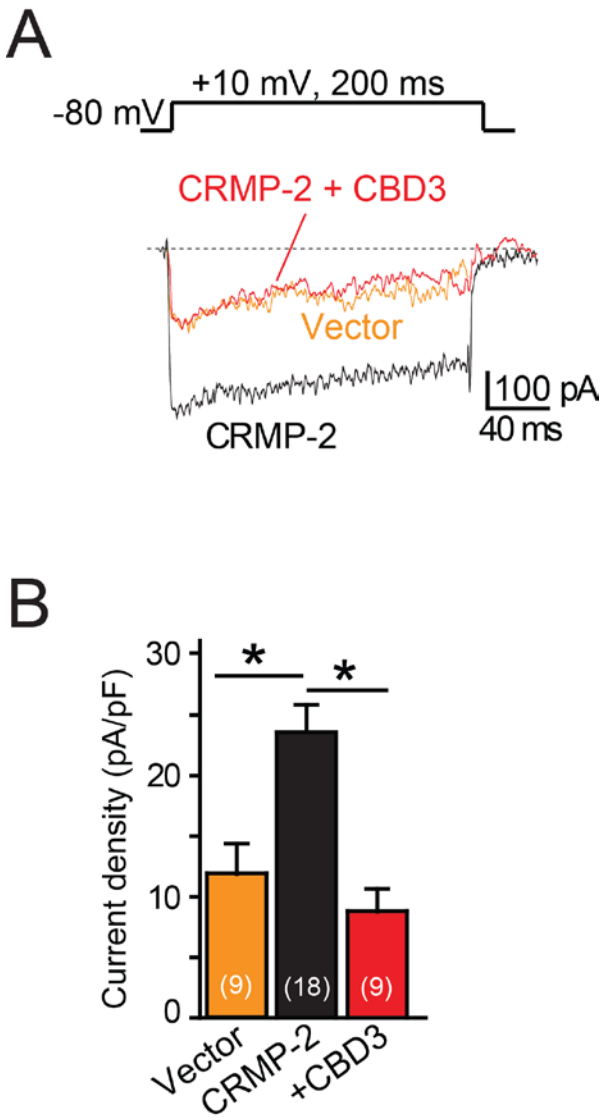

Figure 3.23. CBD3 reverses CRMP-2-mediated enhancement of Ca^{2+}-currents

(**A**) Top displays the voltage protocol used to elicit Ca^{2+} channel currents, bottom displays exemplar traces from hippocampal neurons transfected with vector (EGFP), CRMP-2-EGFP alone, or CRMP-2-EGFP along with CBD3. (**B**) Bar graph depicting the peak current density (pA/pF) at +10 mV for the various transfection conditions. Electrophysiology experiments were performed by Dr. Yuying Wang.

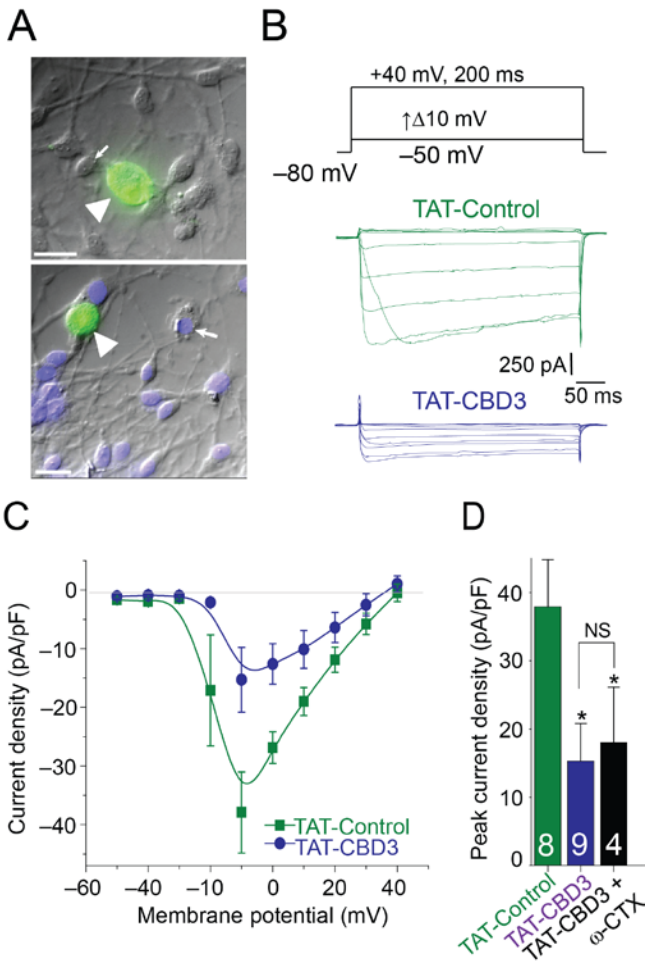

Figure 3.24. TAT-CBD3 reduces Ca^{2+}-currents in primary sensory neurons

(**A**) Representative differential interference contrast/fluorescence images showing robust penetration of FITC-TAT-CBD3 into DRGs (arrowheads) but not other cells (arrows). Nuclei are stained with Hoechst dye in the bottom image. Scale bars, 10 µm. (**B**) Representative current traces from a DRG incubated for 15 min with TAT-Control (10 µM; green) or TAT-CBD3 (10 µM; purple) in response to the voltage steps illustrated at the top. (**C**) Current-voltage relationships for the currents shown in **B** fitted to a b-spline line. Peak currents were normalized to the cell capacitance. (**D**) Peak current density measured at -10 mV for DRGs incubated with TAT-Control, TAT-CBD3 or TAT-CBD3 + 1 µM ω-conotoxin (CTX). The numbers in parentheses represent numbers of cells tested. *P < 0.05 versus TAT-Control. Electrophysiology experiments performed by Dr. Weiguo Zhu and Dr. Yuying Wang.

3.13. TAT-CBD3's effect on CGRP release

As the physiological function of CaV2.2 is to facilitate neurotransmitter release the next logical step was to determine if TAT-CBD3 could prevent neurotransmitter release in sensory neurons. This would further support TAT-CBD3 as a functionally relevant modulator of CaV2.2. CaV2.2 has been shown to regulate release of many different neurotransmitters in sensory neurons, one of particular interest to pain research is calcitonin gene related peptide (CGRP) (Evans et al., 1996; Maggi et al., 1990b). CGRP is a potent neuropeptide that induces vasodilatation and has been linked to pain and inflammation likely due to this action (Brain et al., 1985; Schaible, 1996; Sun et al., 2003). Capsaicin-induced release of CGRP was measured by Dr. Djane Duarte (in collaboration with Dr. Michael Vasko's laboratory) from rat spinal cord slices following a 10 min incubation with either 20 μM TAT-Control or TAT-CBD3 (Figure 3.25). CGRP was measured using a radio-immuno assay to detect immunoreactive CGRP (iCGRP). Slices incubated with TAT-Control displayed a ~9 fold increase in iCGRP in response to Capsaicin exposure whereas those incubated with TAT-CBD3 displayed less than a 3 fold increase compared to basal iCGRP levels. These findings strongly support that inhibition of CaV2.2 by TAT-CBD3 results in a functionally relevant decrease in stimulated release of CGRP. An important note is that TAT-CBD3 incubation did not alter the total content of iCGRP.

3.14. Systemic administration of TAT-CBD3 for the treatment of neuropathic pain

The results to this point strongly support TAT-CBD3 as a novel antagonist to CaV2.2 function as seen by decreases in current density and CGRP release. Based upon these findings and the previous link between CaV2.2 and pain I next asked if TAT-CBD3 could reduce pain using an *in vivo* model of hypersensitivity. Through a collaboration with the laboratory of Dr. Fletcher White and performed by Matthew Ripsch the *in vivo* efficacy of TAT-CBD3 was tested. We utilized a neuropathic pain model in which animals are treated with the anti-retroviral drug dideoxycytidine (ddC) (Bhangoo et al., 2009; Joseph et al., 2004). Nucleoside reverse

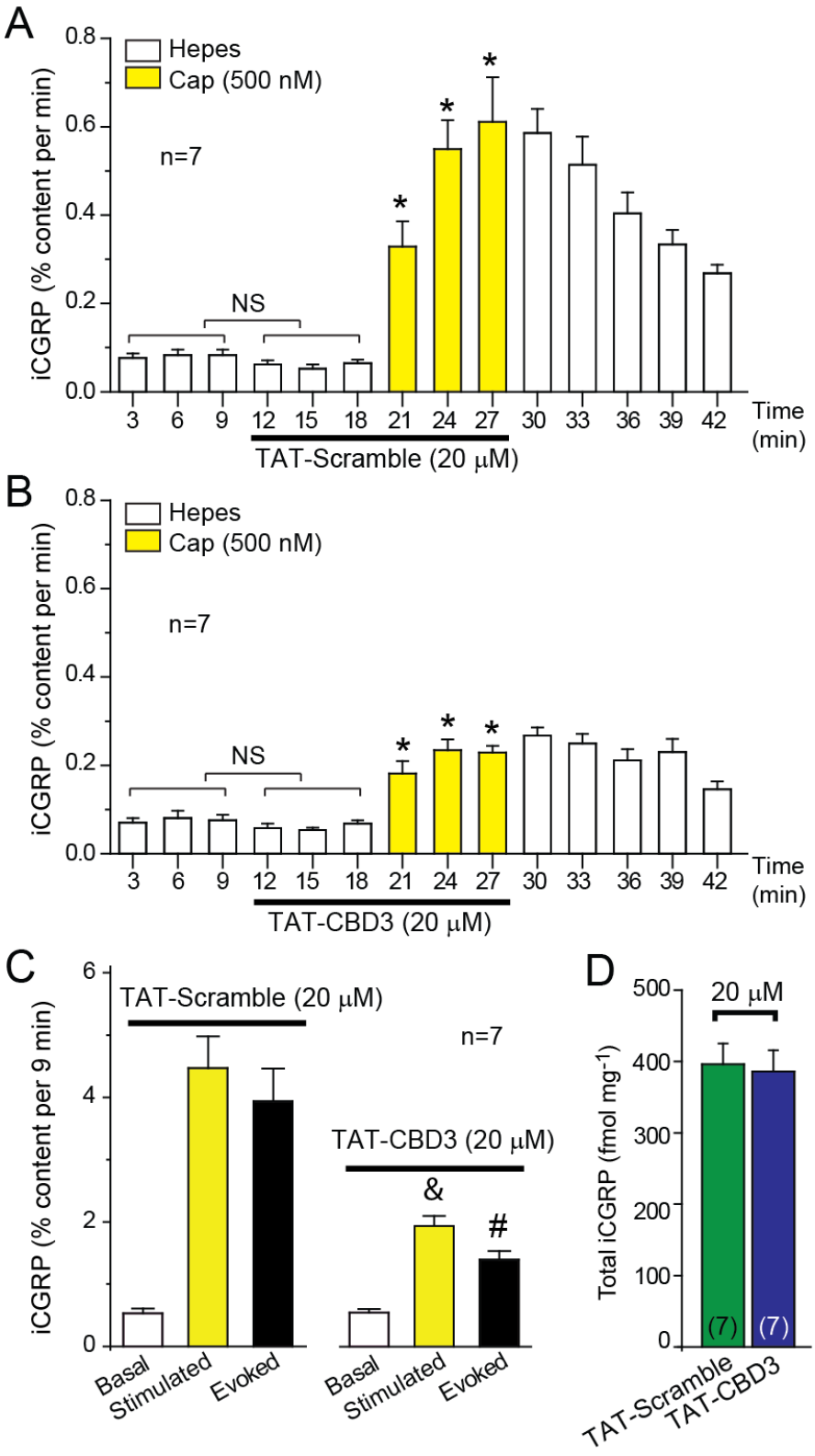
A
Hepes
Cap (500 nM)
n=7
iCGRP (% content per min)
NS
Time (min)
TAT-Scramble (20 μM)
B
Hepes
Cap (500 nM)
n=7
iCGRP (% content per min)
NS
Time (min)
TAT-CBD3 (20 μM)
C
TAT-Scramble (20 μM)
n=7
TAT-CBD3 (20 μM)
iCGRP (% content per 9 min)
Basal
Stimulated
Evoked
D
20 μM
Total iCGRP (fmol mg-1)
(7)
(7)
TAT-Scramble
TAT-CBD3

Figure 3.25. TAT-CBD3 attenuates CGRP release from spinal cord slices

(**A**–**D**) iCGRP release was measured in three 3-min exposures to HEPES buffer alone (white bars), to HEPES buffer with peptides (white), to HEPES buffer containing 500 nM capsaicin (Cap) with peptides (yellow), then to HEPES alone to re-establish baseline (white). Each column represents the mean ± s.e.m. of iCGRP levels in each 3-min perfusate sample, expressed as percentage of total peptide content in the tissues per minute (n = 7 rats). TAT-Control (**A**) or TAT-CBD3 (**B**) was included as indicated by the horizontal bars, *p < 0.05 versus basal iCGRP release in the absence of capsaicin (analysis of variance (ANOVA), Dunnett's post hoc test). Neither peptide altered basal iCGRP release (not significant, NS). (**C**) Basal release is the amount of iCGRP released in the three fractions exposed to HEPES plus peptides. Stimulated release is the amount of iCGRP released in the three fractions exposed to 500 nM capsaicin + peptides. The evoked release was obtained by subtracting iCGRP release during three basal fractions (12–18 min) from that during the three capsaicin-stimulated fractions (21–27 min) and expressed as percentage of total iCGRP content in each group. *P < 0.05 versus the respective TAT-Control using a Student's t-test. (**D**) Total content of iCGRP (in fmol mg−1) is the sum of CGRP released during perfusion and from spinal cord tissue measured at the end of the release experiments. CGRP release experiments were performed by Dr. Djane Duarte.

transcriptase inhibitors such as ddC, which are commonly used to treat AIDS, produce side effects that include painful neuropathies. To induce hypersensitivity using this *in vivo* model, rats are inject once with 25 mg/kg ddc intraperitoneally (i.p.) and 7 days post injection (7 PID) mechanical hypersensitivity is observed by measuring paw withdrawal threshold (PWT) (Figure 3.26). The hypersensitivity is seen as a predictable decrease in PWT. Animals were then treated i.p. with TAT-peptides and PWT was measured 1 h following injection. A significant increase in PWT was seen with injection of TAT-CBD3 at 0.1 mg/kg and complete reversal of hypersensitivity was accomplished by 1 mg/kg. No additional increase in PWT was observed when TAT-CBD3 was increased to 10 mg/kg, suggesting that TAT-CBD3 is targeting hypersensitivity rather than sensitivity in general. TAT-Control did not significantly affect PWT when injected at 1 mg/kg. These results extend the *in vitro* work that was completed using TAT-CBD3 showing that it is effective in treating *in vivo* neuropathy.

Having shown that TAT-CBD3 is effective *in vivo*, I next sought to determine the safety of TAT-CBD3 as it relates to memory and motor function. These two cognitive functions were used in this preliminary safety test for a gauge of any possible side effects that TAT-CBD3 may have. These tests were completed in collaboration with Dr. Xiao-ming Xu's laboratory by Dr. Naikui Liu. The rotarod test was performed to measure for any possible effects on locomotor function, motor coordination, or sedation (Hedgecock et al., 1985). Mice were injected with vehicle, TAT-Control, or TAT-CBD3 and tested using the rotarod using either a fast (left panel) or slow (right panel) acceleration profile (Figure 3.27A). TAT-CBD3, at doses as high as 50 mg/kg, showed no effect on the animals' ability to stay upright on the rotating rod at 1 h or up to 7 days later. This suggests that TAT-CBD3 does not cause severe sedation or observable deficits in locomotor function and coordination. It is, however, important to note that injection of 50

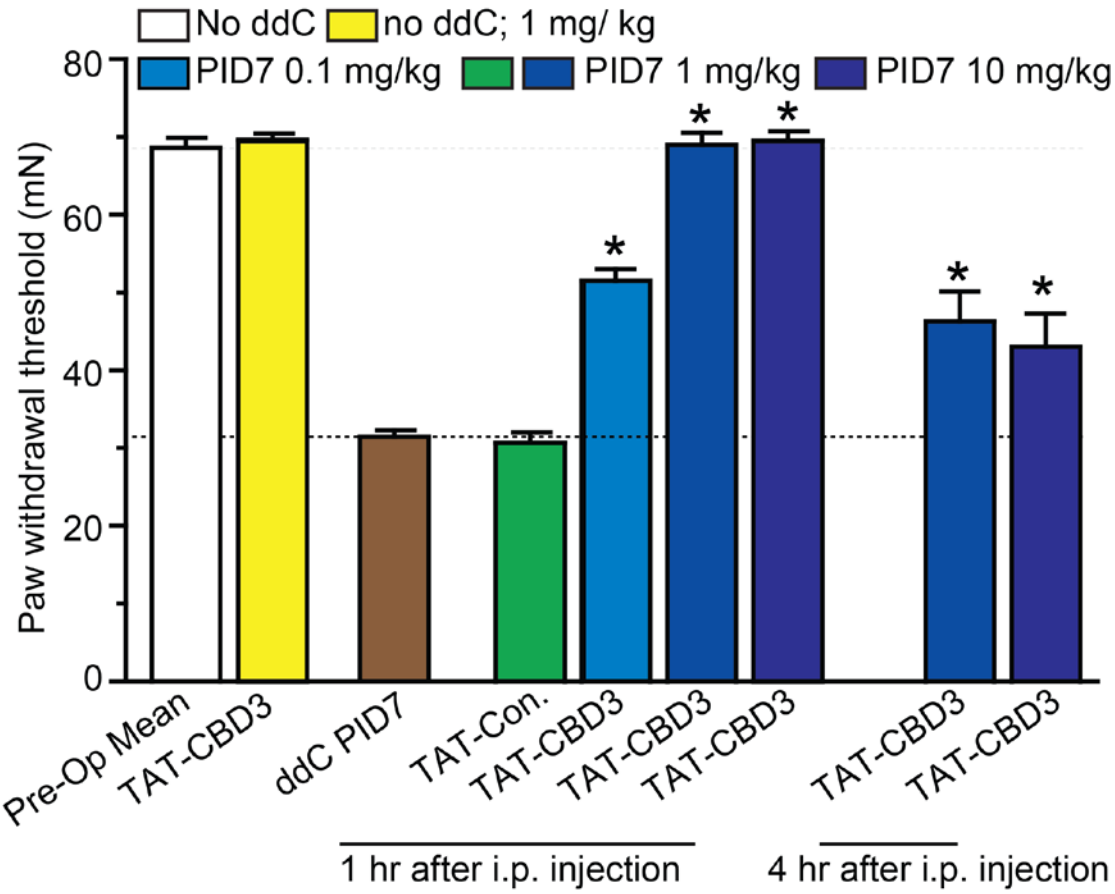

Figure 3.26. Systemic administration of TAT-CBD3 reduces neuropathic hyperalgesia

Adult Sprague dawley rats were given a single injection of ddc and then treated 7 days following injection (PID7) with TAT-CBD3 or TAT-Control. This single injection of ddc induces neuropathic hypersensitivity as observed by a decrease in paw withdrawal threshold (PWT). Reversal of this decrease in PWT is indicative of a reduction in the hypersensitivity associated with neuropathic pain. Response of ddC alone at PID7 is shown in the brown bar. *$p < 0.05$ versus ddC or TAT-Control (ANOVA with Student-Newman-Keuls post hoc test, n = 7). Animal measurements of hypersensitivity were performed by Matthew Ripsch.

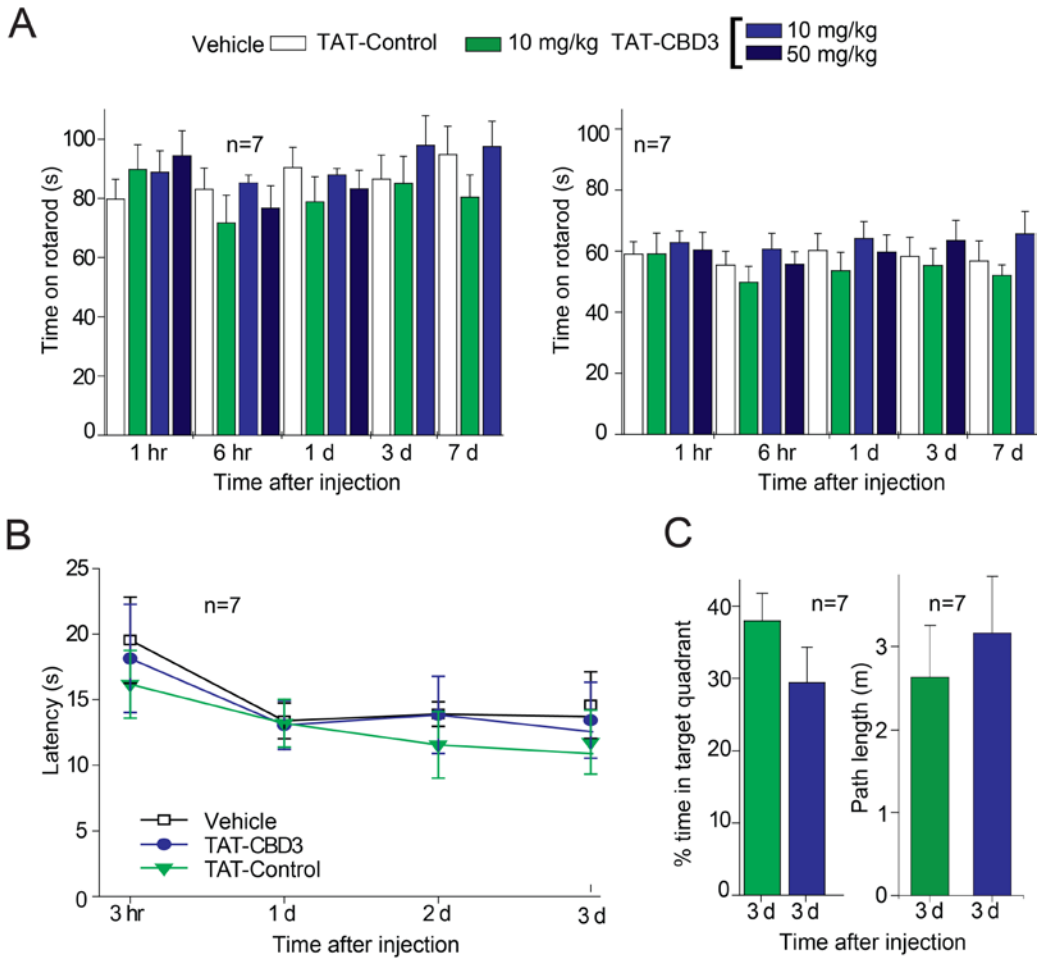

Figure 3.27. TAT-CBD3 does not alter gross motor coordination or memory retrieval

(**A**) Motor coordination of animals treated with either TAT-CBD3 or TAT-Control was assessed using the rotarod test. Latency to fall off a slow (left) or fast (right) rotating rod was recorded for animals treated with the TAT-peptides. There were no significant differences in rotarod performances between groups (ANOVA with Dunnett's post hoc test). (**B**) Memory retrieval ability in mice was measured using the Morris water maze. Latency for mice to find the hidden platform during the test was not different between groups. (**C**) Time spent in target quadrant. There were no significant differences in percentage time spent in target quadrant or path length between groups (Student's t-test). Experiments performed by Dr. Naikui Liu.

mg/kg caused a single transient (< 1 min) motor dysfunction as observed by tail kinking and body contortion. It is unknown the cause of this although there appeared to be no long term effects. Next I sought to determine if TAT-CBD3 led to deficits in memory using the Morris water maze, again in collaboration with Dr. Xu and completed by Dr. Liu. Mice were trained in the Morris water maze for 4 days prior to treatment with TAT-peptides. Following injection animals were tested in the morris water maze at 3 h, 1, 2, and 3days (Figure 3.27B, C). Animals showed no significant deficit in latency to reach the platform at any of these time points. This suggests that TAT-CBD3 does not affect memory retrieval. However, as TAT-CBD3 was only tested after training it is unknown if it affects memory acquisition.

3.15. Conclusions

Prior to the beginning of my research into the interaction between CRMP-2 and CaV2.2 it was unknown if CRMP-2 regulated synaptic transmission. Through the results contained in this Chapter I have shown that by modulating CaV2.2 function CRMP-2 is able to alter neurotransmitter release. CRMP-2 directly interacts with CaV2.2 through a small peptide sequence (CBD3) which interacts with the CaV2.2 cytosolic regions L1 and Ct-d. This interaction is dynamically regulated as depolarization leads to enhanced CaV2.2-CRMP-2 interactions. Importantly CaV2.2 function correlates with CRMP-2 expression, which is likely through an observed regulation of CaV2.2 surface expression by CRMP-2. Collectively the regulation of CaV2.2 by CRMP-2 culminates with enhancement of neurotransmitter release. Furthermore phosphorylation of CRMP-2 by Cdk5 enhances the interaction between CRMP-2 and CaV2.2. This is also supported by the finding that Cdk5 phosphorylation site mutants of CRMP-2 do not enhance CaV2.2 function. The biochemical basis of CRMP-2's regulation of CaV2.2 is supported by the ability of CBD3 to both disrupt the CRMP-2-CaV2.2 complex as well as antagonized CRMP-2-mediated enhancement of CaV2.2 function. Finally the CRMP-2-

CaV2.2 complex is validated as a therapeutic target for neuropathic pain by the observed reversal of pain behavior in animals following systemic administration of the cell penetrant TAT-CBD3.

CaV2.2 functions as both a gate keeper for the requisite Ca^{2+} influx for neurotransmitter release as well as a hub for synaptic proteins in the active zone. The interaction between CRMP-2 and CaV2.2 leads to enhanced surface expression of CaV2.2 culminating in enhanced neurotransmitter release, and therefore identifies CRMP-2 as an important regulator of the pre-synaptic Ca^{2+} channel complex. While this supports CRMP-2 as a functionally relevant modulator of CaV2.2 function it is unknown if CRMP-2 also serves as a scaffold for additional proteins to interact with CaV2.2. CRMP-2 has previously been shown to traffick the TrkB receptor via a multiprotein complex (Arimura et al., 2009b). The trafficking of CaV2.2 by CRMP-2 may employ a similar complex of several proteins all of which are required for mobilization of CaV2.2.

Interestingly I observed that Cdk5-, but not ROCK-, mediated phosphorylation of CRMP is responsible for enhancement of CaV2.2-mediated Ca^{2+} influx. This is particularly intriguing as the Sema3A and LPA pathways induce growth cone collapse via phosphorylation of CRMP-2 by Cdk5 or ROCK, respectively. This suggests that conformational changes in CRMP-2 responsible for growth cone collapse are distinct from that required for regulating CaV2.2. Furthermore this allows cells to select whether a neuron wants to retract and enhance CaV2.2 (Sema3A) or retract without enhancing CaV2.2 (LPA). A neuron's ability to select between these two outcomes may be a vital step in axons deciding what synaptic connections to make. The signaling with regards to CaV2.2 and Cdk5 becomes murky, however, as a recent study found that Cdk5 directly phosphorylates CaV2.2 enhancing its synaptic localization through enhancing RIM's association with CaV2.2 (Su et al., 2012). This finding along with a previous report showing that phosphorylation of CASK by Cdk5 leads to enhanced CaV2.2 synaptic targeting suggests multiple signaling pathways are able to utilize Cdk5 to enhance synaptic transmission via modulating CaV2.2 (Samuels et al., 2007b). It is unknown, however, if Sema3A application for

example will specifically engage Cdk5 phosphorylation of CRMP-2 or if other Cdk5-mediated pathways will also be employed. Additional studies into the selectivity of the pathways of Sema3A, LPA, and growth factors are needed to determine how modulation of CaV2.2 by CRMP-2 may be involved. In addition the observed enhancement of the CRMP-2-CaV2.2 interaction in depolarized synaptosomes may be due in part to Cdk5 activation and subsequent phosphorylation of CRMP-2.

Structural and biochemical studies have demonstrated that CRMPs exist as tetramers (Wang and Strittmatter, 1997). Tetramer formation is stabilized by the presence of divalent cations, whereas in the presence of cation chelating agents almost half of CRMP-2 exists in a monomeric state (Majava et al., 2008). While I have not directly tested whether Cav2.2 binds to a tetrameric or monomeric form of CRMP-2, the latter is a more likely possibility given the presence of chelators in my binding assay buffers. If, however, CRMP tetramers bind Cav2.2, then the subunit composition of the tetramer will be an important determinant of its effect on Cav2.2. The composition of CRMP tetramers will vary due to the differential spatial and developmental patterns of CRMPs expression within the nervous system (Wang and Strittmatter, 1996). Thus, CRMPs, by virtue of their ability to heteromultimerize in multiple combinations, may help in 'fine tuning' the effects on Ca^{2+} channel density, thereby adding another level of complexity in transmitter release regulation. This oligomeric assembly of CRMPs may also serve as the building blocks upon which presynaptic signaling complexes are erected.

CHAPTER 4. NEUROPROTECTION BY TAT-CBD3 THROUGH INHIBITION OF NMDARS

4.1. Introduction

The results from Chapter 3 positioned CRMP-2 as a novel modulator of pre-synaptic function through interaction and modulation of CaV2.2. Prior to the start of my thesis work, two studies potentially linking CRMP-2 to NMDARs suggested that CRMP-2's regulation of Ca^{2+} channels may extend beyond the pre-synaptic space to the post-synaptic zone as well (Al-Hallaq et al., 2007; Bretin et al., 2006). The first study, by Bretin and colleagues, found that CRMP-2 cleavage occurs due to NMDAR activation. These authors also found that CRMP-2 expression increased glutamate toxicity. As CRMP-2 is cleaved following glutamate exposure, they next asked if expression of a cleaved form of CRMP-2 affected neurotoxicity. Notably, they observed that neurons expressing the calpain cleaved form of CRMP-2 had reduced NMDAR responses and decreased neurotoxicity. As overexpression of CRMP-2 was neurotoxic, it appeared then that cleaved CRMP-2 has a dominant negative effect leading to enhanced neuronal survival. Furthermore, NMDAR surface expression was decreased when calpain cleaved CRMP-2 was overexpressed. These findings supported the notion that calpain cleaved CRMP-2 may be neuroprotective by reducing NMDAR surface expression and also by inference that over expression of CRMP-2 is perhaps neurotoxic by upregulating NMDAR surface expression. The second study potentially linking CRMP-2 to NMDARs reported a biochemical complex between CRMP-2 and NR2A and 2B containing NMDARs (Al-Hallaq et al., 2007). In exploring potential regulation of NMDARs by CRMP-2, I began with the hypothesis –based largely on these two reports– that a biochemical interaction between NMDARs and CRMP-2 was key to the link between CRMP-2 expression on glutamate toxicity and that calpain-mediated cleavage of CRMP-2 was an important determinant in the regulation of NMDARs by CRMP-2.

Further support for my investigation into CRMP-2 and NMDARs came from studies on CRMP-2 and neurotoxicity that reported calpain-mediated cleavage of CRMP-2 occurred in response to sundry neurotoxic insults including injury, ischemia, and excitotoxic exposure to glutamate (Bretin et al., 2006; Chung et al., 2005; Hou et al., 2009; Jiang et al., 2007; Touma et

al., 2007; Zhang et al., 2009). Sequence inspection of the CRMP-2 CBD3 peptide that I had identified in Chapter 3 revealed that this peptide was very close to the putative calpain cleavage sites on CRMP-2. Furthermore, the Ca^{2+} binding protein calmodulin apparently shields CRMP-2 from calpain cleavage by binding to a sequence with CRMP-2 that is slightly N-terminal to the CBD3 sequence (Zhang et al., 2009; Zhang et al., 2007). Based on these findings, I hypothesized that the CBD3 peptide could affect calpain-mediated cleavage of CRMP-2 and thus may have neuroprotective effects. Mechanistically, I envisioned that the alteration in calpain-mediated cleavage of CRMP-2 could be neuroprotective by altering NMDAR surface expression. Based upon these hypotheses, in this Chapter I will seek to determine if TAT-CBD3 can alter calpain-mediated cleavage of CRMP-2, affect the functional interaction between CRMP-2 and NMDAR, and protect neurons from glutamate toxicity. Part of the work in this Chapter has been presented in previous publications (Brittain et al., 2011a; Brittain et al., 2012a).

4.2. TAT-CBD3 reduces calpain cleavage of CRMP-2

I first tested if TAT-CBD3 could alter calpain cleavage of CRMP-2 following glutamate activation of calpain. E19 DIV 7 cortical neurons were pre-treated for 10 minutes with TAT peptides and then stimulated for 30 min with 200 μM glutamate and 100 μM D-serine; D-serine has been reported to be the dominant co-agonist for NMDARs (Mothet et al., 2000; Shleper et al., 2005). Lysates from these cells were then immunoblotted with a CRMP-2 antibody that recognizes C-terminal cleaved and full-length CRMP-2. Blots were also probed for β-Tubulin, which served as a loading control. I observed a 55 kDa cleaved fragment of CRMP-2 as well as the 62 kDa full-length CRMP-2 protein (Figure 4.1A), consistent with earlier findings (Bretin et al., 2006; Hou et al., 2009). CRMP-2 cleavage was quantified by densitometry and is reported as the ratio of cleaved CRMP-2 to Tubulin (Figure 4.1B). Exposing neurons to 10 μM TAT-CBD3 prior to stimulation led to a significant reduction in CRMP-2 cleavage at 0.5, 4 and 24 hours following stimulation compared to neurons treated with 10 μM TAT-Control ($p < 0.05$, Student's

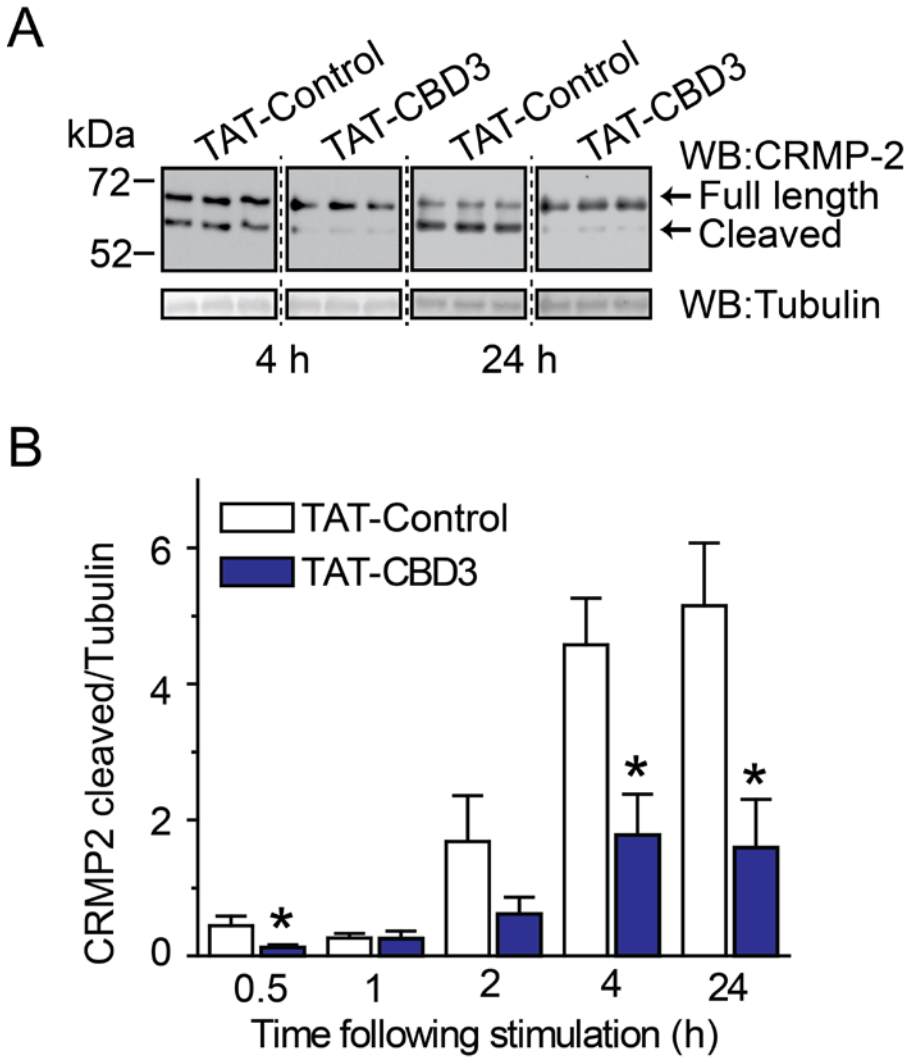

Figure 4.1. TAT-CBD3 attenuates cleaveage of CRMP-2 following glutamate exposure

(**A**) Western blot of CRMP-2 cleavage following excitotoxic challenge. E18-19 DIV7 neurons were stimulated with Glu/Ser for 30 min and lysates made at 4 and 24 h later. Cleavage of CRMP-2 is observed by the appearance of a ~55 kDa band representing cleaved CRMP-2. Tubulin loading controls are also shown. (**B**) Summary of CRMP-2 cleavage at various times following stimulation. Cleavage of CRMP-2 is presented as cleaved CRMP-2/Tubulin (n = 6–12 per condition). Asterisk indicates significant difference compared to time-matched TAT-Control ($p < 0.05$; Student's t-test).

t-test, n=6-12). For example, at 24 hours post-stimulation, neurons exposed to TAT-CBD3 had ~70% less cleaved CRMP-2 compared to neurons exposed to TAT-Control.

In addition to CRMP-2, I also observed that cleavage of the prototypical calpain substrate αII-spectrin (Czogalla and Sikorski, 2005) was inhibited by TAT-CBD3 and that TAT-Control did not alter cleavage compared to vehicle treated neurons (Figure 4.2). This is an important finding as it suggests that TAT-CBD3's inhibition of CRMP-2 cleavage is not specific to CRMP-2 and likely affects multiple calpain substrates. I next asked if the reduction of CRMP-2 cleavage was specific to induction by glutamate. This was tested by pre-incubating neurons with TAT-CBD3 and then inducing non-specific Ca^{2+}-influx with the Ca^{2+} ionophore ionomycin, which has been shown to activate calpain (Lee et al., 2000). Ionomycin-induced cleavage of CRMP-2 was not affected by TAT-CBD3 (Figure 4.3). This result supports that TAT-CBD3 works upstream of calpain activation. To further support this finding I tested TAT-CBD3's ability to alter cleavage of CRMP-2 in lysates. Lysates were generated by homogenizing and subsequent lysis of PN1 rat brains in RIPA #1 before stimulating calpain activation by incubation with 20 mM $CaCl_2$. CRMP-2 cleavage was unaffected by various concentrations of TAT-CBD3, as a control the calpain inhibitor MDL-28170 was also used which greatly attenuated cleavage (Figure 4.4). Consistent with these results, calpain activity (measured in lysates using the fluorogenic calpain substrate *t*-Boc) was also not affected by incubation with TAT-CBD3 (Figure 4.5). Collectively, these findings suggest that that TAT-CBD3 does not prevent CRMP-2 cleavage due to direct modulation of calpain or CRMP-2 *per se*, rather it appears that TAT-CBD3 acts on a target upstream of calpain activation.

4.3. TAT-CBD3 increases cell viability following an excitotoxic insult

Having shown that TAT-CBD3 can attenuate calpain cleavage of CRMP-2 and αII-spectrin following glutamate stimulation this led me to me test if TAT-CBD3 was neuroprotective against excitotoxicity. Calpain and its role in neuronal toxicity has been

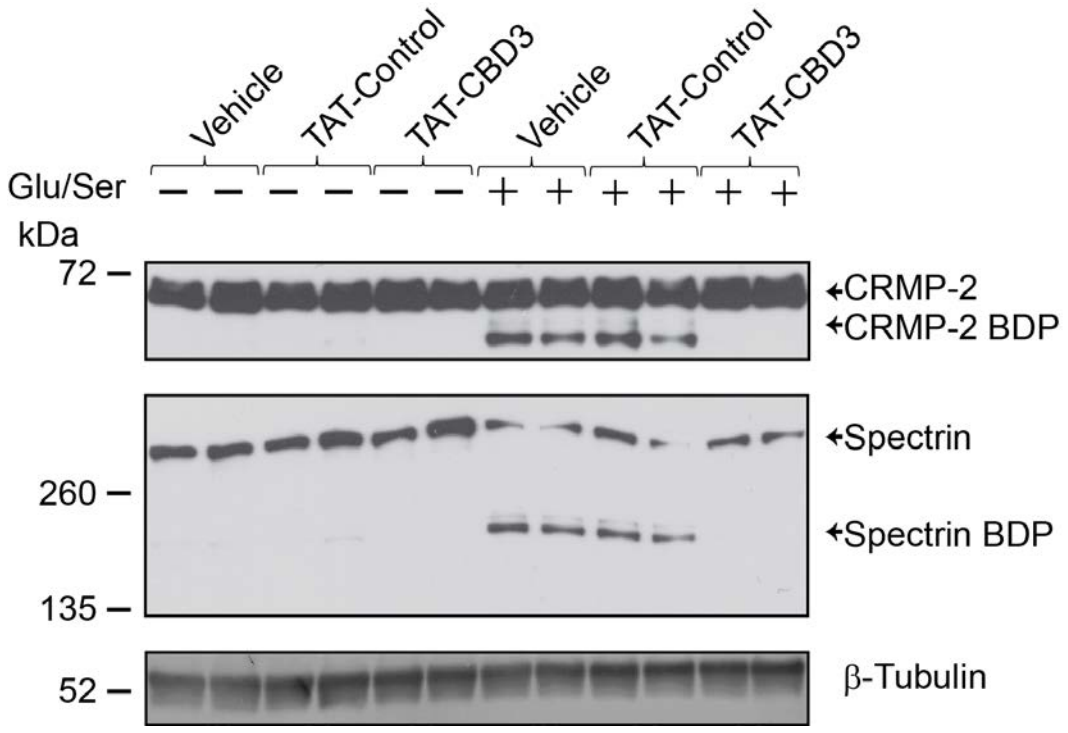

Figure 4.2. TAT-CBD3 prevents cleavage of α-spectrin and CRMP-2 following glutamate exposure

Western blot of CRMP-2 and αII-spectrin cleavage following excitotoxic challenge. E18-19 DIV7 neurons were stimulated with Glu/Ser for 30 min and lysates made 24 h later. Cleavage of αII-spectrin is observed by the appearance of a ~150 kDa band representing cleaved αII-spectrin. Tubulin loading controls are also shown, BDP: breakdown product.

.

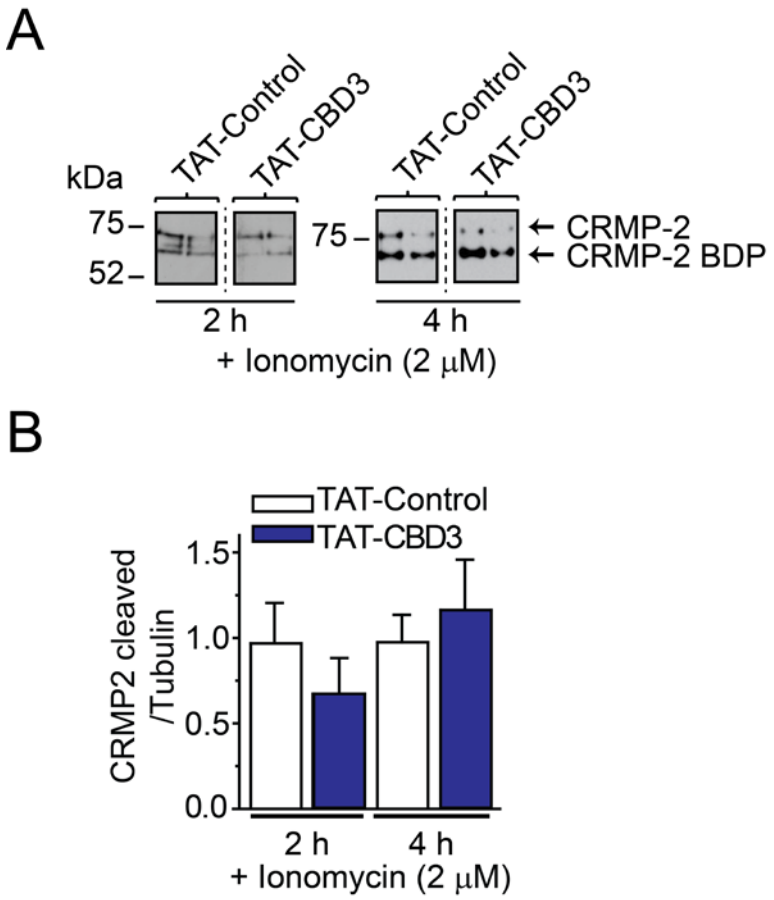

Figure 4.3. TAT-CBD3 does not alter cleavage of CRMP-2 in response to Ionomycin

(**A**) Western blot of CRMP-2 cleavage following treatment with Ionomycin. E18-19 DIV7 neurons were stimulated with Ionomycin for 2 or 4 h and lysates were made following stimulation. (**B**) Summary of CRMP-2 cleavage at 2 and 4 h following stimulation. Cleavage of CRMP-2 is presented as cleaved CRMP-2/Tubulin (n = 5–6 per condition).

.

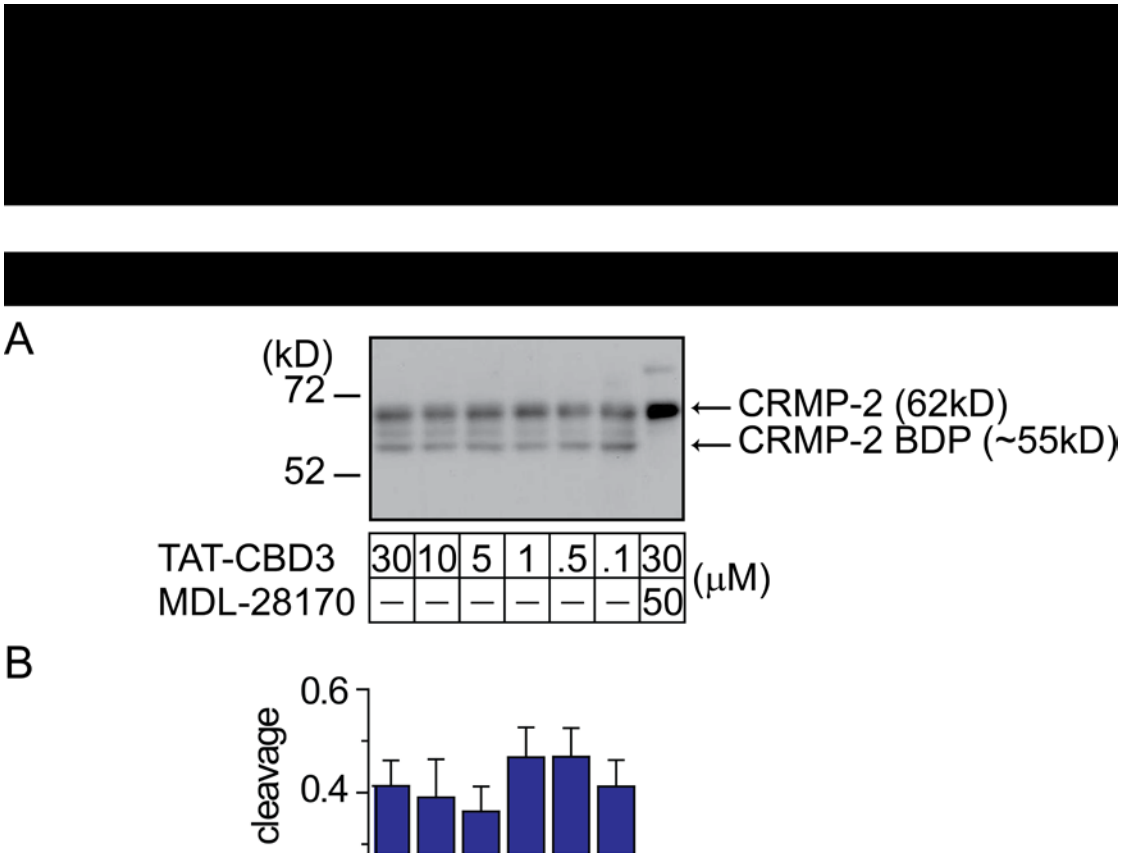

Figure 4.4. TAT-CBD3 does not alter *in vitro* cleavage of CRMP-2

(**A**) Equal amounts of lysates prepared from E18-19 brains were treated for 10 min with TAT-CBD3 (0.1 to 30 μM) or 30 μM TAT-CBD3 + 50 μM MDL28170 and then calpain was activated by addition of 20 mM $CaCl_2$. The cleavage reaction was stopped at 30 min and CRMP-2 cleavage assessed by immunoblotting. (**B**) Bar graph representation of CRMP-2 cleavage, where cleavage is equal to cleaved CRMP-2 / total CRMP-2 (*, $p < 0.05$ vs. all other conditions; n = 4–5 per condition).

.

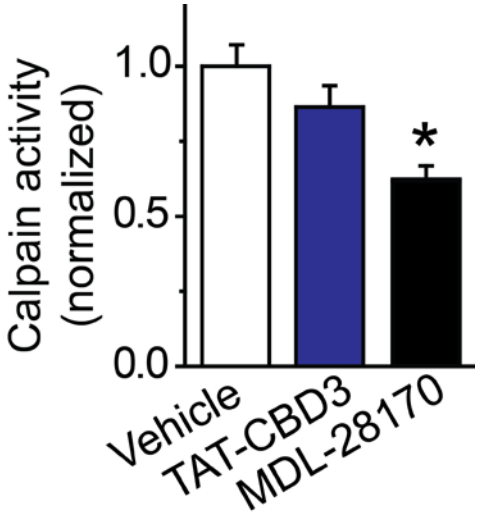

Figure 4.5. TAT-CBD3 does not alter *in vitro* activation of calpain

Lysates were pre-incubated with vehicle (0.1% DMS), TAT-CBD3 (10 μM), or MDL-28170 (50 μM) prior to measuring calpain activity via measurement of cleavage of the fluorogenic calpain substrate *t*-Boc. Values are normalized to vehicle treated lysates (*, $p < 0.05$ vs. vehicle by one-way ANOVA with post-hoc Dunnett's test; n=23-24 from 3 experiments).

.

.

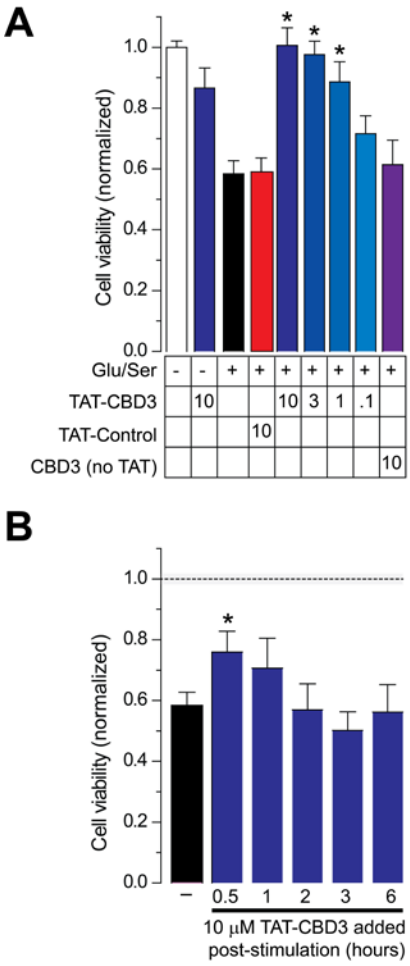

Figure 4.6. Prevention of glutamate-induced reduction in cell viability by TAT-CBD3

(**A**) Cell viability of E18-19 DIV 7 cortical neurons was determined using an MTS cell viability assay. Neurons were incubated with peptides for 10 minutes prior to stimulation with 200 μM glutamate and 100 μM D-serine for 30 minutes. Viability was then measured 24 hours later, with all values normalized to no stimulation control ($n \geq 32$ each from at least four separate experiments). Asterisk indicates significant difference compared to stimulated control ($p < 0.05$). All values are in μM. (**B**) Viability of stimulated neurons was also measured with addition of TAT-CBD3 at various time points following stimulation ($n \geq 16$). Asterisk indicates significant difference compared to stimulated control ($p < 0.05$). The dotted line and shaded box illustrates the normalized cell viability ± SEM in the absence of any stimulation (from **A**).

extensively studied, but despite these studies it is still unclear how cleavage of individual substrates, CRMP-2 for example, affect neuronal survival (Adamec et al., 1998; Bretin et al., 2006; Brorson et al., 1995; Czogalla and Sikorski, 2005; del Cerro et al., 1994; Dutta et al., 2002; Guttmann et al., 2002; Hong et al., 1994; Lee et al., 2000; Rami et al., 1997; Simpkins et al., 2003). Cortical neurons were stimulated as mentioned above with pre-treated for 10 minutes with TAT peptides. Cell viability was measured 24 hours later by MTS cell viability assay, which measures reductase activity in metabolically active cells. Within each experiment cell viability values were normalized to values obtained for unstimulated control neurons. Approximately 58 ± 4% of the neurons survived the Glu/Ser stimulation compared to unstimulated neurons (Figure 4.6A). Neurons pre-treated for 10 min with 10 μM TAT-CBD3 and then stimulated with Glu/Ser completely survived the excitotoxic treatment. Significant neuroprotection by TAT-CBD3 was evident at 3 and 1 μM but not at 0.1 μM. In contrast, pre-treating neurons with 10 μM TAT-Control resulted in cell viability levels (~59 ± 5%, n=48) similar to Glu/Ser-stimulated neurons. Treatment of neurons with 10 μM TAT-CBD3 alone, without stimulation, did not affect cell viability. Application of a CBD3 peptide lacking the TAT cell-penetrating sequence did not prevent cells from Glu/Ser-induced cell death, suggesting that the CBD3 peptide acts on an intracellular target to achieve neuroprotection.

An important aspect of neuroprotective agents is their ability to prevent excitotoxic death when administered post-stimulation. To test if TAT-CBD3 is neuroprotective following stimulation, neurons were treated with 10 μM TAT-CBD3 for 10 minutes at 0.5, 1, 2, 3, and 6 hours after Glu/Ser stimulation and cell viability measured as described. Except for modest, but statistically significant, neuroprotection at 0.5 hour following stimulation (Figure 4.6B), TAT-CBD3 was not effective at later times. Together, the results suggest that: (1) TAT-CBD3 is neuroprotective and (2) the interaction between CRMP-2 and target protein is likely important for mediating the early phase of neuronal death observed following excitotoxic insults.

4.4. Lentiviral-mediated knockdown of CRMP-2 is neuroprotective

My earlier findings showed that TAT-CBD3 protects neurons from an excitotoxic insult while also reducing cleavage of CRMP-2 but raised some important questions: *(1) is the neuroprotection due to inhibition specifically of CRMP-2 and (2) does the activity of TAT-CBD3 require CRMP-2 to be present?* To address if the neuroprotection was due to CRMP-2, cortical neurons were treated with CRMP-2 or scramble shRNA lentiviral particles at 2 DIV. After 5 days, the lentiviral-transduced neurons were pre-treated with TAT peptides for 10 minutes and then stimulated with Glu/Ser and cell viability measured 24 hours later (Figure 4.7). Cell viability was normalized to control neurons (no stimulation) treated with the same virus (scramble vs. CRMP-2 shRNA). CRMP-2 shRNA lentiviral–transduced neurons exhibited a significant increase in cell viability following stimulation compared to scramble shRNA treated neurons when pre-treated with TAT-Control (0.75 ± 0.04 vs. 0.52 ± 0.02, $p < 0.05$, Student's t-test, n=16). Complete neuroprotection was observed in neurons transduced with CRMP-2 shRNA lentivirus and pre-treated with TAT-CBD3 prior to excitotoxic challenge (1.07 ± 0.07; n=16). That neurons transduced with scramble shRNA lentivirus did not exhibit complete neuroprotection with TAT-CBD3 (e.g., compared to ~100% protection in TAT-CBD3 treated cells; Figure 4.6A) can likely be attributed to the alteration of survival by the viral load itself. Nonetheless, these findings demonstrate that it is CRMP-2 itself that mediates the neuroprotection. Furthermore, as TAT-CBD3 is also neuroprotective, it is likely that TAT-CBD3 works through antagonizing a function of CRMP-2.

4.5. Role of CaV2.2 in glutamate toxicity and CRMP-2 cleavage

My previous results in Chapter 3 have shown that CRMP-2 is an important regulator of CaV2.2 and furthermore that TAT-CBD3 in particular targets regulation of CaV2.2 by CRMP-2. Based upon these findings, I wanted to rule out the possibility that TAT-CBD3 was acting in

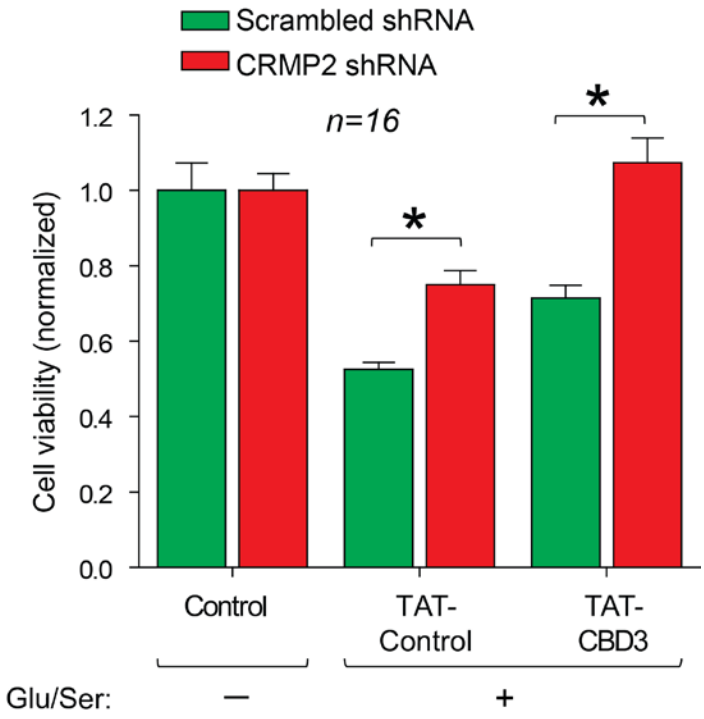

Figure 4.7. CRMP-2 knockdown is neuroprotective

Cortical neurons grown in culture for 2 days were treated with equal titers of scrambled or CRMP-2 shRNA lentivirus. Neurons were then grown for an additional 7 days prior to stimulation as in Figure 4.6. Neurons were treated with 10 μM of TAT-Control or TAT-CBD3 prior to stimulation and cell viability was measured 24 hours later. Values represent average of a single experiment which displayed same qualitative results as two separate experiments, n = 16. Asterisk indicates $p < 0.05$ by Student's t-test compared to scrambled shRNA for same peptide.

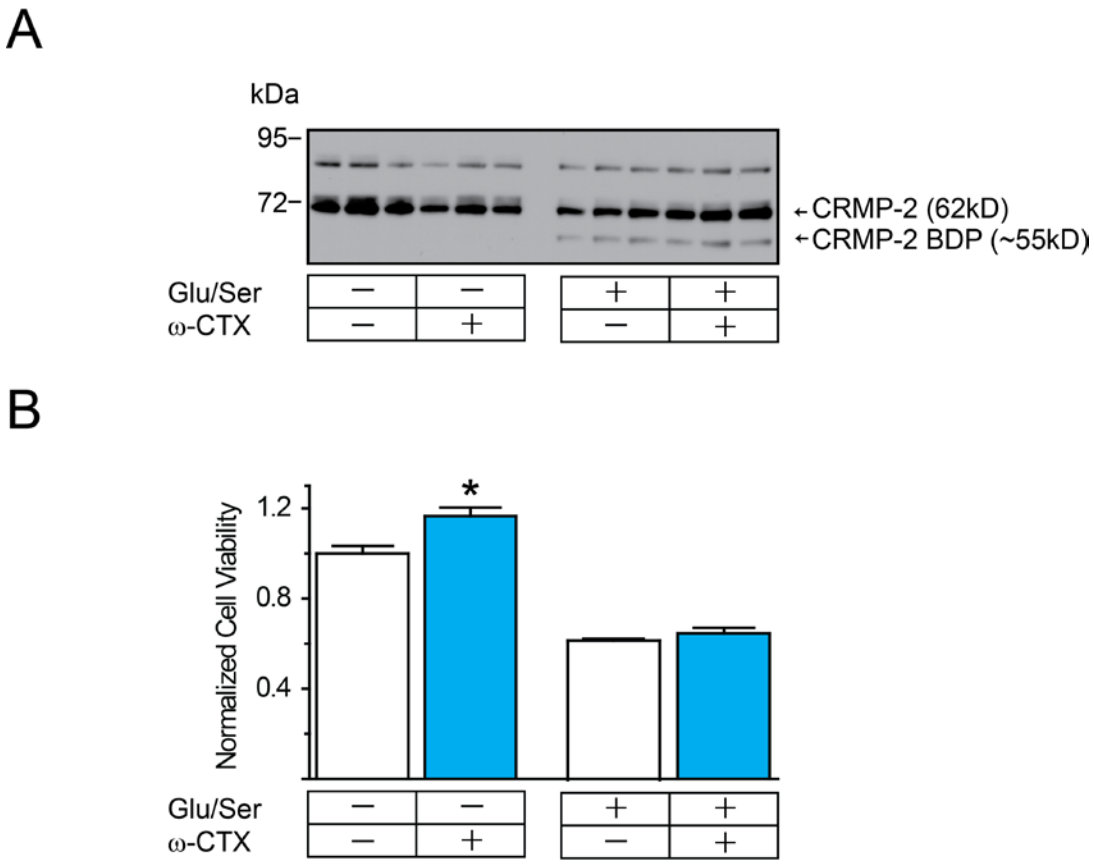

Figure 4.8. Blockade of CaV2.2 by ω-conotoxin GVIA is not neuroprotective and does not reduce CRMP-2 cleavage in response to glutamate stimulation

(**A**) Western blot of CRMP-2 cleavage following excitotoxic challenge with and without ω-conotoxin GVIA (ω-CTX, 1 μM). E18-19 DIV7 neurons were pre-incubated with ω-CTX or vehicle for 10 minutes prior to stimulation with Glu/Ser for 30 min and lysates made 24 h later (n = 6). (**B**) Neurons were stimulated using the same protocol as in panel b. Viability was then measured 24 hours later, with all values normalized to no stimulation control (n = 19 from two separate experiments, asterisk indicates $p < 0.05$ by Student's t-test compared to unstimulated control).

these experiments through inhibition of CaV2.2 activity. E19 DIV 7 Cortical neurons were stimulated using Glu/Ser as previously described with or without pre-incubation with 1 μM ω-CTX for 5 minutes. Lysates were then made 24 hr following stimulation and CRMP-2 cleavage was assessed by immunoblotting (Figure 4.8A). Treatment with ω-CTX with or without stimulation by Glu/Ser had no effect on CRMP-2 cleavage. Based upon this result it can be concluded that Ca^{2+}-influx through CaV2.2 is not a determinant of Glu/Ser-induced cleavage of CRMP-2 and that therefore the mechanism of action of TAT-CBD3 cannot be through inhibition of CaV2.2. Having shown that cleavage of CRMP-2 is not dependent on CaV2.2 activity I wanted to verify that neuronal survival as well was not dependent on CaV2.2 following Glu/Ser. Neurons were pre-incubated with ω-CTX prior to stimulation with Glu/Ser and viability was measured 24 hr later. The blockade of CaV2.2 with ω-CTX did not significantly alter neuronal survival of neurons following Glu/Ser which is indicative that TAT-CBD3 is not neuroprotective through inhibition of CaV2.2 (Figure 4.8B). Neuronal survival in neurons which were not stimulated, however, was significantly increased compared to unstimulated controls. It is unknown why this increase was observed by may be due to preventing of release of endogenous glutamate which could induce a low level of toxicity.

4.6. TAT-CBD3 attenuates NMDAR mediated Ca^{2+} influx

The neuroprotective effect of TAT-CBD3 prior to but not following Glu/Ser stimulation suggests that TAT-CBD3's mode of action may occur early in the glutamate toxicity pathway. Since Ca^{2+} entry is an early event in signaling, I hypothesized that TAT-CBD3 may affect cleavage by reducing Ca^{2+} influx in response to glutamate. During prolonged exposure to glutamate, neurons lose their ability to buffer the large influx of Ca^{2+} resulting in accumulation of toxic levels of cytosolic Ca^{2+} ($[Ca^{2+}]_c$); a phenomenon known as delayed calcium deregulation (DCD) (Nicholls, 2004). To test if TAT-CBD3 alters DCD following glutamate application, the

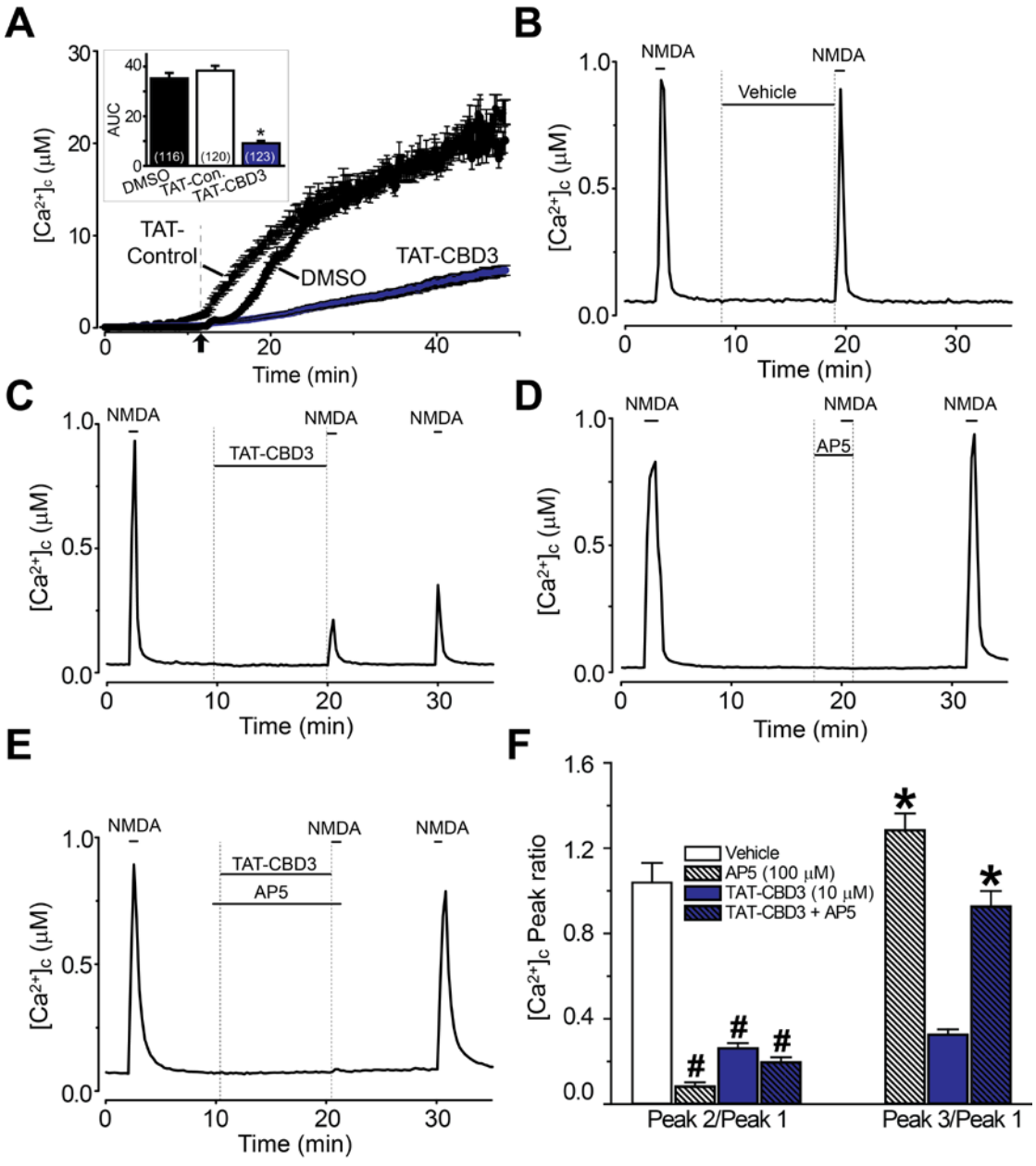
A
B
C
D
E
F
AUC
(116)
(120)
(123)
DMSO
TAT-Con.
TAT-CBD3
TAT-Control
DMSO
TAT-CBD3
Time (min)
NMDA
Vehicle
TAT-CBD3
AP5
[Ca2+]c (μM)
Vehicle
AP5 (100 μM)
TAT-CBD3 (10 μM)
TAT-CBD3 + AP5
[Ca2+]c Peak ratio
Peak 2/Peak 1
Peak 3/Peak 1

.

Figure 4.9. Ca^{2+} influx in response to prolonged glutamate and acute NMDA is attenuated by TAT-CBD3

(**A**) $[Ca^{2+}]_c$ was monitored in E18-19 cortical neurons after prolonged exposure to 200 μM glutamate + 20 μM glycine using the Ca^{2+}-sensitive Fura-2FF. Neurons were treated with vehicle (0.05% DMSO), 10 μM TAT-Control or TAT-CBD3 for 10 minutes prior to stimulation with Glu/Gly. Arrow indicates time of Glu/Gly application. *Inset* graph displays the average area under the curve (AUC), in arbitrary units. Values represent n=116–123 cells obtained from 2 separate experiments for each treatment. (**B**) $[Ca^{2+}]_c$ was monitored in E18-19 cortical neurons using the Ca^{2+}-sensitive dye Fura-2 following application of 50 μM NMDA+ 100 μM glycine. Following application of NMDA, neurons were treated with vehicle (0.05% DMSO) for 10 minutes and then challenged again with NMDA, before a final application ~20 minutes following the first one. (**C-E**) In addition to vehicle, neurons were also treated with either 10 μM TAT-CBD3, 100 μM AP-5, TAT-CBD3 + AP-5, or 1 μM ω-conotoxin GVIA during the 10 minutes in the interim between the 1st and 2nd NMDA applications. (**F**) Bar graph summarizing the ratios of the 2nd and 3rd NMDA applications to the 1st for the various treatment conditions. All values represent at least 95 cells from 2–3 separate experiments. Statistical significance compared to vehicle treated neurons is denoted by an asterisk for P2/P1 ($p < 0.05$), while the # sign denotes significance compared to TAT-CBD3-treated neurons for P3/P1 ($p < 0.05$, one way ANOVA). Ca^{2+} imaging experiments were performed by Tatiana Brustovetsky.

Ca^{2+}-sensitive dye Fura-2FF was used to monitor $[Ca^{2+}]_c$ in collaboration with Dr. Nickolay Brustovetsky's laboratory and performed by Tatiana Brustovetsky. Neurons were incubated with vehicle (0.05 % DMSO) or 10 μM TAT peptides for 10 minutes prior to a 200 μM glutamate + 20 μM glycine (an NMDAR co-agonist (Dingledine et al., 1999; Verdoorn et al., 1987)) challenge (Figure 4.9A). The use of glycine or D-serine for the sake of my experiments appears to be interchangeable as I observed similar amounts of glutamate toxicity with either NMDAR co-agonists. This stimulation led to a sustained increase in $[Ca^{2+}]_c$ throughout the time course of the experiment. Both vehicle and TAT-Control displayed similar increases in $[Ca^{2+}]_c$ during the prolonged exposure to glutamate. In contrast, TAT-CBD3 showed a significant decrease in $[Ca^{2+}]_c$ compared to vehicle and TAT-Control. The changes in $[Ca^{2+}]_c$ following glutamate stimulation, represented by average area under the curve (AUC), was decreased by 78% and 75% compared to that observed in TAT-Control and vehicle-treated neurons, respectively (Figure 4.9A, *inset*). The decrease in DCD and Ca^{2+} influx observed in neurons pre-treated with TAT-CBD3 supports my hypothesis that TAT-CBD3 decreases glutamate-stimulated Ca^{2+} influx. These findings suggest that the neuroprotective effect of TAT-CBD3 as well as the decrease in calpain cleavage of CRMP-2 may occur due to decreased Ca^{2+} influx in the face of glutamate stimulation.

Based on the above observations that TAT-CBD3 reduces Glu/Gly-induced DCD, I next asked if this was through inhibition of NMDAR activity. This was accomplished by measuring Ca^{2+} influx in response to NMDA. Changes in $[Ca^{2+}]_c$ were monitored using the high affinity Ca^{2+} dye Fura-2 after stimulating neurons with 50 μM NMDA + 100 μM glycine. A sharp increase in $[Ca^{2+}]_c$ was observed when NMDA is applied, which returned to baseline upon NMDA removal. When vehicle (DMSO) was applied during the interim between the three NMDA stimulations, no change in $[Ca^{2+}]_c$ amplitude was observed (Figure 4.9B). However, when neurons were treated with 10 μM TAT-CBD3 during this interim period, the second and third responses to NMDA were strongly attenuated (Figure 4.9C).

Having confirmed that TAT-CBD3 reduces the NMDA–initiated Ca^{2+} influx, I next asked if the effect was activity-dependent using the reversible NMDAR inhibitor (2*R*)-amino-5-phosphonopentanoate (AP-5) (Crunelli et al., 1983). When NMDA was applied in the presence of 100 μM AP-5, no $[Ca^{2+}]_c$ increase was observed (Figure 4.9D). However, upon washout of AP-5, NMDA application elicited a $[Ca^{2+}]_c$ increase slightly greater in magnitude to that seen before AP-5 application. NMDA stimulated $[Ca^{2+}]_c$ increase was completely blocked when TAT-CBD3 and AP-5 were co-applied but returned following washout of AP-5 (Figure 4.9E). The ratio of the 2nd to 1st NMDA-induced Ca^{2+} peak (P2/P1) for vehicle treated neurons was 1.05 ± 0.09 whereas incubation with 10 μM TAT-CBD3 reduced the P2/P1 ratio to 0.25 ± 0.03 (Figure 4.9F). The ratio of the 3rd to 1st Ca^{2+} peak (P3/P1) for TAT-CBD3 neurons was 0.33 ± 0.03 suggesting only a minimal recovery of active surface NMDARs. Co-application of TAT-CBD3 with 100 μM AP-5 led to a P2/P1 ratio of 0.19 ± 0.03 and a P3/P1 of 0.93 ± 0.08 indicating recovery of active surface NMDARs. These findings show that inhibition of NMDARs prevents the TAT-CBD3 mediated decrease in NMDA-initiated $[Ca^{2+}]_c$ increase.

I next asked if TAT-CBD3's inhibition of NMDAR-mediated Ca^{2+}-influx was CRMP-2-dependent. Neurons were transfected with CRMP-2 siRNA + GFP at 5 DIV and then Ca^{2+} imaging was performed using a two-pulse NMDA protocol at 7 DIV. Neurons treated with CRMP-2 siRNA exhibited reduced inhibition of NMDAR-mediated Ca^{2+}-influx by TAT-CBD3 (P2/P1 = 0.60 ± 0.09) vs. untransfected controls (P2/P1 = 0.29 ± 0.06, n = 7, $p < 0.05$, Student's t-test). This result suggests that TAT-CBD3's efficacy in reducing NMDAR-mediated Ca^{2+}-influx is CRMP-2–dependent, supporting the notion that TAT-CBD3 antagonizes a function of CRMP-2.

4.7. TAT-CBD3 reduces NR2B surface expression in dendritic spines

The NMDAR is composed of two NR1 subunits and two NR2 subunits that form the heteromeric ligand-gated ion channel. The NR2 subunits present in NMDARs in cortical neurons

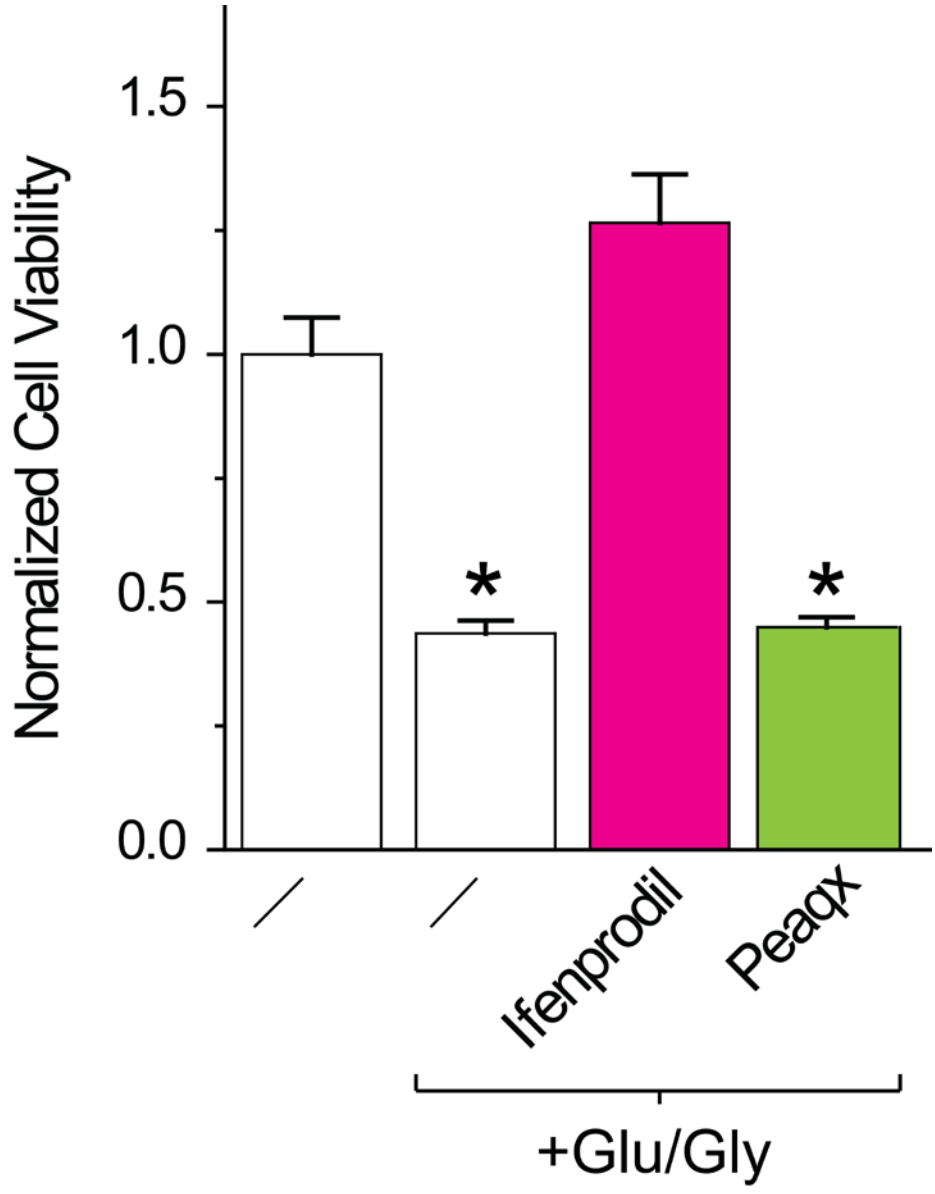

.

Figure 4.10. Blockade of NR2B is completely neuroprotective at 7 DIV

Cortical neurons were grown in culture for 7 days before being stimulated for 30 min with 200 µM glutamate and 20 µM glycine. Neurons were pre-incubated with either Ifenprodil or Peaqx for 10 min prior to stimulation and throughout the exposure to the excitotoxic insult. Values are the average of 32 wells from two separate experiments. Asterisk indicates significant difference compared to no stimulation control ($p < 0.05$, one-way ANOVA with Dunnet's post-hoc test).

7 DIV are primarily NR2A and NR2B. Based upon this is it is likely that TAT-CBD3 is targeting one or both of these subunits. CRMP-2 has been shown to interact with both subunits so it would not be surprising if TAT-CBD3 target both subunits (Bretin et al., 2006). Subunit diversity has been of particular interest in the field of excitotoxicity as the subunit composition of NMDAR appears to alter the extent of glutamate toxicity.(Liu et al., 2007; Mizuta et al., 1998; Zhou and Baudry, 2006). I therefore wanted to determine if TAT-CBD3 displayed subunit specificity. The first step in this was to determine what subunits were responsible for mediating excitotoxicity in my cortical neuron culture. I employed the use of the NR2B and NR2A specific blockers Ifenprodil and Peaqx respectively to accomplish this goal (Auberson et al., 2002; Williams, 1993). Cortical neurons were treated for 10 minutes prior to stimulation and throughout stimulation with 200 μM glutamate and 20 μM glycine for 30 min. At 7 DIV it was found that Ifenprodil, but not Peaqx, was able to completely prevent Glu/Gly-induced toxicity (Figure 4.10). This finding suggests that NR2B is completely responsible for glutamate toxicity at this stage of culture which is consistent with previous findings (Hardingham et al., 2002; Liu et al., 2007; Stanika et al., 2009; Zhou and Baudry, 2006). An extension of this conclusion is that TAT-CBD3 targets NR2B-containing receptors.

As two recent studies showed an association of NMDARs with CRMP-2 and possible regulation of cell-surface expression of the NR2B-containing NMDARs by CRMP-2 (Al-Hallaq et al., 2007; Bretin et al., 2006), I tested if NMDARs are affected by TAT-CBD3 peptide. Additionally, I focused on the NR2B subunit as it appears to be the dominant subunit implicated in excitotoxicity in our cortical neuron cultures. To monitor surface expression of the NR2B containing NMDARs, neurons were pre-treated for 10 minutes with 10 μM of either TAT peptide followed by a 30 minute stimulation with Glu/Ser and then subjected to biotinylation of surface proteins either 30 minutes, 1 or 2 hours after stimulation. Control neurons were treated with peptide for 10 minutes and then incubated for 30 minutes without stimulation before surface proteins were biotinylated. NR2B was mainly detected in the streptavidin-enriched biotinylated

.

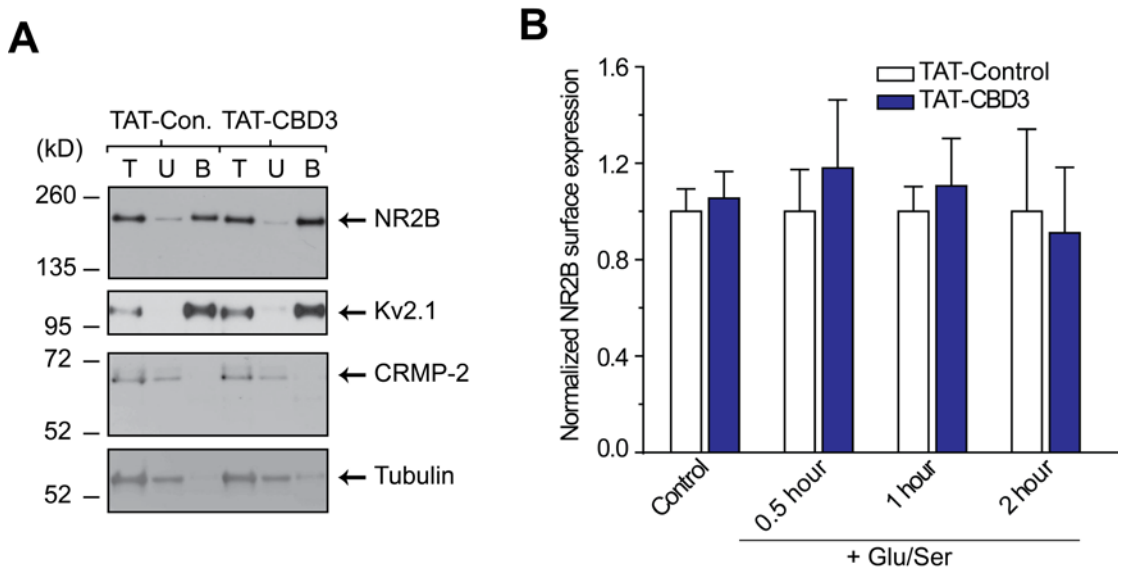

Figure 4.11. TAT-CBD3 does not alter total surface expression of NR2B

(**A**) Representative immunoblots with the indicated antibodies of total lysates (T), unbiotinylated fractions (U), and biotinylated fractions (B) prepared from neurons exposed to TAT-Control or TAT-CBD3 (10 μM each) for 10 minutes. (**B**) Summary of biotinylated (surface) NR2B protein, calculated by densitometry from two experiments. Values were normalized to time matched TAT-Control conditions (n = 6-11 each). Neurons were left untreated (control) or stimulated for 30 min with Glu/Ser followed and biotinylated 0.5 to 2 h later. Levels of surface NR2B were not different in any of the conditions tested ($p > 0.05$; Student's t-test).

fraction (B) with trace amounts in the unbound fraction (U), consistent with a surface-expressed receptor (Figure 4.11A). As a control, the surface expression of the voltage-gated potassium channel 2.1 (Kv2.1) was also found primarily in the biotinylated fraction, consistent with our previous report that CRMP-2 does not affect Kv channel trafficking (17). As expected, the cytosolic proteins CRMP-2 and β-Tubulin were present in the unbound fraction with little to none detected in the biotinylated fractions. NR2B surface expression was calculated as the ratio of biotinylated to total NR2B and then normalized to the ratio observed in neurons treated with TAT-Control for the times indicated. There was no difference in the amount of surface expressed NR2B between TAT-Control and TAT-CBD3 treated neurons in unstimulated neurons or neurons stimulated for 30 minutes with Glu/Ser (Figure 4.11B). Taken together, these results suggest that TAT-CBD3 does not alter surface expression of total NR2B.

Because biotinylation experiments do not address potential localized or spatially restricted changes in surface expression of a protein, I turned to the approach of using the pH sensitive GFP superecliptic pHlourin (SEP) to monitor NR2B surface expression (Miesenbock et al., 1998). SEP fluoresces 20-fold brighter in a neutral pH versus acidic or basic conditions: as proteins on the surface (high fluorescence, ~ pH 7.5) are internalized (low fluorescence, ~ pH 5.5) a strong reduction in fluorescence is observed. The fluorescence of SEP fused to the extracellular domain of NR2B (NR2B-SEP) can therefore be used to observe changes in NR2B-SEP containing NMDARs on the plasma membrane (Kopec et al., 2006). Neurons expressing NR2B-SEP were visualized using confocal fluorescent microscopy as small punctate structures on dendrites (Figure 4.12A), consistent with previous reports showing clustering of NMDARs in dendritic spines (Craig et al., 1994; Kornau et al., 1995). Following acquisition of a 10 minute period of baseline, neurons were incubated with peptides for 20 minutes while continually measuring NR2B-SEP fluorescence. At the end of every experiment, neurons were treated with a pulse of acetic acid (Figure 4.12B). This drop in pH (to ~5.5) caused a near complete loss of fluorescence and verified that the pH sensitivity of SEP was not altered during the course of the

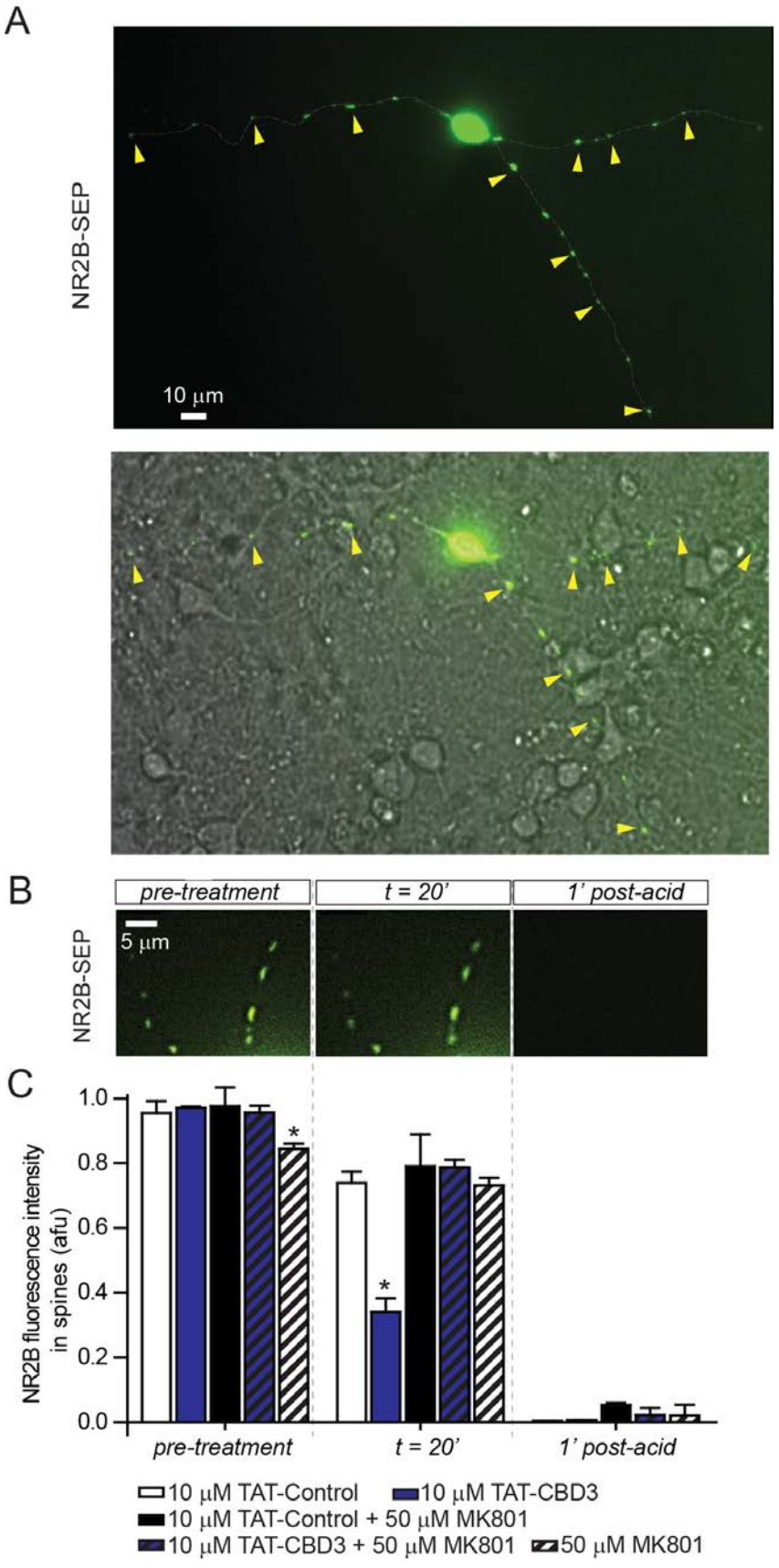
A
NR2B-SEP
10 μm
B
pre-treatment
t = 20'
1' post-acid
NR2B-SEP
5 μm
C
NR2B fluorescence intensity in spines (afu)
1.0
0.8
0.6
0.4
0.2
0.0
*
*
pre-treatment
t = 20'
1' post-acid
10 μM TAT-Control
10 μM TAT-CBD3
10 μM TAT-Control + 50 μM MK801
10 μM TAT-CBD3 + 50 μM MK801
50 μM MK801

Figure 4.12. TAT-CBD3 induces activity-dependent down-regulation of surface NR2B in dendritic spines

Representative deconvolved fluorescent images of surface expressed NR2B-SEP on dendritic spines (**A**, **B**) of transfected neurons before, 20 min after application of TAT-Control, and 1 minute after application of a short acid pulse (pH 5.0). Differential interference contrast image overlaid with a fluorescent image illustrating dendritic spines rich in NR2B (*yellow arrowheads*) is shown in **A** (*bottom panel*). (**C**) Average NR2B-SEP fluorescence intensities of spines in the presence of MK801 alone, or peptides alone or in the presence of peptides and MK801 at the times indicated. Each condition represents 37-70 spines from 3 separate experiments. Asterisk indicates a significant difference compared to TAT-Control ($p < 0.05$; one-way ANOVA with Dunnett's post-hoc). The ordinate represents average intensity in arbitrary fluorescent units (afu). Scale bars are as indicated.

experiment. Incubation of neurons with 10 μM TAT-Control showed no significant change in fluorescence at 20 minutes compared to vehicle. In contrast, incubation with 10 μM TAT-CBD3 caused a ~60% reduction in NR2B-SEP fluorescence (Figure 4.12C). This result suggests that CBD3 can alter dendritic surface NMDARs by inducing internalization of NR2B.

Since NMDAR activity has been linked to surface expression (Barria and Malinow, 2002; Prybylowski et al., 2005; Roche et al., 2001), I tested if inhibition of NMDAR activity could affect TAT-CBD3-induced NR2B internalization. Concomitant addition of the NMDAR antagonist MK801 (50 μM) with 10 μM TAT-CBD3 completely prevented the TAT-CBD3-induced reduction in NR2B-SEP fluorescence observed at 20 minutes following peptide/drug application (Figure 4.12C). Treatment with 50 μM MK801 alone had no effect on NR2B-SEP fluorescence. These results suggest that internalization of NMDARs induced by TAT-CBD3 requires an active NMDAR.

Whereas biotinylation experiments showed that surface expression of NR2B is not altered following TAT-CBD3 exposure, NR2B-SEP fluorescence experiments showed reduced NR2B surface expression in dendrites upon treatment with TAT-CBD3. To address the incongruity between these results, I measured NR2B-SEP fluorescence in cell bodies of neurons following treatment with TAT peptides (Figure 4.13A). NR2B-SEP fluorescence was similar in somas following application of TAT-CBD3 compared to TAT-Control (Figure 4.13B). The finding that somatic NR2B surface expression is unaltered may explain why no reduction in total NR2B surface expression was observed in biotinylation experiments. These observations suggest that TAT-CBD3 induces specific internalization of dendritic NR2B receptors without altering somatic receptors. Collectively, the NR2B-SEP imaging and Ca^{2+} imaging experiments strongly support the conclusion that NMDAR internalization following TAT-CBD3 treatment is activity-dependent.

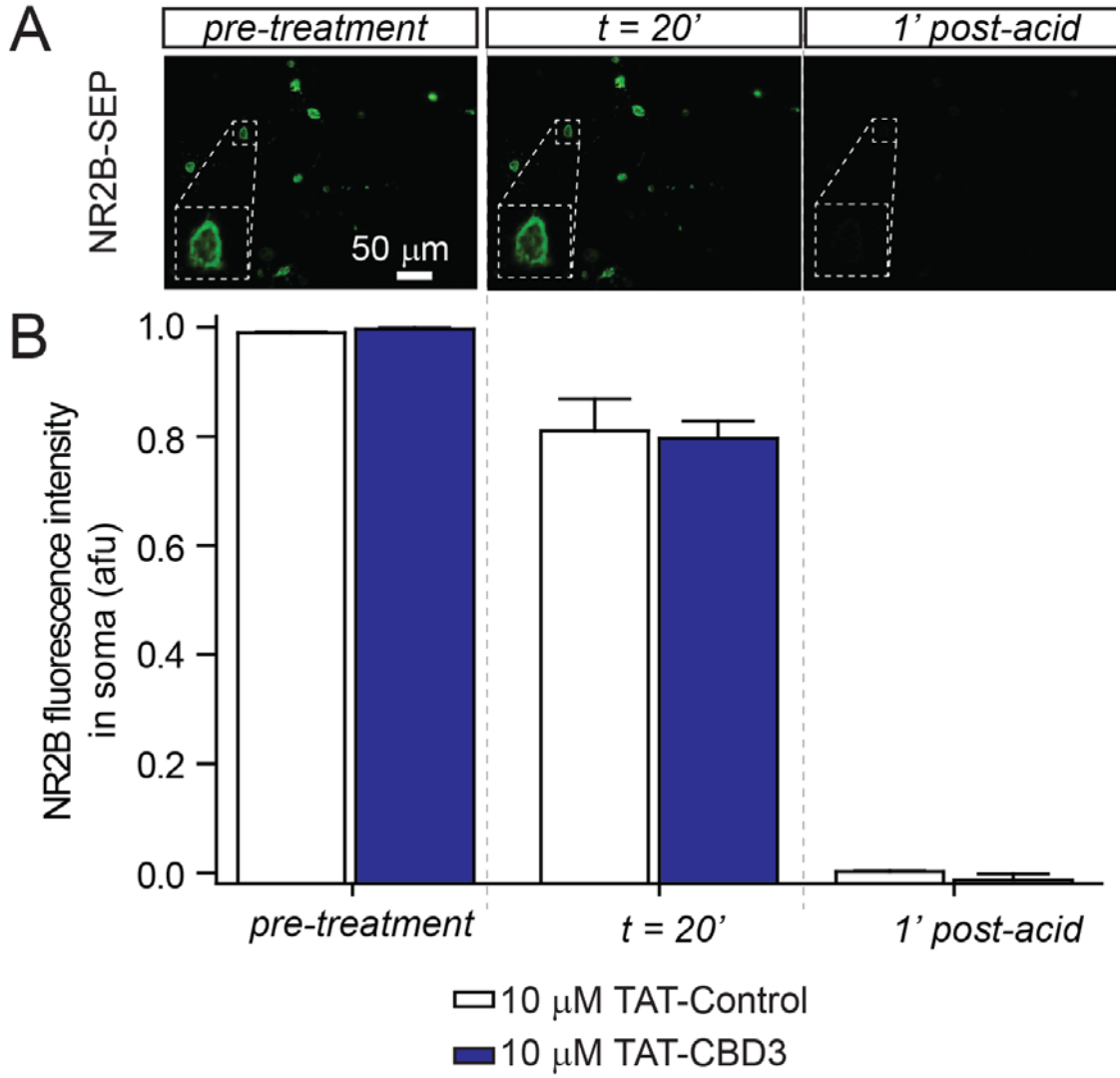

Figure 4.13. TAT-CBD3 does not alter NR2B surface expression in neuron soma

(**A**) Representative fluorescent images of surface expressed NR2B-SEP on soma of transfected neurons before, 20 min after application of TAT-Control, and 1 minute after application of a short acid pulse (pH 5.0). (**B**) Average NR2B-SEP fluorescence intensities in soma in the presence of peptides at the times indicated. Each condition represents 32-34 soma from 3-4 experiments. Asterisk indicates a significant difference compared to time-matched TAT-Control ($p < 0.05$; ANOVA for spines and Student's t-test for soma). The ordinate represents average intensity in arbitrary fluorescent units (afu). Scale bar is as indicated.

4.8. TAT-CBD3 inhibits NMDAR-induced current in hippocampal neurons

The attenuation of NMDA-stimulated Ca^{2+}-influx suggests that TAT-CBD3 acts on the NMDAR. In collaboration with Dr. Gerald Zamponi's laboratory and performed by Dr. Haitou You, we tested if TAT-CBD3 could inhibit NMDA evoked currents in primary neurons. NMDAR currents were recorded from rat hippocampal neuron somas (DIV 7-11) using whole-cell voltage-clamp electrophysiology by stimulating with 50 μM NMDA for 2 seconds with a 30 second interval between stimulations (Figure 4.14A). Following 5 minutes of stable NMDA-stimulated responses (< 5% change between peaks) neurons were perfused with 10 μM TAT-CBD3. TAT-CBD3 induced rapid and strong inhibition of NMDA currents with ~70% block after 5 minutes (Figure 4.14B). Washout with bath solution lacking TAT-CBD3 led to partial recovery of NMDA currents after 10 minutes. These findings place TAT-CBD3 as a modulator of NMDARs and show that TAT-CBD3 directly inhibits NMDA currents.

I hypothesized that the mechanism of TAT-CBD3's inhibition of NMDARs is due to intracellular disruption of CRMP-2-NMDAR signaling. This conclusion is supported by the finding that application of TAT-CBD3 but not CBD3 sans TAT was neuroprotective. While these findings support the conclusion that the TAT penetration peptide is required for neuroprotection by CBD3 it did not directly demonstrate that the target of TAT-CBD3 was intracellular. Therefore, we (performed by Dr. You) tested if intracellular application of TAT-CBD3 inhibits NMDARs. This was tested by measuring NMDA-induced Ca^{2+}-currents in hippocampal neurons with TAT-CBD3 in the recording pipette. In experiments where TAT-CBD3 was applied via the recording pipette, there was no observed decrease in NMDAR Ca^{2+}-currents compared with controls (Figure 4.14C). This finding suggests that TAT-CBD3 does not inhibit NMDARs through an intracellular target, suggesting instead that the observed inhibition of NMDARs by TAT-CBD3 may occur through an extracellular mechanism, such as channel block. This also suggests that the conformation per se of the fused version of the TAT with CBD3 bestows inhibition on the NMDARs, rather than either sequence alone. It is unclear

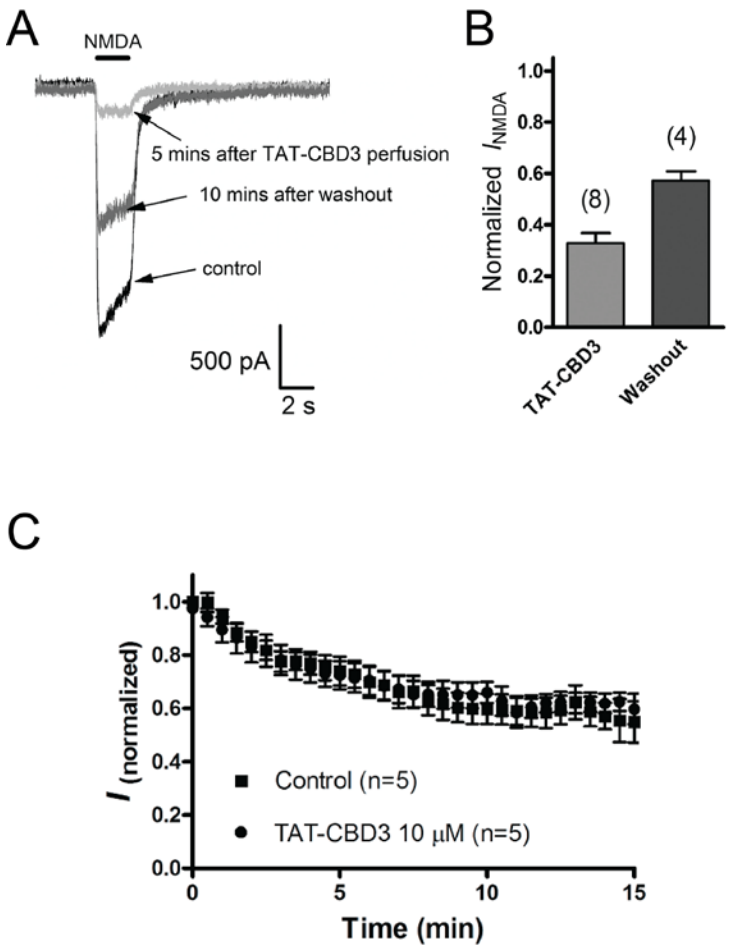

Figure 4.14. TAT-CBD3 decreases NMDA induced current in rat hippocampal neurons via an extracellular target

(**A**) Representative traces from a single neuron, showing a control NMDA trace evoked by 50 μM NMDA (see Methods), NMDA current after 5 min perfusion of 10 μM TAT-CBD3, and NMDA current after 10 min washout of TAT-CBD3. (**B**) Bar graph summarizing the effect of TAT-CBD3 on NMDA current of 8 individual cells; four of those cells lasted long enough to finish a 10-min washout period and partially recovered from TAT-CBD3 effect. (**C**) Ca^{2+} currents were recorded from hippocampal neuron somas in the presence of 10 μM TAT-CBD3 in the recording pipette. Cells were held for 15 min and compared to cells without peptide in the pipette. Electrophysiology experiments were performed by Dr. Haitao You in the laboratory of Dr. Gerald W. Zamponi.

whether the previously observed internalization of NMDARs in response to TAT-CBD3 occurs through the proposed extracellular mechanism or through a distinct intracellular signaling target.

4.9. Interactions between NR2B and CRMP-2

A previous study has reported CRMP-2 as a biochemical binding partner of NMDAR NR2A/B subunits (Al-Hallaq et al., 2007), and hence it is possible that TAT-CBD3 may mediate neuroprotection by disrupting the interaction between CRMP-2 and the NMDAR, rather than via current inhibition. To explore this interaction and determine if TAT-CBD3 affected it, I performed a series of co-immunoprecipitation experiments. Lysates from embryonic day 19 cortical neurons grown for 8 DIV culture were exposed to TAT-CBD3 (100 μM) or TAT-control (100 μM) peptides or vehicle (1% DMSO) for 1 h and immunoprecipitated with an anti-NR2B antibody (recognizes proximal carboxyl-terminus, BD Biosciences) (Figure 4.15A). Immunoblotting of these immunoprecipitations with a CRMP-2 antibody (Sigma) failed to yield a detectable interaction despite detection of PSD-95, a well-established interaction partner of NMDARs (Kornau et al., 1995; Niethammer et al., 1996). Importantly, the interaction between PSD-95 and NR2B was not disrupted by TAT-CBD3, relevant here because disruption of this interaction has neuroprotective properties (Aarts et al., 2002; Martel et al., 2009). The reciprocal co-immunoprecipitation with the anti-CRMP-2 (C4G) antibody on membrane enriched fractions from postnatal day 2 rat brains (Figure 4.15B) also failed to precipitate NR2B. It should be noted that the CRMP-2 antibody C4G was the same as used in the previous study reporting an interaction between CRMP-2 and NMDARs (Al-Hallaq et al., 2007). To rule out epitope specific or conformation specific NMDAR antibodies as the potential reasons for the lack of interaction in our cultures, I used two additional NR2B antibodies that have their epitopes in the N-terminus (NeuroMab) or in the C-terminus (Millipore) (Figure 4.15C). These too failed to resolve an interaction between NR2B and CRMP-2. Bacterially purified CRMP-2-GST fusion protein also failed to pull down NR2B from rat brain lysates or synaptosomes (Figure 4.15D).

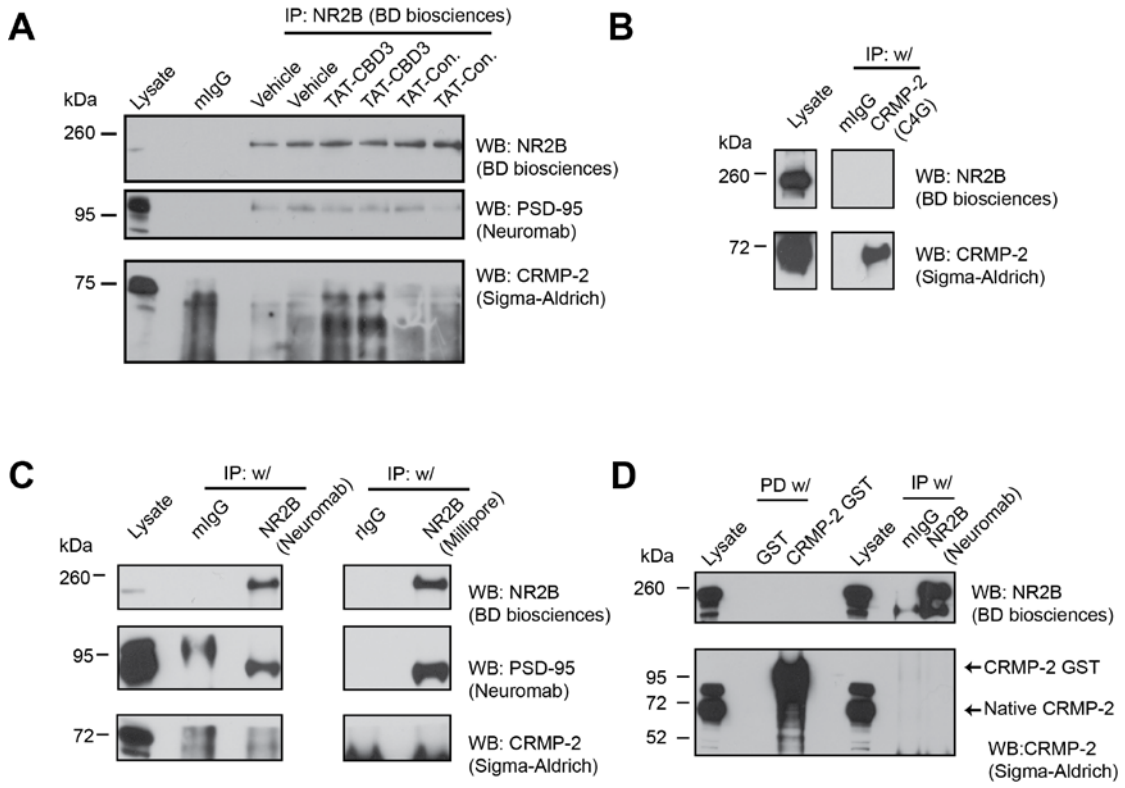

Figure 4.15. CRMP-2 is not found in a complex with NR2B

(**A**) Lysates from E19 DIV 8 cortical neurons were pre-incubated with vehicle (0.5% DMSO), 100 µM TAT-CBD3 or 100 µM TAT-Control prior to performing co-immunoprecipitations using an anti-NR2B antibody. The commercial suppliers of the antibodies are indicated in parentheses. (**B**) PN2 brain fractions were used to perform co-immunoprecipitations using anti-CRMP-2 C4G. (**C**) Cortical neuron lysates were used to co-immunoprecipitate NR2B using two additional NR2B antibodies antibody and immunoblotted as in (**A**). (**D**) Bacterially expressed purified GST (control) or CRMP-2 GST proteins were utilized in pull downs (PD) from cortical neuron lysates along with either a monoclonal IgG (control) or NR2B antibody, and then the immune-captured complexes were blotted with NR2B and CRMP-2 antibodies. Both GST tagged and native CRMP-2 are indicated. Molecular weight markers are indicated in kilodaltons (kDa).

4.10. CONCLUSIONS

In this Chapter I described the neuroprotective effects of a novel peptide (CBD3) derived from the CRMP-2 protein. Knockdown of CRMP-2 itself was neuroprotective. Similarly, incubation with TAT-CBD3 protected neurons from glutamate toxicity, decreased surface expression of NR2B receptors at dendritic spines and reduced NMDAR–mediated Ca^{2+} influx. TAT-CBD3 was also found to inhibit NMDAR-mediated currents in slice recordings and in cultured neurons. Although CRMP-2 was originally discovered as a mediator of axon guidance and outgrowth, recent evidence has suggested that CRMP-2 is also important in excitotoxicity signaling (Bretin et al., 2006; Hou et al., 2009). My results, for the first time, establish CRMP-2 signaling as a *bona fide* target for prevention of glutamate toxicity. The apparent mechanism of action for TAT-CBD3's neuroprotective effect in glutamate toxicity is via attenuation of toxic Ca^{2+}-influx through NMDARs. This mechanism along with previous studies suggests that CRMP-2 modulates NR2B-containing NMDARs (Al-Hallaq et al., 2007; Bretin et al., 2006).

Initial support for CRMP-2 as a potential target in neurotoxicity arose from studies demonstrating cleavage of CRMP-2 by calpain following various forms of neurotoxicity, including focal ischemia (Bretin, Rogemond et al. 2006; Jiang, Kappler et al. 2007; Touma, Kato et al. 2007; Zhang, Ottens et al. 2007). These findings led me to hypothesize that TAT-CBD3 may alter calpain cleavage of CRMP-2, which in turn may be neuroprotective in a cell-based excitotoxic injury model. Consistent with my hypothesis, I observed strong neuroprotection by TAT-CBD3 in neurons stimulated with Glu/Gly. Despite the finding that TAT-CBD3 also reduced calpain cleavage of CRMP-2, this is likely not the mechanism of TAT-CBD3–induced neuroprotection as no reduction in cleavage occurred when TAT-CBD3 was added to *in vitro* cleavage experiments. Rather, it appears that the reduction in cleavage is due to a reduction in glutamate-induced Ca^{2+} influx.

In addition to CRMP-2, cleavage of other members of the CRMP family of proteins has been implicated in neurotoxicity. Collectively, it appears that cleavage of CRMP-3 and CRMP-4

is detrimental to neuronal survival while cleavage of CRMP-2 may be neuroprotective (Bretin et al., 2006; Kowara et al., 2005; Liu et al., 2009). The possible effects cleavage of CRMP-1 and -5 may have on neuronal survival is at present unclear. The CBD3 region of CRMP-2 shares 80% identity with CRMP3 but only 46% and 40% with CRMP-4 and CRMP1, respectively. Given the sequence disparity between the CBD3 regions for CRMPs 1-4 (Figure 3.20), it would be interesting to test if these peptides also have neuroprotective properties. Furthermore, the use of these CBD3 homologues might enable identification of specific residues required for neuroprotection.

A recent study reported that overexpression of a "cleaved" CRMP-2 construct, lacking amino acids 509–572 which are cleaved by calpain, reduced the responsiveness of neurons to glutamate and increased neuronal survival following glutamate-induced toxicity (Bretin et al., 2006). The authors concluded that accumulation of this artificially cleaved CRMP-2 product led to a reduction of surface NMDARs, presumably accounting for the observed neuropreservation. Their study, however, did not examine whether cleavage of *endogenous* CRMP-2 could also be neuroprotective. In this study I initially set out to determine if TAT-CBD3 altered calpain cleavage of CRMP-2 and neuronal survivial following excitotoxicity. Whilst our results show that TAT-CBD3 reduced cleavage of CRMP-2 and was neuroprotective following an excitotoxic insult, this relationship may not be a causal one as it appears that TAT-CBD3-mediated attenuation of NMDAR-mediated Ca^{2+} influx is the likely cause for both neuroprotection and prevention of calpain cleavage of CRMP-2. These findings position CRMP-2 as an important novel modulator of both ligand- (i.e. NMDARs) as well as voltage-gated calcium channels.

Incubation with TAT-CBD3 greatly attenuated DCD during prolonged glutamate exposure as well as reduced Ca^{2+} influx following NMDA application. Perhaps most interesting, however, is the finding that TAT-CBD3 induces activity-dependent internalization of NMDARs as inhibitors of NMDARs (MK801 and AP5) prevented TAT-CBD3's modulation of NMDARs. Although a biochemical interaction between NMDARs and CRMP-2 has been reported (Al-

Hallaq et al., 2007), my attempts to reproduce this interaction were unsuccessful. It is unknown why I was unable to reproduce this interaction, although the interaction may be very weak and therefore difficult to observe. Specifically, the mechanism for TAT-CBD3-induced internalization could be via altering the phosphorylation state of NR2B or by enhancing the interaction between the endocytosis related AP-2 adapter protein. For example, the C-terminus of NR2B contains the AP-2 adaptor protein binding site "YEKL" that is required for clathrin dependent endocytosis (Prybylowski et al., 2005; Roche et al., 2001). Previous work has shown that CRMP-2 interacts with α-adaptin (an AP-2 subunit) and modulates endocytosis of the cell adhesion protein L1, this suggests CRMP-2 could also modulate NR2B endocytosis through an interaction with AP-2 (Nishimura et al., 2003). NR2B receptor trafficking is also regulated by a PDZ binding domain located just adjacent to AP-2 adaptor binding site (Roche et al., 2001). In addition, phosphorylation of the PDZ binding site by casein kinase II leads to receptor internalization (Zhang et al., 2008). TAT-CBD3-initiated NMDAR removal from the membrane could occur via these or as yet undiscovered NMDAR trafficking pathways. The specific removal of NR2B receptors from spines suggests that TAT-CBD3 could be targeting a synaptic trafficking pathway, possibly explaining why somatic receptors are not affected.

In conclusion, the findings presented in this Chapter have identified a novel neuroprotective peptide derived from the protein CRMP-2. This peptide appears to work by inhibiting NMDARs and inducing dendritic spine NMDAR internalization culminating in a reduction of glutamate-induced DCD and NMDA–stimulated Ca^{2+} influx. These findings show that CRMP-2 is not only involved in glutamate-mediated neurotoxicity but may be effectively targeted to prevent excitotoxicity-mediated neuronal death.

CHAPTER 5. DISCUSSION AND CONCLUSION

5.1. Role of CRMPs in modulating release

The pre-synaptic CaV2.2 complex contains many protein components (see Table 1.1.1) and may well contain proteins yet to be identified. In Chapter 3, I characterized the novel CaV2.2 interacting protein CRMP-2. These findings included the discovery of a biochemical as well as a functional interaction leading to the modulation of CaV2.2. Based upon this work CRMP-2 has emerged as an important regulator of CaV2.2. The collective findings from Chapter 3 are visually summarized in Figure 5.1. One of the more interesting findings from these series of experiments was that CRMP-2 over-expression led to an increase in the stimulated release of glutamate. This finding is consistent with the role of CaV2.2 in regulating glutamate release (Wheeler et al., 1994).

While the interaction between CRMP-2 and CaV2.2 suggests that the regulation of neurotransmitter release occurs in response to CRMP-2 expression, other hypotheses are also possible. For example, it is possible that CRMP-2 may have an ultra-structural effect on the synapse, leading to changes in neurotransmitter release. Additional experiments completed in the Khanna laboratory, as enumerated next, have specifically suggested this hypothesis may have some credence. Hippocampal neurons were isolated, grown, and transfected with either EGFP or CRMP-2-EGFP as described in Chapter 2. Following this, neurons were loaded with the amphipathic dye FM4-64 (Invitrogen) by way of stimulation with KCl. This loading protocol specifically leads to labeling of sites where stimulated endocytosis/exocytosis occur and therefore can be used to label active release sites (Pan et al., 2005; Ryan et al., 1993). These release sites are commonly referred to as “boutons” in imaging experiments (Figure 5.2). It was observed that neurons expressing CRMP-2-EGFP had ~3-fold larger boutons compared to EGFP alone. This enhancement in bouton size was observed without a change in the number of boutons. This finding strongly suggests that CRMP-2 is an important determinant in bouton size. It has previously been shown that bouton size correlates with active zone size as well as pre-synaptic

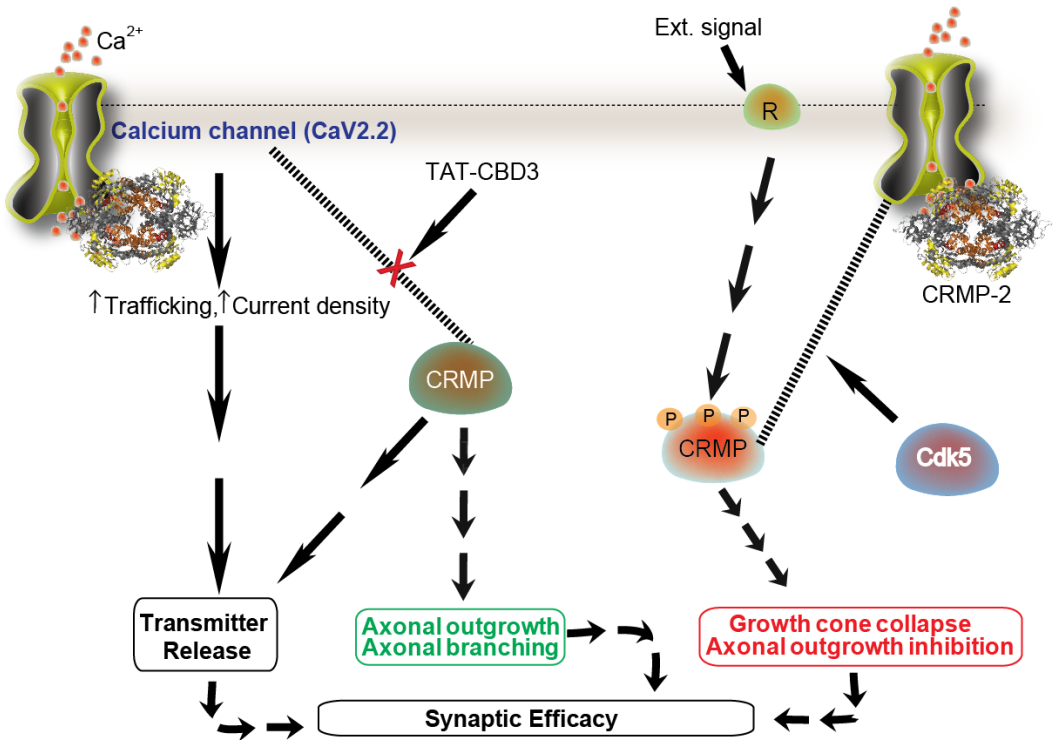

Figure 5.1. CRMP-2 signaling cascade: a novel role for CRMPs in Ca^{2+} channel regulation and transmitter release

Extracellular signals induce growth cone collapse through activation of various kinases pathways. In Chapter 3, I found that CRMP-2 binds to cytoplasmic loops of CaV2.2 and increases its insertion into the membrane, resulting in increased current density culminating into an increase in the release of the neurotransmitter glutamate. In addition, I observed that phosphorylation of CRMP-2 by Cdk5 at Ser-522 is required for CRMP-2-mediated enhancement of CaV2.2 current. I then used the CaV2.2-CRMP-2 interaction disrupting peptide TAT-CBD3 to prevented CRMP-2-mediated regulation of CaV2.2. TAT-CBD3 was then used in both *in vitro* and *in vivo* to target this interaction.

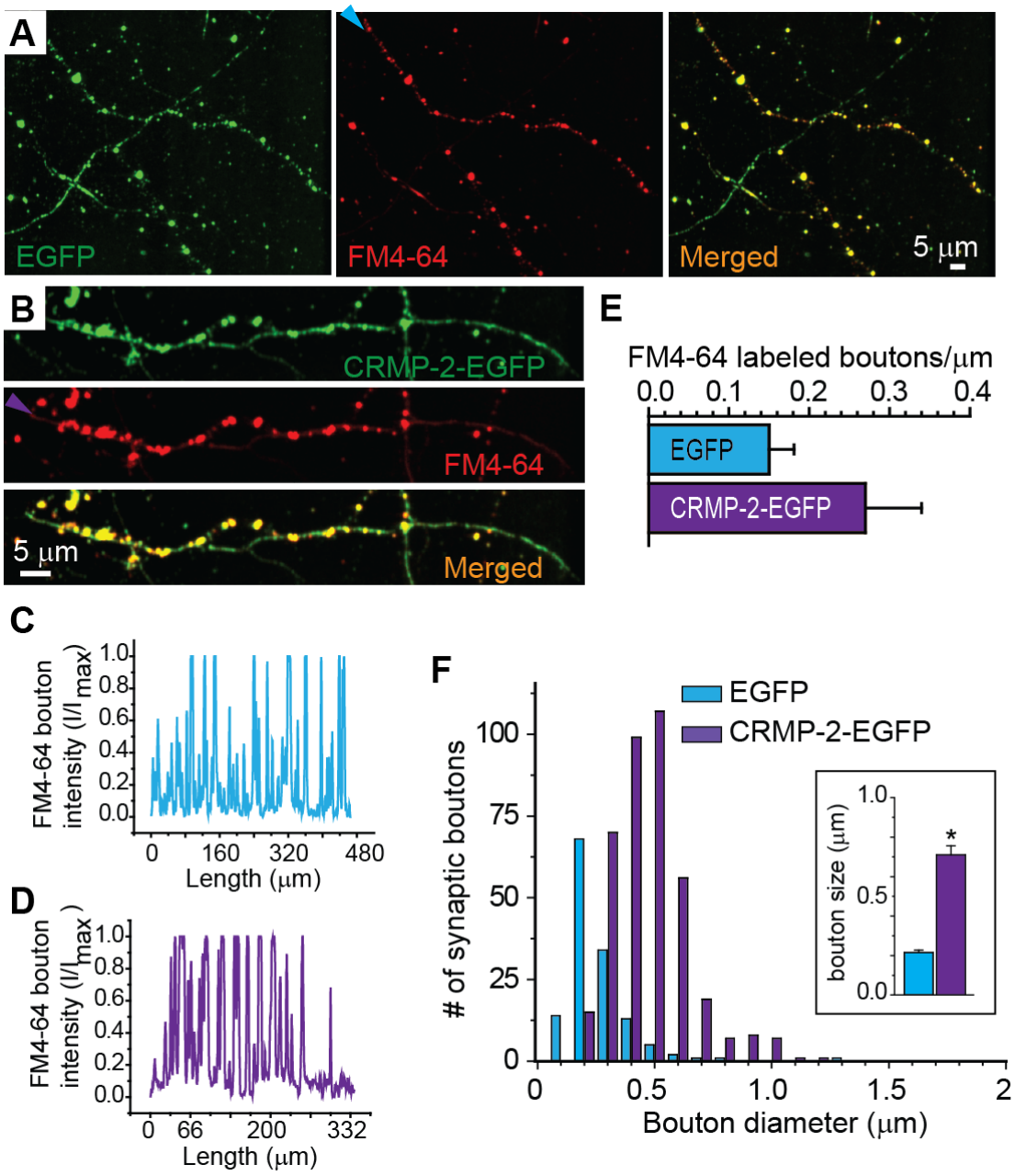
A
EGFP
FM4-64
Merged
5 μm
B
CRMP-2-EGFP
FM4-64
5 μm
Merged
E
FM4-64 labeled boutons/μm
0.0 0.1 0.2 0.3 0.4
EGFP
CRMP-2-EGFP
C
FM4-64 bouton intensity (I/I max)
1.0 0.8 0.6 0.4 0.2 0.0
0 160 320 480
Length (μm)
D
FM4-64 bouton intensity (I/I max)
1.0 0.8 0.6 0.4 0.2 0.0
0 66 200 332
Length (μm)
F
EGFP
CRMP-2-EGFP
# of synaptic boutons
100 75 50 25 0
0 0.5 1.0 1.5 2
Bouton diameter (μm)
bouton size (μm)
1.0 0.5 0.0
*

.

Figure 5.2. An atypical role for CRMP-2: increasing bouton size

Shown are representative pseudocolor images of EGFP (green) andFM4-64 (red) from neurons transfected with EGFP (**A**) or CRMP-2-EGFP (**B**). The arrowheads in **A** and **B** represent axons along which a line scan was performed to quantify the number of boutons (labeled with FM4-64) in EGFP (**C**) and CRMP-2-EGFP (**D**) neurons. Boutons were identified by counting intensity peaks that traversed the 50% maximum intensity level. Representative line intensity staining profiles of the FM4-64 panels in **A** and **B** are shown in **C** and **D**, respectively. (**E**) Summary of the average number of boutons/µm of axon. The density of boutons was not different between EGFP- and CRMP-2-EGFP-expressing neurons (p 0.05). (**F**) Histogram of diameters from boutons of EGFP- and CRMP-2-EGFP-expressing neurons. The largest diameter of each bouton was measured in a double-blind manner; the resulting diameters were grouped into bins of 0.1 µm. Bouton diameters were distributed unimodally in both EGFP- and CRMP-2-EGFP-expressing neurons. (**Inset**) Mean bouton size of EGFP and CRMP-2-EGFP showed the average diameter of boutons to be ~3-fold larger in CRMP-2-EGFP-expressing neurons than in EGFP-expressing neurons ($p < 0.05$, Student's t test).

.

vesicle quantity (Yeow and Peterson, 1991). These findings suggest additional work needs to be done to explore the role of CRMP-2 in neurotransmitter release. Specifically, it may be interesting to determine if CRMP-2 is able to enhance neurotransmitter release without CaV2.2 modulation. This could be accomplished using a Ca^{2+} ionophore, Ca^{2+} uncaging or optogenetics to bypass CaV2.2 and measure neurotransmitter release independent of CaV2.2. In addition, it may be fruitful to look at electron micrographs of neurons transfected with CRMP-2 to determine if the number of vesicles in the pre-synaptic terminal is affected by CRMP-2 expression. Mechanistically, it is likely that CRMP-2 is able to enhance bouton size through interactions with cytoskeleton proteins. That CRMP-2's ability to interact with actin may be responsible for its regulation of bouton size is supported by findings showing that mutation of the actin binding Wiscott-Aldrich syndrome protein (WASP) leads to larger pre-synaptic terminals (Khuong et al., 2010). The interaction between CRMP-2 and actin has had limited exploration, although it is known that phosphorylation does not affect actin binding to CRMP-2 (Arimura et al., 2005). As I found in Chapter 3 that the CRMP-2 S522A mutant is unable to enhance CaV2.2, it would be interesting to assess whether the S522A mutant is able to still increase bouton size.

As described in §1.1, the pre-synaptic terminal is proposed to contain a limited quantity of slots available for CaV2.2. (Cao et al., 2004; Cao and Tsien, 2010). These slots are limiting as over-expression of CaV2.2 does not alter the amplitude of EPSCs or the contribution of CaV2.2 therein (Cao and Tsien, 2010). Based upon the finding that CRMP-2 expression enhances CaV2.2-mediated transmitter release, either CRMP-2 alters the number of slots available, consistent with an observed increase in bouton size, or enhances the open probability of CaV2.2. As single channel recordings of Ca^{2+} channels are technically difficult, it has yet to be determined if CRMP-2's association with CaV2.2 increases the current through CaV2.2. While in the current dissertation I have described the interaction between CaV2.2 and CRMP-2 and further proposed that observed changes in neurotransmitter release occur due to this interaction, the possible role of other CRMP-2 interacting proteins in enhancing neurotransmitter release cannot be

disregarded. CRMP-2 interacts with a litany of proteins (see Table 1.2.2) that are present in the growing axon tip and synapse, which may lead to the observed changes in neuron biology.

An additional question of interest is whether CRMP-2 alters Ca^{2+} channels in other cell types, leading to alterations in Ca^{2+}-dependent release. This is further suggested by my observed interaction between CRMP-2 and CaV1.2 in a neuronal cell line (data not shown). While CaV1.2 is expressed in neurons, it is also expressed in non-neuronal cells such as cardiomyocytes and pancreatic beta cells. Therefore, it would be interesting to test if CRMP-2 is able to regulate release in non-neuronal cells (e.g. insulin release from beta cells). The results of such experiments could lead to the concept of CRMP-2 as a global modulator of release in endocrine cells as well as neurons.

5.2. Role of CRMP-2 as a CaV2.2 trafficking molecule

The initial identification of CRMP-2 as a modulator of axon growth and growth cone collapse suggested that CRMP-2 maybe vital to maintaining proper cytoskeletal organization in the neuron. Subsequent studies further identified CRMP-2 as directly interacting with and modulating tubulin (Fukata et al., 2002). In addition to regulating the polymerization of tubulin, CRMP-2 was found to interact with the kinesin motor protein and through this association transport tubulin along neuron processes (Kimura et al., 2005). The interaction of CRMP-2 with kinesin further suggests that CRMP-2 may possibly link any protein it interacts with to kinesin, and therefore could regulate the protein's trafficking. In order for CRMP-2 to have the observed enhancement of CaV2.2 function, the number of channels on the plasma membrane or the open probability of CaV2.2 must be increased. As CRMP-2's role as a trafficking protein has previously been established, I first tested the hypothesis that CRMP-2 aids in trafficking CaV2.2. Consistent with this hypothesis, I observed an increase in surface expressed CaV2.2 when CRMP-2 was overexpressed. This suggests that CRMP-2 enhances CaV2.2 current through

increasing surface expression of CaV2.2, although it does not rule out that CRMP-2 may also regulate the open probability of CaV2.2.

My initial biochemical characterization found that CRMP-2 is localized to both extrasynaptic and synaptic fractions, which suggests that it may traffick CaV2.2 within these regions (Figure 3.2). I also found CRMP-2 present in both cytosolic and membrane fractions. CRMP-2 is localized to the soma, dendrites, and axons and therefore may interact with CaV2.2 in any of these regions. The rather ubiquitous intracellular distribution of CRMP-2 makes it difficult to determine the precise subcellular localization of the CRMP-2-CaV2.2 complex. While my studies show CRMP-2 enhances CaV2.2 surface expression, it is unknown whether CRMP-2 is responsible for gross trafficking of CaV2.2 (i.e. from the soma to the axon) or micro-trafficking (i.e. from axon tip to active zone). It is also unknown whether CRMP-2 associates with CaV2.2 on the plasma membrane. This question is particularly interesting as CRMP-2 may aid in stabilizing the channel on the membrane, which could be responsible for the observed enhancement of CaV2.2 surface expression.

The strong effect of CRMP-2 knockdown on Ca^{2+} currents in neurons suggests that CRMP-2 is *necessary* for CaV2.2 function (Figure 3.11). Of significant interest, CaV2.2 current is observed in heterologous systems despite limited CRMP-2 expression in these cells, which suggests that rather than directly enhancing CaV2.2 surface expression, CRMP-2 may be dis-inhibiting a negative regulator of CaV2.2 trafficking. This negative regulator would likely be neuron specific, as CRMP-2 expression appears to enhance surface expression in neurons, but may not it heterologous systems. The negative regulation may also represent a channel recycling pathway that, without CRMP-2, may lead to a majority of channels leaving the membrane and being degraded. As CRMP-2 binds to the I-II loop, which has been shown to be an important region for proteasome regulation of CaV2.2, this could be a possible mechanism CRMP-2's regulation of CaV2.2 (Waithe et al., 2011). Assuming that CRMP-2 is responsible for overcoming neuronal specific negative regulators of CaV2.2 would also suggest a mechanism

distinct from the other CaV2.2 subunits. Future work should therefore further explore the precise mechanism of CRMP-2's regulation of CaV2.2 and to determine if it truly is neuronal specific.

In Chapter 3, I observed that phosphorylation of CRMP-2 by Cdk5 enhances the interaction between CRMP-2 and CaV2.2 and that a CRMP-2 S522A mutant is unable to enhance CaV2.2 currents. This suggests that enhanced binding between CRMP-2 and CaV2.2 may be important to CRMP-2 trafficking CaV2.2 to the plasma membrane. It is also known that CRMP-2's affinity for Numb and tubulin is greatly reduced following Cdk5 phosphorylation (Arimura et al., 2005), thus the reduced binding of CRMP-2 to tubulin/Numb maybe a required step in order for CRMP-2 to traffick CaV2.2 to the membrane. Based upon this, I would hypothesize that the interaction between tubulin and CRMP-2 may be instrumental for CaV2.2 to be trafficked from the Golgi to near the membrane, but upon phosphorylation CRMP-2 releases tubulin and allows CaV2.2 to be inserted into the membrane. This would also explain why both CRMP-2 S522A and S522D mutants displayed no enhancement of CaV2.2 current, as proper CaV2.2 trafficking likely requires both phosphorylation states of CRMP-2. This spectulation assumes that S522D acts as a true phospho-mimetic; it is also possible that this mutant does not function as native CRMP-2 phosphorylated at Ser-522 would function. It has been previously reported, however, that the S522D mutant has a subcellular localization similar to phosphorylated CRMP-2 supporting this mutant likely acts as a phospho-mimetic (Yoshimura et al., 2005).

5.3. Role of CRMP-2 in the pre-synaptic Ca^{2+} channel complex

CaV2.2 depends on a variety of protein interactions to traffick to the membrane, associate with vesicle fusion machinery, and target to the synaptic terminal. The protein complement of the pre-synaptic Ca^{2+} channel complex is able to fulfill these needs of CaV2.2 and facilitate its role as a regulator of neurotransmitter release. My results have positioned CRMP-2 as a novel member of the CaV2.2 complex which assists with trafficking CaV2.2 to the membrane. It is likely, however, that the interaction between CaV2.2 and CRMP-2 occurs concomitantly with

other protein interactions. It is also possible that these protein binding partners are a prerequisite for CRMP-2 mediated regulation of CaV2.2. As described above, it may be that CRMP-2 allows CaV2.2 to overcome a negative regulatory pathway specific to neurons. Future studies should therefore attempt to determine what proteins are present in CRMP-2-CaV2.2 complexes. This could be elucidated using sequential co-immunoprecipitation of CRMP-2 and then CaV2.2 in order to isolate proteins interacting with the CRMP-2-CaV2.2 complex. Mass spectrometry could then be performed to identify these proteins.

I found that CRMP-2 is able to bind both the I-II loop and the distal portion of the C-terminus. These regions have many known protein interactions (as shown in Table 1.1) that regulate CaV2.2 trafficking and localization to the synapse. For example, both CASK and Mint-1 bind to CaV2.2 in the distal portion of C-terminus, overlapping with the area where CRMP-2 binds. It would therefore be interesting to determine if CRMP-2 binding interferes with these interactions. Alternatively, the CBD3 peptide could also be useful for these experiments. In other work by Dr. Wang, in the Khanna laboratory, it was found that CRMP-4 expression also leads to enhanced Ca^{2+} currents (Wang et al., 2010). This finding suggests that other CRMPs may also be present in the pre-synaptic Ca^{2+} channel complex and hence could also regulate CaV2.2 and neurotransmitter release. A potential caveat to these findings is that CRMPs exist as heterotetramers and the effects of other CRMPs may therefore occur through enhancing the number of CRMP-2 molecules in the synapse, rather than through direct interaction with CaV2.2. Thus, in order to conclude that direct regulation is responsible for the observed increase in Ca^{2+} currents, it will be useful to examine if other CRMPs interact with CaV2.2

5.4. TAT-CBD3 as a novel therapeutic

In Chapter 3 I discovered and characterized the CRMP-2 peptide CBD3 as a novel CaV2.2 antagonist. Rather than directly targeting CaV2.2, CBD3 acts by disrupting the interaction between CRMP-2 and CaV2.2 which leads to reduced CaV2.2 currents. CBD3

appears to have both an acute and long term effect on CaV2.2 function. When CBD3 was expressed in hippocampal neurons, it antagonized CRMP-2-induced enhancement of Ca^{2+} channel currents. As CBD3 disrupts the interaction between CRMP-2 and CaV2.2, this supports the that conclusion that the interaction between CRMP-2 and CaV2.2 is likely responsible for the observed increase in Ca^{2+} currents. Subsequent creation of TAT-CBD3 (the cell penetrant version of CBD3) allowed me to further investigate the role of the CRMP-2-CaV2.2 interaction in both neurons in a dish as well as in whole animals. Application of TAT-CBD3 was able to sharply attenuate CaV2.2 currents consistent with the time scale in which I observed intracellular penetrance of a FITC-labeled TAT-CBD3. TAT-CBD3 was then shown to inhibit CGRP release in spinal cord slices and reduce hypersensitivity in an animal model of nociception. These findings strongly support TAT-CBD3 as a novel therapeutic to target CaV2.2 related pathology. As Chapter 4 has shown, TAT-CBD3 is also able to target NMDARs which may further enhance its efficacy in targeting neurological disorders.

Further studies on TAT-CBD3, as are ongoing in the Khanna laboratory, are needed to verify its specificity and potential applications. In order to test for specificity of CBD3 peptides, utilizing different cell penetrating motifs such as the model amphipathic peptide (MAP) (Scheller et al., 1999) or the membrane translocation sequence (MTS) of Kaposi fibroblast growth factor (Lin et al., 1995) may be useful, as I found that neither MAP- nor MTS-CBD3 were able to acutely inhibit NMDARs (data not shown). These peptides could therefore be used to specifically inhibit the CRMP-2-CaV2.2 interaction without inhibiting NMDARs. The peptides could then be used to verify that *in vivo* reduction of hypersensitivity occurred solely due to CaV2.2-CRMP-2 inhibition. Conversely, it may be possible that these CBD3 peptides may still target NMDARs (discussed in §5.5), and therefore mutations within CBD3 could remain useful in separating the dual targeting of CaV2.2 and NMDARs by CBD3 peptides. In addition, despite showing that TAT-CBD3 does not alter memory retrieval, it must also be tested in an animal model of memory acquisition to verify that it does not prevent this vital brain function. Further

animal studies, including long term treatment with TAT-CBD3 (several weeks), are also ongoing in the Khanna laboratory. These studies are dual purposed as they may test for any toxicity associated with long term TAT-CBD3 exposure as well as determining whether long term treatment can lead to longer-lasting reversal of hypersensitivity. This last part is of particular importance as we observed that a single dose of TAT-CBD lost ~50% of its efficacy within 4 hours. Ideally, following long term treatment of TAT-CBD3 perhaps given once-a-day, a patient would display complete relief from pain for a prolonged (24 hours) period.

Another potential application of TAT-CBD3 and other CRMP-2 peptides is the treatment of CRMP-2 related neuropathies. CRMP-2 has been linked to many neuropathies several of which were discussed in §1.2.8. One disease linked to CRMP-2 that may particularly benefit from TAT-CBD3 is the neurodegenerative disorder AD. One of the potential mechanisms for the neuronal death associated with AD has been Ca^{2+} deregulation (LaFerla, 2002). As TAT-CBD3 targets Ca^{2+} influx via two independent pathways it may be a viable therapy to reduce Ca^{2+} associated neuronal death? The NMDAR has gained ground as a target for AD specifically due to the success of the AD medication memantine, a NMDAR antagonist (Muir, 2006). Testing TAT-CBD3 in animal models of AD may therefore prove fruitful.

5.5. Role of CRMP-2 in excitotoxicity

In Chapter 4, I identified TAT-CBD3 as a novel neuroprotective compound that prevents neuronal death by reducing Ca^{2+} influx through NMDARs (Figure 5.3). Mechanistically, it appears that TAT-CBD3 works through extracellular inhibition of NMDARs, as well as inducing internalization of dendritic NMDARs. I also observed that knockdown of CRMP-2 leads to reduced neuronal death following glutamate exposure. This is consistent with a previous finding that overexpression of CRMP-2 leads to enhanced glutamate-toxicity (Bretin et al., 2006). However, despite a previous study finding that CRMP-2 is in a biochemical complex with NR2B (Al-Hallaq et al., 2007), I was unable to observe this complex.

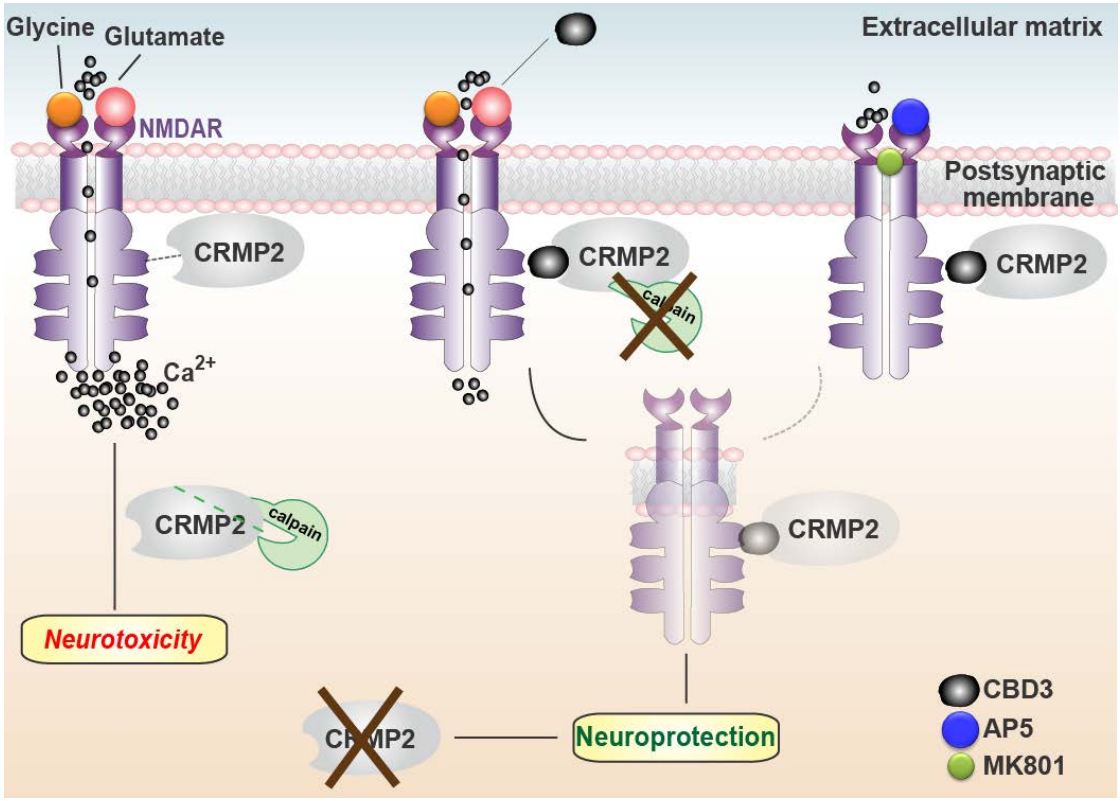

Figure 5.3. CRMP-2's role in neurotoxicity: targeting NMDARs with TAT-CBD3

Extracellular accumulation of glutamate induces hyperactivation of NMDARs leading to toxic influx of Ca^{2+}. This Ca^{2+} build-up leads to activation of many pathways culminating in neurotoxicity including calpain meditated cleavage of CRMP-2. In Chapter 4 I found that knockdown of CRMP-2 using a lentiviral delivered shRNA was neuroprotective. Furthermore I found that application of TAT-CBD3 completely prevented NMDAR-mediated glutamate toxicity. This neuroprotection arose from extracellular inhibition of NMDARs along with selective internalization of dendritic NMDARs. These effects of TAT-CBD3 culminated in preventing toxic accumulation of intracellular Ca^{2+} leading to enhanced neuronal survival. Collectively, Chapter 4 has further implicated CRMP-2 as an important determinant in neurotoxicity and identified TAT-CBD3 as a novel neuroprotective agent.

There have been several studies linking CRMP-2 to neuropathology (see § 1.2.8). The majority of these studies, however, have been proteomic in nature and thus little information has been gleaned on how CRMP-2 contributes to neurological disorders. One of the few areas where CRMP-2 has been explored in past proteomic studies is glutamate-induced excitotoxicity, though there are still many unanswered questions regarding CRMP-2 and neuronal survival in excitotoxicity. NMDAR activation leads to both proteolytic cleavage of CRMP-2 and phosphorylation of CRMP-2 at Thr-555 by CaMKII (Bretin et al., 2006; Hou et al., 2009). Of further interest, it appears that phosphorylation of CRMP-2 may protect CRMP-2 from being cleaved. This presents a potentially complex pathway where CaMKII activation and subsequent phosphorylation prevents simultaneously occurring calpain cleavage of CRMP-2. CaMKII mediated phosphorylation of CRMP-2 is predicted to cause a reduction in axon growth potential through a reduced affinity of CRMP-2 for tubulin and Numb (Arimura et al., 2005). Perhaps more intriguing is that it was observed in this study that overexpression of CRMP-2 prevented glutamate induced alteration of neuritic processes, while a T555A mutant had no effect (Hou et al., 2009). While this suggests that Thr-555 phosphorylation is not an important determinant in neuroprotection, it is unknown, what effect, if any cleavage of CRMP-2 may have on neuronal survival. Alternatively, it has been shown that a calpain cleaved version of CRMP-2 is neuroprotective when overexpressed in neurons, possibly via down regulating NMDAR responses (Bretin et al., 2006). This finding is difficult to interpret, however, because expression of a similarly truncated CRMP-2 leads to a reduction in neuritic process growth, which can likely affect many pathways responsible for glutamate toxicity (Rogemond et al., 2008). It is more likely that expression of this truncated form of CRMP-2 acts as a dominant negative. This could occur either through sequestering native CRMP-2 (through tetramerization) or competing with native CRMP-2 for endogenous protein interactions required for neuritic outgrowth (e.g. tubulin and actin). Therefore, the neuroprotection observed following knockdown of CRMP-2 (Figure 4.7) is entirely consistent with the neuroprotection conferred by the calpain cleaved form of

CRMP-2, in that loss of CRMP-2 function observed with the latter construct is neuroprotective (Bretin et al., 2006). It is then perhaps no surprise that over-expression of full length CRMP-2 enhances neurotoxicity (Bretin et al., 2006).

TAT-CBD3's neuroprotective ability appears to stem from its inhibition of NMDAR-mediated Ca^{2+} influx. This inhibition occurs via an extracellular site of action although I also observed that TAT-CBD3 induced internalization of NMDARs specifically in dendrites. This internalization was not due to disruption of the PSD-95-NR2B interaction (4.15). This suggests that TAT-CBD3 has a dual mode of action through both inhibition of NMDARs and internalization of dendritic receptors. Blockade of NMDARs with MK-801 prevented this internalization. Also of interest is that I observed are my findings that AP-5 co-application with TAT-CBD3 prevents TAT-CBD3's inhibition of NMDAR-mediated Ca^{2+} influx. Although both MK-801 and AP-5 inhibit NMDARs, their mechanisms are entirely different; MK-801 irreversibly blocks the receptor's pore while AP-5 reversibly competes with glutamate for the glutamate binding site on NR2B (See § 1.3.2). Because of this, it is unknown whether the internalization of NMDARs in response to TAT-CBD3 occurs via an intracellular or extracellular site of action. As neither MAP- nor MTS-CBD3 was acutely neuroprotective, these peptides are not able to block NMDAR-mediated Ca^{2+} influx. These peptides may thus be useful for determining both whether intracellular application of CBD3 induces internalization of NMDARs and if long term application is neuroprotective. If long term application of MAP-CBD3 or MTS-CBD3 is able to reduce NMDAR surface expression, this would support CRMP-2 as a regulator of NMDAR function. Future studies should explore if CRMP-2 has a *direct* effect on NMDARs, which could be assesed by measuring surface expression of NR2B following CRMP-2 knockdown.

5.6. Conclusion

In this dissertation, first, I identified and characterized a novel interaction between CRMP-2 and CaV2.2. I further isolated the CBD3 region of CRMP-2 as important to this interaction and utilized CBD3 and its cell penetrant analog TAT-CBD3 to target modulation of CaV2.2 by CRMP-2. TAT-CBD3 was able to successful disrupt CRMP-2's binding to CaV2.2, which resulted in reduced CaV2.2 function and efficacy in CaV2.2-related cell biology and physiology. Second, I identified TAT-CBD3 as a novel neuroprotective agent that works to mitigate glutamate-induced Ca^{2+} toxicity. This finding led to subsequent mechanistic studies identifying a dual mode of action in which NMDARs were inhibited with dendritic NMDARs being internalized.

Collectively, my dissertation work has firmly established CRMP-2 as a novel modulator of synaptic Ca^{2+} channels and has set a solid foundation for the CRMP-2 field to advance both mechanistically and translationally forward.

6. REFERENCES

Aarts, M., Liu, Y., Liu, L., Besshoh, S., Arundine, M., Gurd, J. W., Wang, Y. T., Salter, M. W. and Tymianski, M. (2002). Treatment of ischemic brain damage by perturbing NMDA receptor- PSD-95 protein interactions. *Science* 298, 846-50.

Abbadie, C., McManus, O. B., Sun, S. Y., Bugianesi, R. M., Dai, G., Haedo, R. J., Herrington, J. B., Kaczorowski, G. J., Smith, M. M., Swensen, A. M. et al. (2010). Analgesic effects of a substituted N-triazole oxindole (TROX-1), a state-dependent, voltage-gated calcium channel 2 blocker. *Journal of Pharmacology and Experimental Therapeutics* 334, 545-55.

Adamec, E., Beermann, M. L. and Nixon, R. A. (1998). Calpain I activation in rat hippocampal neurons in culture is NMDA receptor selective and not essential for excitotoxic cell death. *Brain Research. Molecular Brain Research* 54, 35-48.

Adams, D. J. and Gage, P. W. (1976). Gating currents associated with sodium and calcium currents in an Aplysia neuron. *Science* 192, 783-4.

Ahlijanian, M. K., Westenbroek, R. E. and Catterall, W. A. (1990). Subunit structure and localization of dihydropyridine-sensitive calcium channels in mammalian brain, spinal cord, and retina. *Neuron* 4, 819-32.

Al-Hallaq, R. A., Conrads, T. P., Veenstra, T. D. and Wenthold, R. J. (2007). NMDA di-heteromeric receptor populations and associated proteins in rat hippocampus. *J.Neurosci.* 27, 8334-8343.

Altier, C., Dale, C. S., Kisilevsky, A. E., Chapman, K., Castiglioni, A. J., Matthews, E. A., Evans, R. M., Dickenson, A. H., Lipscombe, D., Vergnolle, N. et al. (2007). Differential role of N-type calcium channel splice isoforms in pain. *Journal of Neuroscience* 27, 6363-73.

Altier, C., Garcia-Caballero, A., Simms, B., You, H., Chen, L., Walcher, J., Tedford, H. W., Hermosilla, T. and Zamponi, G. W. (2011). The Cavbeta subunit prevents RFP2-mediated ubiquitination and proteasomal degradation of L-type channels. *Nature Neuroscience* 14, 173-80.

Altier, C., Khosravani, H., Evans, R. M., Hameed, S., Peloquin, J. B., Vartian, B. A., Chen, L., Beedle, A. M., Ferguson, S. S., Mezghrani, A. et al. (2006). ORL1 receptor-mediated internalization of N-type calcium channels. *Nature Neuroscience* 9, 31-40.

Andrade, A., Denome, S., Jiang, Y. Q., Marangoudakis, S. and Lipscombe, D. (2010). Opioid inhibition of N-type Ca2+ channels and spinal analgesia couple to alternative splicing. *Nature Neuroscience* 13, 1249-56.

Arimura, N., Hattori, A., Kimura, T., Nakamuta, S. I., Funahashi, Y., Hirotsune, S., Furuta, K., Urano, T., Toyoshima, Y. Y. and Kaibuchi, K. (2009a). CRMP-2 directly binds to cytoplasmic dynein and interferes with its activity. *Journal of Neurochemistry*.

Arimura, N., Inagaki, N., Chihara, K., Menager, C., Nakamura, N., Amano, M., Iwamatsu, A., Goshima, Y. and Kaibuchi, K. (2000). Phosphorylation of collapsin response mediator protein-2 by Rho-kinase. Evidence for two separate signaling pathways for growth cone collapse. *Journal of Biological Chemistry* 275, 23973-80.

Arimura, N., Kimura, T., Nakamuta, S., Taya, S., Funahashi, Y., Hattori, A., Shimada, A., Menager, C., Kawabata, S., Fujii, K. et al. (2009b). Anterograde transport of TrkB in axons is mediated by direct interaction with Slp1 and Rab27. *Dev Cell* 16, 675-86.

Arimura, N., Menager, C., Fukata, Y. and Kaibuchi, K. (2004). Role of CRMP-2 in neuronal polarity. *Journal of Neurobiology* 58, 34-47.

Arimura, N., Menager, C., Kawano, Y., Yoshimura, T., Kawabata, S., Hattori, A., Fukata, Y., Amano, M., Goshima, Y., Inagaki, M. et al. (2005). Phosphorylation by Rho kinase regulates CRMP-2 activity in growth cones. *Molecular and Cellular Biology* 25, 9973-84.

Artalejo, C. R., Perlman, R. L. and Fox, A. P. (1992). Omega-conotoxin GVIA blocks a Ca2+ current in bovine chromaffin cells that is not of the "classic" N type. *Neuron* 8, 85-95.

Astle, M. V., Ooms, L. M., Cole, A. R., Binge, L. C., Dyson, J. M., Layton, M. J., Petratos, S., Sutherland, C. and Mitchell, C. A. (2011). Identification of a proline-rich inositol polyphosphate 5-phosphatase (PIPP)*collapsin response mediator protein 2 (CRMP2) complex that regulates neurite elongation. *Journal of Biological Chemistry* 286, 23407-18.

Auberson, Y. P., Allgeier, H., Bischoff, S., Lingenhoehl, K., Moretti, R. and Schmutz, M. (2002). 5-Phosphonomethylquinoxalinediones as competitive NMDA receptor antagonists with a preference for the human 1A/2A, rather than 1A/2B receptor composition. *Bioorganic and Medicinal Chemistry Letters* 12, 1099-102.

Baas, P. W. (1997). Microtubules and axonal growth. *Current Opinion in Cell Biology* 9, 29-36.

Barclay, J., Balaguero, N., Mione, M., Ackerman, S. L., Letts, V. A., Brodbeck, J., Canti, C., Meir, A., Page, K. M., Kusumi, K. et al. (2001). Ducky mouse phenotype of epilepsy and ataxia is associated with mutations in the Cacna2d2 gene and decreased calcium channel current in cerebellar Purkinje cells. *Journal of Neuroscience* 21, 6095-104.

Barria, A. and Malinow, R. (2002). Subunit-specific NMDA receptor trafficking to synapses. *Neuron* 35, 345-53.

Bauer, C. S., Nieto-Rostro, M., Rahman, W., Tran-Van-Minh, A., Ferron, L., Douglas, L., Kadurin, I., Sri Ranjan, Y., Fernandez-Alacid, L., Millar, N. S. et al. (2009). The increased trafficking of the calcium channel subunit alpha2delta-1 to presynaptic terminals in neuropathic pain is inhibited by the alpha2delta ligand pregabalin. *Journal of Neuroscience* 29, 4076-88.

Baumann, N. and Pham-Dinh, D. (2001). Biology of oligodendrocyte and myelin in the mammalian central nervous system. *Physiological Reviews* 81, 871-927.

Bean, B. P. (1989). Neurotransmitter inhibition of neuronal calcium currents by changes in channel voltage dependence. *Nature* 340, 153-6.

Bear, M. F. and Malenka, R. C. (1994). Synaptic plasticity: LTP and LTD. *Current Opinion in Neurobiology* 4, 389-99.

Beech, D. J., Bernheim, L. and Hille, B. (1992). Pertussis toxin and voltage dependence distinguish multiple pathways modulating calcium channels of rat sympathetic neurons. *Neuron* 8, 97-106.

Beedle, A. M., McRory, J. E., Poirot, O., Doering, C. J., Altier, C., Barrere, C., Hamid, J., Nargeot, J., Bourinet, E. and Zamponi, G. W. (2004). Agonist-independent modulation of N-type calcium channels by ORL1 receptors. *Nature Neuroscience* 7, 118-25.

Belliotti, T. R., Capiris, T., Ekhato, I. V., Kinsora, J. J., Field, M. J., Heffner, T. G., Meltzer, L. T., Schwarz, J. B., Taylor, C. P., Thorpe, A. J. et al. (2005). Structure-activity relationships of pregabalin and analogues that target the alpha(2)-delta protein. *Journal of Medicinal Chemistry* 48, 2294-307.

Benedict, J. W., Getty, A. L., Wishart, T. M., Gillingwater, T. H. and Pearce, D. A. (2009). Protein product of CLN6 gene responsible for variant late-onset infantile neuronal ceroid lipofuscinosis interacts with CRMP-2. *Journal of Neuroscience Research* 87, 2157-66.

Berg, D., Holzmann, C. and Riess, O. (2003). 14-3-3 proteins in the nervous system. *Nat Rev Neurosci* 4, 752-62.

Bernstein, G. M. and Jones, O. T. (2007). Kinetics of internalization and degradation of N-type voltage-gated calcium channels: role of the alpha2/delta subunit. *Cell Calcium* 41, 27-40.

Beuckmann, C. T., Sinton, C. M., Miyamoto, N., Ino, M. and Yanagisawa, M. (2003). N-type calcium channel alpha1B subunit (Cav2.2) knock-out mice display hyperactivity and vigilance state differences. *Journal of Neuroscience* 23, 6793-7.

Bevers, M. B., Lawrence, E., Maronski, M., Starr, N., Amesquita, M. and Neumar, R. W. (2009). Knockdown of m-calpain increases survival of primary hippocampal neurons following NMDA excitotoxicity. *Journal of Neurochemistry*.

Beyreuther, B. K., Freitag, J., Heers, C., Krebsfanger, N., Scharfenecker, U. and Stohr, T. (2007). Lacosamide: a review of preclinical properties. *CNS Drug Rev* 13, 21-42.

Bezprozvanny, I., Scheller, R. H. and Tsien, R. W. (1995). Functional impact of syntaxin on gating of N-type and Q-type calcium channels. *Nature* 378, 623-6.

Bhangoo, S. K., Ripsch, M. S., Buchanan, D. J., Miller, R. J. and White, F. A. (2009). Increased chemokine signaling in a model of HIV1-associated peripheral neuropathy. *Mol.Pain.* 5:48., 48.

Bichet, D., Cornet, V., Geib, S., Carlier, E., Volsen, S., Hoshi, T., Mori, Y. and De Waard, M. (2000). The I-II loop of the Ca2+ channel alpha1 subunit contains an endoplasmic reticulum retention signal antagonized by the beta subunit. *Neuron* 25, 177-90.

Birnbaumer, L., Qin, N., Olcese, R., Tareilus, E., Platano, D., Costantin, J. and Stefani, E. (1998). Structures and functions of calcium channel beta subunits. *Journal of Bioenergetics and Biomembranes* 30, 357-75.

Boehm, S. and Huck, S. (1996). Inhibition of N-type calcium channels: the only mechanism by which presynaptic alpha 2-autoreceptors control sympathetic transmitter release. *European Journal of Neuroscience* 8, 1924-31.

Bowersox, S. S., Gadbois, T., Singh, T., Pettus, M., Wang, Y. X. and Luther, R. R. (1996). Selective N-type neuronal voltage-sensitive calcium channel blocker, SNX-111, produces spinal antinociception in rat models of acute, persistent and neuropathic pain. *Journal of Pharmacology and Experimental Therapeutics* 279, 1243-9.

Bowser, R., Muller, H., Govindan, B. and Novick, P. (1992). Sec8p and Sec15p are components of a plasma membrane-associated 19.5S particle that may function downstream of Sec4p to control exocytosis. *Journal of Cell Biology* 118, 1041-56.

Bradke, F. and Dotti, C. G. (1999). The role of local actin instability in axon formation. *Science* 283, 1931-4.

Bradke, F. and Dotti, C. G. (2000). Changes in membrane trafficking and actin dynamics during axon formation in cultured hippocampal neurons. *Microscopy Research and Technique* 48, 3-11.

Brain, S. D., Williams, T. J., Tippins, J. R., Morris, H. R. and MacIntyre, I. (1985). Calcitonin gene-related peptide is a potent vasodilator. *Nature* 313, 54-6.

Bredt, D. S. and Snyder, S. H. (1990). Isolation of nitric oxide synthetase, a calmodulin-requiring enzyme. *Proceedings of the National Academy of Sciences of the United States of America* 87, 682-5.

Brehm, P. and Eckert, R. (1978). Calcium entry leads to inactivation of calcium channel in Paramecium. *Science* 202, 1203-6.

Bretin, S., Rogemond, V., Marin, P., Maus, M., Torrens, Y., Honnorat, J., Glowinski, J., Premont, J. and Gauchy, C. (2006). Calpain product of WT-CRMP2 reduces the amount of surface NR2B NMDA receptor subunit. *Journal of Neurochemistry* 98, 1252-65.

Brice, N. L., Berrow, N. S., Campbell, V., Page, K. M., Brickley, K., Tedder, I. and Dolphin, A. C. (1997). Importance of the different beta subunits in the membrane expression of the alpha1A and alpha2 calcium channel subunits: studies using a depolarization-sensitive alpha1A antibody. *European Journal of Neuroscience* 9, 749-59.

Brittain, J. M., Chen, L., Wilson, S. M., Brustovetsky, T., Gao, X., Ashpole, N. M., Molosh, A. I., You, H., Hudmon, A., Shekhar, A. et al. (2011a). Neuroprotection against Traumatic Brain Injury by a Peptide Derived from the Collapsin Response Mediator Protein 2 (CRMP2). *Journal of Biological Chemistry* 286, 37778-92.

Brittain, J. M., Duarte, D. B., Wilson, S. M., Zhu, W., Ballard, C., Johnson, P. L., Liu, N., Xiong, W., Ripsch, M. S., Wang, Y. et al. (2011b). Suppression of inflammatory and neuropathic pain by uncoupling CRMP-2 from the presynaptic Ca(2) channel complex. *Nature Medicine* 17, 822-9.

Brittain, J. M., Pan, R., You, H., Brustovetsky, T., Brustovetsky, N., Zamponi, G. W., Lee, W. H. and Khanna, R. (2012a). Disruption of NMDAR-CRMP-2 signaling protects against focal cerebral ischemic damage in the rat middle cerebral artery occlusion model. *Channels (Austin)* 6.

Brittain, J. M., Piekarz, A. D., Wang, Y., Kondo, T., Cummins, T. R. and Khanna, R. (2009). An atypical role for collapsin response mediator protein 2 (CRMP-2) in neurotransmitter release via interaction with presynaptic voltage-gated calcium channels. *Journal of Biological Chemistry* 284, 31375-90.

Brittain, J. M., Wang, Y., Eruvwetere, O. and Khanna, R. (2012b). Cdk5-mediated phosphorylation of CRMP-2 enhances its interaction with CaV2.2. *FEBS Letters*.

Brodbeck, J., Davies, A., Courtney, J. M., Meir, A., Balaguero, N., Canti, C., Moss, F. J., Page, K. M., Pratt, W. S., Hunt, S. P. et al. (2002). The ducky mutation in Cacna2d2 results in altered Purkinje cell morphology and is associated with the expression of a truncated alpha 2 delta-2 protein with abnormal function. *Journal of Biological Chemistry* 277, 7684-93.

Brorson, J. R., Marcuccilli, C. J. and Miller, R. J. (1995). Delayed antagonism of calpain reduces excitotoxicity in cultured neurons. *Stroke* 26, 1259-66; discussion 1267.

Brot, S., Rogemond, V., Perrot, V., Chounlamountri, N., Auger, C., Honnorat, J. and Moradi-Ameli, M. (2010). CRMP5 interacts with tubulin to inhibit neurite outgrowth, thereby modulating the function of CRMP2. *Journal of Neuroscience* 30, 10639-54.

Brown, M., Jacobs, T., Eickholt, B., Ferrari, G., Teo, M., Monfries, C., Qi, R. Z., Leung, T., Lim, L. and Hall, C. (2004). Alpha2-chimaerin, cyclin-dependent Kinase 5/p35, and its target collapsin response mediator protein-2 are essential components in semaphorin 3A-induced growth-cone collapse. *Journal of Neuroscience* 24, 8994-9004.

Bullock, R., Zauner, A., Woodward, J. and Young, H. F. (1995). Massive persistent release of excitatory amino acids following human occlusive stroke. *Stroke* 26, 2187-9.

Buraei, Z. and Yang, J. (2010). The ss subunit of voltage-gated Ca2+ channels. *Physiological Reviews* 90, 1461-506.

Byk, T., Dobransky, T., Cifuentes-Diaz, C. and Sobel, A. (1996). Identification and molecular characterization of Unc-33-like phosphoprotein (Ulip), a putative mammalian homolog of the axonal guidance-associated unc-33 gene product. *Journal of Neuroscience* 16, 688-701.

Byk, T., Ozon, S. and Sobel, A. (1998). The Ulip family phosphoproteins--common and specific properties. *Eur.J.Biochem.* 254, 14-24.

Calakos, N., Schoch, S., Sudhof, T. C. and Malenka, R. C. (2004). Multiple roles for the active zone protein RIM1alpha in late stages of neurotransmitter release. *Neuron.* 42, 889-896.

Canti, C., Nieto-Rostro, M., Foucault, I., Heblich, F., Wratten, J., Richards, M. W., Hendrich, J., Douglas, L., Page, K. M., Davies, A. et al. (2005). The metal-ion-dependent adhesion site in the Von Willebrand factor-A domain of alpha2delta subunits is key to trafficking voltage-gated Ca2+ channels. *Proceedings of the National Academy of Sciences of the United States of America* 102, 11230-5.

Cao, Y. Q., Piedras-Renteria, E. S., Smith, G. B., Chen, G., Harata, N. C. and Tsien, R. W. (2004). Presynaptic Ca2+ channels compete for channel type-preferring slots in altered neurotransmission arising from Ca2+ channelopathy. *Neuron* 43, 387-400.

Cao, Y. Q. and Tsien, R. W. (2010). Different relationship of N- and P/Q-type Ca2+ channels to channel-interacting slots in controlling neurotransmission at cultured hippocampal synapses. *Journal of Neuroscience* 30, 4536-46.

Carbone, E. and Lux, H. D. (1984). A low voltage-activated calcium conductance in embryonic chick sensory neurons. *Biophysical Journal* 46, 413-8.

Carlin, R. K., Grab, D. J., Cohen, R. S. and Siekevitz, P. (1980). Isolation and characterization of postsynaptic densities from various brain regions: enrichment of different types of postsynaptic densities. *J.Cell Biol.* 86, 831-845.

Carlson, F. D., Society of General Physiologists. and Marine Biological Laboratory (Woods Hole Mass.). (1968). Physiological and biochemical aspects of nervous integration. Englewood Cliffs, N.J.,: Prentice-Hall.

Catterall, W. A. (1988). Structure and function of voltage-sensitive ion channels. *Science.* 242, 50-61.

Catterall, W. A. (1991a). Functional subunit structure of voltage-gated calcium channels. *Science* 253, 1499-500.

Catterall, W. A. (1991b). Structure and function of voltage-gated sodium and calcium channels. *Current Opinion in Neurobiology* 1, 5-13.

Catterall, W. A. and Few, A. P. (2008). Calcium channel regulation and presynaptic plasticity. *Neuron* 59, 882-901.

Catterall, W. A., Perez-Reyes, E., Snutch, T. P. and Striessnig, J. (2005). International Union of Pharmacology. XLVIII. Nomenclature and structure-function relationships of voltage-gated calcium channels. *Pharmacological Reviews* 57, 411-25.

Catterall, W. A., Seagar, M. J., Takahashi, M. and Nunoki, K. (1989). Molecular properties of dihydropyridine-sensitive calcium channels. *Annals of the New York Academy of Sciences* 560, 1-14.

Cerne, R., Rusin, K. I. and Randic, M. (1993). Enhancement of the N-methyl-D-aspartate response in spinal dorsal horn neurons by cAMP-dependent protein kinase. *Neuroscience Letters* 161, 124-8.

Chae, Y. C., Lee, S., Heo, K., Ha, S. H., Jung, Y., Kim, J. H., Ihara, Y., Suh, P. G. and Ryu, S. H. (2009). Collapsin response mediator protein-2 regulates neurite formation by modulating tubulin GTPase activity. *Cellular Signalling* 21, 1818-26.

Chan, A. W., Khanna, R., Li, Q. and Stanley, E. F. (2007). Munc18: A Presynaptic Transmitter Release Site N type (CaV2.2) Calcium Channel Interacting Protein. *Channels* 1, 11-20.

Chaplan, S. R., Pogrel, J. W. and Yaksh, T. L. (1994). Role of voltage-dependent calcium channel subtypes in experimental tactile allodynia. *Journal of Pharmacology and Experimental Therapeutics* 269, 1117-23.

Chapman, E. R. (2008). How does synaptotagmin trigger neurotransmitter release? *Annual Review of Biochemistry* 77, 615-41.

Chen, A., Liao, W. P., Lu, Q., Wong, W. S. and Wong, P. T. (2007a). Upregulation of dihydropyrimidinase-related protein 2, spectrin alpha II chain, heat shock cognate protein 70 pseudogene 1 and tropomodulin 2 after focal cerebral ischemia in rats--a proteomics approach. *Neurochemistry International* 50, 1078-86.

Chen, B. S. and Roche, K. W. (2007). Regulation of NMDA receptors by phosphorylation. *Neuropharmacology* 53, 362-8.

Chen, H., Puhl, H. L., 3rd, Niu, S. L., Mitchell, D. C. and Ikeda, S. R. (2005). Expression of Rem2, an RGK family small GTPase, reduces N-type calcium current without affecting channel surface density. *Journal of Neuroscience* 25, 9762-72.

Chen, J. J., Barber, L. A., Dymshitz, J. and Vasko, M. R. (1996). Peptidase inhibitors improve recovery of substance P and calcitonin gene-related peptide release from rat spinal cord slices. *Peptides.* 17, 31-37.

Chen, L. and Huang, L. Y. (1991). Sustained potentiation of NMDA receptor-mediated glutamate responses through activation of protein kinase C by a mu opioid. *Neuron* 7, 319-26.

Chen, P., Gu, Z., Liu, W. and Yan, Z. (2007b). Glycogen synthase kinase 3 regulates N-methyl-D-aspartate receptor channel trafficking and function in cortical neurons. *Molecular Pharmacology* 72, 40-51.

Chen, Y., Stevens, B., Chang, J., Milbrandt, J., Barres, B. A. and Hell, J. W. (2008). NS21: re-defined and modified supplement B27 for neuronal cultures. *J.Neurosci.Methods.* 171, 239-247.

Chien, A. J., Zhao, X., Shirokov, R. E., Puri, T. S., Chang, C. F., Sun, D., Rios, E. and Hosey, M. M. (1995). Roles of a membrane-localized beta subunit in the formation and targeting of functional L-type Ca2+ channels. *Journal of Biological Chemistry* 270, 30036-44.

Choi, D. W. (1985). Glutamate neurotoxicity in cortical cell culture is calcium dependent. *Neuroscience Letters* 58, 293-7.

Choi, D. W. (1992). Excitotoxic cell death. *J.Neurobiol.* 23, 1261-1276.

Christopherson, K. S., Hillier, B. J., Lim, W. A. and Bredt, D. S. (1999). PSD-95 assembles a ternary complex with the N-methyl-D-aspartic acid receptor and a bivalent neuronal NO synthase PDZ domain. *Journal of Biological Chemistry* 274, 27467-73.

Chung, H. J., Huang, Y. H., Lau, L. F. and Huganir, R. L. (2004). Regulation of the NMDA receptor complex and trafficking by activity-dependent phosphorylation of the NR2B subunit PDZ ligand. *Journal of Neuroscience* 24, 10248-59.

Chung, M. A., Lee, J. E., Lee, J. Y., Ko, M. J., Lee, S. T. and Kim, H. J. (2005). Alteration of collapsin response mediator protein-2 expression in focal ischemic rat brain. *Neuroreport* 16, 1647-53.

Cole, A. R., Causeret, F., Yadirgi, G., Hastie, C. J., McLauchlan, H., McManus, E. J., Hernandez, F., Eickholt, B. J., Nikolic, M. and Sutherland, C. (2006). Distinct priming kinases contribute to differential regulation of collapsin response mediator proteins by glycogen synthase kinase-3 in vivo. *Journal of Biological Chemistry* 281, 16591-8.

Cole, A. R., Knebel, A., Morrice, N. A., Robertson, L. A., Irving, A. J., Connolly, C. N. and Sutherland, C. (2004). GSK-3 phosphorylation of the Alzheimer epitope within collapsin response mediator proteins regulates axon elongation in primary neurons. *Journal of Biological Chemistry* 279, 50176-80.

Cole, A. R., Noble, W., van Aalten, L., Plattner, F., Meimaridou, R., Hogan, D., Taylor, M., LaFrancois, J., Gunn-Moore, F., Verkhratsky, A. et al. (2007). Collapsin response mediator protein-2 hyperphosphorylation is an early event in Alzheimer's disease progression. *Journal of Neurochemistry* 103, 1132-44.

Cole, A. R., Soutar, M. P., Rembutsu, M., Van Aalten, L., Hastie, C. J., McLauchlan, H., Peggie, M., Balastik, M., Lu, K. P. and Sutherland, C. (2008). Relative resistance of Cdk5-phosphorylated CRMP2 to dephosphorylation. *Journal of Biological Chemistry*.

Coppola, T., Magnin-Luthi, S., Perret-Menoud, V., Gattesco, S., Schiavo, G. and Regazzi, R. (2001). Direct interaction of the Rab3 effector RIM with Ca2+ channels, SNAP-25, and synaptotagmin. *Journal of Biological Chemistry* 276, 32756-62.

Cornet, V., Bichet, D., Sandoz, G., Marty, I., Brocard, J., Bourinet, E., Mori, Y., Villaz, M. and De Waard, M. (2002). Multiple determinants in voltage-dependent P/Q calcium channels control their retention in the endoplasmic reticulum. *European Journal of Neuroscience* 16, 883-95.

Cotman, C. W. and Taylor, D. (1972). Isolation and structural studies on synaptic complexes from rat brain. *Journal of Cell Biology* 55, 696-711.

Cox, D. H. and Dunlap, K. (1994). Inactivation of N-type calcium current in chick sensory neurons: calcium and voltage dependence. *Journal of General Physiology* 104, 311-36.

Craig, A. M., Blackstone, C. D., Huganir, R. L. and Banker, G. (1994). Selective clustering of glutamate and gamma-aminobutyric acid receptors opposite terminals releasing the corresponding neurotransmitters. *Proceedings of the National Academy of Sciences of the United States of America* 91, 12373-7.

Crunelli, V., Forda, S. and Kelly, J. S. (1983). Blockade of amino acid-induced depolarizations and inhibition of excitatory post-synaptic potentials in rat dentate gyrus. *J Physiol* 341, 627-40.

Czech, T., Yang, J. W., Csaszar, E., Kappler, J., Baumgartner, C. and Lubec, G. (2004). Reduction of hippocampal collapsin response mediated protein-2 in patients with mesial temporal lobe epilepsy. *Neurochemical Research* 29, 2189-96.

Czogalla, A. and Sikorski, A. F. (2005). Spectrin and calpain: a 'target' and a 'sniper' in the pathology of neuronal cells. *Cellular and Molecular Life Sciences* 62, 1913-24.

D'Ascenzo, M., Vairano, M., Andreassi, C., Navarra, P., Azzena, G. B. and Grassi, C. (2004). Electrophysiological and molecular evidence of L-(Cav1), N- (Cav2.2), and R- (Cav2.3) type Ca2+ channels in rat cortical astrocytes. *Glia* 45, 354-63.

D'Hooge, R. and De Deyn, P. P. (2001). Applications of the Morris water maze in the study of learning and memory. *Brain Res.Brain Res.Rev.* 36, 60-90.

Davies, A., Hendrich, J., Van Minh, A. T., Wratten, J., Douglas, L. and Dolphin, A. C. (2007). Functional biology of the alpha(2)delta subunits of voltage-gated calcium channels. *Trends in Pharmacological Sciences* 28, 220-8.

Davies, J. N. and Zamponi, G. W. (2008). Old proteins, developing roles: The regulation of calcium channels by synaptic proteins. *Channels (Austin)* 2, 130-8.

Dawson, V. L., Dawson, T. M., London, E. D., Bredt, D. S. and Snyder, S. H. (1991). Nitric oxide mediates glutamate neurotoxicity in primary cortical cultures. *Proceedings of the National Academy of Sciences of the United States of America* 88, 6368-71.

De Jongh, K. S., Merrick, D. K. and Catterall, W. A. (1989). Subunits of purified calcium channels: a 212-kDa form of alpha 1 and partial amino acid sequence of a phosphorylation site of an independent beta subunit. *Proceedings of the National Academy of Sciences of the United States of America* 86, 8585-9.

De Waard, M., Hering, J., Weiss, N. and Feltz, A. (2005). How do G proteins directly control neuronal Ca2+ channel function? *Trends in Pharmacological Sciences* 26, 427-36.

De Waard, M., Pragnell, M. and Campbell, K. P. (1994). Ca2+ channel regulation by a conserved beta subunit domain. *Neuron* 13, 495-503.

Deak, F., Xu, Y., Chang, W. P., Dulubova, I., Khvotchev, M., Liu, X., Sudhof, T. C. and Rizo, J. (2009). Munc18-1 binding to the neuronal SNARE complex controls synaptic vesicle priming. *Journal of Cell Biology*.

del Cerro, S., Arai, A., Kessler, M., Bahr, B. A., Vanderklish, P., Rivera, S. and Lynch, G. (1994). Stimulation of NMDA receptors activates calpain in cultured hippocampal slices. *Neuroscience Letters* 167, 149-52.

Deo, R. C., Schmidt, E. F., Elhabazi, A., Togashi, H., Burley, S. K. and Strittmatter, S. M. (2004). Structural bases for CRMP function in plexin-dependent semaphorin3A signaling. *EMBO Journal* 23, 9-22.

Dingledine, R., Borges, K., Bowie, D. and Traynelis, S. F. (1999). The glutamate receptor ion channels. *Pharmacological Reviews* 51, 7-61.

Dodge, F. A., Jr. and Rahamimoff, R. (1967). Co-operative action a calcium ions in transmitter release at the neuromuscular junction. *J Physiol* 193, 419-32.

Dolphin, A. C. (2003a). Beta subunits of voltage-gated calcium channels. *Journal of Bioenergetics and Biomembranes* 35, 599-620.

Dolphin, A. C. (2003b). G protein modulation of voltage-gated calcium channels. *Pharmacological Reviews* 55, 607-27.

Dolphin, A. C. (2006). A short history of voltage-gated calcium channels. *British Journal of Pharmacology* 147 Suppl 1, S56-62.

Donzanti, B. A. and Yamamoto, B. K. (1988). An improved and rapid HPLC-EC method for the isocratic separation of amino acid neurotransmitters from brain tissue and microdialysis perfusates. *Life Sciences* 43, 913-922.

Dooley, D. J., Lupp, A. and Hertting, G. (1987). Inhibition of central neurotransmitter release by omega-conotoxin GVIA, a peptide modulator of the N-type voltage-sensitive calcium channel. *Naunyn-Schmiedebergs Archives of Pharmacology* 336, 467-70.

Dutta, S., Chiu, Y. C., Probert, A. W. and Wang, K. K. (2002). Selective release of calpain produced alphaII-spectrin (alpha-fodrin) breakdown products by acute neuronal cell death. *Biological Chemistry* 383, 785-91.

Edmondson, D. G. and Roth, S. Y. (2001). Identification of protein interactions by far Western analysis. *Curr.Protoc.Cell Biol.* Chapter 17:Unit 17.2., Unit.

Eickholt, B. J., Walsh, F. S. and Doherty, P. (2002). An inactive pool of GSK-3 at the leading edge of growth cones is implicated in Semaphorin 3A signaling. *Journal of Cell Biology* 157, 211-7.

el, F. O., Charvin, N., Leveque, C., Martin-Moutot, N., Takahashi, M. and Seagar, M. J. (1995). Interaction of a synaptobrevin (VAMP)-syntaxin complex with presynaptic calcium channels. *FEBS Letters* 361, 101-105.

Ellinor, P. T., Zhang, J. F., Horne, W. A. and Tsien, R. W. (1994). Structural determinants of the blockade of N-type calcium channels by a peptide neurotoxin. *Nature* 372, 272-5.

Enomoto, H. (2005). Regulation of neural development by glial cell line-derived neurotrophic factor family ligands. *Anat Sci Int* 80, 42-52.

Ertel, E. A., Campbell, K. P., Harpold, M. M., Hofmann, F., Mori, Y., Perez-Reyes, E., Schwartz, A., Snutch, T. P., Tanabe, T., Birnbaumer, L. et al. (2000). Nomenclature of voltage-gated calcium channels. *Neuron* 25, 533-5.

Evans, A. R., Nicol, G. D. and Vasko, M. R. (1996). Differential regulation of evoked peptide release by voltage-sensitive calcium channels in rat sensory neurons. *Brain Research* 712, 265-73.

Evans, R. M. and Zamponi, G. W. (2006). Presynaptic Ca2+ channels--integration centers for neuronal signaling pathways. *Trends in Neurosciences* 29, 617-624.

Faden, A. I., Demediuk, P., Panter, S. S. and Vink, R. (1989). The role of excitatory amino acids and NMDA receptors in traumatic brain injury. *Science* 244, 798-800.

Fatt, P. and Ginsborg, B. L. (1958). The ionic requirements for the production of action potentials in crustacean muscle fibres. *J Physiol* 142, 516-43.

Fatt, P. and Katz, B. (1953). The electrical properties of crustacean muscle fibres. *J Physiol* 120, 171-204.

Fedchyshyn, M. J. and Wang, L. Y. (2005). Developmental transformation of the release modality at the calyx of Held synapse. *Journal of Neuroscience* 25, 4131-40.

Fei, T., Xia, K., Li, Z., Zhou, B., Zhu, S., Chen, H., Zhang, J., Chen, Z., Xiao, H., Han, J. D. et al. (2010). Genome-wide mapping of SMAD target genes reveals the role of BMP signaling in embryonic stem cell fate determination. *Genome Research* 20, 36-44.

Fernandez-Gamba, A., Leal, M. C., Maarouf, C. L., Richter-Landsberg, C., Wu, T., Morelli, L., Roher, A. E. and Castano, E. M. (2012). Collapsin response mediator protein-2 phosphorylation promotes the reversible retraction of oligodendrocyte processes in response to non-lethal oxidative stress. *Journal of Neurochemistry*.

Field, M. J., Cox, P. J., Stott, E., Melrose, H., Offord, J., Su, T. Z., Bramwell, S., Corradini, L., England, S., Winks, J. et al. (2006). Identification of the alpha2-delta-1 subunit of voltage-dependent calcium channels as a molecular target for pain mediating the analgesic actions of pregabalin. *Proceedings of the National Academy of Sciences of the United States of America* 103, 17537-42.

Field, M. J., Hughes, J. and Singh, L. (2000). Further evidence for the role of the alpha(2)delta subunit of voltage dependent calcium channels in models of neuropathic pain. *British Journal of Pharmacology* 131, 282-6.

Finlin, B. S., Crump, S. M., Satin, J. and Andres, D. A. (2003). Regulation of voltage-gated calcium channel activity by the Rem and Rad GTPases. *Proc.Natl.Acad.Sci.U.S.A.* 100, 14469-14474.

Finlin, B. S., Mosley, A. L., Crump, S. M., Correll, R. N., Ozcan, S., Satin, J. and Andres, D. A. (2005). Regulation of L-type Ca2+ channel activity and insulin secretion by the Rem2 GTPase. *J.Biol.Chem.* 280, 41864-41871.

Flynn, R., Chen, L., Hameed, S., Spafford, J. D. and Zamponi, G. W. (2008). Molecular determinants of Rem2 regulation of N-type calcium channels. *Biochemical and Biophysical Research Communications* 368, 827-31.

Foster, A. C. and Wong, E. H. (1987). The novel anticonvulsant MK-801 binds to the activated state of the N-methyl-D-aspartate receptor in rat brain. *British Journal of Pharmacology* 91, 403-9.

Fukada, M., Watakabe, I., Yuasa-Kawada, J., Kawachi, H., Kuroiwa, A., Matsuda, Y. and Noda, M. (2000). Molecular characterization of CRMP5, a novel member of the collapsin response mediator protein family. *Journal of Biological Chemistry* 275, 37957-65.

Fukata, Y., Itoh, T. J., Kimura, T., Menager, C., Nishimura, T., Shiromizu, T., Watanabe, H., Inagaki, N., Iwamatsu, A., Hotani, H. et al. (2002). CRMP-2 binds to tubulin heterodimers to promote microtubule assembly. *Nat Cell Biol* 4, 583-91.

Furukawa, T., Miura, R., Mori, Y., Strobeck, M., Suzuki, K., Ogihara, Y., Asano, T., Morishita, R., Hashii, M., Higashida, H. et al. (1998). Differential interactions of the C terminus and the cytoplasmic I-II loop of neuronal Ca2+ channels with G-protein alpha and beta gamma subunits. II. Evidence for direct binding. *Journal of Biological Chemistry* 273, 17595-603.

Gaetano, C., Matsuo, T. and Thiele, C. J. (1997). Identification and characterization of a retinoic acid-regulated human homologue of the unc-33-like phosphoprotein gene (hUlip) from neuroblastoma cells. *Journal of Biological Chemistry* 272, 12195-201.

Gao, B., Sekido, Y., Maximov, A., Saad, M., Forgacs, E., Latif, F., Wei, M. H., Lerman, M., Lee, J. H., Perez-Reyes, E. et al. (2000). Functional properties of a new voltage-dependent calcium channel alpha(2)delta auxiliary subunit gene (CACNA2D2). *Journal of Biological Chemistry* 275, 12237-42.

Gerber, S. H., Rah, J. C., Min, S. W., Liu, X., de Wit, H., Dulubova, I., Meyer, A. C., Rizo, J., Arancillo, M., Hammer, R. E. et al. (2008). Conformational switch of syntaxin-1 controls synaptic vesicle fusion. *Science* 321, 1507-10.

Geschwind, D. H. and Hockfield, S. (1989). Identification of proteins that are developmentally regulated during early cerebral corticogenesis in the rat. *Journal of Neuroscience* 9, 4303-17.

Goebel-Goody, S. M., Davies, K. D., Alvestad Linger, R. M., Freund, R. K. and Browning, M. D. (2009). Phospho-regulation of synaptic and extrasynaptic N-methyl-d-aspartate receptors in adult hippocampal slices. *Neuroscience* 158, 1446-59.

Gogel, S., Lange, S., Leung, K. Y., Greene, N. D. and Ferretti, P. (2010). Post-translational regulation of Crmp in developing and regenerating chick spinal cord. *Dev Neurobiol* 70, 456-71.

Gomez, L. L., Alam, S., Smith, K. E., Horne, E. and Dell'Acqua, M. L. (2002). Regulation of A-kinase anchoring protein 79/150-cAMP-dependent protein kinase postsynaptic targeting by NMDA receptor activation of calcineurin and remodeling of dendritic actin. *Journal of Neuroscience* 22, 7027-44.

Goo, Y. S., Lim, W. and Elmslie, K. S. (2006). Ca2+ enhances U-type inactivation of N-type (CaV2.2) calcium current in rat sympathetic neurons. *Journal of Neurophysiology* 96, 1075-83.

Good, P. F., Alapat, D., Hsu, A., Chu, C., Perl, D., Wen, X., Burstein, D. E. and Kohtz, D. S. (2004). A role for semaphorin 3A signaling in the degeneration of hippocampal neurons during Alzheimer's disease. *Journal of Neurochemistry* 91, 716-36.

Goshima, Y., Nakamura, F., Strittmatter, P. and Strittmatter, S. M. (1995). Collapsin-induced growth cone collapse mediated by an intracellular protein related to UNC-33. *Nature* 376, 509-14.

Goslin, K. and Banker, G. (1989). Experimental observations on the development of polarity by hippocampal neurons in culture. *J.Cell Biol.* 108, 1507-1516.

Gray, N., Detivaud, L., Doerig, C. and Meijer, L. (1999). ATP-site directed inhibitors of cyclin-dependent kinases. *Current Medicinal Chemistry* 6, 859-75.

Grosshans, D. R., Clayton, D. A., Coultrap, S. J. and Browning, M. D. (2002). LTP leads to rapid surface expression of NMDA but not AMPA receptors in adult rat CA1. *Nature Neuroscience* 5, 27-33.

Grotta, J. C., Picone, C. M., Ostrow, P. T., Strong, R. A., Earls, R. M., Yao, L. P., Rhoades, H. M. and Dedman, J. R. (1990). CGS-19755, a competitive NMDA receptor antagonist, reduces calcium-calmodulin binding and improves outcome after global cerebral ischemia. *Annals of Neurology* 27, 612-9.

Gruner, W. and Silva, L. R. (1994). Omega-conotoxin sensitivity and presynaptic inhibition of glutamatergic sensory neurotransmission in vitro. *Journal of Neuroscience* 14, 2800-8.

Grynkiewicz, G., Poenie, M. and Tsien, R. Y. (1985). A new generation of Ca2+ indicators with greatly improved fluorescence properties. *Journal of Biological Chemistry* 260, 3440-50.

Gu, Y., Hamajima, N. and Ihara, Y. (2000). Neurofibrillary tangle-associated collapsin response mediator protein-2 (CRMP-2) is highly phosphorylated on Thr-509, Ser-518, and Ser-522. *Biochemistry* 39, 4267-75.

Gu, Y. and Ihara, Y. (2000). Evidence that collapsin response mediator protein-2 is involved in the dynamics of microtubules. *Journal of Biological Chemistry* 275, 17917-20.

Guan, K. L. and Rao, Y. (2003). Signalling mechanisms mediating neuronal responses to guidance cues. *Nat Rev Neurosci* 4, 941-56.

Guillaud, L., Setou, M. and Hirokawa, N. (2003). KIF17 dynamics and regulation of NR2B trafficking in hippocampal neurons. *Journal of Neuroscience* 23, 131-40.

Guttmann, R. P., Sokol, S., Baker, D. L., Simpkins, K. L., Dong, Y. and Lynch, D. R. (2002). Proteolysis of the N-methyl-d-aspartate receptor by calpain in situ. *Journal of Pharmacology and Experimental Therapeutics* 302, 1023-30.

Hagiwara, S., Ozawa, S. and Sand, O. (1975). Voltage clamp analysis of two inward current mechanisms in the egg cell membrane of a starfish. *Journal of General Physiology* 65, 617-44.

Hall, R. A. (2004). Studying protein-protein interactions via Blot overlay or Far Western Blot. In *Protein-Protein Interactions, Methods and Application, Methods in Molecular Biology,* vol. 1st, pp. 167-174. Totowa, N.J.: Humana Press.

Hamajima, N., Matsuda, K., Sakata, S., Tamaki, N., Sasaki, M. and Nonaka, M. (1996). A novel gene family defined by human dihydropyrimidinase and three related proteins with differential tissue distribution. *Gene.* 180, 157-163.

Hansen, M. B., Nielsen, S. E. and Berg, K. (1989). Re-examination and further development of a precise and rapid dye method for measuring cell growth/cell kill. *Journal of Immunological Methods* 119, 203-10.

Hardingham, G. E. and Bading, H. (2002). Coupling of extrasynaptic NMDA receptors to a CREB shut-off pathway is developmentally regulated. *Biochimica et Biophysica Acta* 1600, 148-53.

Hardingham, G. E., Fukunaga, Y. and Bading, H. (2002). Extrasynaptic NMDARs oppose synaptic NMDARs by triggering CREB shut-off and cell death pathways. *Nature Neuroscience* 5, 405-14.

Hardy, J. and Selkoe, D. J. (2002). The amyloid hypothesis of Alzheimer's disease: progress and problems on the road to therapeutics. *Science* 297, 353-6.

Hata, Y., Slaughter, C. A. and Sudhof, T. C. (1993). Synaptic vesicle fusion complex contains unc-18 homologue bound to syntaxin. *Nature* 366, 347-51.

Hatakeyama, S., Wakamori, M., Ino, M., Miyamoto, N., Takahashi, E., Yoshinaga, T., Sawada, K., Imoto, K., Tanaka, I., Yoshizawa, T. et al. (2001). Differential nociceptive responses in mice lacking the alpha(1B) subunit of N-type Ca(2+) channels. *Neuroreport* 12, 2423-7.

Haws, C. M., Slesinger, P. A. and Lansman, J. B. (1993). Dihydropyridine- and omega-conotoxin-sensitive Ca2+ currents in cerebellar neurons: persistent block of L-type channels by a pertussis toxin-sensitive G-protein. *Journal of Neuroscience* 13, 1148-56.

Heblich, F., Tran Van Minh, A., Hendrich, J., Watschinger, K. and Dolphin, A. C. (2008). Time course and specificity of the pharmacological disruption of the trafficking of voltage-gated calcium channels by gabapentin. *Channels (Austin)* 2, 4-9.

Hedgecock, E. M., Culotti, J. G., Thomson, J. N. and Perkins, L. A. (1985). Axonal guidance mutants of Caenorhabditis elegans identified by filling sensory neurons with fluorescein dyes. *Developmental Biology* 111, 158-70.

Hendrich, J., Van Minh, A. T., Heblich, F., Nieto-Rostro, M., Watschinger, K., Striessnig, J., Wratten, J., Davies, A. and Dolphin, A. C. (2008). Pharmacological disruption of calcium channel trafficking by the alpha2delta ligand gabapentin. *Proceedings of the National Academy of Sciences of the United States of America* 105, 3628-33.

Hensley, K., Christov, A., Kamat, S., Zhang, X. C., Jackson, K. W., Snow, S. and Post, J. (2010). Proteomic identification of binding partners for the brain metabolite lanthionine ketimine (LK) and documentation of LK effects on microglia and motoneuron cell cultures. *Journal of Neuroscience* 30, 2979-88.

Herlitze, S., Hockerman, G. H., Scheuer, T. and Catterall, W. A. (1997). Molecular determinants of inactivation and G protein modulation in the intracellular loop connecting domains I and II of the calcium channel alpha1A subunit. *Proceedings of the National Academy of Sciences of the United States of America* 94, 1512-6.

Hess, P., Lansman, J. B. and Tsien, R. W. (1984). Different modes of Ca channel gating behaviour favoured by dihydropyridine Ca agonists and antagonists. *Nature* 311, 538-44.

Heuser, J. E., Reese, T. S., Dennis, M. J., Jan, Y., Jan, L. and Evans, L. (1979). Synaptic vesicle exocytosis captured by quick freezing and correlated with quantal transmitter release. *Journal of Cell Biology* 81, 275-300.

Hirning, L. D., Fox, A. P., McCleskey, E. W., Olivera, B. M., Thayer, S. A., Miller, R. J. and Tsien, R. W. (1988). Dominant role of N-type Ca2+ channels in evoked release of norepinephrine from sympathetic neurons. *Science* 239, 57-61.

Hodgkin, A. L. and Keynes, R. D. (1957). Movements of labelled calcium in squid giant axons. *J Physiol* 138, 253-81.

Holm, L. and Sander, C. (1997). An evolutionary treasure: unification of a broad set of amidohydrolases related to urease. *Proteins* 28, 72-82.

Hong, S. C., Goto, Y., Lanzino, G., Soleau, S., Kassell, N. F. and Lee, K. S. (1994). Neuroprotection with a calpain inhibitor in a model of focal cerebral ischemia. *Stroke* 25, 663-9.

Hou, S. T., Jiang, S. X., Aylsworth, A., Ferguson, G., Slinn, J., Hu, H., Leung, T., Kappler, J. and Kaibuchi, K. (2009). CaMKII phosphorylates collapsin response mediator protein 2 and modulates axonal damage during glutamate excitotoxicity. *Journal of Neurochemistry*.

Hou, S. T., Jiang, S. X., Desbois, A., Huang, D., Kelly, J., Tessier, L., Karchewski, L. and Kappler, J. (2006). Calpain-cleaved collapsin response mediator protein-3 induces neuronal death after glutamate toxicity and cerebral ischemia. *Journal of Neuroscience* 26, 2241-9.

Hu, L. Y., Ryder, T. R., Rafferty, M. F., Cody, W. L., Lotarski, S. M., Miljanich, G. P., Millerman, E., Rock, D. M., Song, Y., Stoehr, S. J. et al. (1999a). N,N-dialkyl-dipeptidylamines as novel N-type calcium channel blockers. *Bioorganic and Medicinal Chemistry Letters* 9, 907-12.

Hu, L. Y., Ryder, T. R., Rafferty, M. F., Feng, M. R., Lotarski, S. M., Rock, D. M., Sinz, M., Stoehr, S. J., Taylor, C. P., Weber, M. L. et al. (1999b). Synthesis of a series of 4-benzyloxyaniline analogues as neuronal N-type calcium channel blockers with improved anticonvulsant and analgesic properties. *Journal of Medicinal Chemistry* 42, 4239-49.

Hu, L. Y., Ryder, T. R., Rafferty, M. F., Siebers, K. M., Malone, T., Chatterjee, A., Feng, M. R., Lotarski, S. M., Rock, D. M., Stoehr, S. J. et al. (2000). Neuronal N-type calcium channel blockers: a series of 4-piperidinylaniline analogs with analgesic activity. *Drug Design and Discovery* 17, 85-93.

Huang, Y., Lu, W., Ali, D. W., Pelkey, K. A., Pitcher, G. M., Lu, Y. M., Aoto, H., Roder, J. C., Sasaki, T., Salter, M. W. et al. (2001). CAKbeta/Pyk2 kinase is a signaling link for induction of long-term potentiation in CA1 hippocampus. *Neuron* 29, 485-96.

Huettner, J. E. and Bean, B. P. (1988). Block of N-methyl-D-aspartate-activated current by the anticonvulsant MK-801: selective binding to open channels. *Proceedings of the National Academy of Sciences of the United States of America* 85, 1307-11.

Husi, H., Ward, M. A., Choudhary, J. S., Blackstock, W. P. and Grant, S. G. (2000). Proteomic analysis of NMDA receptor-adhesion protein signaling complexes. *Nature Neuroscience* 3, 661-9.

Huttner, W. B., Schiebler, W., Greengard, P. and De Camilli, P. (1983). Synapsin I (protein I), a nerve terminal-specific phosphoprotein. III. Its association with synaptic vesicles studied in a highly purified synaptic vesicle preparation. *Journal of Cell Biology* 96, 1374-88.

Ikonomidou, C., Stefovska, V. and Turski, L. (2000). Neuronal death enhanced by N-methyl-D-aspartate antagonists. *Proceedings of the National Academy of Sciences of the United States of America* 97, 12885-90.

Ikonomidou, C. and Turski, L. (2002). Why did NMDA receptor antagonists fail clinical trials for stroke and traumatic brain injury? *Lancet Neurol.* 1, 383-386.

Inagaki, H., Kato, Y., Hamajima, N., Nonaka, M., Sasaki, M. and Eimoto, T. (2000). Differential expression of dihydropyrimidinase-related protein genes in developing and adult enteric nervous system. *Histochemistry and Cell Biology* 113, 37-41.

Inagaki, N., Chihara, K., Arimura, N., Menager, C., Kawano, Y., Matsuo, N., Nishimura, T., Amano, M. and Kaibuchi, K. (2001). CRMP-2 induces axons in cultured hippocampal neurons. *Nature Neuroscience* 4, 781-2.

Ip, J. P., Shi, L., Chen, Y., Itoh, Y., Fu, W. Y., Betz, A., Yung, W. H., Gotoh, Y., Fu, A. K. and Ip, N. Y. (2012). alpha2-chimaerin controls neuronal migration and functioning of the cerebral cortex through CRMP-2. *Nature Neuroscience* 15, 39-47.

Ishii, T., Moriyoshi, K., Sugihara, H., Sakurada, K., Kadotani, H., Yokoi, M., Akazawa, C., Shigemoto, R., Mizuno, N., Masu, M. et al. (1993). Molecular characterization of the family of the N-methyl-D-aspartate receptor subunits. *Journal of Biological Chemistry* 268, 2836-43.

Iwasaki, S., Momiyama, A., Uchitel, O. D. and Takahashi, T. (2000). Developmental changes in calcium channel types mediating central synaptic transmission. *Journal of Neuroscience* 20, 59-65.

Iwasaki, S. and Takahashi, T. (1998). Developmental changes in calcium channel types mediating synaptic transmission in rat auditory brainstem. *J Physiol* 509 (Pt 2), 419-23.

Jain, K. K. (2000). Evaluation of memantine for neuroprotection in dementia. *Expert Opin Investig Drugs* 9, 1397-406.

Jarvis, S. E., Magga, J. M., Beedle, A. M., Braun, J. E. and Zamponi, G. W. (2000). G protein modulation of N-type calcium channels is facilitated by physical interactions between syntaxin 1A and Gbetagamma. *Journal of Biological Chemistry* 275, 6388-94.

Jarvis, S. E. and Zamponi, G. W. (2001). Distinct molecular determinants govern syntaxin 1A-mediated inactivation and G-protein inhibition of N-type calcium channels. *Journal of Neuroscience* 21, 2939-48.

Jiang, S. X., Kappler, J., Zurakowski, B., Desbois, A., Aylsworth, A. and Hou, S. T. (2007). Calpain cleavage of collapsin response mediator proteins in ischemic mouse brain. *European Journal of Neuroscience* 26, 801-9.

Jiang, X., Tian, F., Mearow, K., Okagaki, P., Lipsky, R. H. and Marini, A. M. (2005). The excitoprotective effect of N-methyl-D-aspartate receptors is mediated by a brain-derived neurotrophic factor autocrine loop in cultured hippocampal neurons. *Journal of Neurochemistry* 94, 713-22.

Johnson, J. W. and Ascher, P. (1987). Glycine potentiates the NMDA response in cultured mouse brain neurons. *Nature* 325, 529-31.

Jones, L. P., DeMaria, C. D. and Yue, D. T. (1999). N-type calcium channel inactivation probed by gating-current analysis. *Biophysical Journal* 76, 2530-52.

Jones, L. P., Patil, P. G., Snutch, T. P. and Yue, D. T. (1997a). G-protein modulation of N-type calcium channel gating current in human embryonic kidney cells (HEK 293). *J Physiol* 498 (Pt 3), 601-10.

Jones, O. T., Bernstein, G. M., Jones, E. J., Jugloff, D. G., Law, M., Wong, W. and Mills, L. R. (1997b). N-Type calcium channels in the developing rat hippocampus: subunit, complex, and regional expression. *Journal of Neuroscience* 17, 6152-64.

Jones, S. W. and Marks, T. N. (1989). Calcium currents in bullfrog sympathetic neurons. II. Inactivation. *Journal of General Physiology* 94, 169-82.

Joseph, E. K., Chen, X., Khasar, S. G. and Levine, J. D. (2004). Novel mechanism of enhanced nociception in a model of AIDS therapy-induced painful peripheral neuropathy in the rat. *Pain.* 107, 147-158.

Joshi, H. C. and Baas, P. W. (1993). A new perspective on microtubules and axon growth. *Journal of Cell Biology* 121, 1191-6.

Joshi, I. and Taylor, C. P. (2006). Pregabalin action at a model synapse: binding to presynaptic calcium channel alpha2-delta subunit reduces neurotransmission in mice. *European Journal of Pharmacology* 553, 82-8.

Kamata, T., Daar, I. O., Subleski, M., Copeland, T., Kung, H. F. and Xu, R. H. (1998). Xenopus CRMP-2 is an early response gene to neural induction. *Brain Research. Molecular Brain Research* 57, 201-10.

Kammermeier, P. J. and Jones, S. W. (1997). High-voltage-activated calcium currents in neurons acutely isolated from the ventrobasal nucleus of the rat thalamus. *Journal of Neurophysiology* 77, 465-75.

Kaneko, T., Li, L. and Li, S. S. (2008). The SH3 domain--a family of versatile peptide- and protein-recognition module. *Frontiers in Bioscience* 13, 4938-52.

Kang, M. G. and Campbell, K. P. (2003). Gamma subunit of voltage-activated calcium channels. *Journal of Biological Chemistry* 278, 21315-8.

Kang, M. G., Chen, C. C., Felix, R., Letts, V. A., Frankel, W. N., Mori, Y. and Campbell, K. P. (2001). Biochemical and biophysical evidence for gamma 2 subunit association with neuronal voltage-activated Ca2+ channels. *Journal of Biological Chemistry* 276, 32917-24.

Kasai, H., Aosaki, T. and Fukuda, J. (1987). Presynaptic Ca-antagonist omega-conotoxin irreversibly blocks N-type Ca-channels in chick sensory neurons. *Neurosci.Res.* 4, 228-235.

Katayama, Y., Becker, D. P., Tamura, T. and Hovda, D. A. (1990). Massive increases in extracellular potassium and the indiscriminate release of glutamate following concussive brain injury. *Journal of Neurosurgery* 73, 889-900.

Katz, B. and Miledi, R. (1965a). The Effect of Calcium on Acetylcholine Release from Motor Nerve Terminals. *Proceedings of the Royal Society of London. Series B: Biological Sciences* 161, 496-503.

Katz, B. and Miledi, R. (1965b). The Measurement of Synaptic Delay, and the Time Course of Acetylcholine Release at the Neuromuscular Junction. *Proceedings of the Royal Society of London. Series B: Biological Sciences* 161, 483-95.

Kawano, Y., Yoshimura, T., Tsuboi, D., Kawabata, S., Kaneko-Kawano, T., Shirataki, H., Takenawa, T. and Kaibuchi, K. (2005). CRMP-2 is involved in kinesin-1-dependent transport of the Sra-1/WAVE1 complex and axon formation. *Molecular and Cellular Biology* 25, 9920-35.

Kennett, S. B., Roberts, J. D. and Olden, K. (2004). Requirement of protein kinase C micro activation and calpain-mediated proteolysis for arachidonic acid-stimulated adhesion of MDA-MB-435 human mammary carcinoma cells to collagen type IV. *Journal of Biological Chemistry* 279, 3300-7.

Kerr, L. M. and Yoshikami, D. (1984). A venom peptide with a novel presynaptic blocking action. *Nature* 308, 282-4.

Khanna, R., Li, Q., Bewersdorf, J. and Stanley, E. F. (2007a). The presynaptic CaV2.2 channel-transmitter release site core complex. *European Journal of Neuroscience* 26, 547-59.

Khanna, R., Li, Q., Schlichter, L. C. and Stanley, E. F. (2007b). The transmitter release-site CaV2.2 channel cluster is linked to an endocytosis coat protein complex. *European Journal of Neuroscience* 26, 560-74.

Khanna, R., Li, Q., Sun, L., Collins, T. J. and Stanley, E. F. (2006a). N type Ca2+ channels and RIM scaffold protein covary at the presynaptic transmitter release face but are components of independent protein complexes. *Neuroscience* 140, 1201-8.

Khanna, R., Sun, L., Li, Q., Guo, L. and Stanley, E. F. (2006b). Long splice variant N type calcium channels are clustered at presynaptic transmitter release sites without modular adaptor proteins. *Neuroscience* 138, 1115-25.

Khanna, R., Zougman, A. and Stanley, E. F. (2007c). A proteomic screen for presynaptic terminal N-type calcium channel (CaV2.2) binding partners. *J Biochem Mol Biol* 40, 302-14.

Khosravani, H., Zhang, Y., Tsutsui, S., Hameed, S., Altier, C., Hamid, J., Chen, L., Villemaire, M., Ali, Z., Jirik, F. R. et al. (2008). Prion protein attenuates excitotoxicity by inhibiting NMDA receptors. *Journal of Cell Biology* 181, 551-65.

Khuong, T. M., Habets, R. L., Slabbaert, J. R. and Verstreken, P. (2010). WASP is activated by phosphatidylinositol-4,5-bisphosphate to restrict synapse growth in a pathway parallel to bone morphogenetic protein signaling. *Proceedings of the National Academy of Sciences of the United States of America* 107, 17379-84.

Kiedrowski, L., Costa, E. and Wroblewski, J. T. (1992). Glutamate receptor agonists stimulate nitric oxide synthase in primary cultures of cerebellar granule cells. *Journal of Neurochemistry* 58, 335-41.

Kim, C., Jeon, D., Kim, Y. H., Lee, C. J., Kim, H. and Shin, H. S. (2009). Deletion of N-type Ca(2+) channel Ca(v)2.2 results in hyperaggressive behaviors in mice. *Journal of Biological Chemistry* 284, 2738-45.

Kim, C., Jun, K., Lee, T., Kim, S. S., McEnery, M. W., Chin, H., Kim, H. L., Park, J. M., Kim, D. K., Jung, S. J. et al. (2001). Altered nociceptive response in mice deficient in the alpha(1B) subunit of the voltage-dependent calcium channel. *Mol.Cell Neurosci.* 18, 235-245.

Kim, E., Cho, K. O., Rothschild, A. and Sheng, M. (1996). Heteromultimerization and NMDA receptor-clustering activity of Chapsyn-110, a member of the PSD-95 family of proteins. *Neuron* 17, 103-13.

Kimura, T., Watanabe, H., Iwamatsu, A. and Kaibuchi, K. (2005). Tubulin and CRMP-2 complex is transported via Kinesin-1. *Journal of Neurochemistry* 93, 1371-82.

Kisilevsky, A. E., Mulligan, S. J., Altier, C., Iftinca, M. C., Varela, D., Tai, C., Chen, L., Hameed, S., Hamid, J., Macvicar, B. A. et al. (2008). D1 receptors physically interact with N-type calcium channels to regulate channel distribution and dendritic calcium entry. *Neuron* 58, 557-70.

Kisilevsky, A. E. and Zamponi, G. W. (2008a). D2 dopamine receptors interact directly with N-type calcium channels and regulate channel surface expression levels. *Channels (Austin)* 2, 269-77.

Kisilevsky, A. E. and Zamponi, G. W. (2008b). Presynaptic calcium channels: structure, regulators, and blockers. *Handb Exp Pharmacol*, 45-75.

Kiyonaka, S., Wakamori, M., Miki, T., Uriu, Y., Nonaka, M., Bito, H., Beedle, A. M., Mori, E., Hara, Y., De Waard, M. et al. (2007). RIM1 confers sustained activity and neurotransmitter vesicle anchoring to presynaptic Ca2+ channels. *Nature Neuroscience* 10, 691-701.

Klauck, T. M., Faux, M. C., Labudda, K., Langeberg, L. K., Jaken, S. and Scott, J. D. (1996). Coordination of three signaling enzymes by AKAP79, a mammalian scaffold protein. *Science* 271, 1589-92.

Kleckner, N. W. and Dingledine, R. (1988). Requirement for glycine in activation of NMDA-receptors expressed in Xenopus oocytes. *Science* 241, 835-7.

Kodama, Y., Murakumo, Y., Ichihara, M., Kawai, K., Shimono, Y. and Takahashi, M. (2004). Induction of CRMP-2 by GDNF and analysis of the CRMP-2 promoter region. *Biochemical and Biophysical Research Communications* 320, 108-15.

Kohr, G. (2006). NMDA receptor function: subunit composition versus spatial distribution. *Cell and Tissue Research* 326, 439-46.

Kopec, C. D., Li, B., Wei, W., Boehm, J. and Malinow, R. (2006). Glutamate receptor exocytosis and spine enlargement during chemically induced long-term potentiation. *Journal of Neuroscience* 26, 2000-9.

Koplas, P. A., Rosenberg, R. L. and Oxford, G. S. (1997). The role of calcium in the desensitization of capsaicin responses in rat dorsal root ganglion neurons. *J.Neurosci.* 17, 3525-3537.

Kornau, H. C., Schenker, L. T., Kennedy, M. B. and Seeburg, P. H. (1995). Domain interaction between NMDA receptor subunits and the postsynaptic density protein PSD-95. *Science* 269, 1737-40.

Kowara, R., Chen, Q., Milliken, M. and Chakravarthy, B. (2005). Calpain-mediated truncation of dihydropyrimidinase-like 3 protein (DPYSL3) in response to NMDA and H2O2 toxicity. *J.Neurochem.* 95, 466-474.

Kuryatov, A., Laube, B., Betz, H. and Kuhse, J. (1994). Mutational analysis of the glycine-binding site of the NMDA receptor: structural similarity with bacterial amino acid-binding proteins. *Neuron* 12, 1291-300.

LaBonne, C. and Bronner-Fraser, M. (1999). Molecular mechanisms of neural crest formation. *Annual Review of Cell and Developmental Biology* 15, 81-112.

LaFerla, F. M. (2002). Calcium dyshomeostasis and intracellular signalling in Alzheimer's disease. *Nat Rev Neurosci* 3, 862-72.

Lai, M., Wang, F., Rohan, J. G., Maeno-Hikichi, Y., Chen, Y., Zhou, Y., Gao, G., Sather, W. A. and Zhang, J. F. (2005). A tctex1-Ca2+ channel complex for selective surface expression of Ca2+ channels in neurons. *Nat.Neurosci.* 8, 435-442.

LaMotte, R. H., Friedman, R. M., Lu, C., Khalsa, P. S. and Srinivasan, M. A. (1998). Raised object on a planar surface stroked across the fingerpad: responses of cutaneous mechanoreceptors to shape and orientation. *J.Neurophysiol.* 80, 2446-2466.

Lan, J. Y., Skeberdis, V. A., Jover, T., Grooms, S. Y., Lin, Y., Araneda, R. C., Zheng, X., Bennett, M. V. and Zukin, R. S. (2001). Protein kinase C modulates NMDA receptor trafficking and gating. *Nature Neuroscience* 4, 382-90.

Laube, B., Hirai, H., Sturgess, M., Betz, H. and Kuhse, J. (1997). Molecular determinants of agonist discrimination by NMDA receptor subunits: analysis of the glutamate binding site on the NR2B subunit. *Neuron* 18, 493-503.

Lavezzari, G., McCallum, J., Lee, R. and Roche, K. W. (2003). Differential binding of the AP-2 adaptor complex and PSD-95 to the C-terminus of the NMDA receptor subunit NR2B regulates surface expression. *Neuropharmacology* 45, 729-37.

Lee, J., Kim, C. H., Simon, D. K., Aminova, L. R., Andreyev, A. Y., Kushnareva, Y. E., Murphy, A. N., Lonze, B. E., Kim, K. S., Ginty, D. D. et al. (2005). Mitochondrial cyclic AMP response element-binding protein (CREB) mediates mitochondrial gene expression and neuronal survival. *Journal of Biological Chemistry* 280, 40398-401.

Lee, M. S., Kwon, Y. T., Li, M., Peng, J., Friedlander, R. M. and Tsai, L. H. (2000). Neurotoxicity induces cleavage of p35 to p25 by calpain. *Nature* 405, 360-4.

Lee, S., Kim, J. H., Lee, C. S., Kim, Y., Heo, K., Ihara, Y., Goshima, Y., Suh, P. G. and Ryu, S. H. (2002). Collapsin response mediator protein-2 inhibits neuronal phospholipase D(2) activity by direct interaction. *Journal of Biological Chemistry* 277, 6542-9.

Leenders, A. G., Lin, L., Huang, L. D., Gerwin, C., Lu, P. H. and Sheng, Z. H. (2008). The role of MAP1A light chain 2 in synaptic surface retention of CaV2.2 channels in hippocampal neurons. *Journal of Neuroscience* 28, 11333-46.

Leitch, B., Shevtsova, O., Guevremont, D. and Williams, J. (2009). Loss of calcium channels in the cerebellum of the ataxic and epileptic stargazer mutant mouse. *Brain Research* 1279, 156-67.

Letts, V. A., Felix, R., Biddlecome, G. H., Arikkath, J., Mahaffey, C. L., Valenzuela, A., Bartlett, F. S., 2nd, Mori, Y., Campbell, K. P. and Frankel, W. N. (1998). The mouse stargazer gene encodes a neuronal Ca2+-channel gamma subunit. *Nature Genetics* 19, 340-7.

Letts, V. A., Kang, M. G., Mahaffey, C. L., Beyer, B., Tenbrink, H., Campbell, K. P. and Frankel, W. N. (2003). Phenotypic heterogeneity in the stargazin allelic series. *Mamm.Genome.* 14, 506-513.

Leung, T., Ng, Y., Cheong, A., Ng, C. H., Tan, I., Hall, C. and Lim, L. (2002). p80 ROKalpha binding protein is a novel splice variant of CRMP-1 which associates with CRMP-2 and modulates RhoA-induced neuronal morphology. *FEBS Letters* 532, 445-9.

Leveque, C., el Far, O., Martin-Moutot, N., Sato, K., Kato, R., Takahashi, M. and Seagar, M. J. (1994). Purification of the N-type calcium channel associated with syntaxin and synaptotagmin. A complex implicated in synaptic vesicle exocytosis. *Journal of Biological Chemistry* 269, 6306-12.

Leveque, C., Hoshino, T., David, P., Shoji-Kasai, Y., Leys, K., Omori, A., Lang, B., el Far, O., Sato, K., Martin-Moutot, N. et al. (1992). The synaptic vesicle protein synaptotagmin associates with calcium channels and is a putative Lambert-Eaton myasthenic syndrome antigen. *Proceedings of the National Academy of Sciences of the United States of America* 89, 3625-9.

Li, C. Y., Zhang, X. L., Matthews, E. A., Li, K. W., Kurwa, A., Boroujerdi, A., Gross, J., Gold, M. S., Dickenson, A. H., Feng, G. et al. (2006a). Calcium channel alpha2delta1 subunit mediates spinal hyperexcitability in pain modulation. *Pain* 125, 20-34.

Li, D., Wang, F., Lai, M., Chen, Y. and Zhang, J. F. (2005). A protein phosphatase 2calpha-Ca2+ channel complex for dephosphorylation of neuronal Ca2+ channels phosphorylated by protein kinase C. *Journal of Neuroscience* 25, 1914-23.

Li, T., Chalifour, L. E. and Paudel, H. K. (2007a). Phosphorylation of protein phosphatase 1 by cyclin-dependent protein kinase 5 during nerve growth factor-induced PC12 cell differentiation. *The Journal of biological chemistry* 282, 6619-28.

Li, Y., Wu, Y., Li, R. and Zhou, Y. (2007b). The role of 14-3-3 dimerization in its modulation of the CaV2.2 channel. *Channels (Austin)* 1, 1-2.

Li, Y., Wu, Y. and Zhou, Y. (2006b). Modulation of inactivation properties of CaV2.2 channels by 14-3-3 proteins. *Neuron* 51, 755-71.

Liang, H., DeMaria, C. D., Erickson, M. G., Mori, M. X., Alseikhan, B. A. and Yue, D. T. (2003). Unified mechanisms of Ca2+ regulation across the Ca2+ channel family. *Neuron* 39, 951-60.

Liao, G. Y., Wagner, D. A., Hsu, M. H. and Leonard, J. P. (2001). Evidence for direct protein kinase-C mediated modulation of N-methyl-D-aspartate receptor current. *Molecular Pharmacology* 59, 960-4.

Lin, Y. L. and Hsueh, Y. P. (2008). Neurofibromin interacts with CRMP-2 and CRMP-4 in rat brain. *Biochemical and Biophysical Research Communications* 369, 747-52.

Lin, Y. Z., Yao, S. Y., Veach, R. A., Torgerson, T. R. and Hawiger, J. (1995). Inhibition of nuclear translocation of transcription factor NF-kappa B by a synthetic peptide containing a cell membrane-permeable motif and nuclear localization sequence. *Journal of Biological Chemistry* 270, 14255-8.

Liu, W., Zhou, X. W., Liu, S., Hu, K., Wang, C., He, Q. and Li, M. (2009). Calpain-truncated CRMP-3 and -4 contribute to potassium deprivation-induced apoptosis of cerebellar granule neurons. *Proteomics* 9, 3712-28.

Liu, Y., Wong, T. P., Aarts, M., Rooyakkers, A., Liu, L., Lai, T. W., Wu, D. C., Lu, J., Tymianski, M., Craig, A. M. et al. (2007). NMDA receptor subunits have differential roles in mediating excitotoxic neuronal death both in vitro and in vivo. *Journal of Neuroscience* 27, 2846-57.

Llinas, R., Steinberg, I. Z. and Walton, K. (1976). Presynaptic calcium currents and their relation to synaptic transmission: voltage clamp study in squid giant synapse and theoretical model for the calcium gate. *Proceedings of the National Academy of Sciences of the United States of America* 73, 2918-22.

Llinas, R., Steinberg, I. Z. and Walton, K. (1981). Relationship between presynaptic calcium current and postsynaptic potential in squid giant synapse. *Biophysical Journal* 33, 323-51.

Lorenzon, N. M. and Foehring, R. C. (1995). Characterization of pharmacologically identified voltage-gated calcium channel currents in acutely isolated rat neocortical neurons. II. Postnatal development. *Journal of Neurophysiology* 73, 1443-51.

Lu, W. Y., Xiong, Z. G., Lei, S., Orser, B. A., Dudek, E., Browning, M. D. and MacDonald, J. F. (1999). G-protein-coupled receptors act via protein kinase C and Src to regulate NMDA receptors. *Nature Neuroscience* 2, 331-8.

Lubec, G., Nonaka, M., Krapfenbauer, K., Gratzer, M., Cairns, N. and Fountoulakis, M. (1999). Expression of the dihydropyrimidinase related protein 2 (DRP-2) in Down syndrome and Alzheimer's disease brain is downregulated at the mRNA and dysregulated at the protein level. *Journal of Neural Transmission. Supplementum* 57, 161-77.

Ludwig, A., Flockerzi, V. and Hofmann, F. (1997). Regional expression and cellular localization of the alpha1 and beta subunit of high voltage-activated calcium channels in rat brain. *Journal of Neuroscience* 17, 1339-49.

Lukyanetz, E. A., Shkryl, V. M. and Kostyuk, P. G. (2002). Selective blockade of N-type calcium channels by levetiracetam. *Epilepsia* 43, 9-18.

Luscher, C., Xia, H., Beattie, E. C., Carroll, R. C., von Zastrow, M., Malenka, R. C. and Nicoll, R. A. (1999). Role of AMPA receptor cycling in synaptic transmission and plasticity. *Neuron* 24, 649-58.

Ma, C., Shu, Y., Zheng, Z., Chen, Y., Yao, H., Greenquist, K. W., White, F. A. and LaMotte, R. H. (2003). Similar electrophysiological changes in axotomized and neighboring intact dorsal root ganglion neurons. *J.Neurophysiol.* 89, 1588-1602.

Maeno-Hikichi, Y., Chang, S., Matsumura, K., Lai, M., Lin, H., Nakagawa, N., Kuroda, S. and Zhang, J. F. (2003). A PKC epsilon-ENH-channel complex specifically modulates N-type Ca2+ channels. *Nature Neuroscience* 6, 468-75.

Magga, J. M., Jarvis, S. E., Arnot, M. I., Zamponi, G. W. and Braun, J. E. (2000). Cysteine string protein regulates G protein modulation of N-type calcium channels. *Neuron* 28, 195-204.

Maggi, C. A., Giuliani, S., Santicioli, P., Tramontana, M. and Meli, A. (1990a). Effect of omega conotoxin on reflex responses mediated by activation of capsaicin-sensitive nerves of the rat urinary bladder and peptide release from the rat spinal cord. *Neuroscience* 34, 243-50.

Maggi, C. A., Tramontana, M., Cecconi, R. and Santicioli, P. (1990b). Neurochemical evidence for the involvement of N-type calcium channels in transmitter secretion from peripheral endings of sensory nerves in guinea pigs. *Neuroscience Letters* 114, 203-6.

Majava, V., Loytynoja, N., Chen, W. Q., Lubec, G. and Kursula, P. (2008). Crystal and solution structure, stability and post-translational modifications of collapsin response mediator protein 2. *FEBS J* 275, 4583-96.

Malinow, R., Schulman, H. and Tsien, R. W. (1989). Inhibition of postsynaptic PKC or CaMKII blocks induction but not expression of LTP. *Science.* 245, 862-866.

Malmberg, A. B. and Yaksh, T. L. (1994). Voltage-sensitive calcium channels in spinal nociceptive processing: blockade of N- and P-type channels inhibits formalin-induced nociception. *Journal of Neuroscience* 14, 4882-90.

Marangoudakis, S., Andrade, A., Helton, T. D., Denome, S., Castiglioni, A. J. and Lipscombe, D. (2012). Differential Ubiquitination and Proteasome Regulation of CaV2.2 N-Type Channel Splice Isoforms. *Journal of Neuroscience* 32, 10365-9.

Marini, A. M. and Paul, S. M. (1992). N-methyl-D-aspartate receptor-mediated neuroprotection in cerebellar granule cells requires new RNA and protein synthesis. *Proceedings of the National Academy of Sciences of the United States of America* 89, 6555-9.

Martel, M. A., Soriano, F. X., Baxter, P., Rickman, C., Duncan, R., Wyllie, D. J. and Hardingham, G. E. (2009). Inhibiting pro-death NMDA receptor signaling dependent on the NR2 PDZ ligand may not affect synaptic function or synaptic NMDA receptor signaling to gene expression. *Channels (Austin)* 3, 12-5.

Martin, H., Rostas, J., Patel, Y. and Aitken, A. (1994). Subcellular localisation of 14-3-3 isoforms in rat brain using specific antibodies. *Journal of Neurochemistry* 63, 2259-65.

Matthew, W. D., Tsavaler, L. and Reichardt, L. F. (1981). Identification of a synaptic vesicle-specific membrane protein with a wide distribution in neuronal and neurosecretory tissue. *Journal of Cell Biology* 91, 257-69.

Matus, A. I. and Taff-Jones, D. H. (1978). Morphology and molecular composition of isolated postsynaptic junctional structures. *Proceedings of the Royal Society of London. Series B: Biological Sciences* 203, 135-51.

Maximov, A. and Bezprozvanny, I. (2002). Synaptic targeting of N-type calcium channels in hippocampal neurons. *Journal of Neuroscience* 22, 6939-52.

Maximov, A., Sudhof, T. C. and Bezprozvanny, I. (1999). Association of neuronal calcium channels with modular adaptor proteins. *Journal of Biological Chemistry* 274, 24453-6.

McIlhinney, R. A., Le Bourdelles, B., Molnar, E., Tricaud, N., Streit, P. and Whiting, P. J. (1998). Assembly intracellular targeting and cell surface expression of the human N-methyl-D-aspartate receptor subunits NR1a and NR2A in transfected cells. *Neuropharmacology* 37, 1355-67.

McQuarrie, I. G., Grafstein, B. and Gershon, M. D. (1977). Axonal regeneration in the rat sciatic nerve: effect of a conditioning lesion and of dbcAMP. *Brain Research* 132, 443-53.

Meir, A., Ginsburg, S., Butkevich, A., Kachalsky, S. G., Kaiserman, I., Ahdut, R., Demirgoren, S. and Rahamimoff, R. (1999). Ion channels in presynaptic nerve terminals and control of transmitter release. *Physiological Reviews* 79, 1019-88.

Miesenbock, G., De Angelis, D. A. and Rothman, J. E. (1998). Visualizing secretion and synaptic transmission with pH-sensitive green fluorescent proteins. *Nature* 394, 192-5.

Miller, L. C., Swayne, L. A., Chen, L., Feng, Z. P., Wacker, J. L., Muchowski, P. J., Zamponi, G. W. and Braun, J. E. (2003a). Cysteine string protein (CSP) inhibition of N-type calcium channels is blocked by mutant huntingtin. *Journal of Biological Chemistry* 278, 53072-81.

Miller, L. C., Swayne, L. A., Kay, J. G., Feng, Z. P., Jarvis, S. E., Zamponi, G. W. and Braun, J. E. (2003b). Molecular determinants of cysteine string protein modulation of N-type calcium channels. *Journal of Cell Science* 116, 2967-74.

Mines, G. R. (1911). On the replacement of calcium in certain neuro-muscular mechanisms by allied substances. *J Physiol* 42, 251-66.

Minturn, J. E., Fryer, H. J., Geschwind, D. H. and Hockfield, S. (1995a). TOAD-64, a gene expressed early in neuronal differentiation in the rat, is related to unc-33, a C. elegans gene involved in axon outgrowth. *Journal of Neuroscience* 15, 6757-66.

Minturn, J. E., Geschwind, D. H., Fryer, H. J. and Hockfield, S. (1995b). Early postmitotic neurons transiently express TOAD-64, a neural specific protein. *Journal of Comparative Neurology* 355, 369-79.

Mintz, I. M., Sabatini, B. L. and Regehr, W. G. (1995). Calcium control of transmitter release at a cerebellar synapse. *Neuron* 15, 675-88.

Mintz, I. M., Venema, V. J., Swiderek, K. M., Lee, T. D., Bean, B. P. and Adams, M. E. (1992). P-type calcium channels blocked by the spider toxin omega-Aga-IVA. *Nature* 355, 827-9.

Mitsui, N., Inatome, R., Takahashi, S., Goshima, Y., Yamamura, H. and Yanagi, S. (2002). Involvement of Fes/Fps tyrosine kinase in semaphorin3A signaling. *EMBO Journal* 21, 3274-3285.

Mizuta, I., Katayama, M., Watanabe, M., Mishina, M. and Ishii, K. (1998). Developmental expression of NMDA receptor subunits and the emergence of glutamate neurotoxicity in primary cultures of murine cerebral cortical neurons. *Cellular and Molecular Life Sciences* 54, 721-5.

Mochida, S., Saisu, H., Kobayashi, H. and Abe, T. (1995). Impairment of syntaxin by botulinum neurotoxin C1 or antibodies inhibits acetylcholine release but not Ca2+ channel activity. *Neuroscience* 65, 905-15.

Mochida, S., Sheng, Z. H., Baker, C., Kobayashi, H. and Catterall, W. A. (1996). Inhibition of neurotransmission by peptides containing the synaptic protein interaction site of N-type Ca2+ channels. *Neuron* 17, 781-8.

Mochida, S., Westenbroek, R. E., Yokoyama, C. T., Zhong, H., Myers, S. J., Scheuer, T., Itoh, K. and Catterall, W. A. (2003). Requirement for the synaptic protein interaction site for reconstitution of synaptic transmission by P/Q-type calcium channels. *Proceedings of the National Academy of Sciences of the United States of America* 100, 2819-24.

Morinaka, A., Yamada, M., Itofusa, R., Funato, Y., Yoshimura, Y., Nakamura, F., Yoshimura, T., Kaibuchi, K., Goshima, Y., Hoshino, M. et al. (2011). Thioredoxin mediates oxidation-dependent phosphorylation of CRMP2 and growth cone collapse. *Sci Signal* 4, ra26.

Moriyoshi, K., Masu, M., Ishii, T., Shigemoto, R., Mizuno, N. and Nakanishi, S. (1991). Molecular cloning and characterization of the rat NMDA receptor. *Nature* 354, 31-7.

Mothet, J. P., Parent, A. T., Wolosker, H., Brady, R. O., Jr., Linden, D. J., Ferris, C. D., Rogawski, M. A. and Snyder, S. H. (2000). D-serine is an endogenous ligand for the glycine site of the N-methyl-D-aspartate receptor. *Proceedings of the National Academy of Sciences of the United States of America* 97, 4926-31.

Muir, K. W. (2006). Glutamate-based therapeutic approaches: clinical trials with NMDA antagonists. *Curr Opin Pharmacol* 6, 53-60.

Muller, C. S., Haupt, A., Bildl, W., Schindler, J., Knaus, H. G., Meissner, M., Rammner, B., Striessnig, J., Flockerzi, V., Fakler, B. et al. (2010). Quantitative proteomics of the Cav2 channel nano-environments in the mammalian brain. *Proceedings of the National Academy of Sciences of the United States of America* 107, 14950-7.

Nakamura, M., Saatman, K. E., Galvin, J. E., Scherbel, U., Raghupathi, R., Trojanowski, J. Q. and McIntosh, T. K. (1999). Increased vulnerability of NFH-LacZ transgenic mouse to traumatic brain injury-induced behavioral deficits and cortical damage. *Journal of Cerebral Blood Flow and Metabolism* 19, 762-70.

Nebe, J., Vanegas, H. and Schaible, H. G. (1998). Spinal application of omega-conotoxin GVIA, an N-type calcium channel antagonist, attenuates enhancement of dorsal spinal neuronal responses caused by intra-articular injection of mustard oil in the rat. *Experimental Brain Research* 120, 61-9.

Neugebauer, V., Vanegas, H., Nebe, J., Rumenapp, P. and Schaible, H. G. (1996). Effects of N- and L-type calcium channel antagonists on the responses of nociceptive spinal cord neurons to mechanical stimulation of the normal and the inflamed knee joint. *Journal of Neurophysiology* 76, 3740-9.

Nguyen, D., Deng, P., Matthews, E. A., Kim, D. S., Feng, G., Dickenson, A. H., Xu, Z. C. and Luo, Z. D. (2009). Enhanced pre-synaptic glutamate release in deep-dorsal horn contributes to calcium channel alpha-2-delta-1 protein-mediated spinal sensitization and behavioral hypersensitivity. *Mol Pain* 5, 6.

Nicholls, D. G. (2004). Mitochondrial dysfunction and glutamate excitotoxicity studied in primary neuronal cultures. *Curr Mol Med* 4, 149-77.

Nichols, R. A. and Suplick, G. R. (1996). Rapid chelation of calcium entering isolated rat brain nerve terminals during stimulation inhibits neurotransmitter release. *Neuroscience Letters* 211, 135-7.

Niethammer, M., Kim, E. and Sheng, M. (1996). Interaction between the C terminus of NMDA receptor subunits and multiple members of the PSD-95 family of membrane-associated guanylate kinases. *Journal of Neuroscience* 16, 2157-63.

Nishimura, T., Fukata, Y., Kato, K., Yamaguchi, T., Matsuura, Y., Kamiguchi, H. and Kaibuchi, K. (2003). CRMP-2 regulates polarized Numb-mediated endocytosis for axon growth. *Nat Cell Biol* 5, 819-26.

Noda, M., Ikeda, T., Suzuki, H., Takeshima, H., Takahashi, T., Kuno, M. and Numa, S. (1986). Expression of functional sodium channels from cloned cDNA. *Nature* 322, 826-8.

Noda, M., Shimizu, S., Tanabe, T., Takai, T., Kayano, T., Ikeda, T., Takahashi, H., Nakayama, H., Kanaoka, Y., Minamino, N. et al. (1984). Primary structure of Electrophorus electricus sodium channel deduced from cDNA sequence. *Nature* 312, 121-7.

Nowak, L., Bregestovski, P., Ascher, P., Herbet, A. and Prochiantz, A. (1984). Magnesium gates glutamate-activated channels in mouse central neurones. *Nature* 307, 462-5.

Nowycky, M. C., Fox, A. P. and Tsien, R. W. (1985). Three types of neuronal calcium channel with different calcium agonist sensitivity. *Nature* 316, 440-3.

Ogita, K., Okuda, H., Yamamoto, Y., Nishiyama, N. and Yoneda, Y. (2003). In vivo neuroprotective role of NMDA receptors against kainate-induced excitotoxicity in murine hippocampal pyramidal neurons. *Journal of Neurochemistry* 85, 1336-46.

Ohshima, T., Hirasawa, M., Tabata, H., Mutoh, T., Adachi, T., Suzuki, H., Saruta, K., Iwasato, T., Itohara, S., Hashimoto, M. et al. (2007). Cdk5 is required for multipolar-to-bipolar transition during radial neuronal migration and proper dendrite development of pyramidal neurons in the cerebral cortex. *Development* 134, 2273-82.

Olivera, B. M., McIntosh, J. M., Cruz, L. J., Luque, F. A. and Gray, W. R. (1984). Purification and sequence of a presynaptic peptide toxin from Conus geographus venom. *Biochemistry* 23, 5087-90.

Olivera, B. M., Miljanich, G. P., Ramachandran, J. and Adams, M. E. (1994). Calcium channel diversity and neurotransmitter release: the omega-conotoxins and omega-agatoxins. *Annual Review of Biochemistry* 63, 823-67.

Olverman, H. J., Jones, A. W. and Watkins, J. C. (1984). L-glutamate has higher affinity than other amino acids for [3H]-D-AP5 binding sites in rat brain membranes. *Nature* 307, 460-2.

Omkumar, R. V., Kiely, M. J., Rosenstein, A. J., Min, K. T. and Kennedy, M. B. (1996). Identification of a phosphorylation site for calcium/calmodulindependent protein kinase II in the NR2B subunit of the N-methyl-D-aspartate receptor. *Journal of Biological Chemistry* 271, 31670-8.

Onyszchuk, G., He, Y. Y., Berman, N. E. and Brooks, W. M. (2008). Detrimental effects of aging on outcome from traumatic brain injury: a behavioral, magnetic resonance imaging, and histological study in mice. *Journal of Neurotrauma* 25, 153-71.

Pan, P. Y., Cai, Q., Lin, L., Lu, P. H., Duan, S. and Sheng, Z. H. (2005). SNAP-29-mediated modulation of synaptic transmission in cultured hippocampal neurons. *J.Biol.Chem.* 280, 25769-25779.

Park, C. K., Nehls, D. G., Graham, D. I., Teasdale, G. M. and McCulloch, J. (1988). The glutamate antagonist MK-801 reduces focal ischemic brain damage in the rat. *Annals of Neurology* 24, 543-51.

Park, K. D., Morieux, P., Salome, C., Cotten, S. W., Reamtong, O., Eyers, C., Gaskell, S. J., Stables, J. P., Liu, R. and Kohn, H. (2009). Lacosamide isothiocyanate-based agents: novel agents to target and identify lacosamide receptors. *Journal of Medicinal Chemistry* 52, 6897-911.

Parsons, C. G., Danysz, W. and Quack, G. (1999). Memantine is a clinically well tolerated N-methyl-D-aspartate (NMDA) receptor antagonist--a review of preclinical data. *Neuropharmacology* 38, 735-67.

Patil, P. G., Brody, D. L. and Yue, D. T. (1998). Preferential closed-state inactivation of neuronal calcium channels. *Neuron* 20, 1027-38.

Patrakitkomjorn, S., Kobayashi, D., Morikawa, T., Wilson, M. M., Tsubota, N., Irie, A., Ozawa, T., Aoki, M., Arimura, N., Kaibuchi, K. et al. (2008). Neurofibromatosis type 1 (NF1) tumor suppressor, neurofibromin, regulates the neuronal differentiation of PC12 cells via its associating protein, CRMP-2. *Journal of Biological Chemistry* 283, 9399-413.

Patrick, G. N., Zukerberg, L., Nikolic, M., de la Monte, S., Dikkes, P. and Tsai, L. H. (1999). Conversion of p35 to p25 deregulates Cdk5 activity and promotes neurodegeneration. *Nature* 402, 615-22.

Pawlik, M., Otero, D. A., Park, M., Fischer, W. H., Levy, E. and Saitoh, T. (2007). Proteins that bind to the RERMS region of beta amyloid precursor protein. *Biochem.Biophys.Res.Commun.* %20;355, 907-912.

Perin, M. S., Fried, V. A., Mignery, G. A., Jahn, R. and Sudhof, T. C. (1990). Phospholipid binding by a synaptic vesicle protein homologous to the regulatory region of protein kinase C. *Nature* 345, 260-3.

Peterson, B. Z., DeMaria, C. D., Adelman, J. P. and Yue, D. T. (1999). Calmodulin is the Ca2+ sensor for Ca2+ -dependent inactivation of L-type calcium channels. *Neuron.* 22, 549-558.

Petralia, R. S., Al-Hallaq, R. A. and Wenthold, R. J. (2009). Trafficking and Targeting of NMDA Receptors.

Petratos, S., Li, Q. X., George, A. J., Hou, X., Kerr, M. L., Unabia, S. E., Hatzinisiriou, I., Maksel, D., Aguilar, M. I. and Small, D. H. (2008). The -amyloid protein of Alzheimer's disease increases neuronal CRMP-2 phosphorylation by a Rho-GTP mechanism. *Brain* 131, 90-108.

Pragnell, M., De Waard, M., Mori, Y., Tanabe, T., Snutch, T. P. and Campbell, K. P. (1994). Calcium channel beta-subunit binds to a conserved motif in the I-II cytoplasmic linker of the alpha 1-subunit. *Nature* 368, 67-70.

Prybylowski, K., Chang, K., Sans, N., Kan, L., Vicini, S. and Wenthold, R. J. (2005). The synaptic localization of NR2B-containing NMDA receptors is controlled by interactions with PDZ proteins and AP-2. *Neuron* 47, 845-57.

Qin, N., Platano, D., Olcese, R., Stefani, E. and Birnbaumer, L. (1997). Direct interaction of gbetagamma with a C-terminal gbetagamma-binding domain of the Ca2+ channel alpha1 subunit is responsible for channel inhibition by G protein-coupled receptors. *Proc.Natl.Acad.Sci.U.S.A.* 94, 8866-8871.

Quach, T. T., Massicotte, G., Belin, M. F., Honnorat, J., Glasper, E. R., Devries, A. C., Jakeman, L. B., Baudry, M., Duchemin, A. M. and Kolattukudy, P. E. (2008). CRMP3 is required for hippocampal CA1 dendritic organization and plasticity. *FASEB Journal* 22, 401-9.

Quinn, C. C., Chen, E., Kinjo, T. G., Kelly, G., Bell, A. W., Elliott, R. C., McPherson, P. S. and Hockfield, S. (2003). TUC-4b, a novel TUC family variant, regulates neurite outgrowth and associates with vesicles in the growth cone. *Journal of Neuroscience* 23, 2815-23.

Rahajeng, J., Giridharan, S. S., Naslavsky, N. and Caplan, S. (2010). Collapsin response mediator protein-2 (Crmp2) regulates trafficking by linking endocytic regulatory proteins to dynein motors. *Journal of Biological Chemistry* 285, 31918-22.

Raingo, J., Castiglioni, A. J. and Lipscombe, D. (2007). Alternative splicing controls G protein-dependent inhibition of N-type calcium channels in nociceptors. *Nature Neuroscience* 10, 285-92.

Rami, A., Ferger, D. and Krieglstein, J. (1997). Blockade of calpain proteolytic activity rescues neurons from glutamate excitotoxicity. *Neuroscience Research* 27, 93-7.

Rauck, R. L., Wallace, M. S., Burton, A. W., Kapural, L. and North, J. M. (2009). Intrathecal ziconotide for neuropathic pain: a review. *Pain Pract* 9, 327-37.

Reid, C. A., Bekkers, J. M. and Clements, J. D. (1998). N- and P/Q-type Ca2+ channels mediate transmitter release with a similar cooperativity at rat hippocampal autapses. *Journal of Neuroscience* 18, 2849-55.

Reid, C. A., Bekkers, J. M. and Clements, J. D. (2003). Presynaptic Ca2+ channels: a functional patchwork. *Trends in Neurosciences* 26, 683-7.

Rettig, J., Heinemann, C., Ashery, U., Sheng, Z. H., Yokoyama, C. T., Catterall, W. A. and Neher, E. (1997). Alteration of Ca2+ dependence of neurotransmitter release by disruption of Ca2+ channel/syntaxin interaction. *Journal of Neuroscience* 17, 6647-56.

Rhim, H. and Miller, R. J. (1994). Opioid receptors modulate diverse types of calcium channels in the nucleus tractus solitarius of the rat. *J.Neurosci.* 14, 7608-7615.

Ricard, D., Stankoff, B., Bagnard, D., Aguera, M., Rogemond, V., Antoine, J. C., Spassky, N., Zalc, B., Lubetzki, C., Belin, M. F. et al. (2000). Differential expression of collapsin response mediator proteins (CRMP/ULIP) in subsets of oligodendrocytes in the postnatal rodent brain. *Molecular and Cellular Neurosciences* 16, 324-37.

Richman, R. W., Strock, J., Hains, M. D., Cabanilla, N. J., Lau, K. K., Siderovski, D. P. and Diverse-Pierluissi, M. (2005). RGS12 interacts with the SNARE-binding region of the Cav2.2 calcium channel. *Journal of Biological Chemistry* 280, 1521-8.

Richman, R. W. and verse-Pierluissi, M. A. (2004). Mapping of RGS12-Cav2.2 channel interaction. *Methods in Enzymology* 390:224-39., 224-239.

Roche, K. W., Standley, S., McCallum, J., Dune Ly, C., Ehlers, M. D. and Wenthold, R. J. (2001). Molecular determinants of NMDA receptor internalization. *Nature Neuroscience* 4, 794-802.

Rogemond, V., Auger, C., Giraudon, P., Becchi, M., Auvergnon, N., Belin, M. F., Honnorat, J. and Moradi-Ameli, M. (2008). Processing and nuclear localization of CRMP2 during brain development induce neurite outgrowth inhibition. *Journal of Biological Chemistry* 283, 14751-61.

Romero, G., von Zastrow, M. and Friedman, P. A. (2011). Role of PDZ proteins in regulating trafficking, signaling, and function of GPCRs: means, motif, and opportunity. *Advances in Pharmacology* 62, 279-314.

Rubin, R. P. (1970). The role of calcium in the release of neurotransmitter substances and hormones. *Pharmacological Reviews* 22, 389-428.

Ryan, K. A. and Pimplikar, S. W. (2005). Activation of GSK-3 and phosphorylation of CRMP2 in transgenic mice expressing APP intracellular domain. *Journal of Cell Biology* 171, 327-35.

Ryan, T. A., Reuter, H., Wendland, B., Schweizer, F. E., Tsien, R. W. and Smith, S. J. (1993). The kinetics of synaptic vesicle recycling measured at single presynaptic boutons. *Neuron.* 11, 713-724.

Ryan, T. J., Emes, R. D., Grant, S. G. and Komiyama, N. H. (2008). Evolution of NMDA receptor cytoplasmic interaction domains: implications for organisation of synaptic signalling complexes. *BMC Neurosci* 9, 6.

Ryu, M. J., Lee, C., Kim, J., Shin, H. S. and Yu, M. H. (2008). Proteomic analysis of stargazer mutant mouse neuronal proteins involved in absence seizure. *Journal of Neurochemistry* 104, 1260-70.

Saegusa, H., Kurihara, T., Zong, S., Kazuno, A., Matsuda, Y., Nonaka, T., Han, W., Toriyama, H. and Tanabe, T. (2001). Suppression of inflammatory and neuropathic pain symptoms in mice lacking the N-type Ca2+ channel. *EMBO Journal* 20, 2349-56.

Salter, M. W. (1998). Src, N-methyl-D-aspartate (NMDA) receptors, and synaptic plasticity. *Biochemical Pharmacology* 56, 789-98.

Samuels, B. A., Hsueh, Y. P., Shu, T., Liang, H., Tseng, H. C., Hong, C. J., Su, S. C., Volker, J., Neve, R. L., Yue, D. T. et al. (2007a). Cdk5 promotes synaptogenesis by regulating the subcellular distribution of the MAGUK family member CASK. *Neuron.* 56, 823-837.

Samuels, B. A., Hsueh, Y. P., Shu, T., Liang, H., Tseng, H. C., Hong, C. J., Su, S. C., Volker, J., Neve, R. L., Yue, D. T. et al. (2007b). Cdk5 promotes synaptogenesis by regulating the subcellular distribution of the MAGUK family member CASK. *Neuron* 56, 823-37.

Sanderson, J. L. and Dell'Acqua, M. L. (2011). AKAP signaling complexes in regulation of excitatory synaptic plasticity. *Neuroscientist* 17, 321-36.

Sandoval, A., Andrade, A., Beedle, A. M., Campbell, K. P. and Felix, R. (2007a). Inhibition of recombinant N-type Ca(V) channels by the gamma 2 subunit involves unfolded protein response (UPR)-dependent and UPR-independent mechanisms. *J.Neurosci.* 27, 3317-3327.

Sandoval, A., Arikkath, J., Monjaraz, E., Campbell, K. P. and Felix, R. (2007b). gamma1-dependent down-regulation of recombinant voltage-gated Ca2+ channels. *Cell Mol.Neurobiol.* 27, 901-908.

Sans, N., Petralia, R. S., Wang, Y. X., Blahos, J., 2nd, Hell, J. W. and Wenthold, R. J. (2000). A developmental change in NMDA receptor-associated proteins at hippocampal synapses. *Journal of Neuroscience* 20, 1260-71.

Sans, N., Prybylowski, K., Petralia, R. S., Chang, K., Wang, Y. X., Racca, C., Vicini, S. and Wenthold, R. J. (2003). NMDA receptor trafficking through an interaction between PDZ proteins and the exocyst complex. *Nat Cell Biol* 5, 520-30.

Santicioli, P., Del Bianco, E., Tramontana, M., Geppetti, P. and Maggi, C. A. (1992). Release of calcitonin gene-related peptide like-immunoreactivity induced by electrical field stimulation from rat spinal afferents is mediated by conotoxin-sensitive calcium channels. *Neuroscience Letters* 136, 161-4.

Sasaki, Y., Cheng, C., Uchida, Y., Nakajima, O., Ohshima, T., Yagi, T., Taniguchi, M., Nakayama, T., Kishida, R., Kudo, Y. et al. (2002). Fyn and Cdk5 mediate semaphorin-3A signaling, which is involved in regulation of dendrite orientation in cerebral cortex. *Neuron* 35, 907-20.

Sattler, R. and Tymianski, M. (2000). Molecular mechanisms of calcium-dependent excitotoxicity. *Journal of Molecular Medicine* 78, 3-13.

Sattler, R. and Tymianski, M. (2001). Molecular mechanisms of glutamate receptor-mediated excitotoxic neuronal cell death. *Molecular Neurobiology* 24, 107-29.

Sattler, R., Xiong, Z., Lu, W. Y., Hafner, M., MacDonald, J. F. and Tymianski, M. (1999). Specific coupling of NMDA receptor activation to nitric oxide neurotoxicity by PSD-95 protein. *Science* 284, 1845-8.

Schaible, H. G. (1996). On the role of tachykinins and calcitonin gene-related peptide in the spinal mechanisms of nociception and in the induction and maintenance of inflammation-evoked hyperexcitability in spinal cord neurons (with special reference to nociception in joints). *Progress in Brain Research* 113, 423-41.

Schechtman, D., Murriel, C., Bright, R. and Mochly-Rosen, D. (2003). Overlay method for detecting protein-protein interactions. *Methods Mol.Biol.* 233:351-7., 351-357.

Scheller, A., Oehlke, J., Wiesner, B., Dathe, M., Krause, E., Beyermann, M., Melzig, M. and Bienert, M. (1999). Structural requirements for cellular uptake of alpha-helical amphipathic peptides. *J Pept Sci* 5, 185-94.

Schmidtko, A., Lotsch, J., Freynhagen, R. and Geisslinger, G. (2010). Ziconotide for treatment of severe chronic pain. *Lancet* 375, 1569-77.

Scholz, K. P. and Miller, R. J. (1995). Developmental changes in presynaptic calcium channels coupled to glutamate release in cultured rat hippocampal neurons. *Journal of Neuroscience* 15, 4612-7.

Schroeder, J. E., Fischbach, P. S., Zheng, D. and McCleskey, E. W. (1991). Activation of mu opioid receptors inhibits transient high- and low-threshold Ca2+ currents, but spares a sustained current. *Neuron* 6, 13-20.

Schwarze, S. R., Ho, A., Vocero-Akbani, A. and Dowdy, S. F. (1999). In vivo protein transduction: delivery of a biologically active protein into the mouse. *Science.* 285, 1569-1572.

Scott, D. A., Wright, C. E. and Angus, J. A. (2002). Actions of intrathecal omega-conotoxins CVID, GVIA, MVIIA, and morphine in acute and neuropathic pain in the rat. *European Journal of Pharmacology* 451, 279-86.

Scott, V. E., De Waard, M., Liu, H., Gurnett, C. A., Venzke, D. P., Lennon, V. A. and Campbell, K. P. (1996). Beta subunit heterogeneity in N-type Ca2+ channels. *Journal of Biological Chemistry* 271, 3207-12.

Setou, M., Nakagawa, T., Seog, D. H. and Hirokawa, N. (2000). Kinesin superfamily motor protein KIF17 and mLin-10 in NMDA receptor-containing vesicle transport. *Science.* 288, 1796-1802.

Shapovalova, Z., Tabunshchyk, K. and Greer, P. A. (2007). The Fer tyrosine kinase regulates an axon retraction response to Semaphorin 3A in dorsal root ganglion neurons. *BMC Dev Biol* 7, 133.

Sheng, M. (2001). The postsynaptic NMDA-receptor--PSD-95 signaling complex in excitatory synapses of the brain. *Journal of Cell Science* 114, 1251.

Sheng, Z. H., Rettig, J., Cook, T. and Catterall, W. A. (1996). Calcium-dependent interaction of N-type calcium channels with the synaptic core complex. *Nature* 379, 451-4.

Sheng, Z. H., Rettig, J., Takahashi, M. and Catterall, W. A. (1994). Identification of a syntaxin-binding site on N-type calcium channels. *Neuron* 13, 1303-13.

Sheng, Z. H., Yokoyama, C. T. and Catterall, W. A. (1997). Interaction of the synprint site of N-type Ca2+ channels with the C2B domain of synaptotagmin I. *Proceedings of the National Academy of Sciences of the United States of America* 94, 5405-10.

Shistik, E., Ivanina, T., Puri, T., Hosey, M. and Dascal, N. (1995). Ca2+ current enhancement by alpha 2/delta and beta subunits in Xenopus oocytes: contribution of changes in channel gating and alpha 1 protein level. *J Physiol* 489 (Pt 1), 55-62.

Shleper, M., Kartvelishvily, E. and Wolosker, H. (2005). D-serine is the dominant endogenous coagonist for NMDA receptor neurotoxicity in organotypic hippocampal slices. *Journal of Neuroscience* 25, 9413-7.

Simen, A. A., Lee, C. C., Simen, B. B., Bindokas, V. P. and Miller, R. J. (2001). The C terminus of the Ca channel alpha1B subunit mediates selective inhibition by G-protein-coupled receptors. *Journal of Neuroscience* 21, 7587-97.

Simms, B. A. and Zamponi, G. W. (2012). Trafficking and stability of voltage-gated calcium channels. *Cellular and Molecular Life Sciences* 69, 843-56.

Simpkins, K. L., Guttmann, R. P., Dong, Y., Chen, Z., Sokol, S., Neumar, R. W. and Lynch, D. R. (2003). Selective activation induced cleavage of the NR2B subunit by calpain. *Journal of Neuroscience* 23, 11322-31.

Song, X. J., Hu, S. J., Greenquist, K. W., Zhang, J. M. and LaMotte, R. H. (1999). Mechanical and thermal hyperalgesia and ectopic neuronal discharge after chronic compression of dorsal root ganglia. *J.Neurophysiol.* 82, 3347-3358.

Sonkusare, S. K., Kaul, C. L. and Ramarao, P. (2005). Dementia of Alzheimer's disease and other neurodegenerative disorders--memantine, a new hope. *Pharmacological Research* 51, 1-17.

Stanika, R. I., Pivovarova, N. B., Brantner, C. A., Watts, C. A., Winters, C. A. and Andrews, S. B. (2009). Coupling diverse routes of calcium entry to mitochondrial dysfunction and glutamate excitotoxicity. *Proc.Natl.Acad.Sci.U.S.A.* 106, 9854-9859.

Stanley, E. F. (1993). Single calcium channels and acetylcholine release at a presynaptic nerve terminal. *Neuron.* 11, 1007-1011.

Stanley, E. F. (1997). The calcium channel and the organization of the presynaptic transmitter release face. *Trends in Neurosciences* 20, 404-9.

Steinberg, G. K., Saleh, J., DeLaPaz, R., Kunis, D. and Zarnegar, S. R. (1989). Pretreatment with the NMDA antagonist dextrorphan reduces cerebral injury following transient focal ischemia in rabbits. *Brain Research* 497, 382-6.

Stenmark, P., Ogg, D., Flodin, S., Flores, A., Kotenyova, T., Nyman, T., Nordlund, P. and Kursula, P. (2007). The structure of human collapsin response mediator protein 2, a regulator of axonal growth. *Journal of Neurochemistry* 101, 906-17.

Stephens, G. J., Page, K. M., Bogdanov, Y. and Dolphin, A. C. (2000). The alpha1B Ca2+ channel amino terminus contributes determinants for beta subunit-mediated voltage-dependent inactivation properties. *J Physiol* 525 Pt 2, 377-90.

Stephenson, F. A., Cousins, S. L. and Kenny, A. V. (2008). Assembly and forward trafficking of NMDA receptors (Review). *Molecular Membrane Biology* 25, 311-20.

Strack, S. and Colbran, R. J. (1998). Autophosphorylation-dependent targeting of calcium/ calmodulin-dependent protein kinase II by the NR2B subunit of the N-methyl- D-aspartate receptor. *Journal of Biological Chemistry* 273, 20689-92.

Strack, S., McNeill, R. B. and Colbran, R. J. (2000). Mechanism and regulation of calcium/calmodulin-dependent protein kinase II targeting to the NR2B subunit of the N-methyl-D-aspartate receptor. *Journal of Biological Chemistry* 275, 23798-806.

Su, K. Y., Chien, W. L., Fu, W. M., Yu, I. S., Huang, H. P., Huang, P. H., Lin, S. R., Shih, J. Y., Lin, Y. L., Hsueh, Y. P. et al. (2007). Mice deficient in collapsin response mediator protein-1 exhibit impaired long-term potentiation and impaired spatial learning and memory. *Journal of Neuroscience* 27, 2513-24.

Su, Susan C., Seo, J., Pan, Jen Q., Samuels, Benjamin A., Rudenko, A., Ericsson, M., Neve, Rachael L., Yue, David T. and Tsai, L.-H. (2012). Regulation of N-type Voltage-Gated Calcium Channels and Presynaptic Function by Cyclin-Dependent Kinase 5. *Neuron* 75, 675-687.

Suh, Y. H., Terashima, A., Petralia, R. S., Wenthold, R. J., Isaac, J. T., Roche, K. W. and Roche, P. A. (2010). A neuronal role for SNAP-23 in postsynaptic glutamate receptor trafficking. *Nature Neuroscience* 13, 338-43.

Sun, R. Q., Lawand, N. B. and Willis, W. D. (2003). The role of calcitonin gene-related peptide (CGRP) in the generation and maintenance of mechanical allodynia and hyperalgesia in rats after intradermal injection of capsaicin. *Pain* 104, 201-8.

Suzuki, Y., Nakagomi, S., Namikawa, K., Kiryu-Seo, S., Inagaki, N., Kaibuchi, K., Aizawa, H., Kikuchi, K. and Kiyama, H. (2003). Collapsin response mediator protein-2 accelerates axon regeneration of nerve-injured motor neurons of rat. *Journal of Neurochemistry* 86, 1042-50.

Swayne, L. A., Chen, L., Hameed, S., Barr, W., Charlesworth, E., Colicos, M. A., Zamponi, G. W. and Braun, J. E. (2005). Crosstalk between huntingtin and syntaxin 1A regulates N-type calcium channels. *Molecular and Cellular Neurosciences* 30, 339-51.

Swensen, A. M., Herrington, J., Bugianesi, R. M., Dai, G., Haedo, R. J., Ratliff, K. S., Smith, M. M., Warren, V. A., Arneric, S. P., Eduljee, C. et al. (2012). Characterization of the substituted N-triazole oxindole TROX-1, a small-molecule, state-dependent inhibitor of Ca(V)2 calcium channels. *Molecular Pharmacology* 81, 488-97.

Szabo, Z., Obermair, G. J., Cooper, C. B., Zamponi, G. W. and Flucher, B. E. (2006). Role of the synprint site in presynaptic targeting of the calcium channel CaV2.2 in hippocampal neurons. *European Journal of Neuroscience* 24, 709-18.

Tahimic, C. G., Tomimatsu, N., Nishigaki, R., Fukuhara, A., Toda, T., Kaibuchi, K., Shiota, G., Oshimura, M. and Kurimasa, A. (2006). Evidence for a role of Collapsin response mediator protein-2 in signaling pathways that regulate the proliferation of non-neuronal cells. *Biochemical and Biophysical Research Communications* 340, 1244-50.

Takahashi, T., Fournier, A., Nakamura, F., Wang, L. H., Murakami, Y., Kalb, R. G., Fujisawa, H. and Strittmatter, S. M. (1999). Plexin-neuropilin-1 complexes form functional semaphorin-3A receptors. *Cell* 99, 59-69.

Takahashi, Y. (2003). The 14-3-3 proteins: gene, gene expression, and function. *Neurochemical Research* 28, 1265-73.

Takamori, S., Holt, M., Stenius, K., Lemke, E. A., Gronborg, M., Riedel, D., Urlaub, H., Schenck, S., Brugger, B., Ringler, P. et al. (2006). Molecular anatomy of a trafficking organelle. *Cell.* 127, 831-846.

Takata, K., Kitamura, Y., Nakata, Y., Matsuoka, Y., Tomimoto, H., Taniguchi, T. and Shimohama, S. (2009). Involvement of WAVE accumulation in Abeta/APP pathology-dependent tangle modification in Alzheimer's disease. *American Journal of Pathology* 175, 17-24.

Tanabe, T., Takeshima, H., Mikami, A., Flockerzi, V., Takahashi, H., Kangawa, K., Kojima, M., Matsuo, H., Hirose, T. and Numa, S. (1987). Primary structure of the receptor for calcium channel blockers from skeletal muscle. *Nature* 328, 313-8.

Tay, L. H., Dick, I. E., Yang, W., Mank, M., Griesbeck, O. and Yue, D. T. (2012). Nanodomain Ca(2)(+) of Ca(2)(+) channels detected by a tethered genetically encoded Ca(2)(+) sensor. *Nat Commun* 3, 778.

Tedford, H. W. and Zamponi, G. W. (2006). Direct G protein modulation of Cav2 calcium channels. *Pharmacological Reviews* 58, 837-62.

Touma, E., Kato, S., Fukui, K. and Koike, T. (2007). Calpain-mediated cleavage of collapsin response mediator protein(CRMP)-2 during neurite degeneration in mice. *European Journal of Neuroscience* 26, 3368-81.

Tran-Van-Minh, A. and Dolphin, A. C. (2010). The alpha2delta ligand gabapentin inhibits the Rab11-dependent recycling of the calcium channel subunit alpha2delta-2. *The Journal of Neuroscience* 30, 12856-67.

Tuttle, R. and O'Leary, D. D. (1998). Neurotrophins rapidly modulate growth cone response to the axon guidance molecule, collapsin-1. *Molecular and Cellular Neurosciences* 11, 1-8.

Uchida, Y., Ohshima, T., Sasaki, Y., Suzuki, H., Yanai, S., Yamashita, N., Nakamura, F., Takei, K., Ihara, Y., Mikoshiba, K. et al. (2005). Semaphorin3A signalling is mediated via sequential Cdk5 and GSK3beta phosphorylation of CRMP2: implication of common phosphorylating mechanism underlying axon guidance and Alzheimer's disease. *Genes to Cells* 10, 165-79.

Uchida, Y., Ohshima, T., Yamashita, N., Ogawara, M., Sasaki, Y., Nakamura, F. and Goshima, Y. (2009). Semaphorin3A signaling mediated by Fyn-dependent tyrosine phosphorylation of collapsin response mediator protein 2 at tyrosine 32. *Journal of Biological Chemistry* 284, 27393-401.

Uehata, M., Ishizaki, T., Satoh, H., Ono, T., Kawahara, T., Morishita, T., Tamakawa, H., Yamagami, K., Inui, J., Maekawa, M. et al. (1997). Calcium sensitization of smooth muscle mediated by a Rho-associated protein kinase in hypertension. *Nature* 389, 990-4.

Vance, C. L., Begg, C. M., Lee, W. L., Dubel, S. J., Copeland, T. D., Sonnichsen, F. D. and McEnery, M. W. (1999). N-type calcium channel/syntaxin/SNAP-25 complex probed by antibodies to II-III intracellular loop of the alpha1B subunit. *Neuroscience* 90, 665-76.

Varrin-Doyer, M., Nicolle, A., Marignier, R., Cavagna, S., Benetollo, C., Wattel, E. and Giraudon, P. (2012). Human T Lymphotropic Virus Type 1 Increases T Lymphocyte Migration by Recruiting the Cytoskeleton Organizer CRMP2. *Journal of Immunology*.

Varrin-Doyer, M., Vincent, P., Cavagna, S., Auvergnon, N., Noraz, N., Rogemond, V., Honnorat, J., Moradi-Ameli, M. and Giraudon, P. (2009). Phosphorylation of collapsin response mediator protein 2 on Tyr-479 regulates CXCL12-induced T lymphocyte migration. *The Journal of biological chemistry* 284, 13265-76.

Vega-Hernandez, A. and Felix, R. (2002). Down-regulation of N-type voltage-activated Ca2+ channels by gabapentin. *Cellular and Molecular Neurobiology* 22, 185-90.

Verdoorn, T. A., Kleckner, N. W. and Dingledine, R. (1987). Rat brain N-methyl-D-aspartate receptors expressed in Xenopus oocytes. *Science* 238, 1114-6.

Villerbu, N., Gaben, A. M., Redeuilh, G. and Mester, J. (2002). Cellular effects of purvalanol A: a specific inhibitor of cyclin-dependent kinase activities. *International Journal of Cancer* 97, 761-9.

Vincent, P., Collette, Y., Marignier, R., Vuaillat, C., Rogemond, V., Davoust, N., Malcus, C., Cavagna, S., Gessain, A., Machuca-Gayet, I. et al. (2005). A role for the neuronal protein collapsin response mediator protein 2 in T lymphocyte polarization and migration. *Journal of Immunology* 175, 7650-60.

Voets, T., Toonen, R. F., Brian, E. C., de, W. H., Moser, T., Rettig, J., Sudhof, T. C., Neher, E. and Verhage, M. (2001). Munc18-1 promotes large dense-core vesicle docking. *Neuron.* 31, 581-591.

Volbracht, C., van Beek, J., Zhu, C., Blomgren, K. and Leist, M. (2006). Neuroprotective properties of memantine in different in vitro and in vivo models of excitotoxicity. *European Journal of Neuroscience* 23, 2611-22.

Vosler, P. S., Brennan, C. S. and Chen, J. (2008). Calpain-mediated signaling mechanisms in neuronal injury and neurodegeneration. *Molecular Neurobiology* 38, 78-100.

Vuaillat, C., Varrin-Doyer, M., Bernard, A., Sagardoy, I., Cavagna, S., Chounlamountri, I., Lafon, M. and Giraudon, P. (2008). High CRMP2 expression in peripheral T lymphocytes is associated with recruitment to the brain during virus-induced neuroinflammation. *Journal of Neuroimmunology* 193, 38-51.

Waithe, D., Ferron, L., Page, K. M., Chaggar, K. and Dolphin, A. C. (2011). Beta-subunits promote the expression of Ca(V)2.2 channels by reducing their proteasomal degradation. *Journal of Biological Chemistry* 286, 9598-611.

Walker, D., Bichet, D., Campbell, K. P. and De, W. M. (1998). A beta 4 isoform-specific interaction site in the carboxyl-terminal region of the voltage-dependent Ca2+ channel alpha 1A subunit. *J.Biol.Chem.* 273, 2361-2367.

Walker, D., Bichet, D., Geib, S., Mori, E., Cornet, V., Snutch, T. P., Mori, Y. and De, W. M. (1999). A new beta subtype-specific interaction in alpha1A subunit controls P/Q-type Ca2+ channel activation. *J.Biol.Chem.* 274, 12383-12390.

Wang, H. and Oxford, G. S. (2000). Voltage-dependent ion channels in CAD cells: A catecholaminergic neuronal line that exhibits inducible differentiation. *Journal of Neurophysiology* 84, 2888-95.

Wang, L. H. and Strittmatter, S. M. (1996). A family of rat CRMP genes is differentially expressed in the nervous system. *Journal of Neuroscience* 16, 6197-207.

Wang, L. H. and Strittmatter, S. M. (1997). Brain CRMP forms heterotetramers similar to liver dihydropyrimidinase. *Journal of Neurochemistry* 69, 2261-9.

Wang, Y., Brittain, J. M., Wilson, S. M. and Khanna, R. (2010). Emerging roles of collapsin response mediator proteins (CRMPs) as regulators of voltage-gated calcium channels and synaptic transmission. *Communicative and Integrative Biology* 3, 28-61.

Wang, Y., Okamoto, M., Schmitz, F., Hofmann, K. and Sudhof, T. C. (1997). Rim is a putative Rab3 effector in regulating synaptic-vesicle fusion. *Nature* 388, 593-8.

Wang, Y. T. and Salter, M. W. (1994). Regulation of NMDA receptors by tyrosine kinases and phosphatases. *Nature* 369, 233-5.

Washbourne, P., Bennett, J. E. and McAllister, A. K. (2002). Rapid recruitment of NMDA receptor transport packets to nascent synapses. *Nature Neuroscience* 5, 751-9.

Washbourne, P., Liu, X. B., Jones, E. G. and McAllister, A. K. (2004). Cycling of NMDA receptors during trafficking in neurons before synapse formation. *Journal of Neuroscience* 24, 8253-64.

Weber, A. M., Wong, F. K., Tufford, A. R., Schlichter, L. C., Matveev, V. and Stanley, E. F. (2010). N-type Ca2+ channels carry the largest current: implications for nanodomains and transmitter release. *Nature Neuroscience* 13, 1348-1350.

Webster, L. R., Fisher, R., Charapata, S. and Wallace, M. S. (2009). Long-term intrathecal ziconotide for chronic pain: an open-label study. *Journal of Pain and Symptom Management* 37, 363-72.

Weiss, N., Sandoval, A., Kyonaka, S., Felix, R., Mori, Y. and De Waard, M. (2011). Rim1 modulates direct G-protein regulation of Ca(v)2.2 channels. *Pflugers Archiv. European Journal of Physiology* 461, 447-59.

Weiss, N. and Zamponi, G. W. (2012). Regulation of voltage-gated calcium channels by synaptic proteins. *Advances in Experimental Medicine and Biology* 740, 759-75.

Wennemuth, G., Westenbroek, R. E., Xu, T., Hille, B. and Babcock, D. F. (2000). CaV2.2 and CaV2.3 (N- and R-type) Ca2+ channels in depolarization-evoked entry of Ca2+ into mouse sperm. *Journal of Biological Chemistry* 275, 21210-7.

Wenthold, R. J., Prybylowski, K., Standley, S., Sans, N. and Petralia, R. S. (2003). Trafficking of NMDA receptors. *Annual Review of Pharmacology and Toxicology* 43, 335-58.

Westenbroek, R. E., Hell, J. W., Warner, C., Dubel, S. J., Snutch, T. P. and Catterall, W. A. (1992). Biochemical properties and subcellular distribution of an N-type calcium channel alpha 1 subunit. *Neuron* 9, 1099-115.

Westenbroek, R. E., Hoskins, L. and Catterall, W. A. (1998). Localization of Ca2+ channel subtypes on rat spinal motor neurons, interneurons, and nerve terminals. *Journal of Neuroscience* 18, 6319-30.

Westenbroek, R. E., Sakurai, T., Elliott, E. M., Hell, J. W., Starr, T. V., Snutch, T. P. and Catterall, W. A. (1995). Immunochemical identification and subcellular distribution of the alpha 1A subunits of brain calcium channels. *Journal of Neuroscience* 15, 6403-18.

Westphal, R. S., Tavalin, S. J., Lin, J. W., Alto, N. M., Fraser, I. D., Langeberg, L. K., Sheng, M. and Scott, J. D. (1999). Regulation of NMDA receptors by an associated phosphatase-kinase signaling complex. *Science* 285, 93-6.

Wheeler, D. B., Randall, A. and Tsien, R. W. (1994). Roles of N-type and Q-type Ca2+ channels in supporting hippocampal synaptic transmission. *Science* 264, 107-11.

Williams, K. (1993). Ifenprodil discriminates subtypes of the N-methyl-D-aspartate receptor: selectivity and mechanisms at recombinant heteromeric receptors. *Molecular Pharmacology* 44, 851-9.

Williams, M. E., Brust, P. F., Feldman, D. H., Patthi, S., Simerson, S., Maroufi, A., McCue, A. F., Velicelebi, G., Ellis, S. B. and Harpold, M. M. (1992). Structure and functional expression of an omega-conotoxin-sensitive human N-type calcium channel. *Science* 257, 389-95.

Wiser, O., Bennett, M. K. and Atlas, D. (1996). Functional interaction of syntaxin and SNAP-25 with voltage-sensitive L- and N-type Ca2+ channels. *EMBO Journal* 15, 4100-10.

Wo, Z. G. and Oswald, R. E. (1994). Transmembrane topology of two kainate receptor subunits revealed by N-glycosylation. *Proceedings of the National Academy of Sciences of the United States of America* 91, 7154-8.

Wong, F. K. and Stanley, E. F. (2010). Rab3a interacting molecule (RIM) and the tethering of pre-synaptic transmitter release site-associated CaV2.2 calcium channels. *Journal of Neurochemistry* 112, 463-73.

Wong, W., Newell, E. W., Jugloff, D. G., Jones, O. T. and Schlichter, L. C. (2002). Cell surface targeting and clustering interactions between heterologously expressed PSD-95 and the Shal voltage-gated potassium channel, Kv4.2. *J.Biol.Chem.* 277, 20423-20430.

Wu, C. C., Chen, H. C., Chen, S. J., Liu, H. P., Hsieh, Y. Y., Yu, C. J., Tang, R., Hsieh, L. L., Yu, J. S. and Chang, Y. S. (2008). Identification of collapsin response mediator protein-2 as a potential marker of colorectal carcinoma by comparative analysis of cancer cell secretomes. *Proteomics* 8, 316-32.

Wu, H. Y., Yuen, E. Y., Lu, Y. F., Matsushita, M., Matsui, H., Yan, Z. and Tomizawa, K. (2005). Regulation of N-methyl-D-aspartate receptors by calpain in cortical neurons. *Journal of Biological Chemistry* 280, 21588-93.

Wu, L. G., Borst, J. G. and Sakmann, B. (1998). R-type Ca2+ currents evoke transmitter release at a rat central synapse. *Proc.Natl.Acad.Sci.U.S.A.* 95, 4720-4725.

Wu, L. G., Westenbroek, R. E., Borst, J. G., Catterall, W. A. and Sakmann, B. (1999). Calcium channel types with distinct presynaptic localization couple differentially to transmitter release in single calyx-type synapses. *Journal of Neuroscience* 19, 726-36.

Wu, Y., Li, Q. and Chen, X. Z. (2007). Detecting protein-protein interactions by Far western blotting. *Nat.Protoc.* 2, 3278-3284.

Xiong, T., Tang, J., Zhao, J., Chen, H., Zhao, F., Li, J., Qu, Y., Ferriero, D. and Mu, D. (2012). Involvement of the Akt/GSK-3beta/CRMP-2 pathway in axonal injury after hypoxic-ischemic brain damage in neonatal rat. *Neuroscience* 216, 123-32.

Yaka, R., Thornton, C., Vagts, A. J., Phamluong, K., Bonci, A. and Ron, D. (2002). NMDA receptor function is regulated by the inhibitory scaffolding protein, RACK1. *Proceedings of the National Academy of Sciences of the United States of America* 99, 5710-5.

Yamaguchi, K., Tatsuno, M. and Kiuchi, Y. (1998). Maturational change of KCl-induced Ca2+ increase in the rat brain synaptosomes. *Brain and Development* 20, 234-238.

Yamashita, N., Ohshima, T., Nakamura, F., Kolattukudy, P., Honnorat, J., Mikoshiba, K. and Goshima, Y. (2012). Phosphorylation of CRMP2 (collapsin response mediator protein 2) is involved in proper dendritic field organization. *Journal of Neuroscience* 32, 1360-5.

Yang, Y. M. and Wang, L. Y. (2006). Amplitude and kinetics of action potential-evoked Ca2+ current and its efficacy in triggering transmitter release at the developing calyx of held synapse. *Journal of Neuroscience* 26, 5698-708.

Yasuda, T., Chen, L., Barr, W., McRory, J. E., Lewis, R. J., Adams, D. J. and Zamponi, G. W. (2004). Auxiliary subunit regulation of high-voltage activated calcium channels expressed in mammalian cells. *European Journal of Neuroscience* 20, 1-13.

Yeow, M. B. and Peterson, E. H. (1991). Active zone organization and vesicle content scale with bouton size at a vertebrate central synapse. *Journal of Comparative Neurology* 307, 475-86.

Yokoyama, C. T., Sheng, Z. H. and Catterall, W. A. (1997a). Phosphorylation of the synaptic protein interaction site on N-type calcium channels inhibits interactions with SNARE proteins. *The Journal of neuroscience : the official journal of the Society for Neuroscience* 17, 6929-38.

Yokoyama, C. T., Sheng, Z. H. and Catterall, W. A. (1997b). Phosphorylation of the synaptic protein interaction site on N-type calcium channels inhibits interactions with SNARE proteins. *Journal of Neuroscience* 17, 6929-38.

Yoneda, A., Morgan-Fisher, M., Wait, R., Couchman, J. R. and Wewer, U. M. (2012). A CRMP-2 isoform controls myosin II-mediated cell migration and matrix assembly by trapping ROCK II. *Molecular and Cellular Biology*.

Yoshida, H., Watanabe, A. and Ihara, Y. (1998). Collapsin response mediator protein-2 is associated with neurofibrillary tangles in Alzheimer's disease. *Journal of Biological Chemistry* 273, 9761-8.

Yoshikami, D., Bagabaldo, Z. and Olivera, B. M. (1989). The inhibitory effects of omega-conotoxins on Ca channels and synapses. *Annals of the New York Academy of Sciences* 560, 230-48.

Yoshimura, T., Kawano, Y., Arimura, N., Kawabata, S., Kikuchi, A. and Kaibuchi, K. (2005). GSK-3beta regulates phosphorylation of CRMP-2 and neuronal polarity. *Cell* 120, 137-49.

Yu, X. M., Askalan, R., Keil, G. J., 2nd and Salter, M. W. (1997). NMDA channel regulation by channel-associated protein tyrosine kinase Src. *Science* 275, 674-8.

Yuasa-Kawada, J., Suzuki, R., Kano, F., Ohkawara, T., Murata, M. and Noda, M. (2003). Axonal morphogenesis controlled by antagonistic roles of two CRMP subtypes in microtubule organization. *European Journal of Neuroscience* 17, 2329-43.

Yuen, E. Y., Ren, Y. and Yan, Z. (2008). Postsynaptic density-95 (PSD-95) and calcineurin control the sensitivity of N-methyl-D-aspartate receptors to calpain cleavage in cortical neurons. *Molecular Pharmacology* 74, 360-70.

Zamponi, G. W. (2003). Regulation of presynaptic calcium channels by synaptic proteins. *J.Pharmacol.Sci.* 92, 79-83.

Zamponi, G. W., Bourinet, E., Nelson, D., Nargeot, J. and Snutch, T. P. (1997). Crosstalk between G proteins and protein kinase C mediated by the calcium channel alpha1 subunit. *Nature* 385, 442-6.

Zhang, J. F., Randall, A. D., Ellinor, P. T., Horne, W. A., Sather, W. A., Tanabe, T., Schwarz, T. L. and Tsien, R. W. (1993). Distinctive pharmacology and kinetics of cloned neuronal Ca2+ channels and their possible counterparts in mammalian CNS neurons. *Neuropharmacology.* 32, 1075-1088.

Zhang, J. M., Song, X. J. and LaMotte, R. H. (1999). Enhanced excitability of sensory neurons in rats with cutaneous hyperalgesia produced by chronic compression of the dorsal root ganglion. *J.Neurophysiol.* 82, 3359-3366.

Zhang, S., Edelmann, L., Liu, J., Crandall, J. E. and Morabito, M. A. (2008). Cdk5 regulates the phosphorylation of tyrosine 1472 NR2B and the surface expression of NMDA receptors. *Journal of Neuroscience* 28, 415-24.

Zhang, Z., Majava, V., Greffier, A., Hayes, R. L., Kursula, P. and Wang, K. K. (2009). Collapsin response mediator protein-2 is a calmodulin-binding protein. *Cellular and Molecular Life Sciences* 66, 526-36.

Zhang, Z., Ottens, A. K., Sadasivan, S., Kobeissy, F. H., Fang, T., Hayes, R. L. and Wang, K. K. (2007). Calpain-mediated collapsin response mediator protein-1, -2, and -4 proteolysis after neurotoxic and traumatic brain injury. *Journal of Neurotrauma* 24, 460-72.

Zhou, M. and Baudry, M. (2006). Developmental changes in NMDA neurotoxicity reflect developmental changes in subunit composition of NMDA receptors. *Journal of Neuroscience* 26, 2956-63.

Zhu, L. Q., Zheng, H. Y., Peng, C. X., Liu, D., Li, H. L., Wang, Q. and Wang, J. Z. (2010). Protein phosphatase 2A facilitates axonogenesis by dephosphorylating CRMP2. *Journal of Neuroscience* 30, 3839-48.

Zhu, Y. and Ikeda, S. R. (1994). VIP inhibits N-type Ca2+ channels of sympathetic neurons via a pertussis toxin-insensitive but cholera toxin-sensitive pathway. *Neuron* 13, 657-69.

Zilly, F. E., Sorensen, J. B., Jahn, R. and Lang, T. (2006). Munc18-bound syntaxin readily forms SNARE complexes with synaptobrevin in native plasma membranes. *PLoS.Biol.* 4, e330.

Zufferey, R. (2002). Production of lentiviral vectors. *Curr.Top.Microbiol.Immunol.* 261:107-21., 107-121.

Zuhlke, R. D., Pitt, G. S., Deisseroth, K., Tsien, R. W. and Reuter, H. (1999). Calmodulin supports both inactivation and facilitation of L-type calcium channels. *Nature.* 399, 159-162.

7. CURRICULUM VITAE

Joel Matthew Brittain

A. Education

INDIANA UNIVERSITY
Indianapolis, Indiana
Ph.D. Medical Neuroscience (2007-2012)
Mentor: Dr. Rajesh Khanna

UNIVERSITY OF MINNESOTA
Duluth, Minnesota
Bachelor of Science with Honors, *Magna cum laude* – Biochemistry, May 2007

B. Positions and Honors

Other Experience and Professional Memberships:

2009-11	Member, Society for Neuroscience
2010-11	Graduate student organization representative for Medical Neuroscience

Honors:

2006	Undergraduate Research Opportunities Fellow
2006-2007	Summer Undergraduate Research Program Participant
2007	University Fellowship, Indiana University
2009	Outstanding Poster Presentation, Indianapolis Society for Neuroscience
2010	Larry Kays, M.D. Fund Student Fellowship
2010	Educational Enhancement Grant
2011	Gill Thesis Award

C. Peer-reviewed Publications and Presentations

Published Articles:

1. Wilson SM, Schmutzler BS, **Brittain JM**, Dustrude ET, Ripsch MS, Pellman JJ, Yeum TS, Hurley JH, Hingtgen CM, White FA, Khanna R (2012). Inhibition of Transmitter Release and Attenuation of AIDS Therapy-Induced and Tibial Nerve Injury-Related Painful Peripheral Neuropathy by Novel Synthetic Ca^{2+} Channel Peptides. J Biol Chem 287:35065-77

2. **Brittain JM**, Wang Y, Eruvwetere O, Khanna R (2012). Cdk5-mediated phosphorylation of CRMP-2 enhances its interaction with CaV2.2. FEBS Lett 586:3813-8

3. Brittain MK, Brustovetsky T, **Brittain JM**, Khanna R, Cummins TR, Brustovetsky N (2012). Ifenprodil, a NR2B-selective antagonist of NMDA receptor, inhibits reverse Na^{+}/Ca^{2+} exchanger in neurons. Neuropharmacology 63:974-82.

4. Wilson SM, Xiong W, Wang Y, Ping X, Head J D, **Brittain JM**, Gagare PD, Ramachandran PV, Jin X and Khanna R (2012). Prevention of posttraumatic axon sprouting by blocking collapsin response mediator protein 2-mediated neurite outgrowth and tubulin polymerization. Neuroscience 210: 451-66

5. **Brittain JM**, Wang T, Wilson SM, Khanna R (2012) Regulation of CREB signaling through L-Type Ca2+ channels by Nipsnap-2. Channels (Austin) 6: 94-102

6. **Brittain JM,** Pan R, You H, Brustovetsky T, Brustovetsky N, Zamponi GW, Lee WH and Khanna R (2012) Disruption of NMDAR–CRMP-2 signaling protects against focal cerebral ischemic damage in the rat middle cerebral artery occlusion model. Channels (Austin) 6

7. Brittain MK, Brustovetsky T, Sheets PL, **Brittain JM**, Khanna R, Cummins TR, Brustovetsky N (2012) Delayed calcium dysregulation in neurons requires both the NMDA receptor and the reverse Na^{+}/Ca^{2+} exchanger. Neurobiol Dis 46: 109-17

8. **Brittain JM**, Chen L, Wilson SM, Brustovetsky T, Gao X, Ashpole NM, Molosh AI, You H, Hudmon A, Shekhar A, White FA, Zamponi GW, Brustovetsky N, Chen J, Khanna R (2011) Neuroprotection against Traumatic Brain Injury by a Peptide Derived from the Collapsin Response Mediator Protein 2 (CRMP2). J Biol Chem 286: 37778-37792

9. Wilson SM, **Brittain JM**, Piekarz AD, Ballard CJ, Ripsch MS, Cummins TR, Hurley JH, Khanna M, Hammes NM, Samuels BC, White FA, Khanna R (2011) Further insights into the antinociceptive potential of a peptide disrupting the N-type calcium channel-CRMP-2 signaling complex. Channels (Austin) 5: 449-456

10. **Brittain JM**, Duarte DB, Wilson SM, Zhu W, Ballard C, Johnson PL, Liu N, Xiong W, Ripsch MS, Wang Y, Fehrenbacher JC, Fitz SD, Khanna M, Park CK, Schmutzler BS, Cheon BM, Due MR, Brustovetsky T, Ashpole NM, Hudmon A, Meroueh SO, Hingtgen CM, Brustovetsky N, Ji RR, Hurley JH, Jin X, Shekhar A, Xu XM, Oxford GS, Vasko MR, White FA, Khanna R (2011) Suppression of inflammatory and neuropathic pain by uncoupling CRMP-2 from the presynaptic Ca(2) channel complex. Nat Med 17: 822-829

11. Wang Y, Wilson SM, **Brittain JM**, Ripsch MS, Salome C, Park KD, White FA, Khanna R, Kohn H (2011) Merging Structural Motifs of Functionalized Amino Acids and alpha-Aminoamides Results in Novel Anticonvulsant Compounds with Significant Effects on Slow and Fast Inactivation of Voltage-gated Sodium Channels and in the Treatment of Neuropathic Pain. ACS Chem Neurosci 2: 317-322

12. Wang Y, **Brittain JM**, Jarecki BW, Park KD, Wilson SM, Wang B, Hale R, Meroueh SO, Cummins TR, Khanna R (2010) In silico docking and electrophysiological characterization of lacosamide binding sites on collapsin response mediator protein-2 identifies a pocket important in modulating sodium channel slow inactivation. J Biol Chem 285: 25296-25307

13. Wang Y, **Brittain JM**, Wilson SM, Hingtgen CM, Khanna R (2010) Altered calcium currents and axonal growth in Nf1 haploinsufficient mice. Translational Neuroscience 1: 106-114

14. Wang Y, **Brittain JM**, Wilson SM, Khanna R (2010) Emerging roles of collapsin response mediator proteins (CRMPs) as regulators of voltage-gated calcium channels and synaptic transmission. Communicative and Integrative Biology 3: 28-61

15. Chi XX, Schmutzler BS, **Brittain JM**, Wang Y, Hingtgen CM, Nicol GD, Khanna R (2009) Regulation of N-type voltage-gated calcium channels (Cav2.2) and transmitter release by collapsin response mediator protein-2 (CRMP-2) in sensory neurons. J Cell Sci 122: 4351-4362

16. **Brittain JM**, Piekarz AD, Wang Y, Kondo T, Cummins TR, Khanna R (2009) An atypical role for collapsin response mediator protein 2 (CRMP-2) in neurotransmitter release via interaction with presynaptic voltage-gated calcium channels. J Biol Chem 284: 31375-31390

Abstract/Poster Presentations:

1. **Brittain JM**, Duarte DB, Wilson SM, Ballard C, Johnson PL, Liu N, Xiong W, Ripsch MS, Wang Y, Fehrenbacher JC, Fitz JD, Khanna M, Park CK, Ashpole NM, Hudmon A, Meroueh SO, Ji RR, Hurley JH, Jin X, Shekhar A, Xu XM, Oxford GS, Vasko MR, White FA, Khanna R. Session 275. Nov 13, 2011. Society for Neuroscience Meeting, Washington D.C

2. Wilson SM, Xiong W, Head J, **Brittain JM**, Gagare P, Ramachandran P, Jin X, Khanna R. The anticonvulsant Lacosamide inhibits CRMP2-mediated neurite outgrowth in vitro and prevents enhanced excitatory connectivity in an animal model of posttraumatic epileptogenesis. Session 250. Nov 13, 2011. Society for Neuroscience Meeting, Washington D.C.

3. **Brittain JM**, Chen L, Brustovetsky T, Gao X, Wilson SM, Ashpole NM, Molosh AI, You H, Hudmon A, Brustovetsky N, Chen J, Khanna R. Neuroprotection against Traumatic Brain Injury by a Peptide Derived from the Collapsin Response Mediator Protein 2 (CRMP2). Session 426. Nov 14, 2011. Society for Neuroscience Meeting, Washington D.C.

4. **Brittain JM**, Duarte DB, Wilson SM, Ballard C, Johnson PL, Liu N, Xiong W, Ripsch MS, Wang Y, Fehrenbacher JC, Fitz JD, Khanna M, Park CK, Ashpole NM, Hudmon A, Meroueh SO, Ji RR, Hurley JH, Jin X, Shekhar A, Xu XM, Oxford GS, Vasko MR, White FA, Khanna R. Suppression of inflammatory and neuropathic pain by uncoupling CRMP-2 from the presynaptic Ca^{2+} channel complex. July 22, 2011, Midwest Pain Interest Group, Chicago, Il.

5. **Brittain JM**, Piekarz AD, Wang Y, Garcia AS, Cummins TR, Khanna R. An atypical role for CRMP-2 in neurotransmitter release via interaction with presynaptic Ca^{2+} channels. 2010 IUPUI Research Day, Indianapolis, IN.

6. **Brittain JM**, Piekarz AD, Wang Y, Garcia AS, Cummins TR, Khanna R. An atypical role for CRMP-2 in neurotransmitter release via interaction with presynaptic Ca^{2+} channels. Poster 519.4/C73. Oct 20, 2009, Society for Neuroscience Meeting, Chicago, IL.

7. Hingtgen CM, **Brittain JM**, Schmutzler BS, Khanna R. Neurofibromin, CRMP-2 and presynaptic calcium channel proteins control synaptic transmission in a mouse model of neurofibromatosis type 1. Poster 519.5/C74. Oct 20, 2009, Society for Neuroscience Meeting, Chicago, IL.

8. **Brittain JM**, Piekarz AD, Wang Y, Garcia AS, Cummins TR, Khanna R. An atypical role for CRMP-2 in regulation of transmitter release via interaction with presynaptic Ca^{2+} channels. Indianapolis Society for Neuroscience, Indianapolis, IN.

9. Khanna R, **Brittain JM**, Schmutzler BS, Hingtgen CM. Neurofibromin, CRMP-2 and presynaptic calcium channel proteins control synaptic transmission in a mouse model of neurofibromatosis type 1. Poster session 2: P92. June 13-16, 2009, Children's Tumor Foundation conference on Neurofibromatosis, Portland, Oregon.

10. **Brittain JM**, Piekarz AD, Cummins TR, Khanna R. A novel role for CRMP-2 in regulation of transmitter release via interaction with N-type voltage-gated calcium channels. May 20th, 2009, Gill Symposium, Bloomington, IN.

11. **Brittain JM**, Piekarz AD, Cummins TR, Khanna R. A novel role for CRMP-2 in regulation of transmitter release via interaction with N-type voltage-gated calcium channels. February 17 - 22, 2009, Keystone Symposia on *Neurodegenerative Diseases: New Molecular Mechanisms,* Keystone, CO.